ASSESSMENT OF *DEHALOCOCCOIDES MCCARTYI* STRAIN SPECIFIC RESPONSES TO SOIL HETEROGENEITY, PULSED ELECTRON DONOR DELIVERY, AND PER- AND POLYFLUOROALKYL SUBSTANCES

A Dissertation

Submitted by

Jason P. Hnatko

In partial fulfillment of the requirements for the degree of

Doctor of Philosophy

In

Civil and Environmental Engineering

TUFTS UNIVERSITY

May 2020

DISSERTATION COMMITTEE:

Natalie L. Cápiro, PhD, Advisor (*Tufts University/Auburn University)*
Kurt D. Pennell, PhD, Advisor (*Brown University)*
Linda M. Abriola, PhD (*Tufts University*)
Nikhil U. Nair, PhD (*Tufts University)*

Abstract

In situ bioremediation (ISB) is a commonly employed remedy for chlorinated solvent contaminated groundwater. Tetrachloroethene (PCE) and trichloroethene (TCE) ISB utilizes microbial consortia to detoxify contaminants to ethene through microbial reductive dechlorination (MRD). *Dehalococcoides mccartyi (Dhc)* strains are the key contributors to ethene formation. Although ISB has been successful at many sites, contaminant rebound and incomplete dechlorination to *cis*-dichloroethene (*cis*-DCE) and/or vinyl chloride limit ISB's effectiveness. Advancing the understanding of *Dhc* strains harboring reductive dehalogenase (RDase) genes implicated ethene formation (*e.g. vcrA* and *bvcA)* is necessary to expand ISB's implementation as a sustainable groundwater remedy. Subsurface heterogeneity complicates ISB by limiting amendment delivery and exacerbating contaminant rebound. Using an aquifer cell experiment, *Dhc* strain distribution around lenses of varying permeability and organic carbon content was measured. MRD also enhanced mass transfer of TCE from low-permeability materials up to 53% locally over abiotic processes alone. An ISB pilot test and coupled laboratory aquifer cell experiment revealed incomplete MRD of TCE caused by permeability variations affecting local residence times. Increasing average residence time by 50% *in situ* increased the proportion of ethene downgradient from 5% to 46% of chlorinated ethenes and ethene by molar mass. Samples collected during these experiments were also used to examine the impact of periodic electron donor delivery on RDase gene expression, as measured by RNA transcripts associated with ethene formation. *vcrA* transcripts decayed 15-75 times more slowly when electron donor was depleted than in previous studies with depleted electron acceptors. This slow decay of *vcrA* transcripts supports the ISB practice of pulsed electron donor delivery. Lastly, the impact of the class of emerging contaminants, per- and poly-fluoroalkyl substances (PFAS) on *Dhc* strains was investigated using batch reactor and

microcosm experiments. PFAS inhibited *cis*-DCE MRD at concentrations of 11.7 mg/L and higher but the presence of a solid phase prevented inhibition at concentrations up to 53.5 mg/L. The *Dhc* strains responsible for ethene formation shifted from *vcrA*-harboring cells to *bvcA*-harboring cells at high PFAS concentrations. Together, these four studies elucidate *Dhc* strain growth and MRD performance in complex systems, which can help practitioners of ISB implement successful remedies.

Acknowledgements

I would like to thank my advisor, Dr. Natalie Cápiro, for giving me a chance on the softball field and in the laboratory. Your guidance and criticism, even when frustrating, made me approach things scientifically and helped me to successfully navigate this program.

Thank you to my committee members. Dr. Kurt Pennell, you always provided sage advice at the right moment and pushed the work in the right direction. Dr. Linda Abriola, your extensive background was invaluable to formulating problems and ensuring that experiments were designed and conducted to yield useful results. Dr. Nikhil Nair, even though you joined the team late, your suggestions were greatly appreciated, especially in understanding the promotion mechanisms for gene promotion.

To my wife, Lauren. Thank you for your unconditional love and support over these years. We are a great team and got through it together.

Thank you Lurong Yang. Your numerical models are an integral part of this work and I am honored to author several publications with you. I would also like to thank my other collaborators, Dr. Tian Tang, Sam Gaeth, Liyang Chu, Jack Elsey, Dr. Masoud Arshadi, Dr. John Fortner, Dr. John Christ, and Chen Liu. I enjoyed working with you and look forward to finalizing these papers.

This work was made possible by the Vermont Department of Environmental Conservation providing access to the Commerce Street Superfund Site and by the Maine Department of Environmental Protection's assistance with obtaining materials from Loring Air Force Base.

A big thank you and shoutout to my officemates, labmates, and classmates that I have worked closely with over the years. You have always been a great help and it was great to get to know you. There are too many to name but I want to especially single out Tiffany

Duhl, Dr. Tyler Marcet, Dr. Bonnie Lyon-Marion, Caitlin Johnson, Deniz Ranjpour, Amy Hunter, Veronica Gonsalez, Patricia Rosa, Kelly Chin, Jessica Cooper, Lauren Quickel, and Kelly Donohue for your help and patience.

Funding for this research was provided by the Strategic Environmental Research and Development Program (SERDP) under Project ER-2311: Development of an Integrated Field Test/Modeling Protocol for Efficient *In Situ* Bioremediation Design and Performance Uncertainty Assessment and Project ER-2714: Development of Coupled Physiochemical and Biological Systems for *In Situ* Remediation of Mixed Perfluorinated Chemical and Chlorinated Solvent Groundwater Plumes. Thank you to SiREM for providing the KB-1® culture used in these projects.

Table of Contents

List of Tables

List of Figures

List of Abbreviations and Acronyms

1,1,1,-TCA 1,1,1-trichloroethane

AFFFs ..... Aqueous film forming foams

BDI ..... Bio-dechlor Inoculum

bvcA ..... *Vinyl chloride reductase b*

CERCLA ..... Comprehensive Environmental Response, Compensation, and Liability Act

CFC-113 ..... 1,1,2-Trichloro-1,2,2,-trifluoroethane

CMT ..... Continuous multichannel tubing

DCE ..... Dichloroethene

Dhc ..... *Dehalococcoides mccartyi*

DNAPL ..... Dense non-aqueous phase liquid

EGMBE ..... Ethelyne glycol monobutyl ether

EtFOSE ..... n-ethyl sulfonamide ethanol

FTOHs ..... Fluoroetemoer alcohols

FTSAm ..... Fluoroetelomer sulfonamide

FtTAos ..... Fluorotelomer thioether amido sulfonates

GC-FID ..... Gas chromatography with flame ionization detection

Geo ..... *Geobacter* species

GeoSZ ..... *Geobacter lovleyi* strain SZ

HDPE ..... High-density polyethylene

HPLC ..... High pressure liquid chromatography

IARC ..... International Agency for Research on Cancer

IC ..... Ion conductivity

ISB ..... *In situ* bioremediation

K_d ..... adsorption coefficient

LC/MS ..... Liquid chromatography with mass spectrometry

LVI ..... Large volume injection

MCLG ..... Maximum contaminant level goal

MCL ..... Maximum contaminant levels

MRD ..... Microbial reductive dechlorination

mRNA ..... Messenger RNA

MT3DMS ..... Three-dimensional mulit-species modular transport model

NAPL ..... Non-aqueous phase liquid

OC ..... Organic carbon

ORP ..... Oxidation reduction potential

OSHA ..... Occupational Safety and Health Administration

PAPs ..... Polyfluoroalkyl phosphates

PCE ..... Tetrachloroethene

PEL ..... Permissible exposure level

PFAAs ..... Perfluoroalkyl acids

PFAS ..... Per- and poly-fluoroalkyl substances

PFBA ..... Heptafluorobutrycic acid

PFBS ..... Perfulorobutanol sulfonate

PFCAs ..... Perfluoroalkyl carboxylic acids

PFDA ..... Perfluorodecanoate

PFDoA ..... Perfluorododecanoate

PFEtS ..... Perfluoroethanesulfonate

PFHpA ..... Perfluoroheptanoic acid

PFHxA ..... Undecafluorohexanoic acid

PFHxS ..... Perfluorohexanol sulfonate

PFNA ..... Perfluorononanoic acid

PFOA ..... Perfluorooctanoate

PFOS ..... Perfluorooctane sulfonate

PFPeA ..... Perfluoropentanoic acid

PFPrS ..... Perfluoropropanesulfonate

PFSAs ..... Perfluoroalkyl sulfonic acids

PV ..... Pore volume

PVC ..... Poly(vinyl chloride)

qPCR ..... Quantitative polymerase chain reaction

RCRA ..... Resource Conservation and Recovery Act

RDase ..... Reductive dehalogenase

SAMPAP .....EtFOSE-based phosphate diester

SERDP .....Strategic Environmental Research and Development Program

SM.....Supplementary material

TCC.....Triclocarban

TCE.....Trichloroethene

tceA .....*Trichloroethene reductase*

TOC .....Total organic carbon

uHPLC .....Ultra high-performance liquid chromatograph

USEPA..... United States Environmental Protection Agency

VC.....Vinyl chloride

vcrA.....*Vinyl chloride reductase a*

VOCs .....Volatile organic compounds

ASSESSMENT OF *DEHALOCOCCOIDES MCCARTYI* STRAIN SPECIFIC RESPONSES TO SOIL HETEROGENEITY, PULSED ELECTRON DONOR DELIVERY, AND PER- AND POLYFLUOROALKYL SUBSTANCES

1.0 Introduction

In situ bioremediation (ISB) is a commonly employed and effective tool that has been implemented at a variety of sites to degrade contaminants in groundwater and is the *in situ* treatment selected at a majority (57%) of Superfund sites with contaminated groundwater.[1–4] ISB of chlorinated solvents, primarily chlorinated ethenes (tetrachloroethene [PCE] and trichloroethene [TCE]), relies on microorganisms, including *Dehalococcoides mccartyi* (*Dhc)* strains, to transform PCE to benign ethene through microbial reductive dechlorination (MRD).[5–9] Multiple strains of *Dhc* have been identified and those implicated in the transformation of chlorinated ethenes harbor specific reductive dehalogenase (RDase) genes that encode for the critical enzymes of anaerobic organohalide respiration, a microbial metabolic process that has been harnessed for the bioremediation of chlorinated ethene contaminated aquifers.[10] Each *Dhc* strain has the capacity to transform specific chlorinated compounds; however, only a limited number of strains that transform vinyl chloride (VC) to ethene have been identified.[11–14]

Although ISB has been implemented as an effective remedial strategy for PCE and TCE contamination,[1,15,16] many sites exhibit incomplete dechlorination to dichloroethene isomers (DCE) and/or VC, or show rebound of contaminant concentrations when active biostimulation ceases.[17–21] Subsurface heterogeneity complicates implementation of ISB and exacerbates contaminant rebound; amendments delivered through groundwater injection do not effectively distribute into low-permeability regions and, conversely, any compounds retained in low-permeability porous media are slowly released over time.[2,9,22–24] Advancing the understanding of the effect of geological and chemical factors on the growth and activity of the specific *Dhc* strains capable of fully dechlorinating chlorinated ethenes to ethene is critical to supporting the implementation of ISB as a remedy for complex sites. This understanding will be especially valuable in locations where

incomplete dechlorination has been measured or where ISB is believed to be unsuitable, including heterogeneous aquifers with low-permeability and/or high organic carbon lenses.

A variety of factors, including oxygen concentration,[25] pH,[26] type and concentration of electron acceptor,[27,28] temperature,[29] and co-contaminants[30] have been shown to impact specific *Dhc* strains, as measured by the relative abundance of RDase genes. Subsurface porous media heterogeneity may also impact the relative abundance of microorganisms harboring RDase genes, as the presence of such heterogeneity impacts the distribution of contaminants and growth substrates in the surrounding pore water.[31] The presence of specific strains of dechlorinating microbes in and around these low-permeability materials may be able to enhance the release of chlorinated ethenes and transform them to benign ethene as they are released. This process is similar to previously observed bioenhanced dissolution of non-aqueous phase liquids (NAPL).[32–35] However, the effect of subsurface heterogeneity on the distribution of *Dhc* strains during ISB has not been specifically assessed in previous studies. Additionally, the enhancement of back-diffusion from low-permeability porous media by MRD has not been quantified. Chapter 3 presents the results of an aquifer cell experiment designed to elucidate the effect of heterogeneous porous media on the distribution of *Dhc* strains harboring specific RDase genes and the ability of these populations to enhance back-diffusion from low-permeability media.

Heterogeneity also influences the residence time of contaminants, nutrients, and growth substrates in bioactive zones. Average residence time is a parameter often used when designing active pumping or recirculation ISB systems, and if the contact time between contaminants and dechlorinating microorganisms is insufficient, transformation of all contaminants flowing through the bioactive zone will not be achieved.[36] To examine the effect of residence time on the extent of TCE dechlorination by MRD, aquifer cell and pilot-test studies were completed as described in Chapter 4.

Total *Dhc* and strain-specific abundance is typically monitored through quantitative polymerase chain reaction (qPCR) of the 16S rRNA gene and the *tceA*, *vcrA*, and *bvcA* RDase genes in extracted DNA to assess the potential for dechlorination in microbial communities.[37–39] Analysis of DNA is useful to determine changes in total abundance over time, predict remediation performance, and determine the capability of the microbial population to transform PCE to ethene.[38,40,41] However, using only DNA to quantify the abundance of cells provides an incomplete picture of the capacity of the microbial community, as the DNA of genes monitored may be present, but are not being transcribed to produce the corresponding RDase enzyme. RNA transcripts may provide a better measure of active dechlorination as they are only present when the RDase protein is being produced and decay rapidly relative to DNA when electron acceptors are unavailable.[11,42] There has been limited research into the impact of electron donor availability on the expression of RDase genes. To gain a more complete understanding of *Dhc* dechlorination activity during biostimulation, changes in *vcrA* and *bvcA* messenger RNA (mRNA) abundance during ISB were monitored in an aquifer cell experiment following lactate addition and in an *in situ* pilot test before and after lactate amendment as described in Chapter 5.

Per- and polyfluoroalkyl substances (PFAS) have been shown to negatively impact the ability of *Dhc* to transform chlorinated ethenes to ethene.[43] This class of contaminants of emerging concern can be co-located with chlorinated ethenes in groundwater, especially at Department of Defense fire-training areas; therefore, the impact of PFAS on dechlorinating microbes is of particular concern.[44,45] Studies demonstrating inhibition of microbial dechlorination in the presence of PFAS are limited and do not address the impact of PFAS on specific *Dhc* strains.[43,46] A study to further examine the effect of PFAS on *Dhc* strains

and the dechlorination capacity of a culture containing multiple *Dhc* strains is presented in Chapter 6.

The research presented in this dissertation strives to address the following identified research gaps:

- There is a critical need for systematic, high-resolution, laboratory investigations of biomass and *Dhc* strain distributions in realistic, multi-dimensional, chemically and physically heterogeneous systems as the strain-specific biomass distribution can influence the release of contaminants from low-permeability and highly sorbing materials.
- Although laboratory experiments have correlated longer residence time with increased TCE dechlorination, field-scale studies demonstrating the effect of residence time on the extent of TCE biodegradation are lacking. Because average hydraulic residence time is often used when designing active pumping or recirculation ISB systems, it is essential to link this parameter to the extent of TCE degradation by MRD.
- Studies of RDase expression have focused on the impact of electron acceptor (chlorinated ethene) variability but information on the effect of varying electron donor availability during bioremediation is lacking.
- Although PFAS have been shown to inhibit MRD by *Dhc*, their impacts on specific *Dhc* strains and on the dechlorination performance of cultures containing multiple *Dhc* strains has not been examined. In order to treat chlorinated ethenes in plumes comingled with PFAS, the conditions under which *Dhc* activity is inhibited must be better understood.

This work addresses these knowledge gaps by enhancing the understanding of factors that impact *Dhc* activity and growth in order to assist in the implementation of ISB at

complex sites impacted by chlorinated ethenes. Specifically, the experiments described below were designed to address the following objectives:

- To assess the impact of soil heterogeneity on the relative abundance of *Dhc* strains harboring RDase genes within a multi-dimensional system with realistic groundwater flow conditions and to quantify the extent of bioenhanced back-diffusion from low-permeability porous media within the system (Chapter 3);
- To determine the impact of residence time on the extent of TCE degradation through laboratory- and pilot-scale studies using similar configurations (Chapter 4);
- To examine the expression of RDase genes (via RNA analysis) in response to electron donor delivery during biostimulation in laboratory and field systems (Chapter 5); and
- To determine the impact of PFAS mixtures on PCE and TCE biodegradation by a culture containing multiple strains of *Dhc* and changes in *Dhc*-strain specific population growth in aqueous systems and in systems with porous media.

Overall, the four studies completed and detailed below seek to enhance the understanding of *Dhc* strains and their associated RDase genes, emphasizing those implicated in complete transformation to ethene and the factors that impact their abundance and expression. This information may be used by practitioners of ISB to design efficient remedies and avoid some of the pitfalls that prevent complete dechlorination of chlorinated ethenes to benign ethene.

2.0 Background

Many chemicals, including the chlorinated ethenes tetrachloroethene (PCE) and trichloroethene (TCE), as well as per- and poly-fluorinated substances (PFAS), have been developed and used for many years, then later recognized as hazardous to human health and/or the environment. This research focuses on these two classes of compounds as they are recognized health hazards and are common contaminants in soil and groundwater. Improper use and disposal of these chemicals has led to widespread soil and groundwater contamination, which can bring people into contact with these compounds through contaminated drinking water, wash water, soil, and vapor intrusion. The recognition of adverse health impacts caused by PCE and TCE exposure has led to their regulation, and requirements to remediate these compounds to safe levels when they are detected in soil and groundwater. Similarly, there is growing evidence that PFAS exposure can cause a myriad of known and suspected health effects, leading governments to issue health advisories.

While there are many soil and groundwater remediation technologies, bioremediation has become the most used treatment for groundwater impacted by chlorinated ethenes[1] due to its low cost, ability to treat low concentrations of contamination, and sustainability.[7,22,47–50] Increased understanding of *Dehalococcoides mccartyi* (*Dhc)* strains, specifically strains harboring reductive dehalogenase (RDase) genes implicated in the biotransformation of chlorinated ethenes, has contributed to the acceptance and implementation of *in situ* bioremediation (ISB) as a remedy for chlorinated ethene groundwater contamination.[8,9,12,51] In order to improve the performance of ISB and to reduce contaminant levels to safe concentrations over shorter timeframes, it is essential to continue advancing the understanding of chlorinated ethene bioremediation microbiology, specifically factors that impact the abundance of specific microbial strains and species. Background information

on chlorinated ethene use and disposal, their health impacts, and the current state of chlorinated ethene bioremediation is provided below. A brief background on PFAS, contaminants of emerging concern that may impact ISB is provided. This background includes information on the use and disposal of PFAS at chlorinated ethene contaminated sites and on the lack of *in situ* treatment technologies.

2.1 Use, Manufacture, and Disposal of Chlorinated Ethenes

The chlorinated ethenes TCE and PCE were often used as solvents and are often referred to as chlorinated solvents. TCE was one of the earliest dry-cleaning solvents when the industry developed in the 1930s, although it was replaced by PCE in the 1950s; PCE continues to be used in commercial and industrial dry cleaning with 70-80% of dry cleaners using it at the primary cleaning solvent.[52–55] Chlorinated ethenes are still manufactured and used in large quantities with 324 million pounds of PCE and 172 million pounds of TCE manufactured in or imported to the United States in 2015.[56,57] These chemicals also continue to be released into the environment with a reported 2.2 million pounds of TCE and 0.9 million pounds of PCE being released throughout 2016.[58] The ongoing use and release of these compounds necessitates advanced remediation technologies to efficiently manage and remediate contaminated sites.

After being phased out as a dry-cleaning solvent and natural oil extraction solvent, TCE was, and is currently, used in vapor degreasing and cleaning metal parts, with smaller quantities of TCE used as a component of other chemical products such as adhesives, paint-strippers, paints, and textile spotting fluids.[52,54] In addition to its use in dry cleaning, PCE is used as a chemical intermediate to produce fluorinated compounds including hydrofluorocarbon refrigerants 134a and 124 and as a cleaning solvent. TCE is used in the production of poly(vinyl chloride) (PVC) and hydrochloroflurocarbons.[52–54,59]

In addition to ongoing releases, historic use and improper disposal of chlorinated ethenes has led to soil and groundwater contamination at numerous sites.[7,60,61] PCE and TCE are the volatile organic compounds (VOCs) most frequently detected above maximum contaminant levels (MCLs) and are listed on the Comprehensive Environmental Response, Compensation, and Liability Act (CERCLA) Priority List.[5,6,62] Moran et al. (2007) examined data from groundwater samples collected across the United States (5,068 United States Geological Survey wells) and found detectable levels of PCE in 11% of wells and TCE in 5% of wells at concentrations ranging from 0.02 to 4,800 µg/L PCE and 0.02 to 230 µg/L TCE. Many of the estimated 100,000 sites where contamination prevents unlimited use of and unrestricted exposure to the property are impacted by chlorinated ethenes, as they represent some of the most persistent contaminants worldwide.[7,63] The ubiquity of these compounds makes them the most common contaminant at Superfund sites where they continue to persist in groundwater at 78% of sites and in soil at 49% of sites.[1] At U.S. Department of Defense Sites, TCE and PCE have been reported at concentrations above remedial goals in 69% and 59% of sites, respectively.[7]

2.2 Use, Manufacture, and Disposal of Per- and poly-fluoroalkyl Substances

PFAS encompass a variety of compounds with useful properties, such as low boiling points relative to molecular weight and unique partitioning behaviors with hydrocarbons and water.[64] These properties enabled PFAS to be used in a variety of products including firefighting aqueous film forming foams (AFFFs); surface coating protection on cardboard, carpets, leather, and textiles; nonstick cookware; and breathable, waterproof membranes.[65–67]

Perfluoroalkyl acids (PFAAs) are a subset of PFAS that are generally found in the environment from direct release or from the degradation of precursor substances. PFAAs can be further classified as perfluoroalkyl carboxylic acids (PFCAs) or perfuloroalkyl

sulfonic acids (PFSAs) depending on the functional group at the end of the fluorinated hydrocarbon backbone.[68,69] Of the PFAAs, perfluorooctane sulfonate (PFOS) and perfluorooctanoate (PFOA) are the most frequently detected and widely studied PFSA and PFCA, respectively.[66,70–73]

AFFFs, which represent a major source of PFAS in the environment, are complex mixtures which typically contained significant quantities of PFAA precursor molecules (e.g. fluorotelomer alcohols [FTOHs] and fluorotelomer thioether amido sulfonates [FtTAoS]), PFAAs (e.g. PFOS and perfluorohexanol sulfonate [PFHxS]), and other PFAS.[67,74–77] Approximately 200 different fluorinated organic chemicals, divided into 40 classes, have been detected at AFFF impacted sites, including the shortest-chain PFAAs: perfluoroethanesulfonate (PFEtS) and perfluoropropanesulfonate (PFPrS).[74,75,78] As of 2004, an estimated 9.9 million gallons of AFFF concentrate containing PFAS was in storage and available for use in the U.S. by the U.S. military, civilian airports, fire departments, oil refineries, and other users, indicating potential sources of PFAS to the environment and an ongoing disposal liability.[79] The wide variety of PFAS contained in AFFF includes anionic (25%), zwitterionic (55%), and cationic (13%) compounds.[74]

Where AFFF containing PFAS has been used or released, PFAS have been detected at high concentrations in soil and groundwater. Moody and Field (1999) reported plumes of PFAS contaminated groundwater, associated with fire-training sites at US military bases where AFFFs were used (e.g. NAS Fallon, NV, Tyndall Air Force Base, FL, and Wurtsmith Air Force Base, MI), with concentrations up to 7.09 mg/L. In Sweden, PFOS concentrations of up to 2.9 mg/L were measured in groundwater collected from a fire training area.[81]

Releases of PFAS associated with AFFF typically occur at the ground's surface and, while compounds often accumulate in the aquifer's capillary fringe, some conditions may cause PFAS to migrate deeper into groundwater, though these processes are not well

understood.[67] Cationic and zwitterionic PFAS adsorb to soil particles and are likely to remain in source zones near the site of release. They have been shown to have non-linear Freundlich or Langmuir sorption isotherms with sorption dependent on organic carbon content and electrostatic interactions with iron-containing minerals.[67,82–84] The overall ecological toxicity of PFAS likely depends on the specific mixture of compounds that an organism is exposed to; a study of PFOS found higher toxicity in wild tree swallows exposed to a suite of PFAS compounds when compared to laboratory-raised birds that were only exposed to PFOS.[85]

In many aquifers, both chlorinated ethenes and PFAS are found together as co-contaminants. Many fire-training areas used AFFFs to extinguish fires fed by off-specification fuels and waste solvents, some of which were comingled with chlorinated ethenes, resulting in the co-release of PCE, TCE, and PFAS to soil and groundwater.[44,45]

2.3 Health Risks

The presence of chlorinated ethenes and PFAS in the environment is of concern due to their negative effects on human health, causing them to be regulated and/or monitored contaminants. The adverse health effects of PCE and TCE have been documented for many years, as far back as at least 1945, and disposal has been regulated by the United States Environmental Protection Agency (USEPA) since the 1976 Resource Conservation and Recovery Act (RCRA).[86] The health effects of PFAS are still being assessed but recent studies showing adverse effects have led to USEPA provisional health advisories for PFOA and PFOS.[87]

2.3.1 Health effects of chlorinated ethenes

Acute inhalation of chlorinated ethenes can cause death as seen in accidental worker exposures and animal studies.[88–96] In non-fatal doses, inhalation of chlorinated ethenes has acute effects on the central nervous system similar to the effects of drunkenness including

loss of body control, dizziness, drowsiness and fatigue, loss of consciousness, headache, euphoria, loss of vision and hearing, nausea, and memory loss.[97–106] Chronic exposure to chlorinated ethenes, specifically TCE, is linked to neurological effects, including Parkinson's disease, memory loss, mood swings, nerve damage, impaired motor function, decreased intelligence test scores, increases in mood disorders, and psychotic behavior with impaired cognitive function.[97,107–115] Additional health effect from chronic exposure include cardiovascular damage such as Raynaud's phenomenon, asthma, and ischemic heart disease,[98,116–119] and liver damage, including cirrhosis, lesions, and increased liver weight.[120–130] Inhalation of solvent vapors can be a concern during environmental remediation through the intrusion of vapors from groundwater, through the vadose zone, and into buildings.[131,132]

There is substantial evidence that TCE and vinyl chloride (VC) are carcinogenic to humans, leading the International Agency for Research on Cancer (IARC) to classify them as Group 1, carcinogenic to humans.[133,134] There is less evidence linking PCE to cancer; it is classified by IARC as Group 2A, possible carcinogenic to humans.[135] Specifically, TCE has been linked to kidney cancer[136–140] and VC with liver cancers.[141–151] Chlorinated ethenes are also linked to non-Hodgkin's lymphoma, leukemia, liver cancer, bladder and urinary cancer, multiple myeloma, lunch cancer, lymphatic/hematopoietic cancers, and gallbladder cancer.[117,136,147,151–168]

Due to these health effects, the Occupational Safety and Health Administration (OSHA) regulates PCE and TCE vapors with a permissible exposure level (PEL) of 25 ppm.[169] VC, a compound produced during the biodegradation of PCE and TCE, is more harmful to health than the parent compounds as reflected in its lower OSHA PEL of 1 ppm.[169] PCE, TCE, and VC are also regulated as drinking water contaminants with a USEPA maximum contaminant level (MCL) of 5 µg/L for PCE and TCE and 2 µg/L for VC.[170] USEPA has

also issued a maximum contaminant level goal (MCLG) of 0 µg/L for all three compounds.[170]

2.3.2 Health effects of per- and poly-fluoroalkyl substances

The health effects of PFAS compounds are not as well understood as those of chlorinated ethenes, but recent research has shown negative effects of these chemicals. There are no reported cases of death due to acute PFAS exposure but an oral LD_{50} value of 540 mg/kg has been reported for rats fed PFOA.[171,172] PFOA and other PFAS have been linked to kidney disease,[173] diabetes,[173,174] and liver toxicity.[175] Chronic exposure to PFAS, including PFOA, PFOS, perflurodecanoate (PFDA), and perfluorododecanoate (PFDoA), has been linked to liver damage, asthma, changes in cholesterol levels, and cardiovascular damage such as high blood pressure, peripheral arterial disease, stroke, and myocardial infarction.[173,176–192] Studies of communities exposed to PFAS in drinking water have identified correlations between exposure and instances of ulcerative colitis, impaired vaccine antibody responses, damage to reprodutive health, and delayed neurological development.[193–201] Similar immunolgical and reproductive effects have been reported in animal studies.[172,186,192,202–209]

There is limited information on the carcinogenicity of PFAS compounds. Only PFOA has been evaluated by IARC who classify it as Group 2B, possibly carcinogenic to humans.[210] PFOA has been linked to kidney, bladder, and testicular cancers as well as mesothelioma.[173,188,211–215] Low level exposure, associated with contaminated drinking water, has not been correlated to elevated risk of cancer.[210,214]

In 2009, due to the growing understanding that ingestion of PFAS poses a risk to human health, the USEPA issued provisional health advisories for PFOA and PFOS in drinking water at concentrations of 0.4 µg/L and 0.2 µg/L, respectively.[87] While not enforceable as MCLs, if the provisional health advisory concentrations are exceeded, water suppliers

should take action to reduce exposure to these compounds.[216] In addition to PFOS and PFOA, four other PFAS: perfluorobutanol sulfonate (PFBS), PFHxS, perfluoroheptanoic acid (PFHpA), and perfluorononanoic acid (PFNA), have been added to the USEPA's list of unregulated contaminants to be monitored in public water systems.[217]

2.4 Remediation of Chlorinated Ethenes

Chlorinated solvents are colorless, volatile liquids with a distinctive sweet smell, and have unique properties that complicate remediation.[5,218,219] The chlorinated solvents examined in this work are chlorinated ethenes, consisting of two carbon atoms double-bonded and one to four chlorine atoms. The highly chlorinated compounds, PCE (four chlorine atoms) and TCE (three chlorine atoms), are relatively insoluble in water with average reported aqueous solubilities of 1.7 and 11 mol/m^3 (282 and 1,445 mg/L), respectively, and are the least volatile of the chlorinated ethenes with a vapor pressures of 2,600 and 9,700 Pa.[220–222] By removing chlorine atoms, PCE can be transformed to TCE, TCE to *cis*- or *trans*-1,2-dichloroethene (DCE), DCEs to VC, and VC to non-chlorinated, non-toxic ethene. As chlorine atoms are removed, the compounds become more soluble in water and more volatile.[218,223–225] Each compound is more dense than water and can form a dense non-aqueous phase (DNAPL) when concentrations exceed the aqueous solubility.[222,225,226] PCE and TCE readily adsorb to soil particles, primarily to those with organic carbon compounds, but also to clay cations, as measured by an adsorption coefficient (K_d).[227–232] In order to be removed, these compounds must be desorbed from soil and present as free solutes in the aqueous phase.[233]

The earliest methods of remediating chlorinated ethene releases relied on physical processes, including soil excavation to treat source areas and in-place containment (barriers) and groundwater extraction with physical treatment (pump and treat) to treat dissolved plumes. Soil venting or thermal treatment were used to remove vapor phase

contaminants in both source areas and plumes.[222,234–238] Physical removal of contaminants, especially via pump and treat systems, is costly, requires disposal of extracted contaminants in another location, and is complicated by aquifer heterogeneity, DNAPL source architecture, sorption to soil particles, and entrapment of contaminants between soil grains.[223,234,236,239–241] These complications have led to a proliferation of *in situ* degradation technologies, including chemical oxidation and bioremediation, where contaminants are transformed to non-toxic compounds without removing them from the subsurface.[234,241,242]

Some form of *in situ* treatment technology, including bioremediation, chemical treatment, permeable reactive barriers, air sparging, or thermal treatment, is currently used as a groundwater treatment remedy at 69% of Superfund sites with active remediation.[1] The most popular *in situ* groundwater treatment technologies involve degradation of the compound in the subsurface. *In situ* chemical remediation and ISB were selected as the *in situ* treatment in 46% and 57% of Superfund groundwater remedies between 2012 and 2014, respectively.[1] ISB uses microorganisms to transform chlorinated ethenes in groundwater to non-toxic ethene. As a treatment technology, ISB involves modifying environmental conditions to encourage growth of a microbial community conducive to biodegradation. This is accomplished through biostimulation (the addition of nutrients and substrates), bioaugmentation (the addition of specific microbial species), or a combination of both.[234,242–246]

In situ chemical remediation provides rapid transformation of chlorinated ethenes, but is the *in situ* technology most prone to rebound of contaminant when active remediation ends.[2,247,248] Rebound is generally caused by diffusion of contaminants from DNAPL and low-permeability materials where chemical reagents did not achieve contact with the contaminant, or from reactions between the reagent and naturally occurring minerals that deplete the injected reagent; rebound is exacerbated by the short residence time of many

chemical amendments in the treated zone.[247,249,250] In contrast, during ISB, conditions conducive to contaminant degradation can be maintained after biostimulation ends, reducing the potential for contaminants to rebound to concentrations above MCLs.[244,251–253] After 70 months of sucrose injections for bioremediaiton of PCE, Suthersan et al. (2013) observed elevated total organic carbon for at least 30 months after injections, with continued transformation of PCE to ethene, which the authors attributed to the decay of biomass providing an ongoing source of electron donor. In the traditional view of chlorinated ethene remediation, physical-chemical remediation techniques were preferred for source zones where DNAPL and high concentrations were expected, while ISB was a remedy only for dissolved plumes; however, more recently, ISB has been explored and utilized as a remedy for source zones as well as dissolved plumes.[32,35,254–257]

While ISB is a popular remedy and is successful at many sites, it has limitations and challenges that make it an ongoing area of research. Incomplete transformation of PCE and TCE to ethene, and the associated increase in DCE and VC concentrations, is of significant concern when implementing ISB.[18,19,239,258,259] Delivery of remediation amendments in heterogeneous soils complicates both chemical remediation and ISB and can result in untreated regions of aquifers and back diffusion from these locations.[22,243] Advancing the understanding of the microbial communities involved in ISB is essential to overcoming its limits and increasing its effectiveness as a treatment technology.

2.4.1 Biological processes regulating chlorinated ethene bioremediation

The microbial processes that transform chlorinated ethenes include organohalide respiration, co-metabolism, and aerobic oxidation.[9,218,239] During anaerobic reductive dechlorination, a form of organohalide respiration, chlorinated ethenes are used as an electron acceptor in an energy-producing metabolic reaction.[39,239,260] Co-metabolism can occur during both aerobic or anaerobic processes when microbes using other metabolic

pathways also degrade chlorinated ethenes without yielding a direct benefit to the organism.[261–265] Some microorganisms, including *Polaromonas vaculata, Mycobacterium* strains, and *Nocardioides* strain JS614, can utilize less chlorinated compounds (e.g., VC) as an electron donor in an aerobic oxidation reaction when oxygen is present as an electron acceptor.[266–274]

The reductive dechlorination of PCE and TCE under anoxic conditions, the most critical pathway for ISB, is a sequential process, producing hydrochloric acid and chlorinated intermediaries, with transformation of PCE to TCE to *cis*-1,2-DCE to VC to ethene being the most commonly observed pathway.[258,260,275,276] The reductive dechlorination reaction is thermodynamically favorable and allows microorganisms to obtain energy and grow using this metabolic pathway.[277,278] While thermodynamically favorable, anaerobic reductive dechlorination yields less energy than other forms of microbial respiration making it unlikely to occur if alternate electron acceptors (oxygen and nitrate) are present, as indicated by an oxidation-reduction potential (ORP) greater than -200 mv.[242,279–281] There is also evidence of dihaloelimination in which 1,2-dichloroethane was transformed to ethene without forming VC as an intermediary product but this has not been observed in the degradation of *cis*-1,2-DCE.[282]

Not all species capable of anaerobic reductive dechlorination are able to perform each step in the sequential transformation of PCE to ethene. Several species can transform PCE and TCE to *cis*-DCE, including *Dehalospirillum multivorans*, *Enterobacter agglomerans, Desulfitobacterium* sp. strain PCE1, *Dehalobacter restrictus, Desulurmona chloroethnica,* and *Geobacter lovleyi* strain SZ (*Geo*SZ).[283–289] *Dehalococcoides* species (*Dhc*), specifically strains of *Dehalococcoides mccartyi* (previously known as *Dehalococcoides ethanogeneses)*, are the most widely-studied and utilized microorganisms capable of transforming PCE and TCE to ethene.[8,19,290–292] *Dhc* is a gram-neutral, disc-shaped, coccoid

cell bacterium in the phylum *Chloroflexi* that cannot use oxygen, nitrate, or sulfate as electron acceptors, making them obligate anaerobes.[292]

Multiple strains of *Dhc*, with differing capacities for reductive dechlorination, have been identified and are typically differentiated by the RDase genes they contain.[12] Strains 195 and FL2 have been shown to rapidly transform PCE and/or TCE to VC, but not to ethene; strain 195 slowly transforms VC to ethene, likely in a co-metabolic process.[51,276,292] *Dhc* strains BAV1, VS, KB-1/VC, and GT are able to transform VC to ethene in a metabolic dechlorination reaction resulting in more rapid transformation than co-metabolic reactions.[13,14,293,294] Strains FL2 and GT can also metabolically transform TCE to *cis*-DCE, but cannot degrade PCE, while strain BAV1 can co-metabolically transform PCE and TCE to DCE.[14,51,293,295] A *Dhc* strain that converts PCE to *trans*-DCE has also been identified as strain MB.[296]

The identity of *Dhc* strains and their capability to perform reductive dechlorination is determined by the RDase enzymes they produce to catalyze the dechlorination of chlorinated ethenes and the associated RDase genes that encode for the enzymes.[10,37] RDase genes that have been characterized include *pceA* and *tceA* in *Dhc* strain 195, *vcrA* in *Dhc* strains VS, WBC-2, 11G, and GT, *bvcA* in *Dhc* strain BAV1, and *pteA* in *Dhc* strain 11a5.[51,293,297–303] PCE reductase (*pceA* and *pteA* genes) catalyzes the transformation of PCE to TCE, TCE reductase (*tceA* gene) catalyzes the transformation of TCE to VC, Vinyl chloride reductase (*vcrA* gene) catalyzes the transformation of *cis*-DCE, *trans*-DCE, and VC to ethene, and Vinyl chloride reductase b (*bvcA* gene) catalyzes the transformation of *cis*-DCE and VC to ethene.[10,290,301] Additional metabolic genes are found in strains of *Dhc* that are capable of organohalide respiration using compounds other than chlorinated ethenes including triclorobenzene and 1,2-dichloropropane.[304–307] Recent evidence has

emerged that the *vcrA* gene may be contained on extrachromosomal circular elements which may increase the transfer of RDase genes between strains of *Dhc*.[308]

Monitoring total *Dhc* 16S rRNA and RDase gene abundance is useful to predict remediation performance and assess the need for bioaugmentation.[40,41,309] Quantitative polymerase chain reaction (qPCR) and loop-mediated isothermal amplification (LAMP) can be used to target specific nucleotide sequences, allowing the quantification of total *Dhc* and other microorganisms through the 16S rRNA gene and the identification and quantification of *Dhc* strains through the RDase genes.[37,310] If the strains and associated RDase genes implicated in transformation to ethene (*vcrA* and *bvcA*) are not present, or are present in low numbers, complete transformation to ethene is unlikely and additional organisms must be added to the subsurface through bioaugmentation.[19,20,244,311] A survey of samples collected at sites undergoing active bioremediation or monitored natural attenuation identified a correlation between higher ethene concentrations and total *Dhc* 16S rRNA and VC RDase (*bvcA and vcrA)* gene abundances greater than 10^7 and 10^6 copies/L, respectively, especially when the ratio of total *Dhc* to VC RDases was near one.[38] Conversely, incomplete dechlorination occurs (PCE, TCE, and DCE predominate) when VC RDase genes are absent or present at less than 10^5 copies/L, even if total *Dhc* 16S rRNA abundance is greater than 10^7 copies/L.[38]

Dhc have specific environmental and nutritional requirements including hydrogen as an electron donor, acetate as a carbon source, and vitamin B_{12} (cyanocobalamin) as a cofactor to produce RDase enzymes.[27,291,292,312,313] For bioremediation, *Dhc* are typically grown in a mixed culture where fermenting bacteria (including *Desulfovibrio, Eubacterium, Clostridium, Acetobacterium*, *Citrobacter*, and *Spirochetes)* transform fermentable substrates (lactate or other biostimulation additives) to acetate and produce hydrogen. Other community members, including species from the *Geobacter, Clostridium,*

Pelosiinus, Dendrosorobacter, Sporotalea, Desulfovibrio, Acetobacterium, and *Methanosarcina* genera produce the necessary corrinoids, including B_{12}.[42,314–324]

2.4.2 Bioremediation studies

ISB pilot studies began in the early 1990s trying to stimulate aerobic co-metabolic degradation by injecting methane and oxygen into the subsurface and successfully demonstrated biostimulation to transform VC to ethene.[325] Harkness et al. (1999) demonstrated successful bioaugmentation in a laboratory setting where columns bioaugmented with the Pinellas culture, isolated from the Department of Energy's Pinellas site (Largo, FL), were able to transform TCE to ethene. This culture was then used at the Dover Air Force Base (Dover, DE) and was shown to complete the transformation to ethene *in situ* when provided with lactate as an electron donor and carbon source.[244] Investigation and implementation of ISB continued with additional successful demonstrations, primarily in aquifers consisting of coarse and fine grained porous media.[2,19,327–329] Although ISB has been established as a practical remedy for chlorinated ethene remediation, contaminant rebound and incomplete dechlorination to DCE and VC are often observed. In order to address these issues, research into implementing ISB in heterogeneous porous media, low-permeability aquifers, and contaminated fractured bedrock is ongoing.[330–333]

In both field and laboratory studies, ISB has been shown to work successfully in chlorinated ethene source zones where high concentrations and DNAPL may be present.[32,35,251,254,334,335] ISB can successfully remediate source zones by incorporating bio-enhanced dissolution, in which the breakdown of highly chlorinated ethenes near a concentrated source lowers the aqueous concentration, thus increasing the driving force necessary to dissolve residual DNAPL, and transforms parent compounds to less chlorinated ethenes with higher solubilities.[32,33,257,311,336–338] Similarly, biological activity in higher permeability zones, where bioremediation amendments are easily distributed, may

facilitate the back diffusion of compounds from low-permeability materials into higher flow regions. MRD decreases the total mass of the contaminant in solution, thus increasing the driving force and causing mass transfer from low-permeability regions to high flow regions, even if biomass growth does not occur in the low-permeability matrix.[331,339,340] There is also evidence of biofilm formation by dechlorinating microorganisms, which may act as a sink for contaminants migrating from low-permeability areas and decrease the overall mass flux from residual contamination trapped in low-permeability regions.[341–343] *Dhc* strains will play an important role in attenuating releases from low-permeability media, affecting contaminant rebound rates and long-term plume management. Thus, understanding the distribution of *Dhc* strains in heterogeneous porous media, and the factors that affect these distributions, is essential to designing effective remedies for chlorinated ethene contamination in real-world systems.

The availability of electron acceptors has been shown to determine the abundance of *Dhc* strains harboring specific RDase genes.[28,344–346] Liang et al. (2015) prepared culture bottles with KB-1®, a commercially-available dechlorinating consortium (SiREM; Guelph, ON), maintained on TCE and methanol, as a parent culture. Each culture was then enriched with TCE, *cis*-DCE, or VC as electron acceptors, and the *vcrA* and *tceA* genes were most abundant in cultures provided with TCE, while *bvcA* was most abundant in cultures where *cis*-DCE was the available electron acceptor.[28] In cultures where VC was the only electron acceptor, only the *vcrA* gene was present while, in cultures provided with *cis*-DCE, cells harboring *bvcA* was favored.[28,346] Johnson et al. (2005) found that transcription of the *tceA* gene increased with the duration of TCE or DCE exposure, but did not increase if PCE or VC was the only available electron acceptor. The total abundance of the *tceA* gene increased when TCE was provided as an electron acceptor.[347] At two TCE-contaminated field sites bioaugmented with KB-1®, the relative abundance of RDase genes shifted as

dechlorination progressed, with *bvcA* most abundant while *cis*-DCE was the predominant contaminant and the relative abundance of *vcrA* increasing as *cis*-DCE was transformed to VC.[346] Variation in RDase gene abundance with electron acceptor availability has also been shown in column studies in which all RDase genes were present at the inlet, where PCE was introduced, but the only the *vcrA* and *bvcA* genes were present in downgradient locations where only *cis*-DCE and VC were detected.[27,344]

The presence of high aqueous concentrations of chlorinated ethenes, associated with the presence of DNAPL, affects the abundance of dechlorinating microorganisms and RDase genes, similar to the availability of electron acceptors.[35,255,257] In a mixed culture, *GeoSZ* was three orders of magnitude more abundant than *Dhc* in a DNAPL source zone, but, downgradient of the DNAPL source, total *Dhc* abundance was within 1 order of magnitude of *GeoSZ* abundance.[257] Cápiro et al. (2015), examining the distribution of *GeoSZ*, *Dhc*, and RDase genes around PCE DNAPL pools and ganglia in a two-dimensional aquifer cell, also found that planktonic *GeoSZ* was more abundant than planktonic *Dhc* in the source zone area. Late in the experiment, when PCE and TCE were depleted from the source zone and residence time was increased using flow interruptions, the relative abundance of planktonic *Dhc* increased relative to the *GeoSZ* abundance.[35] In regions of pooled PCE DNAPL, cells harboring the *vcrA* gene were most abundant with the *tceA* and *bvcA* genes making up 23% and 2% of the total planktonic RDase genes, respectively. In more sparse DNAPL ganglia regions, cells harboring the *vcrA* gene were still most abundant, but the *tceA* gene made up a smaller proportion (10%) of the planktonic RDase genes.[35]

The availability and type of electron donor also affects the composition of the dechlorinating community. A recent study has shown variability in the strains of *Dhc* (as identified by sequencing the *Dhc* 16S rRNA gene) when columns, inoculated with the *Dhc*-containing Bachman Road culture, were provided with different types of electron donors,

but did not report changes to specific RDase genes.[348] In columns continuously provided with whey electron donor, *Dhc* strains associated with the Cornell group (strain 195) predominated, while strains from the Pinellas group (strain FL2) predominated in columns with infrequent amendments of vegetable oil.[293,348] Electron donor limitations also affect the strains of *Dhc* and associated RDase genes in mixed cultures. In a culture containing strains of *Dhc* harboring both the *vcrA* and *tceA* genes (derived from aquifer material at sites in Corvallis, OR and Victoria, TX), long-term electron donor limitation caused cells with *tceA* to outcompete cells with *vcrA,* preventing transformation of DCE to VC and ethene.[349] After a long-term (2,000-day) period of electron donor limitation, the cells harboring *vcrA* were still present at low concentration and were able to recover after additional electron donor was provided, allowing the culture to once again complete the transformation of TCE to ethene.[349]

Geochemical parameters, including oxygen concentration, nitrogen availability, temperature, and pH, have also been shown to impact the abundance of RDase genes and tend to most inhibit cells harboring the *vcrA* gene, one of the genes necessary for metabolic transformation of VC to ethene.[25,26,29,350–352] In an oxygen exposure study, a mixed strain *Dhc* culture, Bio-dechlor Inoculum (BDI), retained the ability to rapidly transform TCE to VC after 30-days of oxygen exposure but the transformation rate of VC to ethene was reduced, likely due to the preferential survival of strain FL2, capable of slower, co-metabolic transformation of VC to ethene.[25] Using the KB-1® enrichment culture, Heavner et al. (2018) found that the *Dhc* strain harboring *bvcA* recovered after exposure to oxygen while cells harboring *vcrA* did not. The availability of nitrogen (as NH_4) was shown to increase dechlorination rates and encourage the growth of Pinellas-type *Dhc* at the expense of Cornell-type *Dhc.*[352]

When exposed to elevated temperatures, increasing from 15°C to 35°C (similar to temperatures on the perimeter of a traditional thermal treatment site or in a low temperature thermal treatment), *Dhc* strains harboring the *bvcA* gene increased in abundance preferentially when compared to cells harboring the *vcrA* gene.[29] Fletcher et al. (2011), using OW Consortium, a culture with only *tceA* and *vcrA*, found that incubation above 40°C for 49 days, followed by cooling to 24°C, caused the culture to lose the ability to transform VC to ethene, indicating that higher temperatures negatively impacted *Dhc* cells harboring the *vcrA* gene.

Low pH has been shown to have a detrimental effect on *Dhc* growth and dechlorination ability, which is of significant concern because hydrochloric acid is produced during reductive dechlorination, thus lowering the pH of the groundwater.[254,353,354] *Dhc* strains harboring the *vcrA* gene were more susceptible to low pH (5.5) stress than cells harboring the *tceA* gene. When pH was restored to neutral (7.2) after 40-days of low pH exposure, the surviving *Dhc* population was unable to complete the transformation of PCE to ethene and stalled at VC, adding further evidence that cells harboring the *tceA* gene were more resilient in non-ideal conditions.[26]

Co-contaminants can impact microbial reductive dechlorination and affect specific strains of *Dhc.* Chloroform has been shown to inhibit chlorinated ethene biodegradation by KB-1® microbes[355] and 1,1,2-Trichloro-1,2,2,-trifluoroethane (CFC-113) inhibited transformation of *cis*-1,2,-DCE by the *Dhc*-containing consortium SDC-9.[356] The presence of co-contaminants 1,1,1-trichloroethane (1,1,1-TCA) and triclocarban (TCC) have also been shown to reduce dechlorination rates by *Dhc*-containing cultures.[357,358] In addition to reducing dechlorination rates, co-contaminants such as 1,2-Dichloroethane can alter the population structure of dechlorinating consortia, favoring *Dhc* cells harboring the *tceA* gene at the expense of cells harboring the *vcrA* gene.[30]

There is limited information available on the specific effect of heterogeneous porous media on the distribution of *Dhc* and RDase genes at the interface between soils of differing hydraulic conductivity. Cápiro et al. (2014) examined the effect of different porous media on the attachment of *Dhc* and *Geo*SZ cells in column experiments during active dechlorination, and found that fewer cells were associated with the aqueous phase in Appling soil, with a lower hydraulic conductivity and higher organic carbon content, than in Federal Fine Ottawa sand, but did not measure RDase genes. When deprived of electron donor, *Dhc* cells rapidly detached from soil and were found to be associated with the aqueous phase.[359]

The effect of soil heterogeneity on the distribution of DNAPL into pools and ganglia has been examined, along with the distribution of RDase genes and *Dhc* cells in these source zone regions, but there are no studies of the spatial and temporal dynamics relative to soil heterogeneity in dissolved plumes. Field studies have shown that *Dhc* cells are able to penetrate low-permeability media, including clays, but delivering the necessary amendments to low-permeability regions is still a challenge, especially in heterogeneous aquifers.[22,331,332] There is also evidence that *Dhc* cells can grow and dechlorinate in biofilms, the formation of which may be affected by soil properties and gradients in nutrient availability which then, in turn, affect the transport of compounds in and out biofilm containing regions and complicate amendment delivery.[341–343,360]

In larger, field-scale studies, researchers have identified variations in dechlorinating populations across large scales, but have not examined the effect of small-scale heterogeneity. In a study examining multiple sites, the total *Dhc* population was correlated with dissolved organic carbon concentration, likely acting as an electron donor.[361] The abundance of cells harboring the *vcrA* gene correlated with VC concentrations, while the abundance of cells harboring *bvcA* and *tceA* genes made up a larger portion of the *Dhc*

population in less reduced aquifers, likely due to the impact of oxidative stress on cells harboring *vcrA*.[25,361] In a study of sediments across multiple sites, the distribution of RDase genes was dependent on depth, but did not correlate with the concentration of VC.[362]

Due to the importance of bioenhanced dissolution and diffusion in limiting contaminant rebound during and after ISB, it is important to understand the dynamics of microbial populations in relation to low-permeability and high organic carbon soils in a heterogeneous aquifer. These regions are likely to have higher contaminant concentrations in mature plumes and are likely to receive fewer nutrients and amendments using traditional ISB injection techniques. To advance the understanding of these phenomenon, an aquifer cell experiment with heterogeneous porous media was used to quantify the effect of soil heterogeneity and electron acceptor availability on the distribution of *Dhc* 16S rRNA and RDase genes (Chapter 3).

The hydraulic residence time of contaminants and remediation amendments in a treatment zone is a key ISB design parameter and can be controlled by well positioning and, if active pumping is used for recirculation or hydraulic containment, by extraction rates.[36,363,364] Increasing average residence time can increase chlorinated ethene degradation in air sparging systems,[365] permeable adsorptive barriers,[366,367] permeable reactive barriers,[368] and during *in situ* chemical oxidation.[369] In laboratory experiments, longer residence time is correlated with increased dechlorination of TCE.[370–372] Aquifer heterogeneity complicates the design of ISB as average residence time differs from local residence times when permeability is non-uniform. Despite laboratory studies demonstrating the impact of residence-time on dechlorination, field-scale studies and studies incorporating heterogeneity are lacking. Demonstrating that insufficient hydraulic residence time in a bioactive treatment zone causes incomplete dechlorination during bioremediation will improve the implementation of bioremediation as a remedy for groundwater contaminated

with TCE. An *in situ* pilot test and corresponding laboratory aquifer cell study were used to demonstrate the impact of residence time and heterogeneity on the extent of TCE biodegradation (Chapter 4).

Quantifying RDase gene abundance through DNA provides information on the *Dhc* strains that are present and their capability to perform reductive dechlorination, as described above, but it does not measure which cells are actively performing MRD. RNA transcripts may provide a better measure of the potential for dechlorination activity as they are only present when the RDase enzyme is being produced and decay rapidly relative to DNA when electron acceptors are depleted.[42] By examining RNA, Lee et al. (2006) demonstrated the effect of electron acceptor availability as, in a pure culture of *Dhc* strain 195, the *tceA* gene was expressed when TCE and *cis*-DCE were present, but was depleted to a stable concentration after about 2 days without those electron acceptors. Subsequently, the *vcrA* gene was expressed as long as a chlorinated ethene was present, but it also degraded to a low level after VC was transformed to ethene.[42]

In a mixed culture collected from Zenne River (Belgium) sediment, Doğan-Subaşi et al. (2014) also identified an increase in *tceA* and *vcrA* gene transcripts when chlorinated ethenes were present. The *tceA* gene was upregulated while TCE was present, but the abundance of gene transcripts decreased after TCE was dechlorinated. The *vcrA* gene transcript increased in abundance as *cis*-DCE was formed but, in contrast to Lee et al. (2006), remained elevated after the VC concentration was reduced to undetectable levels.[11] In samples collected from a TCE-impacted aquifer in Fort Lewis, WA, the *vcrA and bvcA* genes were found to be highly expressed by the *Dhc* cells while *tceA* transcripts were detected infrequently and with lower abundance, despite the presence of TCE in the groundwater.[373]

While electron acceptor availability correlates to RDase gene abundance and expression in laboratory batch experiments, the low expression of the *tceA* gene at the Fort Lewis site may indicate that there are other factors impacting the expression of RDase genes in more complex systems. Studies examining the impact of varying electron donor availability on RDase gene expression are lacking but would be useful to determine dechlorination capability during the common practice of pulsed electron donor delivery. To address this need, samples were collected from an *in situ* pilot test and aquifer cell experiment where lactate was supplied intermittently. These samples were analyzed for RDase RNA transcript abundance to determine which RDase genes were expressed during MRD (Chapter 5).

2.5 Remediation of Per- and Poly-fluoroalkyl Substances

PFAS are considered persistent in the environment with no known natural pathways of photolysis, hydrolysis, or biodegradation to a benign end point.[374] Several PFAS compounds are known to adsorb to soil and the extent and rate of adsorption is affected by co-contaminants, including NAPLs, and by the presence of other surfactants.[374,375] Currently, pump and treat remediation systems are used to contain PFAS plumes, but are unlikely to fully remediate aquifers do to the sorption and low solubility of the compounds.[376,377] A variety of technologies are available to remove (activated carbon, ion exchange, nanofiltration, or reverse osmosis)[67,73,378–387] or destroy (photo-, sono-, or thermo-chemical processes)[377,388–402] PFAS compounds in process water from pump and treat systems, wastewater treatment plants, and drinking water purification facilities. Traditional water treatment technologies, deployed to treat wastewater, drinking water, or extracted groundwater for remediation (e.g. coagulation, flocculation, sedimentation, and filtration), are not typically effective in removing PFAS from water due to the low concentrations and high hydrophobicity of these contaminants.[69,380–382,398,403]

In situ treatments for PFAS contaminated groundwater have not been implemented on a commercial-scale. There is some evidence that permanganate and persulfate may degrade PFOS and/or PFOA, but require specific temperature and pH controls that may not be practical on a large scale.[404,405] During *in situ* activated persulfate treatment of a mixed plume of chlorinated solvents and PFAAs, the presence of PFAAs did not reduce the effectiveness of treatment for chlorinated ethenes and PFAA concentrations declined after treatment, possibly due to destruction of PFAA compounds by persulfate.[406]

2.5.1 Biodegradation of PFAS

PFAS were typically manufactured and used as large fluorotelomers (e.g. fluorotelomer alcohols [FTOH], n-ethyl sulfonamide ethanol [EtFOSE], or polyfluoroalkyl phosphates [PAPs]), which have been shown to degrade to PFAAs, also known as terminal PFAS.[407–411] Aerobic biodegradation of FTOH yields unsaturated fluorotelomer acids and PFCAs, primarily PFOA, undecafluorohexanoic acid (PFHxA), and perfluoropentanoic acid (PFPeA).[409,412] Microorganisms in aerobic wastewater treatment plant sludge were used to degrade 6:2 fluorotelomer sulfonamide alkylamine and 6:2 fluorotelomer sulfonamide alkylbetaine, common AFFF fluorotelomers, to form shorter-chain PFCAs, including PFHxA and PFPeA, plus FTOH and 6:2 fluorotelomer sulfonamide (FTSAm), indicating that the sulfonamide group of the parent compound was not transformed during biodegradation.[413] In anaerobic activated wastewater sludge, C^{14} labeled 8:2 FTOH degraded to shorter chain FTOHs and PFCAs (PFOA, PFNA, PFHxA) with some evidence of defluorination identified by C^{14} labeled carbon dioxide and an increase in free fluorine ions.[414] Similar results were observed when a microbial community from aerobic soils were exposed to 8:2 FTOH or 6:2 FTOH, but PFOA and PFHxA produced by the microbes did not degrade further.[414–416] Anaerobic wastewater sludge-derived microbes have not been shown to degrade 6:2 fluorotelomer sulfonic acid (FTSA) or PFAAs, such as PFOS and PFBS, even at incubations of 32 weeks to 3.4 years.[417]

Bacteria derived from marine sediments were able to degrade EtFOSE to PFOS, PFOA, and other fluorinated sulfonamides but a higher molecular weight EtFOSE-based phosphate diester (SAMPAP) was recalcitrant to biodegradation.[418] Similarly, 8:2 fluorotelomer stearate monoester was transformed to 8:2 FTOH and stearic acid, then FTOH was degraded to PFCAs, primarily PFOA.[419] Aerobic microcosm studies using soil microbial communities and Ansul AFFF showed that FtTAoS degrades to fluorotelomer sulfonates and PFCAs with additional unidentified intermediate products, but did not monitor fluoride ion concentration to detect defluorination of the PFAS.[420] The white-rot fungus, *Phanerochaete chrysosporium* was also shown to degrade 6:2 FTOH, primarily to polyfluoroalkylcarboxylic acids with the formation of fewer PFCAs, 5.9% by molar mass.[421]

Although there is evidence that perfluoroalkyl compounds can be biotransformed, the degradation may be limited to non-fluorinated portions of the molecule, resulting in PFOS, PFOA, or other unidentified end products.[44,67,73,422] A community of denitrifying, iron reducing, and sulfate reducing bacteria was able to transform PFOA and PFOS to shorter chain PFAAs (heptafluorobutrycic acid [PFBA], PFPeA, PFHxA, PFBS, and other unidentified compounds) with a measurable increase in free fluorine.[423] Microbial cleavage of the C-F bond by microbes in KB-1® has been shown for two branched, unsaturated PFAS (perfluoro(4-methylpent-2-enoic acid and 4,5,5,5-tetrafluoro-4-(trifluoromethyl)-2-pentenoic acid).[424] Although the fully saturated compounds tested (PFOA, perfluoro-3,7-dimethyloctanoic acid, and 4,5,5,5-tetrafluoro-4-(trifluoromethyl) pentanoic acid) were not biodegraded, this single study may suggest the possibility of additional microbial transformations of PFAS.[424] Overall these microbial processes are likely to lead to the accumulation of PFAAs in aquifers contaminated with AFFF, necessitating study of their impact on ISB.

2.5.2 Impact of PFAS on dechlorinating microorganisms

Although there is no well understood pathway for the biotransformation of fully-saturated PFAAs, their presence affects the bioremediation of other compounds, including chlorinated ethenes, which are often present in mixed plumes. Although PFOS and other PFCAs were not shown to impact the methanogenic activity of anaerobic wastewater sludge, even at concentrations as high as 500 mg/L,[417] other studies have shown negative impacts of PFAS on microorganisms. Degradation of soil organic matter by soil microorganisms was impeded by PFAS in soil, with PFSAs exhibiting greater toxicity than PFCAs, and with longer-chain PFAAs having greater toxicity than shorter chain PFAAs.[425] A study of the community structure of soil microbes exposed to PFAS revealed inhibition of some species (*Latescibacteria* and *Chloroflexi)* but stimulation of others (*Firmicutes, Acidobacteria,* and *Actinobacteria)* with an overall increase in the abundance of bacteria but a decrease in bacterial diversity.[426] Fitzgerald et al. (2019) showed that AFFF, a PFAS-mixture, and individual PFAS could all inhibit microbial degradation of 2,4,-dichlorophenol and change the microbial community structure. In a study of toluene-degrading bacteria, the rate of toluene degradation was not affected by the presence of PFAAs but there were indications of stress on the microbial cells, including flocculation and an increased transcription of stress-genes.[428]

TCE degradation by *Dhc* was found to be inhibited by PFAA concentrations in excess of 66 mg/L in a methanogenic culture containing *Dhc* strain 195.[43] A similar study found that TCE dechlorination by *Dhc* was inhibited by AFFF from Ansul and National foam, but was not inhibited by 3M AFFF.[46] In order to use ISB to treat chlorinated ethenes in plumes mixed with PFAS, the conditions under which *Dhc* activity is inhibited must be better understood. A series of batch reactor and microcosm experiments was used to examine the impact of PFAAs on *Dhc* strains and dechlorination rates (Chapter 6).

3.0 Bioenhanced back diffusion and population dynamics of *Dehalococcoides mccartyi* strains in heterogeneous porous media

This work was accepted for publication in *Chemosphere* on April 17, 2020. Co-author Lurong Yang performed the numerical modeling portions of this work, specifically sections 3.3.4, 3.4.1, and 3.4.3 and Appendix A1.6. The Supplementary Material submitted for publication with this work is provided as Appendix A.

3.1 Abstract

Diffusion, sorption-desorption, and biodegradation influence chlorinated solvent storage in, and release (mass flux) from, low-permeability media. Although bioenhanced dissolution of non-aqueous phase liquids has been well-documented, less attention has been directed towards biologically-mediated enhanced diffusion from low-permeability media. This latter process was investigated using a heterogeneous aquifer cell, packed with 20-30 mesh Ottawa sand and lenses of varying permeability (1.0×10^{-12}-1.2×10^{-11} m^2) and organic carbon (OC) content (<0.1-2%), underlain by trichloroethene (TCE)-saturated clay. Initial contaminant loading was attained by flushing with 0.5mM TCE. Total chlorinated ethene removal by hydraulic flushing was then compared for abiotic and bioaugmented systems (KB-1® SIREM; Guelph, ON). A numerical model incorporating coupled diffusion and (de)sorption, facilitated quantification of bio-enhanced TCE release from low-permeability lenses, which ranged from 6-53%. Although *Dehalococcoides mccartyi (Dhc)* 16S rRNA genes were uniformly distributed throughout the porous media, strain-specific distribution, as indicated by the reductive dehalogenase (RDase) genes *vcrA*, *bvcA*, and *tceA*, was influenced by physical and chemical heterogeneity. Cells harboring *bvcA* comprised 44% of the total RDase genes in the lower clay layer and media surrounding high OC lenses, but only 2% of RDase genes at other locations. Conversely, cells harboring the *vcrA* gene comprised 50% of RDase genes in low-permeability media compared with 85% at other locations. These results demonstrate the influence of microbial

processes on back diffusion, which was most evident in regions with pronounced contrasts in permeability and OC content. Bioenhanced mass transfer and changes in the relative abundance of *Dhc* strains likely impact bioremediation performance in heterogeneous systems.

3.2 Introduction

Engineered bioremediation, including bioaugmentation and biostimulation, has been implemented as an effective remedial strategy to transform tetrachloroethene (PCE) and trichloroethene (TCE) to benign ethene, and has resulted in reduced site cleanup times compared to natural attenuation.[15,19,335] In close proximity to non-aqueous phase liquid (NAPL) contaminants, it is well documented that the process of microbial reductive dechlorination (MRD) can enhance organic phase dissolution rates over abiotic dissolution alone, leading to decreased longevity of the source zone.[35,257,311,337] Two mechanisms involved in this enhancement are: (1) the transformation of contaminants to higher solubility daughter products, and (2) an increase in the concentration gradient between the NAPL and the surrounding aqueous phase (dissolution driving force).

While engineered bioremediation has been successfully implemented at many sites, numerous sites have also exhibited incomplete dechlorination to dichloroethene isomers (DCE) and/or vinyl chloride (VC)[18–20], or have demonstrated rebound of contaminant concentrations after biostimulation.[17,21] Contaminant rebound is often exacerbated by the presence of subsurface heterogeneity, where contaminant mass sequestered in low-permeability porous media can be slowly released over time through diffusion and desorption.[2,22–24] Subsurface heterogeneity also complicates bioremediation because amendments delivered through groundwater injection are unable to effectively penetrate low-permeability media.[9,22,24] Despite these challenges, bioremediation has been shown to be effective in aquifers with physical heterogeneity, including clay tills.[331,332] Further,

biological activity in higher permeability zones, where amendments are more easily distributed, can facilitate the back diffusion of compounds from low-permeability zones to higher flow regions by increasing the driving force for mass transfer.[331,339,340]

The widespread application of MRD for treatment at chlorinated solvent sites has been largely due to the extensive study of *Dehalococcoides mccartyi* (*Dhc*) strains.[8,14,39,51,276,289,292] This work has shown that numerous strains can contribute to the transformation of the PCE and TCE to benign ethene. Specific transformation steps are carried out by *Dhc* strains harboring reductive dehalogenase (RDase) genes, including *tceA*, (TCE to VC), *vcrA* (*cis*-DCE to ethene), and *bvcA* (all DCE isomers to ethene).[292,362] RDase genes are routinely monitored to assess the dechlorination capability of specific microbial communities.[37,332,361,373]

While previous studies have examined responses of specific *Dhc* strains to perturbations in geochemistry,[25,26,29] few have explored the influence of coupled physical and chemical heterogeneity on *Dhc* strain growth and activity, despite the role of specific *Dhc* strains and the influence of subsurface conditions on the successful application of bioremediation. Instead, experimental studies have generally been limited to batch and one-dimensional homogeneous column experiments examining the relationship between electron donor and acceptor concentration and the abundance of RDase genes.[11,27,28,344] Such experimental systems, however, do not reproduce the heterogeneity present in real aquifers. Conversely, field-scale studies, examining microbial population variations between sites or across large areas[361,362,373] did not resolve microbial spatial distributions at the scale that will control enhanced contaminant mass transfer and its contribution to remedial effectiveness. Only one study examining the impacts of NAPL saturation heterogeneity on *Dhc* strain distribution has been performed in a heterogeneous multi-dimensional system,[35] but the influence of physical heterogeneity was not addressed.

Mathematical models can be used to extrapolate laboratory results to the field-scale and to delineate the impact of individual biogeochemical processes. In prior studies, models have been used to quantify the effect of back diffusion in both field- and bench-scale systems (2-D) incorporating heterogeneous permeability domains.[429–432] However, these investigations have not accounted for coupled processes, including diffusion, sorption, and biotransformation. Changes in physical-chemical properties (e.g., diffusivity, solubility, sorptive capacity, volatility) as parent compounds are biotransformed to daughter products will also influence the remediation of the sequestered mass in low-permeability soils. To date, no studies have utilized numerical models to quantify the impact of enhanced biotransformation on back diffusion in heterogeneous media.

Due to the potential impacts of bioremediation on contaminant mass transfer from low-permeability zones, there is a critical need for systematic, high-resolution, laboratory investigations of biomass and *Dhc* strain distributions in realistic, multi-dimensional, chemically and physically heterogeneous systems. The overall objective of this study was to improve our understanding of the contribution of bioremediation to mass transfer between the bulk media and regions of low-permeability and higher organic carbon. A laboratory-scale, multi-dimensional aquifer cell, packed with five porous media of varying permeability and organic carbon (OC) content, was employed to study chlorinated ethene (TCE) diffusion from low-permeability regions under abiotic and biotic conditions. A modified version of a three-dimensional multi-species modular transport model (MT3DMS), incorporating information on physical and sorption heterogeneity, was used to generate predictions of back diffusion under abiotic conditions for comparison with experimental data following bioaugmentation. The spatial and temporal variation abundance of *Dhc* 16S rRNA and RDase genes was monitored throughout the experiment and in soil samples collected at the conclusion of the experiment. These data were used to

determine the extent of biologically-enhanced back diffusion as a function of physical heterogeneity, contaminant distribution, and the distribution of total and specific *Dhc* strain abundance.

3.3 Materials and Methods

3.3.1 Aquifer cell setup and preparation

The aquifer cell (63.5 cm length × 38 cm height × 1.4 cm thickness) was constructed from two 1.4 cm thick glass panels held in an aluminum frame, with sampling ports aligned in four vertical columns following the procedures of Cápiro et al. (2015) and Suchomel et al. (2007) (Figure 3-1). Clay collected from the Commerce Street Superfund Site (Williston, VT) was dried, ground with a mortar and pestle, re-saturated with a 100 mg/L TCE solution, and emplaced in the bottom 3 cm of the aquifer cell to create a lower confining layer. Above the clay layer, the aquifer cell was packed with ASTM International Standard 20-30 mesh sand (US Silica Company; Ottawa, IL) under water-saturated conditions. Four 5 cm (height) × 14 cm (length) lenses were emplaced, so that sampling ports were located downgradient from each lens. Lens materials consisted of Webster soil (Iowa State University Agricultural Experiment Station; Ames, IA), Appling soil (University of Georgia Agricultural Experiment Station; Eastville, GA), F-95 sand (Fisher Scientific; Hampton, NH), and a loamy sand collected from the Commerce Street site (Figure 3-1). All porous media was sterilized via autoclave, liquid cycle at 121°C for 30 minutes, prior to packing. Additional porous media information can be found in Table 3-2 and the Supplementary Material (SM), provided as Appendix A.

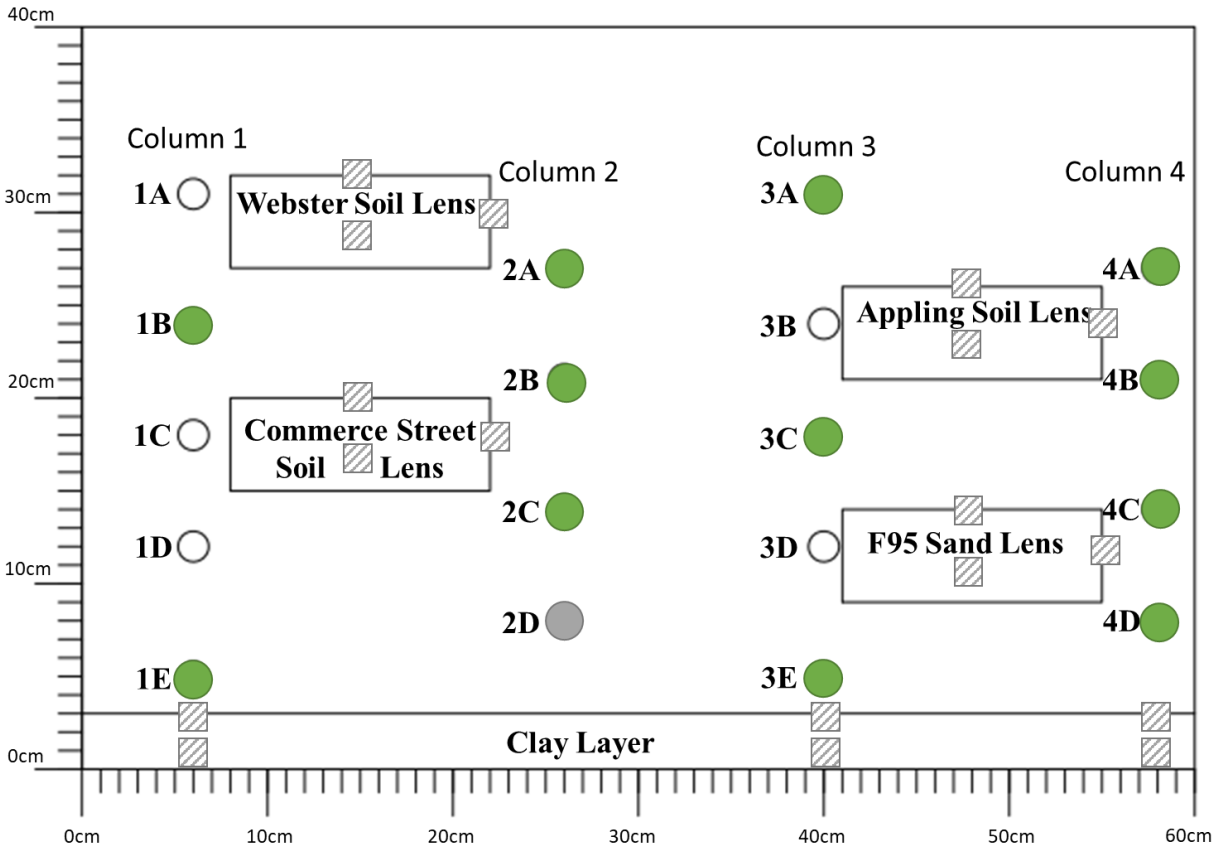

Figure 3-1. Aquifer cell layout and sample locations. Aqueous sampling ports sampled throughout experiment, final 7 rounds only, and additional soil sample locations.

After packing, flow was established in the aquifer cell using a constant head influent system described by Cápiro et al. (2015). Influent solutions were prepared in a 5 L Mariotte bottle, and a flow rate of 0.10 (during biotic treatment) to 2.60 (during bromide tracer test) mL/min was maintained by adjusting the height of the influent and effluent reservoirs (Table 3-1). These flow rates correspond to seepage (pore-water) velocities of 7.47-82.5 cm/day and residence times of 0.77-8.5 days.

3.3.2 Non-reactive tracer and abiotic back diffusion experiments

A conservative tracer test was performed using 10 mM sodium bromide (Fisher Scientific; Hampton, NH) and 0.075 mM sodium fluorescein (Sigma Aldrich; St. Louis, MO) solution as described in Appendix A1.2. The abiotic back diffusion experiment was completed in

two phases that are detailed in Table 3-1. Briefly, after the tracer test, an influent solution of 0.5 mM TCE and 10 mM sodium bromide was maintained for 15.9 pore volumes (PVs) to simulate historic mass loading (plume development). This duration was based on model predictions estimating a minimum of 15 PVs to allow bromide and TCE to fully penetrate low-permeability materials. Following the loading stage, the influent was changed to a 10 mM sodium chloride solution (without TCE) to flush TCE and bromide from the aquifer cell. During this abiotic flushing period, 1.6 mL samples were collected periodically from 12 sampling ports using a Fusion 200 syringe pump (Chemyx; Stafford, TX) to draw samples at a rate of 0.1 mL/min (10% of the background flow rate). Effluent samples (1.6 mL) were also collected from a 20 mL sampling bulb in the effluent line. Sample aliquots (1.0 mL) were used to measure chlorinated ethenes (TCE, *cis*-DCE, and VC) and ethene concentrations using a gas chromatograph equipped with a flame-ionization detector (GC-FID) and the remaining sample volume (0.6 mL) was analyzed for bromide concentrations by ion chromatography. Details of the analytical methods are provided in Appendix A1.3. The 12 sampling port locations were selected based upon their locations relative to the clay and soil lenses and to provide a sampling port downgradient of each lens.

Table 3-1. Aquifer cell experimental parameters

	Bromide Tracer		**Abiotic Experiment**	
Phase	**Bromide Plume Development**	**Bromide Flushing**	**Bromide/TCE Plume Development**	**Abiotic Flushing**
Avg. Flow Rate (mL/min)	2.4	2.4	1.0	0.93
Duration (PVs)	0.63	2.3	15.9	8.9
Duration (days)	0.21	0.79	13	8
Influent Solution	10 mM sodium bromide and 0.075 mM sodium fluorescein	10 mM sodium chloride	10 mM sodium bromide	10 mM sodium chloride
Influent TCE	0 mM	0 mM	0.5 mM	0.01 mM
Sampling Frequency	1/0.04 PVs (effluent only)		1/0.06 to 1/3.9 PVs (effluent and ports)	

	Biotic Experiment						
Phase	**TCE Plume Develop-ment I**	**TCE Plume Develop-ment II**	**TCE Plume Develop-ment III**	**BIOAUGMENTATION**	**Establish Microbial Community**	**Biotic Treatment I**	**Biotic Treatment II**
Avg. Flow Rate (mL/min)	0.51	0.71	0.39		0.27	0.21	0.16
Duration (PVs)	12.9	6	3.7		2.6	5.8	1.5
Duration (days)	21	7	8		8	23	8
Influent Solution	10 mM sodium chloride	Mineral Salts Medium with 10 mM sodium lactate			Mineral Salts Medium with 10 mM sodium lactate		
Influent TCE	0.5 mM	0.5 mM	0.5 mM		0.5 mM	0.04 mM	0.01 mM
Sampling Frequency	1/0.23 to 1/1.2 PVs (effluent and ports)						

3.3.3 Biotic degradation experiment

Following the abiotic back diffusion experiment, the cell was again pre-loaded with TCE over a 22.6 PV injection period. To achieve conditions appropriate for MRD, TCE loading was conducted in three phases (Table 3-1). After an initial preloading using a 0.5 mM TCE influent solution (TCE Plume Development I), anoxic conditions were established by introducing a bacterial growth medium, augmented with 10 mM sodium lactate and 0.5 mM TCE, as the influent (TCE Plume Development II). The medium was prepared according to Löffler et al., (2005), incorporating the modifications reported in Cápiro et al.

(2015). Prior to bioaugmentation (TCE Plume Development III), the flow rate was reduced to approximately 0.39 mL/minute (34 cm/day seepage velocity; 1.8-day residence time) to provide sufficient residence time for biodegradation reactions to occur. The aquifer cell was then bioaugmented with the KB-1® inoculum (SiREM; Guelph, Ontario), a methanogenic dechlorinating consortium containing *Acetobacerium sp., Geobacter sp. (Geo)*, and multiple *Dhc* strains harboring the *vcrA*, *bvcA, and tceA* RDase genes. This consortium was selected based upon its widespread application in the field, previous use in field-scale bioremediation applications, and demonstrated capability to dechlorinate PCE to ethene.[13,314,337] Initial gene abundances of 2.4×10^7, 9.8×10^7, 2.9×10^6, and 6.0×10^5 gene copies/mL of the *Dhc* 16S rRNA, *vcrA*, *bvcA*, and *tceA* genes, respectively, were measured in the inoculating culture. The inoculum was diluted in sterile growth medium to provide approximately 10^4 *Dhc* cells/mL of pore water, the cell density suggested by previous studies to yield ethene at acceptable rates.[38,39] Twenty mL of dilute inoculum was then injected at a rate of 0.1 mL/min into each of the 18 sampling ports using a syringe pump in an effort to create a uniform distribution.

Following bioaugmentation, the influent of medium, lactate, and TCE was maintained for 2.6 PVs to establish the microbial community. The influent TCE concentration was then reduced to 0.04 mM for 5.8 PVs (Biotic Treatment I) and to 0.01 mM for 1.5 PVs (Biotic Treatment II) as shown in Table 3-1. Samples (1.0 to 2.6 mL) were collected from the selected sampling ports and from the effluent throughout the experiment. These samples were analyzed for chlorinated ethenes and ethene by GC-FID as described above, with additional 0.5 mL aliquots analyzed for volatile fatty acids (VFAs) by high pressure liquid chromatography (HPLC). The remaining sample volume was centrifuged and frozen for microbial quantification via quantitative polymerase chain reaction (qPCR) as described in Appendix A1.5.[35,37] An additional port (2D, Figure 3-1), located near the clay layer, was

sampled once ethene was the only compound detected in the effluent (6.6 PVs after bioaugmentation) to monitor diffusion from the clay. Following the final round of aqueous port sampling, the aquifer cell was destructively sampled to measure sorbed-phase chlorinated ethenes and attached biomass at specific locations (at the sampling port locations, in the clay confining layer, and within and around each lens, see Appendix A for details).

3.3.4 Numerical simulation

A modified version of MT3DMS[435] was used to simulate bromide tracer and abiotic TCE back diffusion experiments, and to quantify bioenhanced chlorinated ethene and ethene diffusion. This model was coupled with MODFLOW (McDonald and Harbaugh, 1988) to simulate transient flow conditions. In MT3DMS, aqueous transport of non-reactive components is represented by a traditional advection-dispersion-reaction equation (Appendix A1.6, equation (1)). In this work, TCE sorption to solids was represented as a linear, equilibrium process (Appendix A1.6, equation (2)).

Initial model parameter values (Table 3-2) were obtained from published experiments conducted with the same porous media. Data from the bromide tracer experiment were used to characterize the flow field and fit hydraulic parameters (hydraulic conductivity and dispersivity coefficients) in the numerical model. Details of breakthrough curve fitting are provided in Appendix A2.1. A comparison of simulated and measured TCE (sorptive) and bromide (conservative) concentrations at sampling ports and in the effluent during the abiotic flushing experiment facilitated calibration of the linear sorption coefficients (K_d). Porosity was calculated from experimental measurements of soil mass and emplaced volume. Free-solution diffusivity values for bromide and TCE were 2.01×10^{-5} cm^2/s and 7.99×10^{-6} cm^2/s, respectively.[436,437] A tortuosity of 0.67[438,439] was used to obtain the effective diffusivity used in the model following the method of Yang et al. (2018).

Table 3-2. Initial and calibrated model parameters for aquifer cell transport simulations

	Published Values			Model Calibrated Values		Measured[a]
Porous Media	Organic Carbon Content (% mass)	Hydraulic Conductivity (m/day)	Linear Sorption Coefficient K_d(L/kg)	Hydraulic Conductivity (m/day)	Linear Sorption Coefficient K_d(L/kg)	Porosity, ϕ (-)
ASTM 20/30	N/A	330[b]	N/A	200	0	0.45
Webster Soil	1.96%[c]	0.86[d]	2.47[e]	0.6	4.16	0.51
Appling Soil	0.66%[c]	10.2[f]	0.83[e]	5	0.95	0.33
Commerce St. Soil	0.09%[g]	1.7-6.9[g]	0.13[g]	5	0.13	0.3
F-95 Sand	0.01%[c]	1.9[h]	0.006[i]	1	0.0013	0.28
Commerce St. Clay	0.30%[g]	N/A	0.35[g]	0.05	0.40	0.78

a. Measured in this experiment by mass added and aquifer cell volume
b. Taylor et al., 2001
c. Marcet et al., 2018b
d. Marcet, 2014
e. Calculated by $K_d = Orgranic\ Carbon\ Content * K_{OC}$ using the organic carbon content from Marcet et al., 2018b and $K_{OC} = 126\ L/kg$ for TCE from Pankow et al., 1996
f. Pennell et al., 1995
g. Gaeth, 2017
h. Chen et al., 2007
i. Joo et al., 2008
j. N/A = not available

The total molar sum of chlorinated ethene and ethene concentrations (total ethenes) observed during the biotic experiment were compared with model predictions of concentrations expected in the absence of MRD to assess the influence of biotransformation on diffusion and desorption (bioenhancement of back diffusion). Detailed descriptions of model simulation procedure, domain discretization, and boundary conditions are provided in Appendix A1.6.

3.4 Results and Discussion

3.4.1 Desorption and diffusion under abiotic conditions

Measurements from the abiotic flushing experiment were used in conjunction with model simulations to investigate the influence of sorption and diffusion on the removal of sorbing (i.e., TCE) and non-sorbing (i.e., bromide) solutes (Figure 3-2). One PV after reducing the solute influent concentrations, the concentrations dropped rapidly, with the effluent TCE and bromide concentrations reduced to 16.9% and 8.5% of the loading concentrations, respectively. After 9 PVs of flushing, TCE concentrations were one order-of-magnitude lower than the input concentration, while bromide concentrations were two orders-of-magnitude lower than the input concentration. Based on model simulations, the TCE mass retention percentages from each porous material at the final flushing time were 2.7%, 51.5%, 26.4%, 2.6%, 4.1%, and 20.1% in the background sand, Webster lens, Appling lens, Commerce Street lens, F-95 sand lens, and clay layer, respectively. This higher retention of TCE in comparison to that of bromide (which had 1.9% mass retention in the clay layer and 0.3% in other locations) is attributed primarily to the influence of sorption.

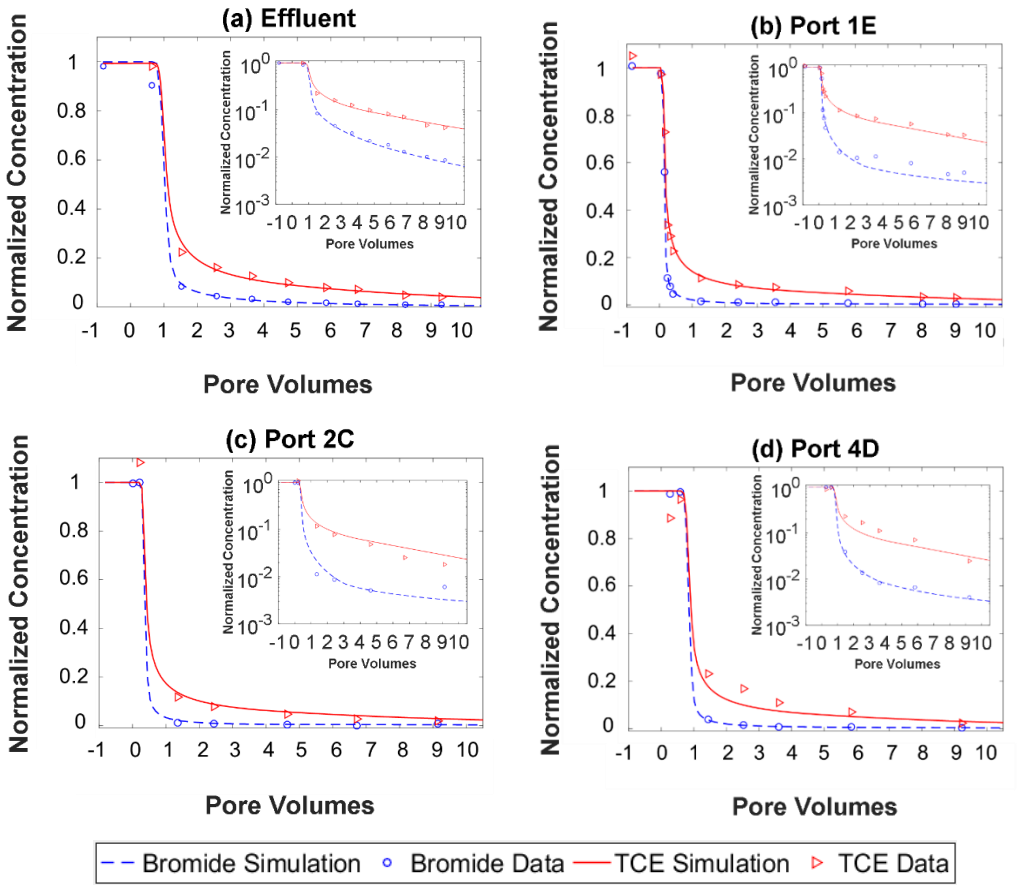

Figure 3-2. Comparison of experiment observations and calibrated model simulations of bromide and TCE concentrations (normalized by input concentration) plotted in linear and log scale (inset) during abiotic flushing experiment in (a) effluent (b) port 1E (c) port 2C and (d) port 4D. Influent TCE and bromide concentrations were switched to 0.01 and 0.0 mM at time zero (PV=0), respectively Experiment data: circle—bromide, triangle—TCE; Simulation: dashed line—bromide, solid line—TCE. Figure by Lurong Yang.

Measurements and model predictions of bromide and TCE concentrations during the abiotic flushing period are presented in Figure 3-2 for the effluent, a port above the clay layer [1E], a port downgradient of the Commerce Street lens [2C], and a port downgradient of the F95 sand lens [4D]. These locations were selected based upon their proximity to low-permeability materials that can retain contaminant mass and thus, support back diffusion and desorption. The agreement between model predictions and experimental measurements indicates that the model is capable of capturing measured bromide and TCE back diffusion under abiotic conditions, with goodness of fits of 0.91 and 0.95 in the effluent, 0.88 and 0.91 at port 1E, 0.99 and 0.86 at port 2C, and 0.98 and 0.84 at port 4D

for bromide and TCE, respectively. Although the geometry of the low-permeability compartments was digitized based on images of the aquifer cell, fine-scale variations in lens shape and compaction of the material may partially account for the discrepancies between model simulations and experimental measurements.

3.4.2 Biodegradation results

The biotic experiment utilized a TCE loading approach similar to that employed during the abiotic experiment. Following bioaugmentation, *cis*-DCE was detected in the effluent after 0.2 PVs (5% of the total ethenes), VC was detected after 2 PVs (1% of total ethenes), and ethene after 3.4 PVs (4% of total ethenes). When the influent TCE concentration was lowered to 0.04 mM, 2.6 PVs after bioaugmentation, the effluent molar composition was 90% *cis*-DCE and 10% VC (Figure A-5[a]). Approximately 6.1 PVs after bioaugmentation, 3.4 PVs after lowering the influent TCE concentration to 0.04 mM, ethene was the only analyte detected in the effluent. However, *cis*-DCE continued to be detected at concentrations of 0.07-0.08 mM in sampling ports located near the influent chamber (1A and 1E, Figure 3-1) and at 0.02-0.03 mM in the ports located in columns 2 and 3 (Figure 3-1), indicating rapid biotransformation of TCE to *cis*-DCE and slower transformation to VC and ethene.

When the influent TCE concentration was further reduced to 0.01 mM (9 PVs after bioaugmentation), ethene persisted in the effluent at 0.04-0.06 mM, indicating additional mass inputs from diffusion and desorption from the low-permeability lenses and clay. Ethene concentrations were sustained at 0.01-0.02 mM in all ports except those impacted by the clay (1E and 3E) and the higher OC lenses (3A, 4A, and 4B) where higher ethene concentrations were measured (Figure A-5). The highest concentrations, 0.04-0.06 mM, were measured in the bottom ports (1E and 3E), where TCE continued to be released from the underlying clay layer (Figure A-6 [b] and [d]). Downgradient of the high OC Webster

and Appling lenses (ports 3A, 4A, and 4B), ethene was detected at concentrations up to 0.03 mM.

At the conclusion of the experiment, TCE was detected in soil samples collected from the clay layer, Webster lens, and Appling lens with average concentrations of 1.94 μg/g (±0.57 μg/g), 0.022 μg/g (±0.016 μg/g), and 0.37 μg/g (±0.19 μg/g), respectively. Due to the high detection limit for *cis*-DCE (0.0026 mM) as described in Appendix A1.3, this compound was only detected in the clay layer at an average concentration of 49 μg/g (±23 μg/g). Throughout the experiment, lactate, acetate, and/or propionate were detected in all samples indicating excess electron donor. Total VFA concentrations in sampling ports and effluent averaged 3.69mM (±1.71mM) and 2.37mM (±0.21mM), respectively.

3.4.3 Desorption and diffusion under abiotic and biotic conditions

To explore the influence of MRD on chlorinated ethene mass transfer, a synthetic abiotic flushing experiment (with the same influent conditions but without MRD) was created by numerical simulation and model predictions compared with measurements of total ethenes during the biotic experiment. Under biotic conditions, TCE transformed to the lesser-chlorinated transformation products, which have higher diffusivities, higher solubilities, and lower sorption coefficients than TCE. This transformation increases the mobility of the compounds, thus increasing the driving force for back diffusion, resulting in microbially-enhanced mass elution. As the comparative simulation used the same flow rate and input concentration of TCE as the MRD experiment, comparison of aqueous mass (measured biotic vs. modeled abiotic) at sampling locations indicates the influence of MRD on contaminant mass transfer. An expression to quantify the extent of bioenhanced back diffusion and desorption was developed as:

$$\delta_{MRD} = \frac{CM_{exp} - CM_{sim}}{CM_{sim}} \times 100\% \quad (3)$$

Here, δ_{MRD} is a measure of the effective enhancement of TCE diffusion and desorption by MRD, CM_{exp} is the total ethene molar mass calculated using experimental data for a specific location (e.g., effluent or sampling port), and CM_{sim} is the TCE molar mass calculated using the model simulation at the same location. CM_{exp} or CM_{sim} is calculated by a stepwise summation of the discrete data of total concentration $\sum_{i_{t=0}}^{i_{t=final}}(total\ concentration)_{i_t} * (time\_interval)_{i_t} * (flow\ rate)_{i_t}$. Predicted and measured concentrations of total ethenes in the effluent and selected ports are compared in Figure 3 with subplots for the two ports with the highest δ_{MRD} values, both located at the bottom of the aquifer cell (near the clay layer).

The δ_{MRD} values (Figure 3-3) reveal that total ethene mass elution was enhanced by MRD, with δ_{MRD}>0 calculated at all sampling locations (12% for the effluent and 6%-53% at the sampling ports). Sampling ports directly impacted by mass transfer from low-permeability layers displayed more pronounced differences from abiotic simulations than ports located downgradient of more permeable materials. For example, ports 1E and 3E, in close proximity to the clay layer (lowest permeability and higher sorption capacity than background sand), displayed the highest MRD enhancements of 40% and 53%, respectively. Similar enhancements were observed in other locations near low-permeability zones (Figure A-6). The ports immediately downgradient from the Webster (port 2A), Commerce Street (port 2B and 2C), and F-95 soil lenses (port 4C and 4D) were associated with bioenhanced mass transfer ranging from 20-35%. Lower enhancement (7-12%) was measured in the effluent, attributed to dilution from the more permeable, less sorptive zones. However, the lowest δ_{MRD} was measured at port 4B, immediately downgradient from the Appling soil lens, which has a higher organic carbon content than the Commerce Street and F95 lenses. This observation may be attributed to volatilization losses; TCE biodegradation products (*cis*-DCE, VC, and ethene) have higher volatility than TCE and

the location of this port is nearest to air-water contact surface of the aquifer cell. Thus, the volatilization losses from the water table in the vicinity of port 4B may have resulted in a reduction in measured chlorinated ethene mass, and an underestimation of total δ_{MRD}. As the effluent represents the integrated effect of all locations in the aquifer cell, the δ_{MRD} calculated for the effluent may also be underestimated due to volatilization.

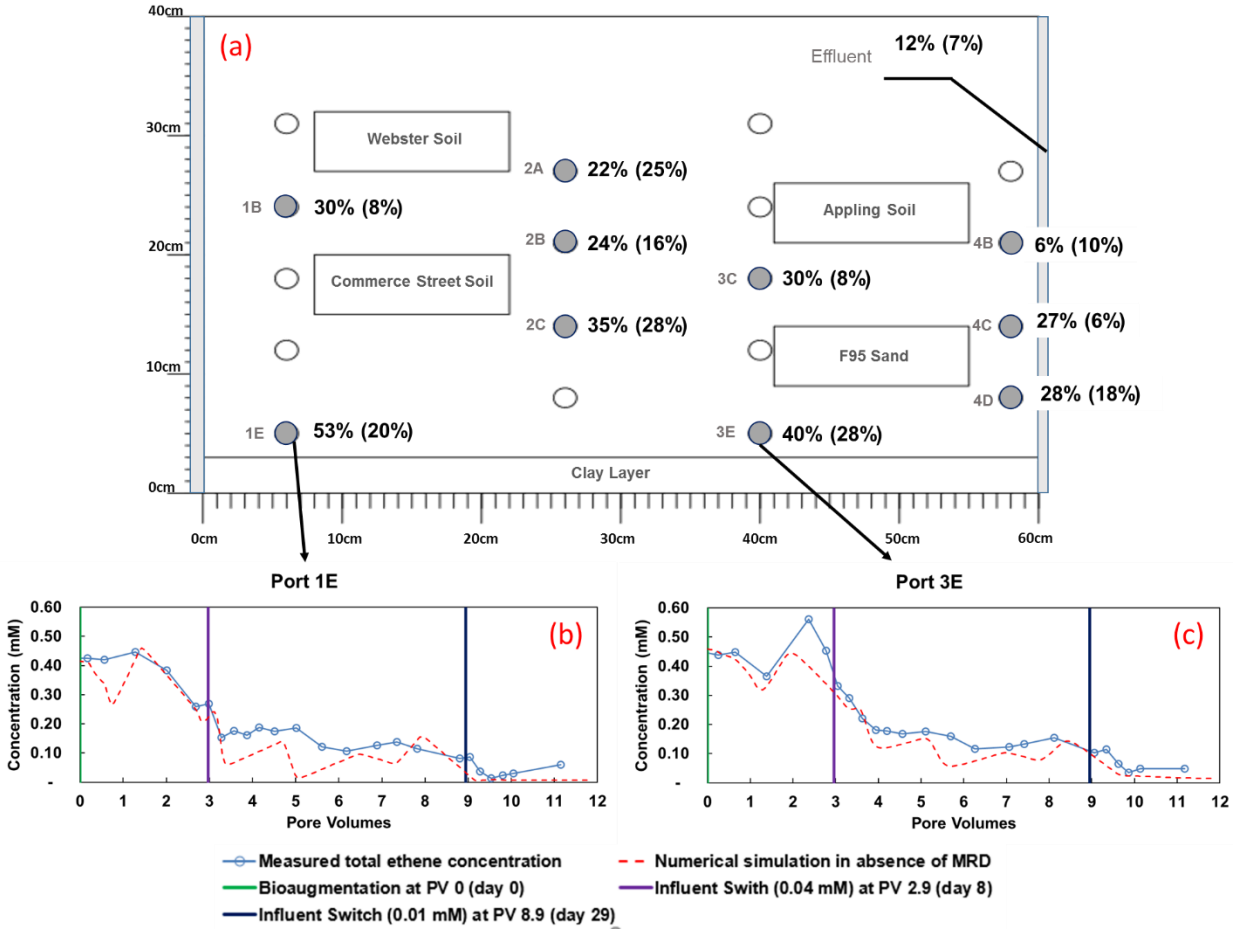

Figure 3-3. Bioenhancement of back diffusion and desorption in the heterogeneous aquifer cell; (a) δ_{MRD} (%) in effluent and selected ports where percentage values were calculated for the period from the lowering of the influent TCE concentration (PV 2.9) to the end of the experiment, and over the period of the entire biotic experiment (shown in parentheses), (b) and (c) show the total molar concentration of chlorinated ethenes and ethene during biotic experiment compared with model simulations without MRD for port 1E and 3E, respectively. Figure by Lurong Yang.

3.4.4 Growth of Dehalococcoides population

Total *Dhc* abundance, as measured by the 16S rRNA gene, increased from a 12-port average of 2.84×10^5 $\pm4.43\times10^5$ cells/mL following bioaugmentation (0.5-0.9 PVs) to

3.78×10^{7} $\pm1.50\times10^{7}$ cells/mL at the conclusion of the experiment (Figure A-7, Table A-1). At an intermediate sampling time, 5.2 PVs after bioaugmentation, *Dhc* abundance varied 3 orders-of-magnitude across the domain, with the highest abundance in downgradient ports (columns 3 and 4, average abundance 7.07×10^{7} $\pm4.6\times10^{7}$ cells/mL), where higher concentrations of *cis*-DCE and VC were present, and the lowest in the upgradient ports (columns 1 and 2, average abundance 9.64×10^{6} $\pm6.12\times10^{6}$ cells/mL). This observation may be explained by the fact that *Geo* cells are more efficient than *Dhc* cells at transforming TCE to *cis*-DCE and can outcompete *Dhc* when TCE is present (i.e., at upgradient ports).[257,449] *Dhc* abundance was higher where *cis*-DCE and VC were the available electron acceptors (i.e., downgradient ports, Figure A-7). The uniform *Dhc* population at the conclusion of the experiment, when all measurements were within one order-of-magnitude, may reflect electron acceptor limitations and an associated lack of competition by *Geo* in the last phase of the experiment (lowest TCE influent). During the period of higher TCE influent concentration (2.6 PVs), *Geobacter lovely strain SZ (GeoSZ)* abundance, as measured by qPCR of the 16S rRNA gene, increased from an initial value of 7.95×10^{1} cells/mL to an average of 2.17×10^{6} $\pm2.34\times10^{6}$ cells/mL, but growth ceased after influent TCE was lowered (Table A-1).

In solid phase samples collected at the conclusion of the experiment, total *Dhc* abundance was uniform in the background samples (collected from sand corresponding to the sampling port locations), averaging 6.58×10^{7} $\pm1.44\times10^{8}$ cells/ mass of porous media containing 1 mL of water. Within the lenses, *Dhc* abundance was approximately two to four times higher throughout the Appling and Webster lenses, but four to six times lower in the Commerce Street and F-95 sand lenses. In samples collected from the clay layer, *Dhc* abundance was more than one order-of-magnitude lower than in the background (Table A-1). Growth of *Dhc* cells in and around low-permeability materials was

responsible for the measured bioenhancement of back diffusion. Although aqueous samples were not collected from the clay layer and lenses to quantify chlorinated ethene transformation within these materials, the increase in *Dhc* abundance and detection of *cis*-DCE in the clay suggests active MRD. MRD in the clay layer, and/or at the interface between the clay and background materials, was supported by either the diffusion of supplied VFAs into the clay or components of the clay that could be used as an electron donor, leading to the highest δ_{MRD} (40% and 53%) measured in Ports 1E and 3E, directly above the clay (Figure 3-3(a)).

At sampling port locations, cell abundances measured in co-located aqueous and sand samples were used to estimate the number of cells attached to the solid phase by subtracting the planktonic cells from the total cells (combined planktonic and solid phase associated cells) in the wet porous media at the same location. All measurements of gene copies in porous media were normalized by moisture content and porosity, and reported as the mass of porous media that would contain 1 mL of pore water when saturated, as in Amos et al., (2009). In all but 3 locations, 77-100% of the cells were found to be associated with the aqueous phase. This condition is typical of cells lacking necessary growth substrates, and is consistent with the depleted electron acceptor (chlorinated ethenes) conditions after lowering the TCE influent to 0.01mM.[359] Although the ratio of attached and unattached cells could not be calculated during active MRD, previous studies suggest active dechlorination was carried out by attached cells.[34,257,359,371] While microbial transport is possible, its impact was minimized by inoculating the aquifer cell through all ports. Cápiro et al. (2014) reported that *Dhc* strains grow as attached cells in systems where substrates are available. Similarly, in this study, the growth of populations of cells harboring specific RDase genes occurred in locations where substrates were available, likely as attached cells. Downgradient from the Webster and Appling lenses (port 4B), which continued to release

electron acceptor through diffusion and desorption, 53% of the *Dhc* 16S rRNA gene copies measured were associated with the solid phase. Near the influent (ports 1B and 1E), where TCE had been introduced throughout the experiment, most of the cells (90% and 74%, respectively) were attached to the solid phase, as sufficient electron acceptor was available.

3.4.5 Distribution of RDase genes

Immediately after bioaugmentation, the *tceA* gene was most abundant in the first column of ports, near the 0.5 mM TCE influent, comprising 43-99% of the total RDase genes (Figure A-8). After 2.6 PVs (Figure 3-4), *tceA* continued to be predominate (65-85% of total RDase genes) in ports 3A and 4C, where a measurable concentration of VC had not been detected. At later times (5.2 PVs and 9.8 PVs after bioaugmentation, Figures 3-4 and A-7), cells harboring the *tceA* gene only comprised a substantial proportion of the total RDase genes more than 30%) near the influent (port 1B), downgradient of the Commerce Street lens (port 2C), and above the clay layer (ports 1E and 2D). These are locations where TCE was introduced or stored in low-permeability, high-sorption regions. At the conclusion of the experiment, *tceA* was the only RDase gene detected in the clay sample collected 5 cm below Port 1E, where highest TCE [2.7 μg/g] and *cis*-DCE [95 μg/g] concentrations were measured. The *tceA* gene was also detected in the center of the Webster, Commerce Street, and F-95 lenses, accounting for 15%, 19%, and 45% of the total RDase genes, respectively. Cells harboring the *tceA* gene were associated with the solid phase (31%-100% attached) in all port locations but four, indicating that cells harboring *tceA* may be able to remain attached even when lacking a growth substrate. In ports 1B, 2C, 4C, and 4D, only 0-7% of the *tceA* genes measured were associated with the solid phase. Although *Dhc* cells were present, these locations were not impacted by the clay or high OC lenses; chlorinated ethenes were flushed rapidly from these regions, as reflected in the lowest ethene concentrations measured at the conclusion of the experiment.

As cells in these locations faced the greatest electron acceptor limitation, fewer remained attached to the solid phase at the conclusion of the experiment.

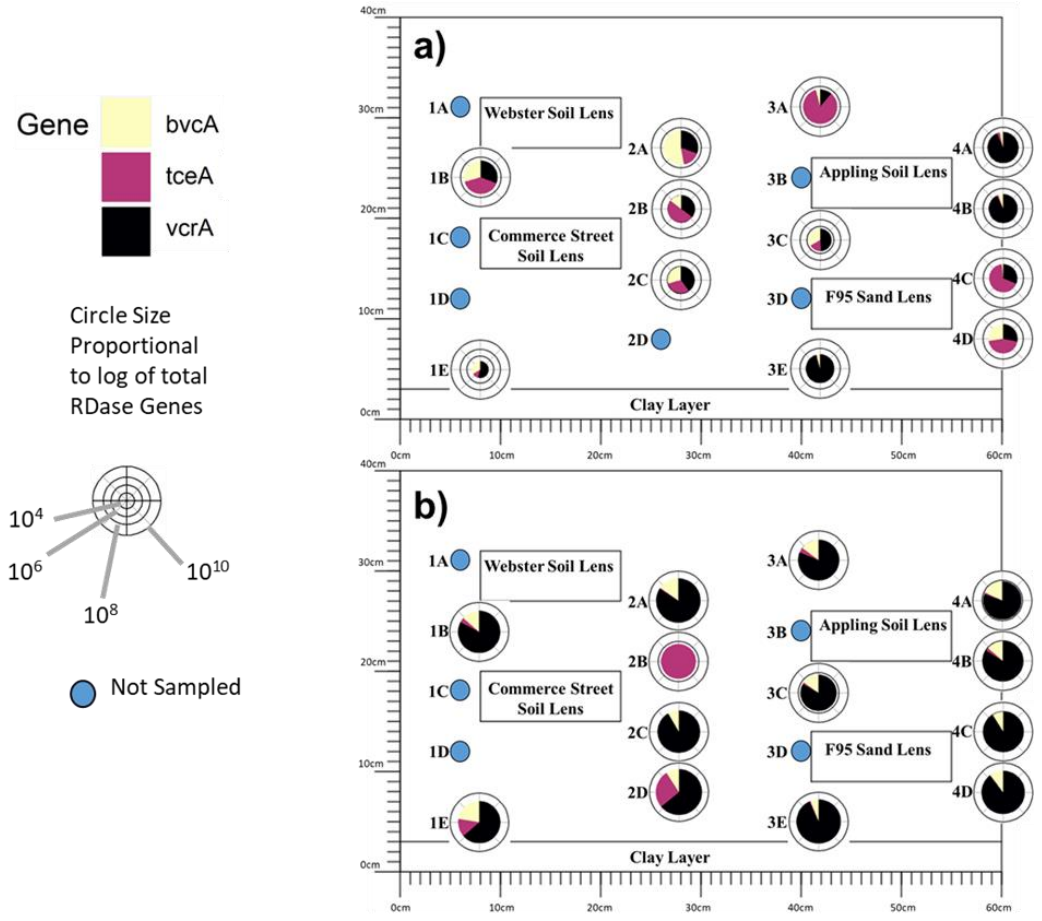

Figure 3-4. Aqueous RDase gene abundance and composition (a) 2.6 PVs (8 days) following bioaugmentation and (b) final aqueous samples, 9.8 PVs (37 days) following bioaugmentation.

In columns 3 and 4 (further downgradient), where *cis*-DCE and VC were detected due to upgradient transformation of TCE, cells harboring the *vcrA* gene were more abundant than other *Dhc* cells in samples collected 0.6 and 2.6 PVs after bioaugmentation, comprising 62-99% and 70-85% of the RDase genes detected, respectively. By the end of the experiment, 81-92% of the RDase genes detected in the aqueous phase were *vcrA* in all but 2 ports (1E, and 2D, both above the TCE-containing clay and in the upgradient half of the aquifer cell). Similarly, nearly all of the *Dhc* cells in the background porous media harbored

the *vcrA* gene (75-100%) in solid phase samples collected at the conclusion of the experiment, except where TCE continued to diffuse from the Commerce Street lens (port 2B) and clay layer (port 2E), as shown on Figure 3-5. As with the *Dhc* 16S rRNA gene abundance, nearly all (93-100%) of the *vcrA* genes measured at port sample locations were associated with the aqueous phase samples with a few exceptions. In ports 1B, 1E, and 4B, 45-87% of the *vcrA* genes detected were associated with the solid phase, likely due to the accessibility of electron acceptor near the influent and downgradient of the high-OC Webster soil lens.

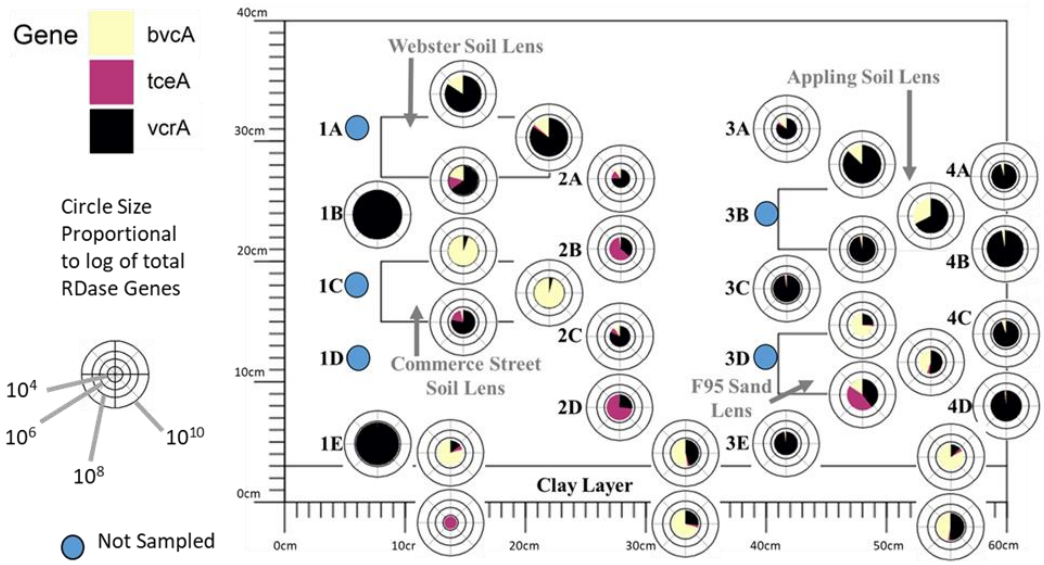

Figure 3-5. RDase gene abundance and composition in soil samples at end of experiment, 9.8 PVs (37 days) following bioaugmentation.

Cells harboring the *bvcA* gene made up a small proportion of the population (0-9%) at early time (0.6 PVs), except where the total RDase gene abundance was lowest (Port 2B, 28%, and Port 3C, 18%). Subsequently (PVs 2.6 and 5.2), the *bvcA gene* comprised larger proportion of the total RDase genes (27-53%) in the aqueous phase at locations where TCE and *cis*-DCE were present (downgradient from lenses at Ports 2A, 2B, 2C, 3A, 3C, 4C, and 4D) and near the influent (Ports 1B and 1E). At the conclusion of the experiment, when only ethene was detected, *bvcA* abundance was relatively uniform (avg. 1.1×10^7 $\pm5.6\times10^6$

copies/mL) comprising 6-22% of the total aqueous phase RDase genes. In biomass collected from the solid phase, *bvcA* made up a greater proportion of the RDase genes detected in the clay layer (47-83%), along the top and downgradient edges of the Commerce Street (94-96%) and F-95 sand lenses (44-73%), and on the downgradient edge of the Appling soil lens (32%), locations that served as an ongoing source of chlorinated ethenes. Similar to *vcrA*, cells harboring *bvcA* were primarily associated with the aqueous phase (93-100%). The 16S rRNA and RDase gene copies contained in each sample are included as Table A-1. Overall, the abundance of RDase genes exceeded the abundance of *Dhc* 16S rRNA genes by an average of 3.64-fold ±5.61, which is consistent with previous studies.[35,361,450]

The spatial variation in the proportion of cells harboring each RDase gene is a result of the physical properties of the lens materials and their effect on the mass transfer of electron acceptors (i.e., chlorinated ethenes). The Webster and F-95 lenses had the lowest hydraulic conductivity, which impeded the flushing of TCE from these lenses and resulted in longer exposure of cells to TCE and *cis*-DCE, thus favoring cells harboring the *tceA* and *bvcA* genes.[28,451] Although Appling soil has a hydraulic conductivity equal to the Commerce Street material (Table 3-2), its position further downgradient from the influent chamber facilitated rapid TCE flushing during biotic treatment as TCE daughter products were measured in nearby ports, thereby increasing the TCE concentration gradient between the lens and the surrounding background material. This rapid flushing of TCE favored *Dhc* cells harboring the *vcrA* gene (87%). The overall abundance of RDase genes was approximately one order-of-magnitude lower in the clay, 1.64×10^{6} $\pm9.05\times10^{5}$ gene copies/mass of porous media containing 1 mL of water, when compared with the background porous media and lenses (4.60×10^{7} $\pm1.19\times10^{8}$ gene copies/mass of porous media containing 1 mL of water). This result is consistent with the low hydraulic

conductivity of the clay that limits penetration of the inoculum into the clay and impedes electron donor delivery.

3.5 Conclusions

The heterogeneous aquifer cell, packed with porous media representing a range of permeabilities and OC content, enabled examination of the influence of heterogeneity on contaminant mass transfer at a higher resolution than would be possible at the field-scale. Here, MRD enhanced back diffusion by 12% over abiotic conditions alone, with local enhancements up to 53% measured where TCE was stored in low-permeability and high-OC lenses, resulting in increased overall mass flux of chlorinated ethenes from the aquifer cell. Future work on modeling of bioremediation performance should incorporate bioenhanced desorption and diffusion to improve the accuracy of predicted cleanup times, especially in formations with high permeability contrasts. In particular, bioehancement may substantially affect cleanup times in aquifers with thick low-permeability zones or interbedded high- and low-permeability materials. Under such conditions, more detailed modeling will likely reduce predicted cleanup times and may allow bioremediation to be proposed as a remedy in locations where it was previously thought to be inefficient or infeasible.

Subsurface heterogeneity represented in the aquifer cell resulted in variations in the availability of electron acceptor, shifting the *Dhc* strains present from cells harboring *tceA* in locations where TCE was available to cells harboring *vcrA* where VC was available. Cells harboring *bvcA* were most abundant near low-permeability, high OC materials where *cis*-DCE was available due to the preferential utilization of this electron acceptor. The observed shift in the predominant *Dhc* strain with changes in electron acceptor abundance demonstrates the importance of maintaining a robust dechlorinating community harboring multiple RDase genes and monitoring multiple strains to obtain more complete information

for the assessment of bioremediation progress. If the necessary strains are present, the dechlorinating microbial population (e.g., *Geo* and *Dhc* strains) adapts to changes in electron acceptor availability caused by the transport of chlorinated ethenes into and out of low-permeability and highly sorptive soils. Such shifts in the microbial population allow efficient transformation of chlorinated ethenes to ethene over the course of a bioremediation application.

The detailed experimental and mathematical modeling assessment of bioaugmentation and biostimulation in the heterogeneous aquifer cell revealed that:

- Differences in hydraulic conductivity and OC content-controlled desorption and back diffusion of sequestered chlorinated solvents from OC and low-permeability zones.
- Organohalide respiring bacteria enhance the mass transfer of TCE out of the low-permeability regions over abiotic dissolution processes alone.
- The greatest bioenhancement of back diffusion occurred in regions of contrasting hydraulic conductivity and organic carbon content.
- Model simulations accounting for heterogeneity in physical and chemical properties quantified local bioenhancement of back diffusion up to 53%
- *Dhc* cells were capable of penetrating low-permeability porous media including clays, contributing to enhanced back diffusion.
- The distribution of specific *Dhc* strains was influenced by the availability of electron acceptors within and near soils of differing physical properties.

Acknowledgements

Funding for this research was provided by the Strategic Environmental Research and Development Program (SERDP) under Contract W912HQ-13-C-0011, Project ER-2311: Development of an Integrated Field Test/Modeling Protocol for Efficient *In situ* Bioremediation Design and Performance Uncertainty Assessment. The authors thank Samuel Gaeth, Jessica Cooper, and Tian Tang for their assistance with sampling and data analysis, and SiREM for providing the KB-1® culture used in the aquifer cell experiment. The contents of this chapter have not been subject to agency review and do not necessarily represent the views of the sponsoring agency.

Appendix A. Supplementary data

The supplementary material contains additional details on the porous media, tracer test, analytical and sampling methods and a detailed description of the numerical model. Additional gene abundance, chlorinated ethene and ethene, and MRD enhancement results are also included.

4.0 Impact of residence time on extent of trichloroethene biodegradation

The work presented in this chapter is being prepared for publication in conjunction with a numerical model prepared by Lurong Yang which will further explore the impact of residence time and electron donor delivery on trichloroethene biodegradation. The supplementary material prepared for submission is included as Appendix B.

4.1 Abstract

Although biostimulation and bioaugmentation are widely used *in situ* remediation technologies, incomplete dechlorination resulting in the accumulation of *cis*-dichloroethene (*cis*-DCE) and vinyl chloride (VC) continues to plague many sites, preventing remediation to concentrations below maximum contaminant levels. Incomplete dechlorination is exacerbated by subsurface heterogeneity, including variations in porous media hydraulic conductivity, which controls the residence time of contaminants and amendments in different regions of a treatment zone. The average residence time is a design parameter that can be adjusted by controlling flow rates, injection frequencies, and the positioning of injection and extraction wells; however, subsurface heterogeneity will cause some regions to have higher or lower effective residence times. The effect of average residence time on the extent of trichloroethene (TCE) biodegradation was examined using a field pilot test and a similarly sized laboratory aquifer experiment. In both systems, TCE was partially dechlorinated to a mixture of *cis*-DCE, VC, and ethene when the average pore-water velocity was 7 cm/day (8-day residence time in aquifer cell and 14 days in pilot test). Decreasing the average pore-water velocity to 4.8 cm/day (21-day residence time) in the pilot test increased the proportion of ethene measured downgradient from 5% to 46% of chlorinated ethenes and ethene (molar composition), while the proportion of *cis*-DCE decreased from 75% to 28%. Similarly, in the aquifer cell, decreasing the pore-water velocity to 3.8 cm/day (16-day residence time) increased the proportion of ethene in the

effluent from 41% to 78% of chlorinated ethenes and ethene and decreased the proportion of *cis*-DCE from 27% to 5%. These results demonstrate that increasing average residence time will increase the extent of biotransformation, a useful strategy if incomplete transformation is observed and local *in situ* heterogeneity is not well characterized.

4.2 Introduction

Although chlorinated solvents continue to persist in groundwater at thousands of sites,[5,6,62] bioremediation has become a well-established remedy to treat tetrachloroethene (PCE) and trichloroethene (TCE) plumes.[1,234,242–245] Bioremediation of PCE and TCE typically relies on microbial reductive dechlorination (MRD) under anoxic conditions: a sequential process with transformation of PCE to TCE to *cis*-1,2-dichloroethene (*cis*-DCE) to vinyl chloride (VC) to ethene being the most commonly observed pathway.[258,260,275,276] While several species can transform PCE and TCE to *cis*-DCE, including *Dehalospirillum multivorans*, *Dehalobacter restrictus*, and *Geobacter lovleyi* strain SZ (*Geo*SZ),[283,284,287–289] strains of *Dehalococcoides mccartyi (Dhc)* are the most widely-studied and utilized microorganisms capable of transforming PCE and TCE to ethene.[8,19,290–292] Despite the capability of microorganisms to transform PCE and TCE to ethene, and the successful implementation of bioremediation at some sites, incomplete transformation of PCE and TCE and the associated increase in DCE and VC concentrations is of concern when implementing bioremediation.[18,19,239,258,259]

Hydraulic residence time of contaminants and remediation amendments in the treatment zone is a key design parameter that can be controlled by well position and by active pumping for recirculation or hydraulic containment.[36,363,364] Increasing average residence time can increase chlorinated ethene degradation in air sparging systems,[365] permeable adsorptive barriers,[366,367] permeable reactive barriers,[368] and during *in situ* chemical oxidation.[369] In laboratory experiments, longer residence time is correlated with increased

dechlorination of PCE and TCE.[35,254,370–372] Despite these laboratory studies, field-scale studies demonstrating the effect of varying residence time on the extent of TCE biodegradation are lacking. Verifying that insufficient hydraulic residence time in a bioactive treatment zone causes incomplete dechlorination during bioremediation, and quantifying the extent of this influence, will improve the implementation of bioremediation as a remedy for groundwater contaminated with chlorinated ethenes.

This study examines the effect of residence time variations on the extent of TCE biodegradation during an *in situ* bioremediation pilot test performed at the Commerce Street Superfund Site (Williston, VT). Materials from the site were also used to prepare a two-dimensional laboratory aquifer cell experiment designed to mimic the pilot test and allowing for more frequent and distributed sampling of the system. Using the pilot test and aquifer cell experiments, this work aims to demonstrate the utility of average hydraulic residence time as a design parameter to predict the extent of contaminant degradation in a heterogeneous aquifer by determining the extent of TCE degradation at various average hydraulic residence times.

4.3 Methods

4.3.1 Pilot test site description

The Commerce Street Superfund Site is located in an industrial park where TCE is the primary groundwater contaminant. To design the pilot test, a site investigation was completed in the vicinity of 237 Commerce Street. The investigation consisted of five continuous multi-channel tubing (CMT) wells installed in two transects (Figure 4-1). Each CMT well consisted of seven discrete channels screened at similar depths as described in Appendix B5.0. The site investigation revealed that the pilot-test area was downgradient of a suspected TCE source-zone, and that TCE was naturally being transformed to *cis*-DCE, with a total chlorinated ethene concentration averaging 0.14 (±0.05) mM in well

CMT-6 on the upgradient side of the pilot-test (Figure 4-1). Detailed site characterization data are provided in the supplemental material (SM), included as Appendix B, and in Abriola et al. (2019).

The aquifer generally consists of fine grain sand with increasingly fine sands and silts in deeper depths, culminating in a layer of dense, silty clay beginning at 10.7 to 12.2 m bgs (Table B-2); permeability ranges from 1.04×10^{-13} to 1.02×10^{-12} m^2 in the pilot test area and generally decreased with depth (Table B-1). Prior to implementing the pilot test, aquifer conditions were well suited to microbial reductive dechlorination with an average pH of 7.42 (±0.38) and an average oxidation reduction potential (ORP) of -152.8 (±23.3) mV measured in wells CMT-1, CMT-2, CMT-3, CMT-4, and CMT-5 (Figure 4-1). Naturally-occurring organic matter in the aquifer likely facilitated the observed natural attenuation of TCE to *cis*-DCE, with groundwater dissolved organic carbon concentrations ranging from 0.80 to 4.9 mg C/L measured in the pilot test area.

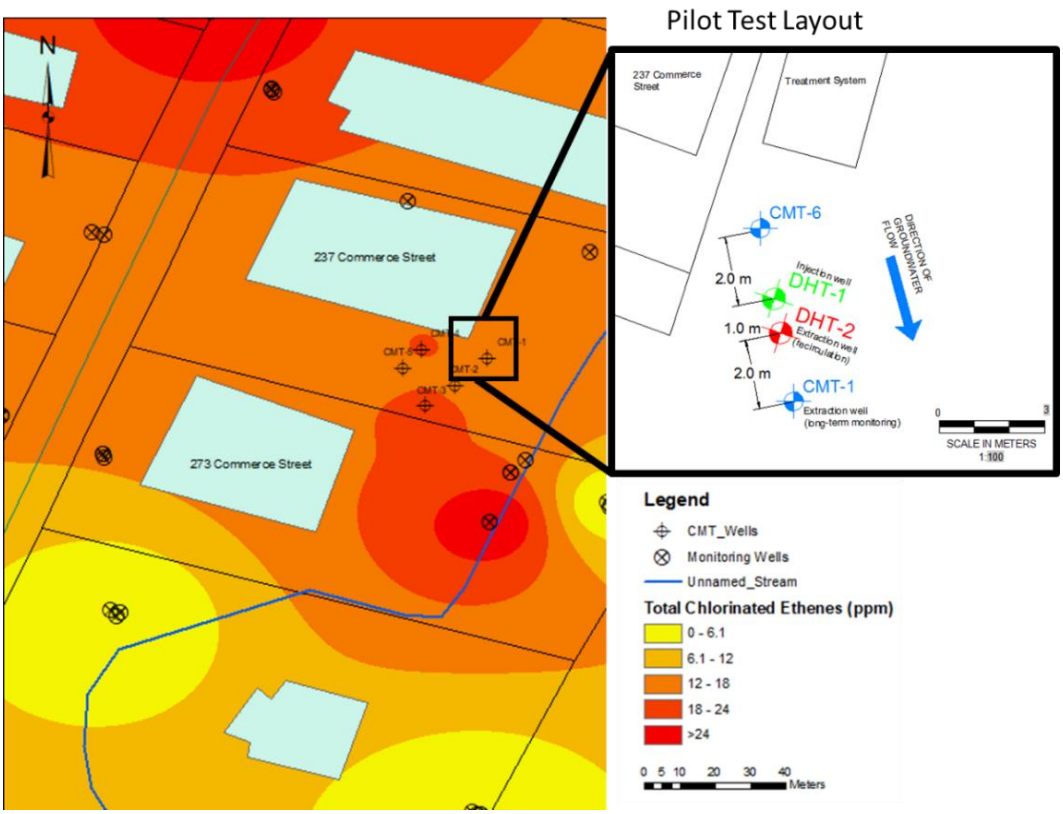

Figure 4-1. Interpolated total chlorinated ethene (TCE, *cis*-DCE, VC) concentrations (ppm) in August-September 2014 for deep (>9.1 m below surface) groundwater samples and location and layout of pilot test (inset). The interpolation was based on available concentration measurements from wells displayed in the maps.

Prior to bioaugmentation, the average aqueous *Dhc* abundance was 1.88×10^{6} ($\pm8.35\times10^{5}$) cells/L across the 9.48-9.63 m bgs and 10.9-11.1 m bgs channels of the CMT-wells with no observed spatial trends. In a soil sample collected from the 10.9 to 11.9 m bgs depth of the CMT-4 borehole, total *Dhc* abundance was 1.08×10^{7} cells/gram of wet soil. The reductive dehalogenase (RDase) genes, *vcrA (*implicated in metabolic transformation to ethene) and *tceA* (implicated in co-metabolic transformation to ethene), were not detected. Although the *Dhc* 16S rRNA gene abundance measured suggested a sufficient population for dechlorination,[38,39] the lack of *Dhc* cells harboring specific RDase genes explained the accumulation of *cis*-DCE and the absence of VC and ethene observed at the site and suggested the need for bioaugmentation. *Dhc* abundance was measured by quantitative

polymerase chain reaction (qPCR) of the *Dhc* 16S rRNA gene which is present as a single gene copy per *Dhc* cell.[37]

4.3.2 Design and implementation of the Pilot Test

The pilot test consisted of two injection and monitoring wells (DHT-1 and DHT-2) installed as 2-inch diameter PVC-wells, screened between 10.1-10.7 m bgs. In addition, a sixth CMT well, CMT-6, with 6 screened intervals (6.25-6.40, 7.92-8.08, 8.84-8.99, 9.60-9.75, 10.4-10.5, and 11.1-11.3 m bgs) was situated 5 m upgradient of CMT-1, to allow monitoring of constituents entering the pilot test area. A previously installed CMT well, CMT-1, screened similarly to CMT-6, was used as an extraction well during the pilot test. Pumping rates for each phase of the pilot test were determined using a regional groundwater flow simulation model implemented in MODFLOW Flex and capable of predicting the residence time of groundwater between DHT-1 and DHT-2 based on the extraction rate in CMT-1 (Appendix B8.0).

The treatment system consisted of four pumps and two tanks housed in a treatment trailer with high density polyethylene tubing (HDPE) tubing connected to wells DHT-1, DHT-2, and CMT-1. Three Masterflex peristaltic pumps (Cole Parmer; Vernon Hills, IL) were used to extract groundwater from DHT-2 and CMT-1 while a Series I HPLC pump (Scientific Systems Inc.; State College, PA) was used to inject amendments into DHT-1. The effluent treatment system consisted of a submersible pump, a 10-micron bag filter, a 0.1-micron bag filter, and a 208.2 L (55-gallon) vessel of activated carbon. After treatment, extracted water was discharged to the unnamed brook east of the site.

The pilot test system was operated in three configurations over the course of the experiment with the parameters shown in Table 4-1a. Immediately preceding and throughout the pilot test, groundwater samples were collected from CMT-6, CMT-1, DHT-1, and DHT-2 twice per month for chloroethene and volatile fatty acid (VFA) analysis, and monthly for

biological analysis using the methods described in Appendix B2.0. During operation of the pilot test, groundwater samples from the extraction wells were collected from a sample port in the treatment trailer connected to the extraction tubing without additional purging.

Table 4-1. Operating parameters for a) Pilot test and b) Aquifer cell experiment

a)

Phase:	Bromide Tracer/lactate loading	Lactate Recirculation	Bioaug-mentation	Lactate/ Biomass Recirculation	Long-term Monitoring	Monitoring w/ Reduced Flow Rate
Duration (days)	4	3	1	14	62	44
Pore Water Velocity (cm/d)	14.3	14.3	14.3	7.15	7.15	4.76
Residence Time (days)	7	7	7	14	14	21
Injections	10 mM bromide; 5 mM lactate; 0.85 g/L KB-1 Primer®	5 mM lactate; 0.85 g/L KB-1 Primer®	1.5 L of KB-1® inoculum	5 mM lactate; 0.85 g/L KB-1 Primer®	1 pulse of 13.1 mM lactate (14 days)	1 pulse of 37 mM lactate (22 days)

b)

Phase:	Bromide Tracer/TCE loading	Lactate Recirculation	Bioaug-mentation	Lactate/ Biomass Recirculation	Long-term Monitoring	Monitoring w/ Reduced Flow Rate	Monitoring w/ Higher Flow Rate
Duration (days)	37	10	1	14	88	74	9
Pore Water Velocity (cm/d)	15	15	7.5	7.5	7.5	3.75	11.3
Residence Time (days)	4	4	8	8	8	16	5.3
Injections	10 mM bromide; 50 mg/L erioglaucine A; 0.3 mM TCE	0.3 mM TCE; 10 mM lactate	100 mL of dilute KB-1® inoculum	0.3 mM TCE; 10 mM lactate	0.3 mM TCE; 2 pulses of 10 mM lactate (7 days each)	0.3 mM TCE; 1 pulse of 5 mM lactate (14 days)	0.3 mM TCE; 1 pulse of 5 mM lactate (4 days)

- **Step 1 – Lactate Recirculation (Establish Bioactive Zone)**

During Step 1, groundwater was extracted from DHT-2 and reinjected into well DHT-1 at a target flow rate of 16.5 mL/min to achieve a target residence time of 7 days (seepage velocity of 14 cm/day). A 38 L pulse containing 11.7 g/L bromide (conservative tracer), 5 mM lactate (a microbial electron donor and carbon source), and 0.85 g/L KB-1 Primer® (used to create more ideal conditions for bioaugmentation, e.g., neutral pH, dissolved oxygen below 0.5 mg/L and ORP below -150 mV [SiREM, Guelph, ON]) was delivered

over 1.5 days at approximately 17 mL/min, as shown in Table 4-1. Following this 38 L pulse, extracted groundwater was amended with 5 mM lactate and 0.85 g/L of KB-1 Primer® prior to reinjection. A bromide probe (Cole Parmer; Vernon Hills, IL) was placed in the flow stream from the DHT-2 pump to monitor the breakthrough of the bromide pulse (Appendix B10). Additional bromide and VFA samples were collected from the extracted water to quantify the breakthrough of injected fluids. Step 1 continued for 7 days to ensure that lactate passed through the target zone, anoxic conditions were established, and electron donor was available for the PCE-to-ethene dechlorinating consortia, introduced in Step 2.

- **Step 2 – Bioaugmentation (Distribute Microorganisms)**

Step 2, bioaugmentation, encompassed inoculation of the site and maintenance of conditions suitable for the growth of the dechlorinating consortia. During Step 2, the recirculation system continued to operate between wells DHT-1 and DHT-2. On day 8, 1.5 L of a PCE-to-ethene microbial inoculum, KB-1® (SiREM; Guelph, ON), was delivered into well DHT-1 to establish an initial *Dhc* population of approximately 10^6 cells/L within the 1 m treatment zone. The system continued to operate with a 7-day residence time (17 mL/min) in a recirculation mode (with lactate and KB-1 Primer® amendment) in an effort to create an anoxic zone conducive to the growth and activity of the introduced KB-1® inoculum. Following the completion of bromide tracer measurements in the downgradient well (DHT-2), system operation was continued in a recirculation mode for an additional week at a decreased flow rate of 8.5 mL/min, which corresponds to a seepage velocity of 7 cm/day and a doubled residence time of 14 days (Table 4-1a). This longer residence time within the treatment zone was designed to promote complete detoxification of TCE to ethene.

- **Step 3 – Pumping and Monitoring (Assess Performance)**

Following Step 2, the target zone between DHT-1 and DHT-2 had a well-established community of dechlorinating organisms and conditions suitable for organohalide

respiration. At this time, the recirculation system was disconnected and wells DHT-1 and DHT-2 were used for groundwater monitoring. During Step 3, groundwater was extracted from the lowest three depths of CMT-1 at approximately 450 mL/min (14-day residence time between DHT-1 and DHT-2; 7.15 cm/d pore water velocity) to maintain hydraulic control of the contaminant plume and ensure that VOC-impacted groundwater migrated into the bioactive zone and was captured by monitoring wells (Table 4-1a). After 62 days (76 days following bioaugmentation), the extraction rate was reduced to 300 mL/min to provide a longer residence time of 21 days between DHT-1 and DHT-2 (4.76 cm/day pore water velocity).

During Step 3, 2 pulses of lactate and KB-1 Primer® were introduced into DHT-1 to maintain conditions suitable to biotransformation of TCE to ethene. The first pulse of 75 L of 13.1 mM lactate and 0.85 g/L KB-1 Primer® was injected at 3.5 mL/min over the course of 14 days beginning 16 days after bioaugmentation. The second pulse was also 75 L, containing 37 mM lactate and 3.4 g/L KB-1 Primer® injected at 2.8 mL/min over the course of 23 days, beginning 48 days after bioaugmentation. The injection rates and lactate concentrations were selected based on predictions of the pore water volume flowing through the treatment zone (using the regional groundwater flow model [Appendix B8.0]) so that a concentration of at least 5 mM VFAs was achieved downgradient.

4.3.3 Aquifer cell experiment

A 63.5 cm (length) × 38 cm (height) × 1.4 cm (thickness) aquifer cell (Figure 4-2) was constructed with an aluminum frame held by two 1.4 cm thick glass panels and configured with eighteen sampling ports, aligned in four vertical columns of four or five ports.[35] Silty clay recovered from the 12.2 to 12.8 m depth of borehole CMT-2 at the Commerce Street Site was dried, ground with a mortar and pestle, then re-saturated with a 0.76 mM TCE solution and emplaced in the bottom 3 cm of the aquifer cell to create a contaminated lower confining layer. Above the clay, the aquifer cell was packed under water saturated

conditions with soil materials collected from the 6.40 to 10.7 m depth of borehole DHT-2 at the Commerce Street site, collected as described in Appendix B. This core was opened in an anoxic chamber (Coy Laboratory Products, Inc; Grass Lake, MI) and separated into sections representing 15 cm (6-inches) of borehole depth. Each discrete section was homogenized by mixing with a scoop, placed in Ziploc® bags, then packed in the aquifer cell within 1 hour to maintain the native microbial population. The discrete sections of soil cores were placed in 4 to 6 cm layers in the aquifer cell to recreate the stratigraphy of the field site (Figure 4-2). Details of the permeability (B7.2), grain size (B7.2), organic carbon (B7.3), and sorption capacity (B7.3) of Commerce Street materials are provided in the SM (Appendix B).

After packing, flow was established in the aquifer cell using a constant head influent system as described by Cápiro et al. (2015). Anoxic site groundwater (Appendix B1.0) was prepared in a 5 L Mariotte bottle and the flow rate was controlled by adjusting the heights of the influent and effluent to maintain a flow rate between 0.10 and 0.20 mL/min; a corresponding seepage (pore-water) velocity of 12.5 to 25 cm/day and a residence time of 4.8 to 9.5 days. A bromide and erioglaucine A (blue dye) tracer test was performed in the aquifer cell as described in Appendix B10.0.

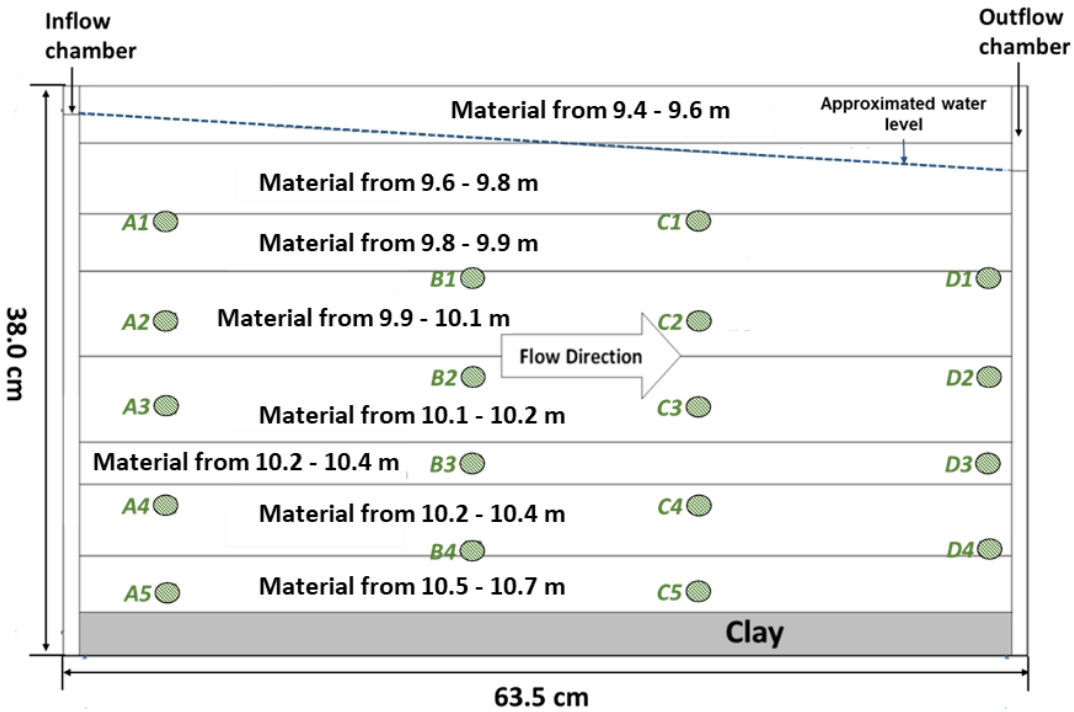

Figure 4-2. Aquifer cell configuration and sampling port locations: ◍. Packed layers indicated by horizontal lines.

After the tracer experiment, the aquifer cell was operated in several phases to mimic the pilot test as shown in Table 4-1b. To establish a uniform background contaminant concentration, the aquifer cell was flushed with a 0.3 mM (40 mg/L) TCE solution, prepared with anoxic site groundwater, at a flow rate of 0.2 mL/min (25 cm/day seepage velocity), for a period of 32 days (Table 4-1b). The aquifer cell was then reconfigured for recirculation to mimic the pilot test. Here the effluent was removed with a peristaltic pump (Cole Parmer; Vernon Hills, IL) at a rate of 0.1 mL/min (12.5 cm/day seepage velocity), amended with 100 mM lactate stock at 0.01 mL/min to achieve a concentration of 10 mM lactate, and reinjected into the aquifer cell (Table 4-1b).

After 10-days of recirculation, the aquifer cell was bioaugmented with KB-1® inoculum. The SiREM-provided inoculum was first diluted 1:320 in anoxic site groundwater amended with 10 mM lactate. Twenty mL was then injected at a rate of 1 mL/min into each of 5 sampling ports nearest the inlet (matching the pilot test injection in the upgradient well),

using a syringe pump to yield a target concentration of approximately 10^6 *Dhc* cells/L of pore water. This cell abundance has been demonstrated sufficient for complete transformation of TCE to ethene.[49,453,454] Recirculation with lactate amendment continued for an additional 14 days following bioaugmentation to distribute the inoculum throughout the aquifer cell (Table 4-1b).

After recirculation, the flow regime was changed back to a head-driven system without recirculation, to match the long-term monitoring phase of the pilot test. An influent solution of anoxic groundwater, amended with 0.3 mM TCE, was employed for the remainder of the experiment. A flow rate of approximately 0.1 mL/min was maintained for 88 days, after which the flow was reduced to 0.05 mL/min for 64 days, then increased to 0.15 mL/min for the final 15 days (Table 4-1b). Lactate pulses of 1.0 L (approximately 1 pore volume) were introduced throughout the experiment. Over the course of the experiment lactate was introduced as 2 pulses of 10 mM during the first long-term monitoring phase, 1 pulse of 5 mM during the monitoring with reduced flow rate phase, and 1 pulse of 5 mM during the monitoring with higher flow rate phase (Table 4-1b). The pulses began 17.8, 59.7, 102, and 168 days after the end of the recirculation phase (Figure 4-5).

4.4 Results and Discussion

4.4.1 Pilot test

At the end of recirculation, VFA analysis of samples collected from DHT-1 and DHT-2 contained lactate, acetate, and propionate with a total VFA concentration of 12.8 mM in the injection well and 6.0 mM in downgradient well DHT-2 as shown on Figure 4-3. During subsequent lactate pulses, lactate and acetate were measured in the injection well while only acetate and propionate were measured downgradient. This mixture of acetate and propionate (lactate fermentation products) indicated an active microbial community and distribution of electron donor throughout the pilot test area. In well DHT-2, VFA concentrations decreased after each pulse but remained at concentrations above 0.28 mM

total VFAs in all samples collected. These results indicate enough mixing of VFAs in the pilot test area to maintain detectable quantities between lactate pulses, supporting conditions suitable for MRD.

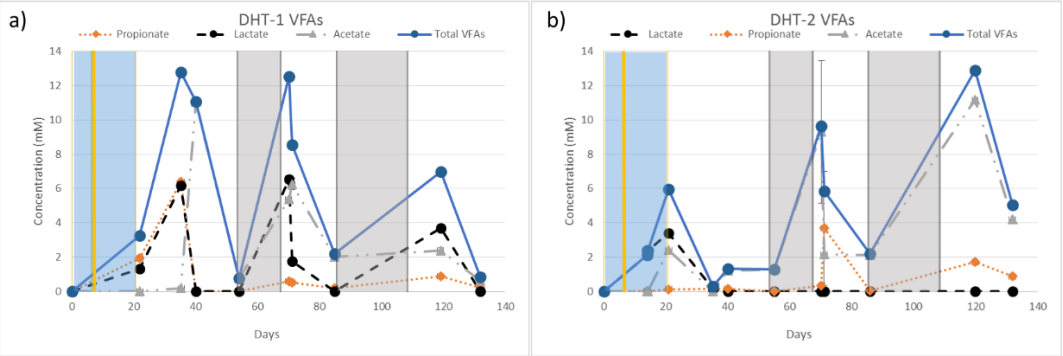

Figure 4-3. VFA concentrations in injection well DHT-1 and downgradient well DHT-2 during pilot test. Vertical lines in each panel represent, from left to right: 1. Beginning of recirculation with lactate; 2. Bioaugmentation 3. End of recirculation; 4. Beginning of lactate pulse; 5. End of lactate pulse; 6. Beginning of lactate pulse; and 7. End of lactate pulse.

Prior to beginning the pilot test, *cis*-DCE was the only chlorinated ethene detected in the pilot test area with concentrations of 0.14 mM in the CMT-6 channel 10.4-10.5 m bgs (upgradient) and 0.11 mM in well DHT-2, the downgradient pilot test well monitored throughout the experiment. Over the course of the pilot test, the *cis*-DCE concentration upgradient (CMT-6) remained steady but slightly higher than the initial sample, averaging 0.17 (±0.013) mM (Figure 4-4). Downgradient of the pilot test, VC and ethene were first detected 14 days after bioaugmentation (the residence time between DHT-1 and DHT-2 during this phase), reaching concentrations of 0.015 mM VC and 0.006 mM ethene after 33.5 days (day 40.5; Figure 4-4).

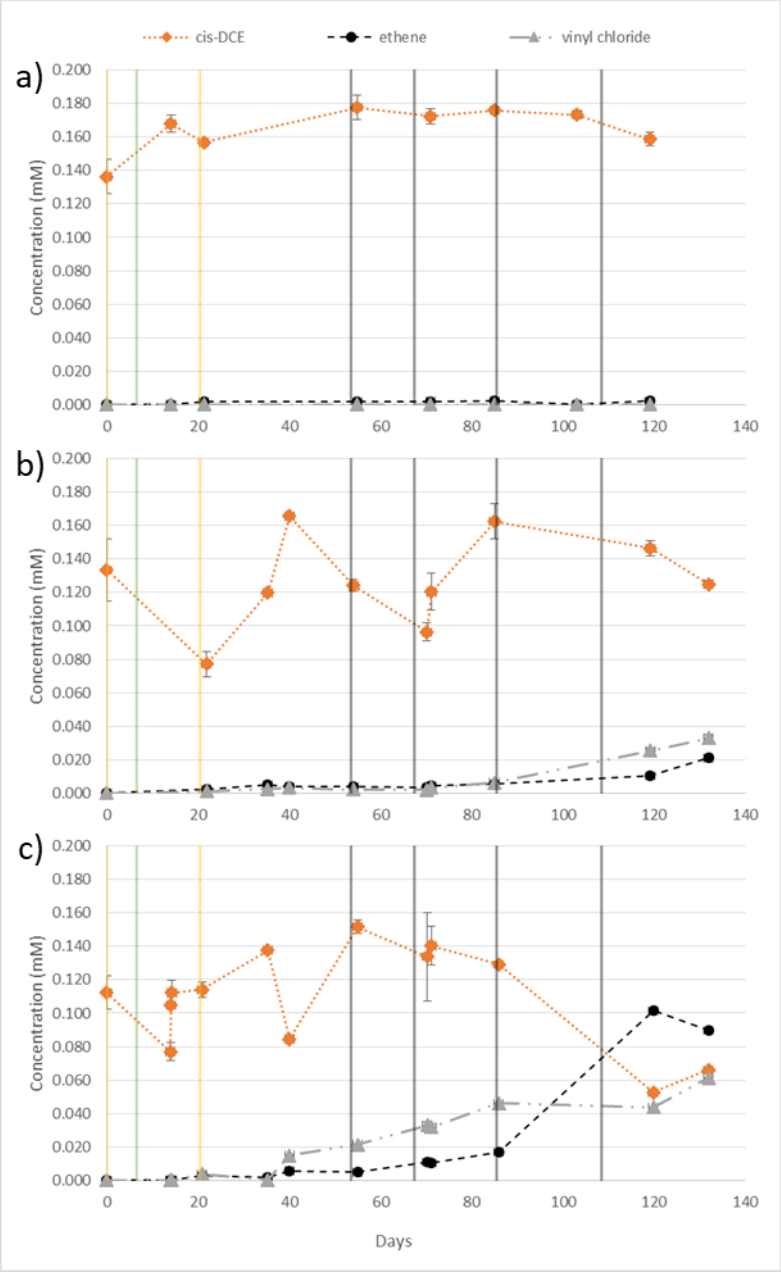

Figure 4-4. Chlorinated ethene and ethene concentrations in a) CMT-6-2, upgradient of injection well, b) DHT-1, injection well, and in c) DHT-2, downgradient of injection well. Vertical lines represent, from left to right: 1. Beginning of recirculation with lactate; 2. Bioaugmentation 3. End of recirculation; 4. Beginning of lactate pulse; 5. End of lactate pulse; 6. Beginning of lactate pulse; and 7. End of lactate pulse.

After an additional 15 days, the VC and ethene concentrations remained nearly unchanged (0.021 and 0.005 mM, respectively). During this period, groundwater quality parameters, including ORP and pH remained stable and conducive to MRD. Thus, the likely explanation for the lack of continued dechlorination between day 40.5 and 55.5 (Figure 4-

4) was decreasing electron donor availability. This conclusion is supported by the measurements of total VFA concentrations in DHT-2 which were reduced to 0.28 mM 14 days after ending the lactate recirculation phase (day 35; Figure 4-3). After the first lactate pulse, VC and ethene concentrations continued to increase reaching concentrations of 0.046 and 0.017 mM, respectively, 79.4 days after bioaugmentation (day 86.4) with the *cis*-DCE concentration decreasing slightly from a peak of 0.15 to 0.13 mM. During this phase of the pilot test, conditions were conducive to MRD, the *Dhc* population reached a stable abundance (Figure B-6), and was capable of transforming a portion of the total chlorinated ethenes to ethene (5%). Thus, the lack of complete dechlorination to ethene was likely due to insufficient residence time of contaminants and amendments in the region between DHT-1 and DHT-2.

In order to assess the effect of residence time on the extent of dechlorination, the extraction rate in DHT-1 was reduced to increase groundwater plume residence time in the pilot test area from 14 to 21 days (4.8 cm/day pore water velocity) at the beginning of the second lactate pulse (day 82, 75 days following bioaugmentation). The maximum ethene concentration of 0.10 mM measured during the pilot test occurred on day 120 (113 days following bioaugmentation, 38 days after reducing the flow rate, and 5 days after the end of the second lactate pulse), while the VC concentration remained stable at 0.04 mM and the *cis*-DCE concentration decreased to 0.053 mM. In the final samples collected 12 days later, the ethene concentration in DHT-2 began to decrease slightly while VC and *cis*-DCE concentrations increased, once again indicating a decrease in electron donor availability. Throughout the experiment, the ORP and pH in the treatment zone were maintained at -330.0 to -225.2 mv and 6.8 to 6.9, respectively, by the addition of KB-1 Primer®.

By reducing the extraction rate to increase residence time by 50%, the proportion of ethene in the downgradient well increased from approximately 5% of chlorinated ethene and

ethenes by molar mass (total ethenes) to 46% while the proportion of *cis*-DCE declined from 79% to 28%, demonstrating the importance of maintaining sufficient residence time to achieve complete dechlorination of TCE to ethene.

Total *Dhc* abundance, measured in samples collected from wells DHT-1 and DHT-2 during the pilot test, increased from 6.2×10^4 and 4.9×10^4 cells/L, respectively, prior to bioaugmentation to 1.8×10^8 and 2.7×10^6 cells/L at the end of the recirculation phase (Figure B-6). After an additional 32 days, *Dhc* abundance in DHT-1 and DHT-2 were nearly identical at 5.0×10^8 cells/L and remained constant until the flow rate was reduced, after which it continued to increase to a maximum abundance of 1.8×10^{10} and 1.6×10^{10} cells/L in samples collected from DHT-1 and DHT-2, respectively.

Bioaugmentation with KB-1® successfully provided a viable *Dhc* population with sufficient abundance to transform *cis*-DCE to ethene over the duration of the pilot test as seen in the chlorinated ethene and ethene results (Figure 4-4). The lactate pulses were rapidly fermented (Figure 4-3) and provided a growth substrate to increase the *Dhc* population (Figure B-6). When the residence time of contaminants and amendments in the pilot test area was 14 days, the growth of *Dhc* stalled and the extent of *cis*-DCE dechlorination remained constant. Reducing the pumping rate in CMT-1 increased the residence time of contaminants and amendments in the region between DHT-1 and DHT-2 to 21 days, increasing the extent of transformation of *cis*-DCE to ethene and allowing the *Dhc* population to continue to increase in abundance.

4.4.2 Aquifer cell experiment

As soon as lactate was introduced to the aquifer cell, at the beginning of recirculation, a portion of the influent TCE was transformed to *cis*-DCE by the native microbial population, similar to conditions at the site (Figure 4-5a). After bioaugmentation, TCE was no longer detected and effluent ethene concentrations began to increase. The ethene

concentration in the effluent peaked at 0.31 mM at the end of the recirculation phase as chlorinated ethenes were reintroduced in the influent as *cis*-DCE and VC and had additional time to be dechlorinated. Following recirculation, the electron donor (VFAs) was flushed from the aquifer cell to a minimum concentration of 0.38 mM (Figure 4-5b) and the effluent ethene concentration dropped to 0.10 mM as the *cis*-DCE and VC concentrations increased from 0.09 and 0.01 mM to 0.17 and 0.02 mM, respectively.

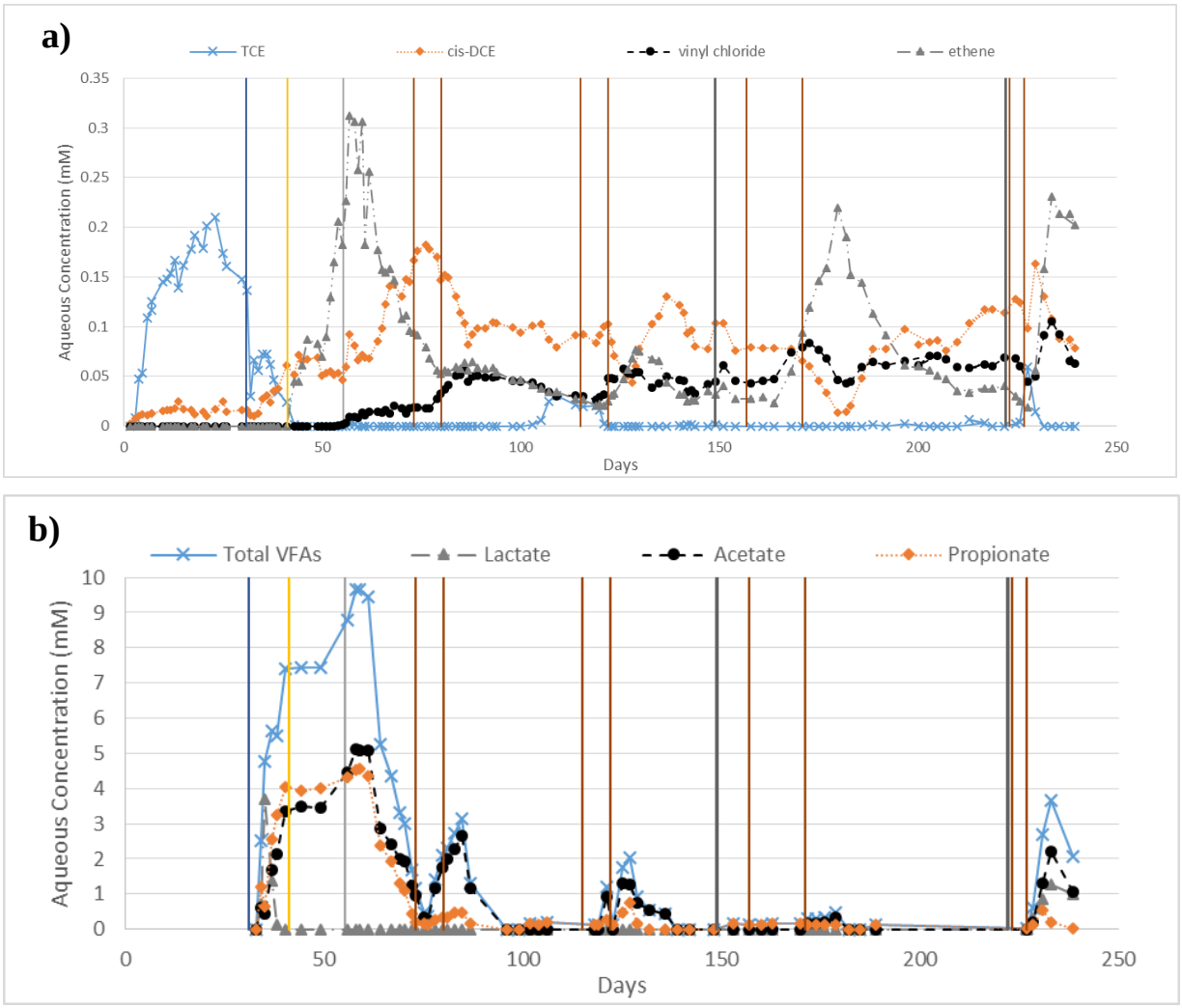

Figure 4-5. a) Chlorinated ethene and ethene concentrations in aquifer cell effluent. b) VFA concentrations in aquifer cell effluent. Vertical lines represent, from left to right: 1. Beginning of recirculation with lactate; 2. Bioaugmentation 3. End of recirculation; 4. Beginning of lactate pulse; 5. End of lactate pulse; 6. Beginning of lactate pulse; 7. End of lactate pulse; 8. Decrease in flow rate; 9. Beginning of lactate pulse; 10. End of lactate pulse; 11. Increase in flow rate; 12. Beginning of lactate pulse; 13. End of lactate pulse.

At each lactate pulse, effluent VFAs increased for a period of 1 to 2 PVs (Figure 4-5b) and the influent TCE was degraded to a mixture of *cis*-DCE, VC, and ethene (Figure 4-5a). TCE, comprising up to 18% of the total ethenes, was observed in the effluent 5 PVs after the first lactate pulse as the electron donor was limited to the point that TCE to *cis*-DCE transformation was impeded. A majority of the TCE introduced into the aquifer cell was transformed into *cis*-DCE, VC, and ethene for up to 4.4 PVs (35 days) after a lactate pulse. Analysis of VFAs in the aquifer cell effluent, however, revealed large spikes in concentration, primarily acetate, lasting only 1 to 2 PVs after each lactate pulse, with VFAs were no longer detected afterward. The absence of measurable VFAs coupled with measurements of continued dechlorination suggests that an electron donor and carbon source was present in the background groundwater solution as dissolved organic carbon (Figure 4-5b).

After the second lactate pulse (day 115 [PV 13.8] to day 122 [PV 14.6]), while the flow rate was maintained at 0.1 mL/min to provide a 8-day residence time, the influent TCE was transformed to a combination of to 60% cis-DCE, 23% VC, and 17% ethene on a molar basis at the effluent. Reducing the flow rate to 0.05 mL/min, resulting in a 16-day residence time, resulted in an effluent containing 5% cis-DCE, 17% VC, and 78% ethene, after introducing a lactate pulse. When the flow rate was then increased to 0.15 mL/min and a 5mM lactate pulse was introduced, the proportion of ethene in the effluent decreased to 54% while the VC and *cis*-DCE proportions increased to 23% and 22%, respectively.

Dhc abundance was measured in aqueous samples collected from the sampling ports at three times during the aquifer cell experiment: 1 to 2 days before the end of recirculation, 20 to 25 days after the first lactate pulse, and at the conclusion of the experiment. These data exhibit little change in the total *Dhc* abundance, with an average across the ports of 3.26×10^{8} ($\pm 5.02\times10^{8}$), 7.80×10^{8} ($\pm1.68\times10^{9}$), and 2.69×10^{8} ($\pm2.59\times10^{8}$) cells/L in each

round of sampling, respectively. The data suggest that a sufficient population of *Dhc* was distributed throughout the aquifer cell during recirculation and remained relatively constant over the course of the experiment.

The extent of ethene formation was highly dependent on the residence time and the availability of electron donor in the heterogeneous layers. The erioglaucine A tracer test revealed a high permeability layer in the center of the aquifer cell with lower permeability layers above and below (Appendix B10.0). Numerical modeling performed by Lurong Yang estimated a permeability of 3.4×10^{-12} m^2 in the faster flowing center region and permeabilities of 1.4×10^{-12} m^2 above and 1.0×10^{-12} m^2 below. Due to this heterogeneity, the residence time in the high permeability layer was lower than the average residence time in the aquifer cell. This lower residence time was not sufficient to fully transform influent TCE to ethene, resulting in the observed mixture of *cis*-DCE, VC, and ethene in the effluent. As the aquifer cell was packed with material from the field site and the layer were constructed to mimic *in situ* heterogeneity (Figure 4-2), a similar high permeability region was likely present in the pilot test. The presence of a high permeability region in the aquifer cell and pilot test contributed to the measurements of incomplete dechlorination as *cis*-DCE flowed through these regions without sufficient residence time to be transformed to VC and ethene by *Dhc*.

The results of this aquifer cell and pilot test study provide insight into the effect of soil heterogeneity on residence time and corresponding dechlorination. Increasing the average residence time increased the extent of chlorinated ethene biodegradation and can be a useful tool if incomplete dechlorination is observed and subsurface heterogeneity is not well characterized.

4.5 Conclusions

The average residence time of contaminants and amendments in a bioactive zone determined the extent of TCE biodegradation in this in this comparative study incorporating a laboratory aquifer and field pilot test of similar dimensions. Increasing the average residence time from 8 days to 16 days (7.5 to 3.8 cm/day seepage velocity) in the aquifer cell experiment increased the proportion of ethene in the effluent from 17% of total ethenes on a molar basis to 78% ethene. Similarly, in the field-pilot test, a 50% increase in average residence time (from 14 days to 21 days [7.2 to 4.8 cm/day seepage velocity]) increased the proportion of ethene in the downgradient well from 5% to 46% of total ethenes on a molar basis.

The results of this work also provide evidence that heterogeneity in soil properties influenced the complete dechlorination of TCE to ethene. The aquifer cell tracer experiment revealed the existence of a high permeability layer in the center of the system. As the aquifer cell was packed to mimic the conditions in the pilot test area, it is likely that similar heterogeneity exists at the field site. Due to this heterogeneity, local residence times varied from the predicted average residence time and allowed contaminants in the treatment zone to reach the downgradient location without being fully transformed to ethene. Increasing the average residence time in the treatment zone is a useful tool to increase the extent of chlorinated solvent biodegradation, especially if aquifer heterogeneity is unknown.

The coupling of a pilot test and laboratory experiment revealed that:

- Increasing residence time increased the extent of ethene formation.
- Spatial heterogeneity in aquifer hydraulic conductivity caused a portion of chlorinated ethenes to pass through the treatment area without being fully

transformed, despite an average residence time predicted to yield complete dechlorination.

The data collected during these experiments was used in numerical models by Lurong Yang to further explore the impact of residence time and electron donor delivery on MRD. This work will be combined for publication.

Acknowledgements

Funding for this research was provided by the Strategic Environmental Research and Development Program (SERDP) under Contract W912HQ-13-C-0011, Project ER-2311: Development of an Integrated Field Test/Modeling Protocol for Efficient *In Situ* Bioremediation Design and Performance Uncertainty Assessment. The contents of this document have not been subject to agency review and do not necessarily represent the views of the sponsoring agency.

Appendix B. Supplementary data

The supplementary material contains additional details on the porous media, chemicals, and growth medium; chemical, biological, and physical analytical methods; well installation and groundwater sampling methods; additional site background data; and tracer test results.

5.0 *Dehalococcoides mccartyi* reductive dehalogenase gene expression during pulsed lactate delivery

The contents of this chapter are currently being prepared as a manuscript for publication.

5.1 Abstract

The potential for *in situ* bioremediation of chlorinated solvents is often evaluated by the abundance of *Dehalococcoides mccartyi (Dhc)* 16S rRNA and reductive dehalogenase (RDase) gene DNA abundance. Due to the long life of DNA in the environment, these measurements do not measure which cells are actively performing microbial reductive dechlorination (MRD), the process of detoxifying tetrachloroethene and trichloroethene to ethene. Measurements of RNA transcripts are thought to better measure active MRD as they decay rapidly when electron acceptors are depleted, with a half-life of 4 to 24 hours. This study examined *vcrA* and *bvcA* RDase gene and transcript abundance in a laboratory aquifer cell experiment and *in situ* field pilot test, both bioaugmented with KB-1® (SiREM; Guelph, ON) and using pulsed lactate injections to provide an electron donor and carbon source. In the aquifer cell experiment, after electron donor was depleted, *vcrA* RNA transcripts were found to decrease by 7.46-fold over 47 days, while the abundance of *vcrA* DNA gene copies remained constant (0.47-fold decrease) over the same time period. The exponential decay of *vcrA* transcripts corresponded to an average half-life of 15.3 (±1.68) days that is in stark contrast to the 4.8- to 24-hour half-life reported for *vcrA* when electron acceptor is limited. In the pilot test, *vcrA* and *bvcA* DNA abundance increased 2.13- and 2.49-fold, respectively, 34 days after an electron donor pulse and remained stable. The abundance of *vcrA* and *bvcA* RNA transcripts also increased by a similar amount, 2.65- and 2.49-fold, respectively, but the increased lagged the increase in DNA abundance by 12 days. This study supports the current practice of pulsed electron donor delivery as *Dhc* strain specific RNA is not rapidly depleted when electron donor is limited and will remain up-regulated as cells await future electron donor amendments.

5.2 Introduction

In situ bioremediation (ISB) of chlorinated solvents relies on *Dehalococcoides mccartyi (Dhc)* strains to fully transform chlorinated ethenes to non-toxic ethene.[8,9,19,290,291] To evaluate the potential for biotransformation, total *Dhc* abundance and specific RDase gene abundance are often measured by quantitative polymerase chain reaction (qPCR) from extracted DNA.[40,41,309] Quantifying RDase gene abundance through DNA provides information on the *Dhc* strains that are present and their capability to perform reductive dechlorination, but it does not measure which cells are actively performing microbial reductive dechlorination (MRD). RNA transcripts may provide a better measure of the potential for dechlorination activity as they are only present when the RDase protein is being produced and have been demonstrated to decay rapidly relative to DNA in the absence of chlorinated ethenes (electron acceptor).[42]

Electron acceptor availability has been correlated with RDase gene abundance and expression in laboratory batch experiments.[11,42,455,456] Waller et al. (2005) found that the *bvcA* gene was transcribed regardless of which chlorinated electron acceptor was present and that *vcrA* was transcribed during TCE degradation. *tceA* transcription has been found to be upregulated during TCE and DCE exposure but not during exposure to other chlorinated compounds, including PCE, vinyl chloride (VC), and 2,3-dichlorophenol.[347,458] The *bvcA* and *vcrA* genes may be part of a two-component signal transduction system where control of these RDase genes responds to multiple stimuli.[457] The *tceA* gene, on the other hand, is located in a different part of the genome, not near this transcriptional regulator, which may cause this gene to respond to different stimuli.[457]

In a field study conducted at a TCE-contaminated landfill at the Fort Lewis military base (Tacoma, WA), the *tceA* gene was expressed in RNA transcripts in lower amounts than expected based on the gene copies detected in DNA which may indicate that there are other

factors impacting the expression of RDase genes in more complex systems.[373] In a survey of multiple field sites, Liang et al. (2017) correlated *vcrA* transcript abundance with DCE, VC, and methane concentrations, while *bvcA* transcript abundance was correlated only with *cis*-DCE concentration. Higher temperatures cause *vcrA* expression to be upregulated, but this increase did not correlate to increased dechlorination activity.[351] Similarly, Amos et al. (2008) found that RDase transcripts did not correlate with dechlorination activity following exposure to oxygen and that the detection of RNA did not, on its own, indicate active cells. No studies have examined the impact of electron donor availability on *Dhc* RDase gene transcripts. Understanding the conditions that favor RDase expression is essential to designing systems that will fully transform chlorinated ethenes to ethene and to prevent accumulation of *cis*-DCE and VC.

In a flowing system with intermittent delivery of electron donor, typical of *in situ* bioremediation systems, both electron acceptor and electron donor concentration and composition vary over time, likely affecting the expression of RDase genes, as measured by RNA transcript abundance. To assess the impact of intermittent electron donor delivery on RDase transcript abundance, samples were collected during a two-dimensional aquifer cell experiment and a field pilot test performed at the Commerce Street Superfund Site in Williston, VT. Both experiments were performed under similar conditions with pulsed lactate amendment and bioaugmentation using KB-1® (SiREM; Guelph, ON). RDase DNA and RNA were measured to determine the expression of RDase genes in response to electron donor delivery to further the understanding of conditions under which RDase genes are expressed or repressed.

5.3 Methods

5.3.1 Aquifer cell and pilot test experiments

Aqueous samples for RDase DNA and RNA analysis were collected during the aquifer cell and pilot test experiments described in Sections 4.3.2 and 4.3.3, respectively. Samples collected during these experiments were preserved with RNAlater™ (Invitrogen; Carlsbad, CA), and stored at -80°C for extraction and analysis. From the aquifer cell, samples from an upgradient column of ports (ports 1A, 1C, and 1E [Figure5-1]) and a corresponding downgradient column of ports (ports 3A, 3C, and 3E [Figure 5-1]) were selected for analysis. Samples collected over 3 rounds (167-172, 182-185, and 214-218 days after bioaugmentation) had been preserved with RNAlater™ during the experiment and were processed as described below. These samples were collected at the conclusion of a lactate pulse and as lactate and other VFAs were flushed from the system to examine the impact of decreasing electron donor availability (Figure 5-3). Samples from pilot test well DHT-2 (Figure 4-1), collected on days 86, 120, and 132 of the pilot test, were selected for analysis as they were collected at the start of lactate addition in upgradient well DHT-1 (day 86) and after the lactate pulse ended (days 120 and 132).

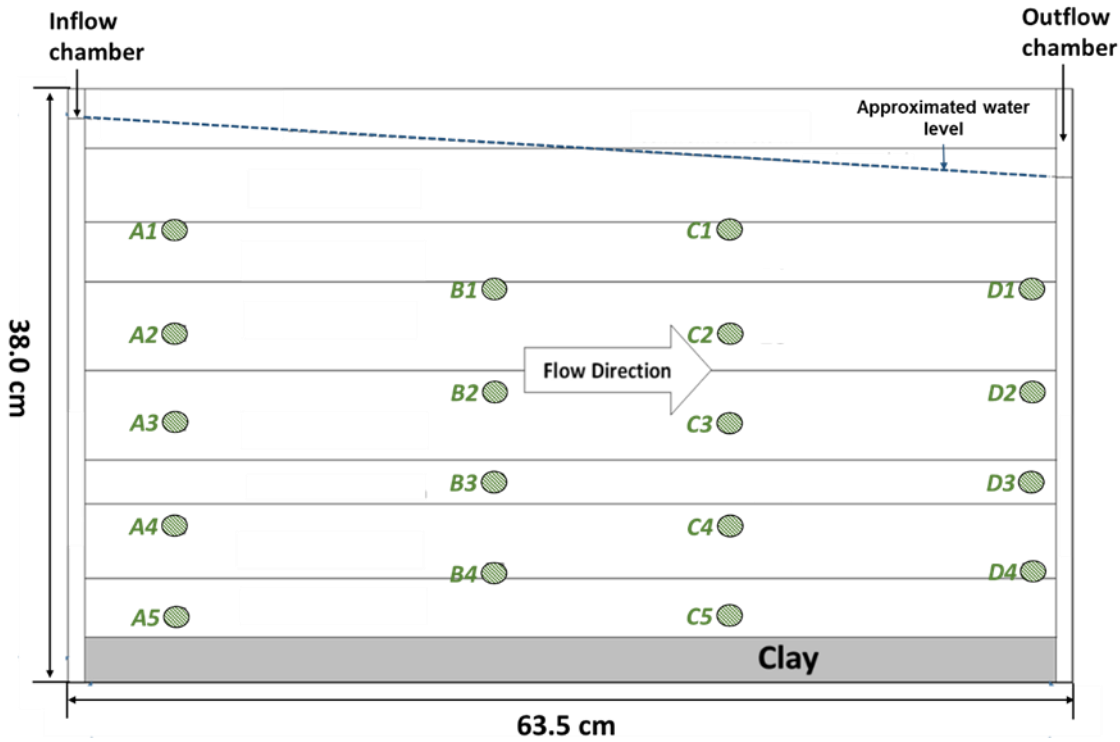

Figure 5-1. Aquifer cell configuration and sampling port locations: ◍. Packed layers indicated by horizontal lines.

5.3.2 RNA/DNA extraction and transformation

For field samples, where a large quantity of cells was collected via filtration of 340 to 800 mL of groundwater through a Sterivex cartridge (MilliporeSigma; Burlington, MA), the MoBio PowerSoil Total RNA Isolation Kit with DNA Elution Accessory Kit (Qiagen; Hilden, Germany) was used to purify both DNA and RNA. Prior to extraction, the filter was thawed on ice and the RNAlater™ was removed by pushing it through the filter cartridge using a 5.0 mL syringe. The PowerSoil Total RNA Isolation Kit with DNA Elution Accessory Kit did not yield quantifiable amounts of DNA when used for small (1 mL) samples collected from the aquifer cell. For 1 mL aquifer cell samples, RNA and DNA were simultaneously extracted using the Qiagen Allprep DNA/RNA mini kit in accordance with manufacturer's instructions. Samples were thawed on ice and centrifuged at 8,000×g for 15 minutes to pellet cells. RNAlater™ was then removed using a sterile pipette.

A 10 µL aliquot of extracted RNA was transformed to complementary DNA (cDNA) via reverse transcription using the Qiagen QuantiTect Reverse Transcription kit (Qiagen; Hilden, Germany). This kit includes a DNase digestion step to remove DNA contamination from extracted RNA so no additional cleanup was performed. After transformation, gene abundance was measured via qPCR using previously established methods described in Appendix A1.5. Both extracted DNA and cDNA (representing RNA transcripts) were analyzed for *vcrA*, *bvcA*, and *tceA* RDase gene abundance.

5.4 Results and Discussion

5.4.1 Aquifer cell experiment

In the aquifer cell, the *bvcA* and *tceA* genes were not detected in DNA or cDNA samples above the quantification limit of 10^3 cells per sample. The *vcrA* gene and *vcrA* gene transcripts were detected and quantified in aquifer cell samples (Figure 5-2).

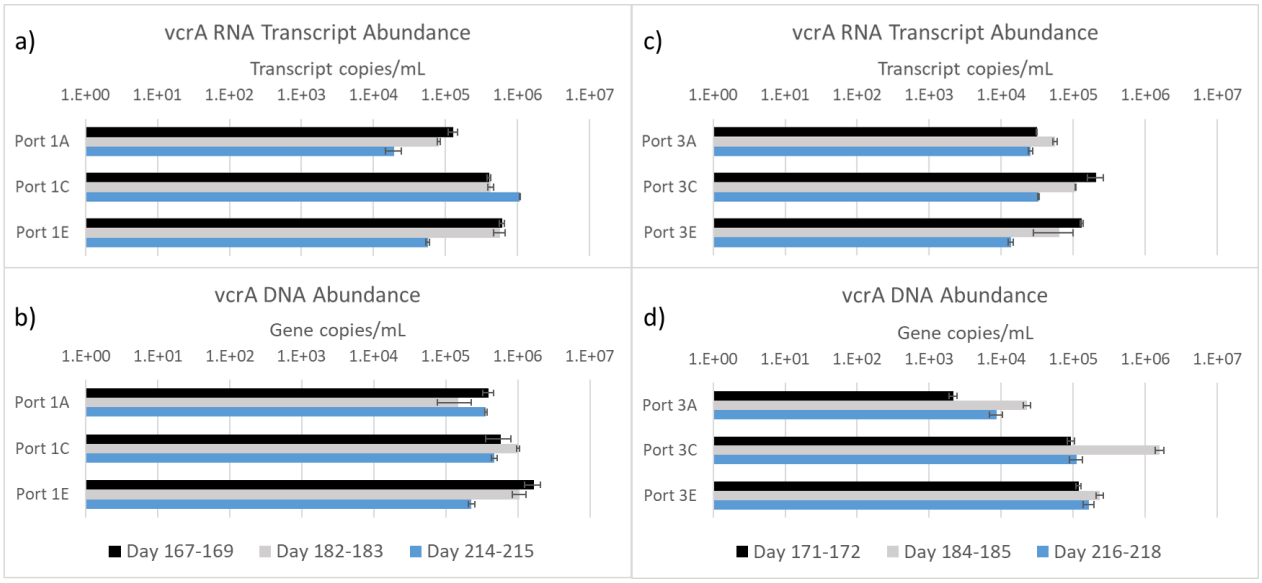

Figure 5-2. Abundance of *vcrA* a) RNA transcripts in upgradient ports, b) DNA gene copies in upgradient ports, c) RNA transcripts in downgradient ports, and d) DNA gene copies in downgradient ports

In all ports except 1C, *vcrA* RNA transcripts decreased by approximately 1 order of magnitude after electron donors (VFAs) were depleted to undetectable concentrations of <0.001 mM (Figure 5-3), from an average of 2.21×10^5 ($\pm2.01\times10^5$) transcript copies/mL

on days 167-172 to an average of 2.97×10^4 ($\pm1.50\times10^4$) transcript copies/mL on days 214-218 (7.46-fold decrease). In contrast, *vcrA* DNA abundance remained constant over time in most ports (ports 1A, 1C, 3C, 3E), decreased in port 1E, and increased port 3A, with an average abundance of 4.77×10^5 ($\pm6.23\times10^5$) gene copies/mL on days 167-172 and an average abundance within one order of magnitude (47%) on days 214-218 (2.24×10^5 [$\pm1.69\times10^5$] gene copies/mL, 0.47-fold decrease). The increase in *vcrA* transcription abundance observed in Port 3A between day 172 and 185 is likely due to its position in the low-permeability region of the aquifer cell (Appendix B10.0) causing the longer retention of VFAs measured (Figure 5-3).

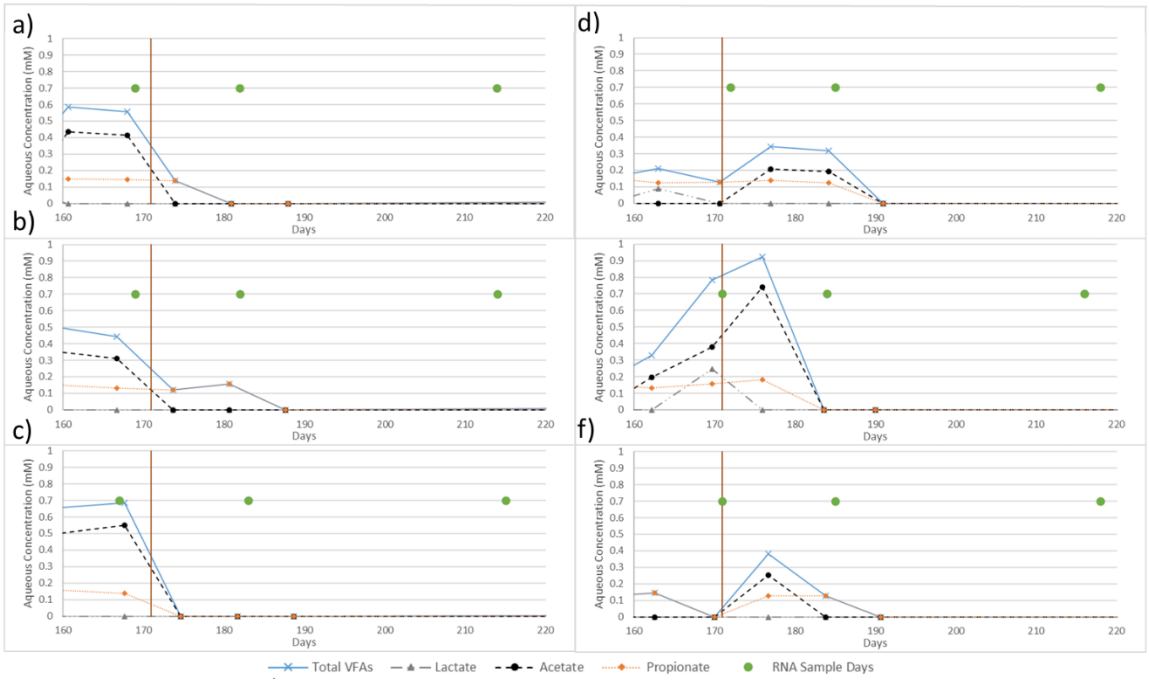

Figure 5-3. VFA concentrations measured in aquifer cell ports a) 1A, b) 1C, c) 1E, d) 3A, e) 3C, and f) 3E. Vertical line represents end of lactate pulse.

The abundance of *vcrA* RNA transcripts demonstrated a weak positive correlation ($r^2=0.29$) with VFA concentration in samples collected from the aquifer cell ports (Figure 5-3), as defined by a correlation coefficient (r^2) greater than 0.20.[460] On the other hand, *vcrA* DNA abundance showed no correlation ($r^2=0.024$) with VFA concentration (Figure 5-4). The correlation between VFA concentration and *vcrA* transcript abundance is caused by the

decline in gene transcripts when electron donor is depleted, despite the continued presence of cells harboring the *vcrA* gene (as measured in extracted DNA). After the end of the lactate pulse (day 171), *vcrA* transcript abundance declined exponentially (r^2=0.23) while *vcrA* gene abundance had an order of magnitude lower correlation to an exponential function (r^2=0.016) (Figure 5-5).

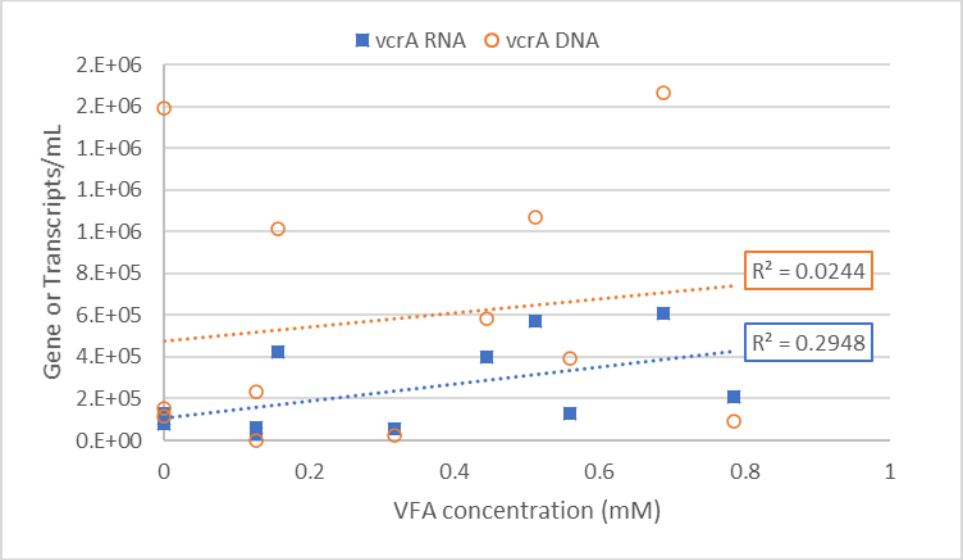

Figure 5-4. *vcrA* RNA transcript and DNA gene abundance vs. VFA concentration in aquifer cell sampling ports.

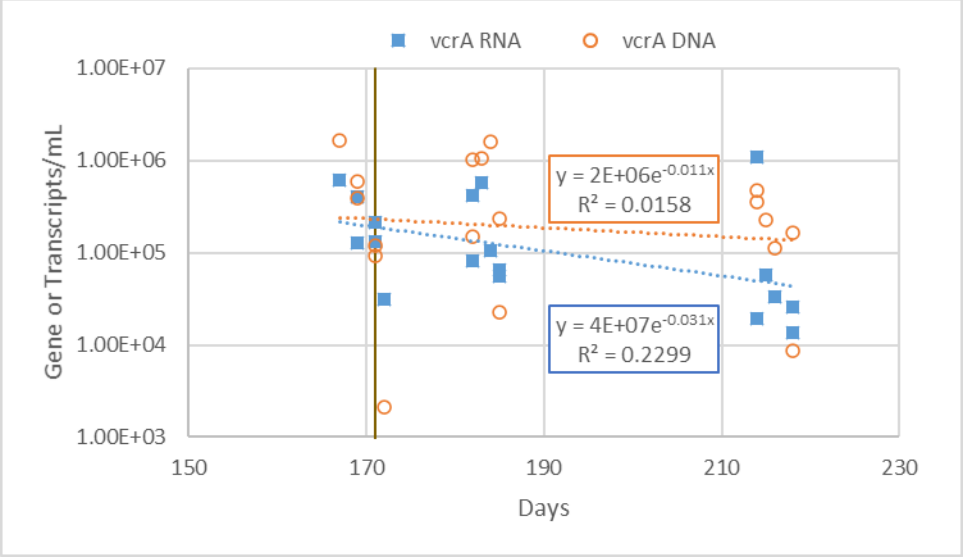

Figure 5-5. *vcrA* RNA transcript and DNA gene abundance over time in aquifer cell sampling ports, logarithmic scale.

In locations where RNA abundance decreased over time due to depletion of electron donor (Ports 1A, 1E, 3C, and 3E), an exponential decay function was fit to the data (Figure 5-6). These decay rates correspond to an average *vcrA* RNA transcript half-life of 15.3 (±1.68) days after electron donor is depleted to undetectable concentrations. This half-life is much longer than the 4.8 hour half-life reported by Lee et al. (2006) and the 1.0 day half-life approximated from data provided by Doğan-Subaşi et al. (2014). In both previous studies, the decline in *vcrA* transcripts was measured after the electron acceptor (chlorinated ethenes) was depleted to undetectable concentrations. The longer half-life measured in this study suggest that the *vcrA* gene continues to be transcribed in *Dhc* cells while chlorinated ethenes are present, even in the absence of detectable concentrations of electron donor. This finding supports the current ISB practice of periodic (pulsed) electron donor delivery as *Dhc* cells may continue to produce *vcrA* transcripts during periods of limited electron donor.

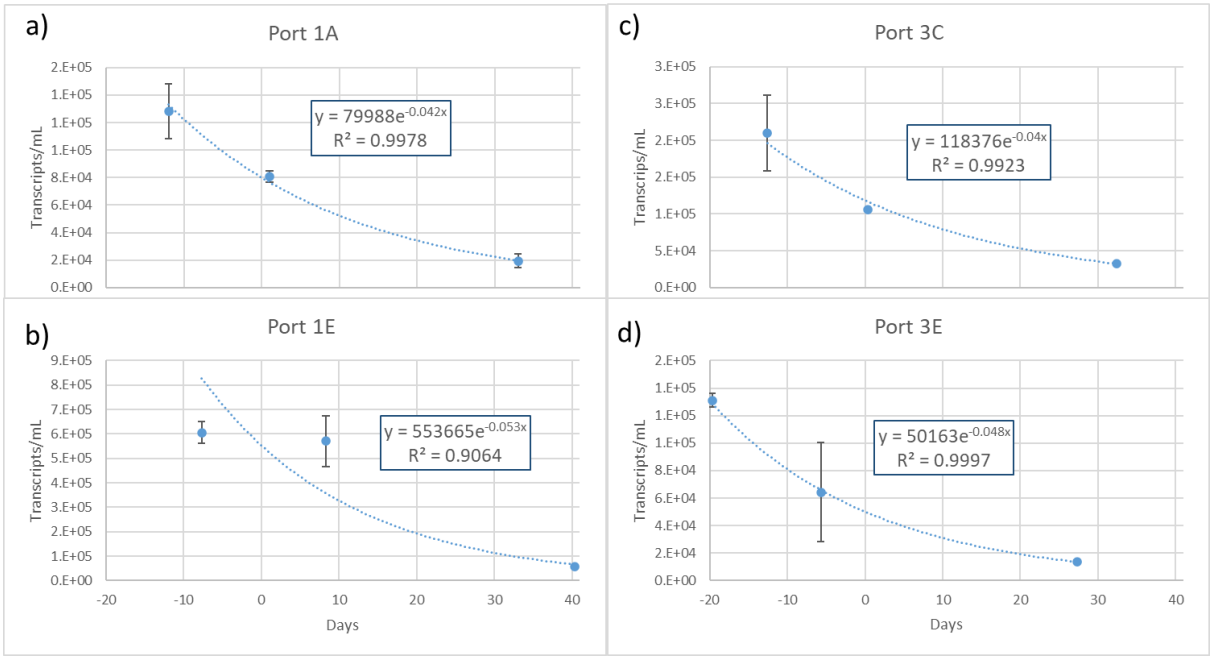

Figure 5-6. Exponential decay of *vcrA* transcripts in a) Port 1A, b) Port 1E, c) Port 3C, and d) Port 3E. Day 0 is the first sample in which no VFAs were detected.

DNA and RNA abundances were also compared with chlorinated ethene and ethene concentrations measured in the sampling ports during the aquifer cell experiment (Figure 5-7). RNA and DNA abundances were generally at their maximum when ethene concentrations were highest (except in ports 1C [DNA and RNA], 3C [DNA], and 3E [RNA]) and declined as the concentrations of more highly chlorinated ethenes (*cis*-DCE and TCE) increased. The decline in RNA and DNA abundance, and corresponding increase in *cis*-DCE and TCE, is likely due to the decline in electron donor discussed above, the absence of which limited the amount of MRD. Because the electron donor was depleted, there are insufficient data to determine if the shift in electron acceptor (chlorinated ethene) concentrations impacted the growth of *Dhc* cells harboring *vcrA* or the expression of *vcrA* transcripts.

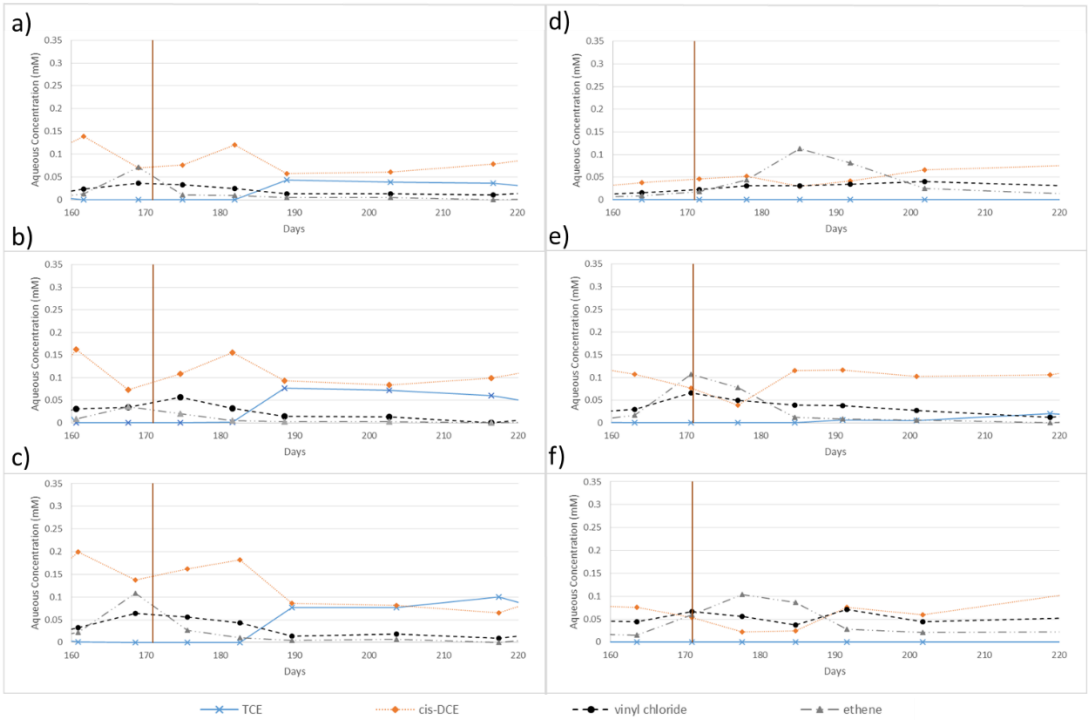

Figure 5-7. Chlorinated ethene and ethene concentrations measured in aquifer cell ports a) 1A, b) 1C, c) 1E, d) 3A, e) 3C, and f) 3E. Vertical line represents end of lactate pulse.

The abundance of *vcrA* DNA and RNA in the aquifer cell correlated with *cis*-DCE concentration (r^2=0.45 and 0.23, respectively [Figure 5-8]) but did not correlate with TCE,

VC, or ethene concentrations (r^2 ranging from 0.001 to 0.032). This correlation is likely due to the growth of *Dhc* cells harboring the *vcrA* gene when electron acceptor (*cis*-DCE) is available and subsequent expression of this gene as measured by RNA transcripts. TCE is not used as an electron acceptor for metabolic reductive dechlorination by *Dhc* cells harboring *vcrA* so the lack of correlation is expected. VC and ethene are daughter products of *cis*-DCE biodegradation by *Dhc* cells harboring the *vcrA* gene. The concentration of these compounds did not correlate with *vcrA* RNA and DNA abundance at the same location, likely due to the transport of these compounds downgradient after they were formed. Additional spatial analysis of *vcrA* DNA and RNA abundance compared with chlorinated ethene concentrations is warranted to assess the relationship between chlorinated ethene and RDase gene and transcript abundance under conditions of electron donor limitation.

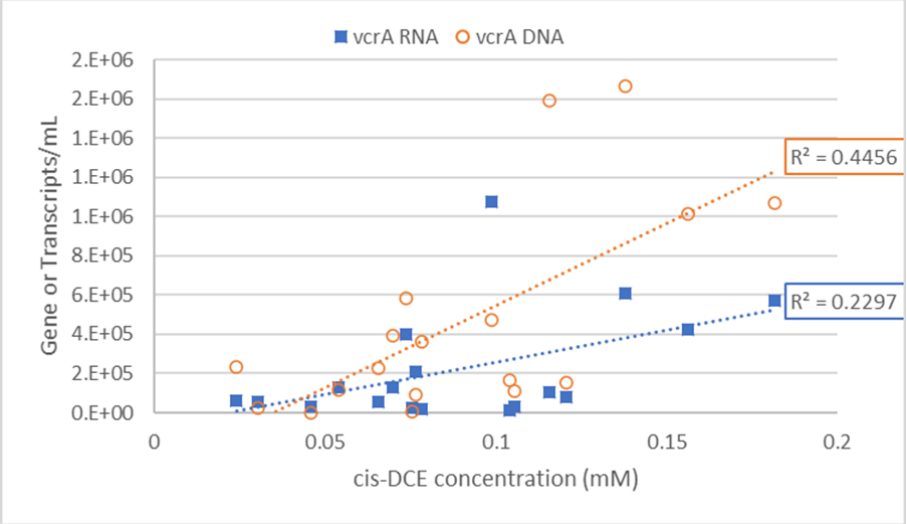

Figure 5-8. *vcrA* RNA transcript and DNA gene abundance vs. *cis*-DCE concentration in aquifer cell sampling ports.

5.4.2 Pilot test

In samples collected during the pilot test, both *vcrA* and *bvcA* genes were detected in DNA and cDNA samples, likely due to the larger volume of sample collected and extracted (Figure 5-9). The *tceA* gene was not detected in either DNA or cDNA, possibly due to the

lack of substrate (TCE) to promote the growth of *Dhc* cells harboring this RDase. In the pilot test, samples were collected as electron donor concentrations in DHT-2 increased, then decreased (Figure 5-10). Both *vcrA* DNA gene and RNA transcript abundance increased by 2.13- to 3.65-fold, respectively after electron donor concentrations increased, although the increase in RNA transcripts lagged the increase in DNA gene copies by 12 days. After 34 days from the beginning of the lactate injection, the abundance of *vcrA* and *bvcA* DNA gene copies increased 2.13- and 2.49-fold, respectively, while the abundance of gene transcripts increased only 1.18- and 1.46-fold, respectively. In the next sample, 46 days from the start of the lactate pulse, the increase in RNA transcript abundance was similar to the increase in DNA gene copies with a 3.65-fold increase in *vcrA* RNA transcripts, a 2.65-fold increase in *vcrA* DNA gene copies, a 2.45-fold increase in *bvcA* RNA transcripts, and a 2.49-fold increase in *bvcA* DNA gene copies (after 34-days; *bvcA* DNA abundance declined afterward).

The abundance of *vcrA* DNA and RNA did not decline as electron donor (VFAs) and electron acceptor (chlorinated ethenes) were detected at each sample time. The abundance of *bvcA* RNA transcripts increased over time after the VFA concentration increased, from 2.83×10^2 (±9.76) transcripts/mL to 6.91×10^2 (±49.0) transcripts/mL. The abundance of *bvcA* DNA, however, increased to 5.05×10^3 ($\pm3.08\times10^2$) transcripts/mL when VFA concentrations were highest (12.9 mM), but declined to 1.36×10^3 (±31.4) transcripts/mL as electron donor concentration decreased to 5.06 mM total VFAs, possibly due to the higher efficiency of *Dhc* cells harboring *vcrA* cells compared with cells harboring *bvcA*.[37,361]

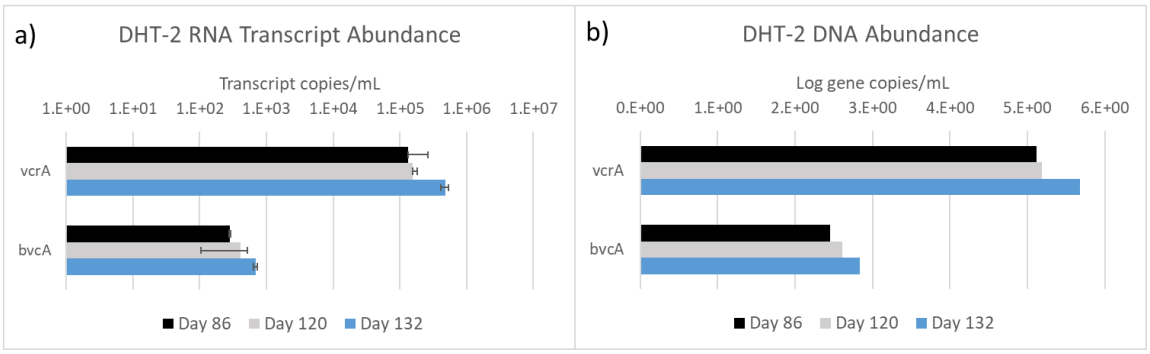

Figure 5-9. Abundance of *vcrA* and *bvcA* a) RNA transcript copies and b) DNA gene copies in pilot test well DHT-2

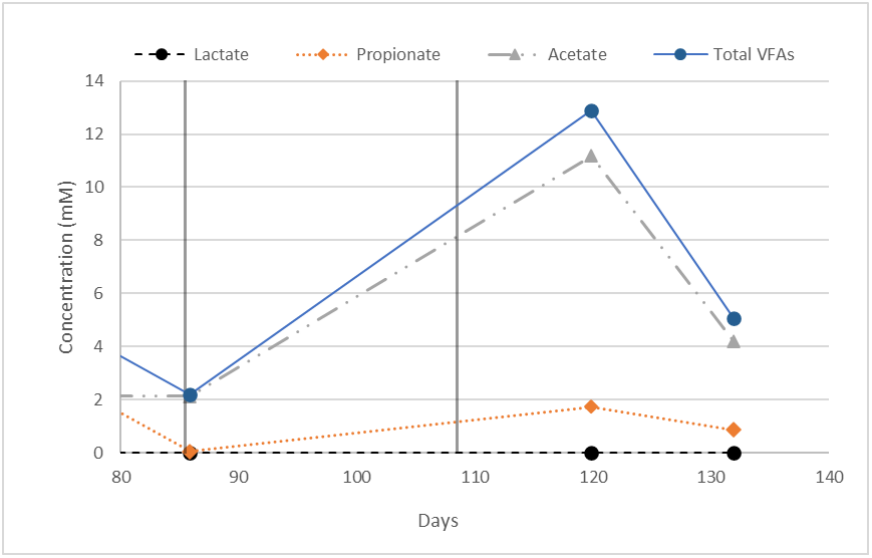

Figure 5-10. VFA concentrations measured in pilot test well DHT-2. RNA/DNA samples collected at same time points as VFA samples.

5.5 Conclusions

As previously reported, the transcription of RDase genes, measured by RNA abundance, is promoted by the type and availability of electron acceptor.[11,42,347,455–458] The absence of electron donor did not appear to cause down-regulation of *vcrA* gene transcription and the abundance of *vcrA* transcripts decreased 7.46-fold when electron donor was depleted to undetectable concentrations (<0.001 mM). The decline in *vcrA* gene transcripts occurred slowly, with a half-life of 15.3 (±1.68) days. This contrasts with a half-life of 4.8- to 24-hours when electron acceptor is depleted.[11,42] The abundance of *vcrA* DNA decreased less than 1 order of magnitude over time, even when the electron donor was depleted (compared with a 7.46-fold decrease in transcripts). The discrepancy is likely caused by the detection

of *vcrA* DNA in inactive cells and the detection of *vcrA* RNA transcripts only in active cells.

Increasing electron donor availability first increased the abundance of *vcrA* and *bvcA* DNA, indicating increase growth of cells harboring these genes. Increased RDase gene transcripts were detected in the following sampling round (12 days later) as the newly grown cells transcribed the *vcrA* and *bvcA* gene in response to the presence of electron acceptors (chlorinated ethenes).

This study supports the current practice of pulsed electron donor delivery as RDase RNA is not rapidly depleted when electron donor is limited and will remain up-regulated as cells await future electron donor amendments. Because *vcrA* transcripts do not decay rapidly if electron acceptor is present while electron donor is depleted, *vcrA* transcript abundance is not necessarily indicative of active MRD, an observation that has been made in previous studies.[25,351]

Acknowledgements

Funding for this research was provided by the Strategic Environmental Research and Development Program (SERDP) under Contract W912HQ-13-C-0011, Project ER-2311: Development of an Integrated Field Test/Modeling Protocol for Efficient *In situ* Bioremediation Design and Performance Uncertainty Assessment. The contents of this document have not been subject to agency review and do not necessarily represent the views of the sponsoring agency.

6.0 Strain-specific response of *Dehalococcoides mccartyi* to perfluoroalkyl substances and impact on microbial reductive dechlorination

The contents of this chapter are currently being prepared as a manuscript for publication, which will be supplemented with additional measurements of gene abundance and with estimates of dechlorination rates derived from fitting the data to a numerical model. Supplementary material for this submission is included as Appendix C.

6.1 Abstract

Although bioremediation is a common remedy for groundwater contaminated by chlorinated solvents, per- and polyfluoroalkyl substances (PFAS) have been shown to inhibit microbial reductive dechlorination (MRD), the process that detoxifies tetrachloroethene (PCE) and trichloroethene (TCE) to ethene. As PFAS are commonly co-located with chlorinated solvent groundwater plumes, their impact on the microbial species capable of MRD, particularly *Dehalococcoides mccartyi (Dhc)*, are of critical concern for bioremediation of chlorinated ethenes. Batch reactor experiments were prepared with an aqueous solution containing a mixture of ten perfluoroalkyl acids (PFAAs) and microcosm experiments were prepared with the same PFAA mixture plus soil collected from Loring Air Force Base (Aroostook County, ME). Experiments, bioaugmented with KB-1® (SiREM; Guelph, ON), were completed to assess the impact of PFAAs on MRD by a PCE to ethene methanogenic dechlorinating consortium containing *Acetobacterium sp.*, *Geobacter sp. (Geo)*, and relying on *Dhc* strains to complete the transformation to ethene. Although PFAA concentrations of 11.7 to 49.8 mg/L increased the time required to transform *cis*-DCE to ethene by 18% to 37% (6.0-13 days) in batch reactors, the presence of a solid phase eliminated this effect in microcosms with initial aqueous PFAA concentrations as high as 53.5 mg/L. Batch reactors containing 61.7 and 101 mg/L PFAAs did not fully transform PCE to ethene over the 48 day experiment, while microcosms

initially containing 120 mg/L PFAA completely dechlorinated PCE within 28 days. This time to transform PCE to ethene, however, was slightly longer (16%, 5 days) in microcosms containing 120 mg/L than in those containing 53.5 mg/L PFAAs. Examination of the *Dhc* strain-specific reductive dehalogenase genes implicated in the transformation of chlorinated ethenes to ethene revealed that high concentrations of PFAAs promoted the growth of *Dhc* strains harboring *bvcA* rather than cells harboring the *vcrA* gene. A microbial consortium containing multiple *Dhc* strains (KB-1®) was able to transform PCE to ethene even at PFAA concentrations of 120 mg/L when porous media was present, indicating that MRD can be implemented to treat chlorinated ethenes in plumes comingled with PFAAs.

6.2 Introduction

In situ bioremediation (ISB) of chlorinated solvents, including the ubiquitous groundwater contaminants tetrachloroethene (PCE) and trichloroethene (TCE), is an effective remedy that has been implemented at numerous sites.[1–4,15] Chlorinated solvents rarely occur in isolation and the presence of co-contaminants can impact bioremediation performance.[355–357,461] Per- and polyfluoroalkyl substances (PFAS) are a class of contaminants of emerging concern that are often found co-located in aquifers contaminated with chlorinated solvents.[44,45] PFAS were used in a variety of products including firefighting aqueous film forming foams (AFFFs), surface coating protection on cardboard, carpets, leather, and textiles, nonstick cookware, and breathable, waterproof membranes.[65–67] Many fire-training areas used AFFFs to extinguish fires fed by off-specification fuels and waste solvents, some of which were comingled with chlorinated solvents, resulting in the co-release of PCE, TCE, and PFAS to soil and groundwater.[44,45] In source areas associated with AFFF use, including at NAS Fallon (NV), Tyndall Air Force Base (FL), and Wurtsmith Air Force Base (MI), Moody and Field (1999) reported plumes of PFAS contaminated groundwater with total PFAS concentrations up to 7.09 mg/L.

PFAS encompass a large class of compounds including more than 4,000 chemicals registered with the chemical abstract service.[462] Many of these compounds are degraded into the environment to fully-fluorinated perfluoroalkyl acids (PFAAs), also known as terminal PFAS.[68,407–409,411,418] Although there is no well understood pathway for the biotransformation of PFAAs, their presence affects the bioremediation of other compounds, including chlorinated solvents. Weathers et al. (2016) reported that TCE degradation by *Dehalococcoides mccartyi (Dhc) strain 195* was inhibited by PFAA concentrations in excess of 66 mg/L in a methanogenic culture. A similar study found that TCE dechlorination by *Dhc* was prevented by 0.3% solutions of neat AFFF from Ansul and National foam, but was not inhibited by 3M AFFF, with total PFAS concentrations ranging from 30 to 120 mg/L in all experiments.[46] In order to treat chlorinated solvents in plumes mixed with PFAS, the conditions under which *Dhc* strain-specific activity is inhibited must be better understood.

Current field implementations of PCE and TCE bioremediation rely on *Dhc* strains, to complete the transformation of PCE to benign ethene.[5–9] Multiple strains of *Dhc* have been identified and those implicated in transformation of chlorinated ethenes harbor specific reductive dehalogenase (RDase) genes.[10] Each *Dhc* strain has the capacity to transform specific chlorinated compounds but only a limited number of strains that transform vinyl chloride (VC) to ethene have been identified.[11–14] *Dhc* strains harboring the *tceA* gene have been shown to metabolically transform PCE/TCE to *cis*-dichloroethene (*cis*-DCE) and co-metabolically transform *cis*-DCE to VC and VC to ethene while strains harboring the *bvcA* and *vcrA* genes are able to transform DCE to VC and VC to ethene metabolically, resulting in more efficient transformation and limiting the accumulation of *cis*-DCE and VC during ISB.[10,290,301]

Because specific *Dhc* strains are necessary to fully transform PCE to ethene, understanding the strain-specific impacts of co-contaminants is essential to successful implementation of ISB. Geochemical parameters, including oxygen concentration, temperature, and pH, have been shown to impact the abundance of RDase genes and tend to most inhibit cells harboring the *vcrA* gene, one of the genes necessary for metabolic transformation of VC to ethene.[25,26,29,350,351] The presence of co-contaminants such as 1,1,1-trichloroethane and triclocarban has also been shown to impact specific *Dhc* strains with both compounds having a greater impact on cells harboring *vcrA* than cells harboring *tceA.*[30,358] Although Weathers et al. (2016) demonstrated that PFAAs can inhibit TCE degradation by *Dhc* strain 195 (harboring the *tceA* gene), they did not examine the strain-specific impact of PFAAs, inhibition in a culture containing multiple *Dhc* strains, or inhibition of *Dhc* strains that metabolically transform VC to ethene. Additionally, the presence of a solid phase has been shown to minimize or prevent inhibition of microbial reductive dechlorination at low pH and at high PCE and TCE concentrations as soil particles provide microenvironments where microbes are not exposed to the high concentrations present in the bulk liquid.[35,463] Similarly, the inhibition of microbial reductive dechlorination (MRD) by PFAAs measured in batch reactor experiments may not occur at the same aqueous PFAA concentrations if a solid phase is present.

A series of batch reactor and microcosm experiments were completed to provide insight into the conditions under which PFAAs can inhibit microbial reductive dechlorination and to assess the impact of these compounds on specific *Dhc* strains. All reactors were prepared with a mixture of 10 PFAAs observed *in situ* with total PFAA concentrations ranging from 0 to 138.5 mg/L. Experiments were bioagumented with KB-1® (SIREM; Guelph, ON), a methanogenic dechlorinating consortium containing *Acetobacterium sp., Geobacter sp. (Geo),* and multiple *Dhc* strains harboring the *vcrA, bvcA, and tceA* RDase genes.[13,314]

Microcosm experiments containing soil from a PFAS-contaminated site were used to assess the impact of a solid phase on the effects measured in batch reactor experiments. RDase genes were quantified to provide insight into the strain-specific responses of *Dhc* to PFAAs and into the conditions under which inhibition may impede successful ISB. This study aims to determine the impact of PFAAs on *Dhc* biodegradation rates and population growth, *Dhc* strain-specific impacts of these compounds, and the effect of a solid phase on inhibition and strain distribution.

6.3 Materials and Methods

6.3.1 Chemicals and porous media

Sodium sulfide nonahydrate (Fisher Scientific; Hampton, NH) and L-cysteine (Sigma Aldrich; St. Louis, MO) were used as reductants to maintain anoxic conditions and sodium DL-lactate solution, 60% w/w (Sigma Aldrich; St. Louis, MO) was used as an electron donor. TCE (ACS reagent, >99.5%) with a density of 1.46 g/mL was obtained from Sigma Aldrich; St. Louis, MO and PCE (99% extra pure) with a density of 1.62 g/mL from Acros Organics (Fisher Scientific; Hampton, NH). Aqueous solutions were prepared in deionized water produced by a Milli-Q® Integral Water Purification System (EMD Millipore; Burlington, MA).

PFAAs were obtained from Sigma Aldrich (St. Louis, MO) as nonaflurobutane-1-sulfonic acid (PFBS) 97%, heptafluorobutrycic acid (PFBA) 98%, perfluoropentanoic acid (PFPeA) 97%, tridecaluorohexane-1-sulfonic acid potassium salt (PFHxS) >98%, undecafluorohexanoic acid (PFHxA) >97%, perfluoroheptanoic acid (PFHpA) 99%, heptadecafluorooctanesulfonic acid potassium salt (PFOS) >98%, perfluorooctanoic acid (PFOA) 95%, perfluorononanoic acid (PFNA) 97%, and perfluorodecanoic acid (PFDA) 98%. Ethlyene glycol monobutyl ether (EGMBE) was obtained from Fisher Chemical (Hampton, NH) and was used to increase the solubility of PFAAs in select experiments.

Porous media used in microcosms consisted of surficial soils recovered via shovel in the vicinity of soil boring AA07SB04 at Loring Air Force Base (Aroostook County, ME) in October 2017. This location, approximately 30 m northeast of the Crash Fire Station, had been impacted by PFAS from AFFF with measured concentrations of 3.57 mg/kg PFOS, 0.015 mg/kg PFOA, and 0.001 mg/kg PFBS.[464] The soil contains 1.7% organic carbon by mass as measured using the method in Appendix C1.0.

The liquid phase used in the batch reactors consisted of an anoxic growth medium modified from the recipe of Löffler et al. (2005) to reduce the total ionic strength to prevent precipitation PFOS at high concentrations (PFOS solubility is affected by salt concentration[465]). The ionic strength of the medium was reduced from 102.7 mM to 19.9 mM by reducing the concentration of 100x salts solution to 12.5% of the original concentration, reducing the sodium bicarbonate buffer from 30 mM to 10 mM, and reducing the concentrations of trace element solution, Se/Wo solution, L-cysteine, and sodium sulfide by 50% each. The medium was prepared with 5 mM lactate as an electron donor.

6.3.2 Batch reactor and microcosm configurations

Batch (without porous media) and microcosm (with porous media) reactor transformation studies were completed to assess the impact of terminal PFAS on microbial reductive dechlorination by a mixed-community culture capable of transforming PCE and TCE to ethene. This culture (KB-1®; SiREM; Guelph, ON) contains *Acetobacterium sp., Geo*, and multiple *Dhc* strains harboring the *vcrA, bvcA, and tceA* RDase genes.[13,314] In contrast to previous work that identified impacts on MRD by *Dhc* strain 195 in the presence of a mixture of 11 PFAAs at equal concentrations,[43] this work utilized a mixture of 10 PFAAs, in ratios that approximate those measured in groundwater at the fire training area of Loring Air Force Base (Aroostook County, ME), and a commercially available dechlorinating

consortium to create more realistic conditions. To prevent the perfluorooctane sulfonate (PFOS) concentration from exceeding 25 mg/L at the highest mixture concentrations, its proportion of was reduced from the 44.3% of total PFAS observed at the site to 15-20% of total PFAS and the proportions of other compounds were increased as shown in Table 6-1 (columns 1 and 2). When PFOS was added to the PFAS mixture at concentrations above 25 mg/L, its measured concentration was lower than the mass added, likely due to precipitation of PFOS from the low salts growth medium.

Table 6-1. Composition of PFAA Mixture in Batch Reactor Experiments

PFAA	% total PFAAs (by mass) in Loring AFB Overburden	% total PFAAs (by mass) in Batch Reactors	% total PFAAs (by mass) in EGMBE Batch Reactors	% total PFAAs (by mass) in Microcosms (initial)	% total PFAAs (by mass) in Microcosms (final)
PFBS	0.43%	5.67%	5.30%	4.43%	4.95%
PFBA	3.74%	6.41%	6.95%	10.2%	10.9%
PFPeA	13.3%	14.9%	14.3%	18.1%	18.9%
PFHxS	14.5%	17.9%	14.7%	13.9%	14.7%
PFHxA	10.2%	10.7%	15.7%	18.7%	18.7%
PFHpA	5.20%	6.30%	7.21%	6.17%	6.56%
PFOS	44.3%	22.7%	20.0%	15.4%	12.3%
PFOA	7.02%	9.33%	9.70%	8.56%	9.00%
PFNA	1.13%	3.45%	3.63%	3.21%	3.46%
PFDA	0.17%	2.59%	2.46%	1.28%	0.68%

Experiments were performed in 160 mL glass serum bottles capped with butyl rubber stoppers (Chemglass Life Sciences; Vineland, NJ) and aluminum crimp caps (Chemglass Life Sciences; Vineland, NJ). All reactors were prepared at room temperature in an anaerobic chamber containing an atmosphere of 97% N_2/3% H_2 (Coy Laboratory Products; Grass Lake, MI). Batch reactors were prepared with an aqueous volume of 120 mL; microcosm experiments were prepared with 100 mL of aqueous volume and 14.7–18.6 g of porous media.

A PFAS solution was prepared by dissolving 10 PFAAs in pre-prepared medium to create a stock solution with a total PFAA concentration of 101-122 mg/L. The ratio of PFAAs was configured to simulate the relative concentrations observed at Loring AFB (Table 6-1), although the PFOS concentration was reduced to prevent it from precipitating at high total PFAA concentrations and the concentrations of other compounds were increased. The stock solution was used to create 6 sets of 5 batch reactors containing initial measured concentrations of 101 mg/L, 61.7 mg/L, 49.8 mg/L, 26.5 mg/L, 11.7 mg/L, and 0 mg/L total PFAAs (Table C-1), above and below the 66 mg/L total PFAA concentration shown to impact *Dhc* strain 195.[43] Reactors were then amended with 15 mL of low salts growth medium containing PCE and TCE to provide average initial concentrations in each batch reactor of 0.039 (±0.004) mM PCE and 0.18 (±0.02) mM TCE. For the highest concentration reactors, the PCE/TCE solution was prepared in medium containing 101 mg/L PFAAs to maintain the target PFAA concentrations. Reactors were also amended with 0.5 mL of 200x Wolin vitamin[466] solution to provide nutrients necessary for microorganisms. In each set of 5 batch reactors, 3 reactors were bioaugmented with 6 mL of KB-1® inoculum (SIREM; Guelph, ON), while 2 reactors received 6 mL of low salts growth medium to maintain the same volume as the biologically active reactors. These two reactors were sterilized via autoclave to serve as abiotic controls.

To achieve PFAS concentrations above the 110 mg/L used by Weathers et al. (2006), a set of batch reactor experiments were prepared using 1% ethylene glycol monobutyl ether (EGMBE) by volume. This solvent, also known as butyl carbitol, was used in formulations of AFFF and could be present in PFAS plumes from fire-training or firefighting activities.[44] Batch reactors with EGMBE were prepared as described above with initial measured concentrations of 119.8 mg/L, 53.5 mg/L, 25.9 mg/L, 12.8 mg/L, and 0 mg/L total PFAAs (Table C-2); a set of positive control reactors were also prepared with no PFAAs or

EGMBE. At each concentration three reactors were bioaugmented and two were sterilized as described above.

Microcosm experiments were prepared in an anaerobic chamber with 14.7–18.6 g of porous media collected from Loring Air Force Base (Aroostook County, ME) and 100 mL of reduced salt growth medium containing a PFAA mixture similar to that used in the batch reactors (Table 6-1). Microcosms containing initial measured concentrations of 119.8 mg/L, 53.5 mg/L, 25.9 mg/L, 12.8 mg/L, and 0 mg/L total PFAAs (Table C-2) were prepared in the same manner as the batch reactors. Negative control microcosms were not autoclaved to maintain the physical-chemical properties of the soil, instead 10 mg/L of sodium azide was added to inhibit reductive dechlorination. An additional six microcosms were prepared without bioaugmentation and without sodium azide to assess the dechlorinating capability of the native microbial population. Three of these reactors were prepared with 12.8 mg/L PFAAs and three were prepared without PFAAs. In subsequent sections, microcosms are referred to by the initial measured concentrations of PFAAs listed above although the aqueous concentrations decreased as described in Section 6.4.4.

6.3.3 Batch reactor sampling

After bioaugmentation, 1.0 to 2.5 mL samples were collected every 2 to 7 days from each of the reactors using a sterile 25-gauge needle (Becton, Dickinson and Company; Franklin Lakes, NJ) and polypropylene syringe (Becton, Dickinson and Company; Franklin Lakes, NJ). During sampling, 1.0 to 3.0 mL of nitrogen gas was injected to maintain atmospheric pressure in the bottles prior to collecting aqueous samples. Sample aliquots of 1.0 mL were analyzed for chlorinated ethenes by gas chromatography with flame ionization detection (GC-FID). Additional sample aliquots of 1.0 mL were prepared for future DNA extraction and quantitative polymerase chain reaction (qPCR) analysis by centrifugation as described in Section 6.3.5 below. After centrifugation, the aqueous phase was analyzed for VFA and

fluoride concentrations by ion chromatography (IC). The remaining 0.5 mL sample volume was analyzed for PFAS by liquid chromatography with tandem mass spectrometry (LC/MS-MS). Samples for PFAS analysis were placed in a 15 mL high-density polyethylene (HDPE) bottles containing 9.5 mL of 4M equivalent sodium hydroxide (20:1 dilution) and stored at 4°C prior to analysis. At the time of analysis samples were further diluted into an 80:20 water: methanol solution as necessary to ensure that the expected concentration fell within the calibration range of the analytical instrument.

6.3.4 Chemical analytical methods

Samples for chlorinated ethene and ethene analysis were placed into headspace analysis vials immediately after collection and analyzed within 24-hours. Chlorinated ethene and ethene concentrations were measured using an Agilent 7890B GC system with a DB-625 column and FID (Agilent Technologies; Santa Clara, CA).[336] Samples were introduced to the GC by a Telemark HT3 headspace autosampler (Teledyne Technologies; Thousand Oaks, CA) using a constant heating program.

Targeted analysis of PFAS was based on a modification of EPA Method 537 that employs large volume injection (LVI).[375,467] Quantification was achieved using a Waters Xevo TQ-S triple quadrupole mass spectrometer equipped with a Waters Acquity ultra high performance liquid chromatograph (uHPLC). To achieve analyte separation, a Waters BEH C-18 column (1.7 µm dia., 2.1 × 50 mm) was operated at a flow rate of 0.4 mL/min with an eluent gradient consisting of 2 mM ammonium acetate in water or methanol. The mass spectrometer was operated in negative electrospray ionization and multiple reaction monitoring modes. The method is currently able to detect 40 PFAS, precursors, and C-13 labeled standards with a total run time of approximately 10 min and detection limits ranging from 5 to 20 ng/L. LVI (50 µL) was used to improve sensitivity without the use of solid phase extraction.

Volatile fatty acids (VFAs) and fluoride were measured by ion conductivity (IC) using a Dionex ICS-2100 IC system with IonPac AS-18 Fast column (Thermo Scientific; Waltham, MA). Soil organic and inorganic carbon content was determined using a total organic carbon (TOC)-L analyzer (Shimadzu; Kyoto, Japan) using the subtraction method (total carbon minus inorganic carbon equals organic carbon).[442]

6.3.5 Biological analytical methods

Aqueous biomass samples (1 mL) were prepared by room temperature centrifugation at 15,000 rpm (21,130×g) for 15 minutes using an Eppendorf 5424 centrifuge with 5424R rotor (Eppendorf; Hamburg, Germany). After removing the supernatant, pellets were stored at -20°C. Microbial genomic DNA was extracted from the pellets using the QIAamp DNA Mini Kit (Qiagen; Hilden, Germany) and following the manufacturer's protocol. Extracted DNA was stored at -20°C until qPCR analysis.

Dhc strain abundance was quantified by qPCR analysis targeting the *Dhc* 16S rRNA gene with additional analysis targeting the *tceA, vcrA, and bvcA* RDase genes. All qPCR analyses were measured in triplicate using a Step One Plus Real-Time PCR System (Applied Biosystems; Foster City, CA) under standard operating conditions and TaqMan-based chemistry. Primers and probes were obtained from IDT Technologies (Coralville, IA) or ThermoFisher and the TaqMan Universal PCR Master Mix from Applied Biosystems (Foster City, CA). For each analysis, a standard curve was generated using 10-fold serial dilutions of a stock solution containing a known concentration of plasmid DNA with a single copy of the target gene.[37]

6.4 Results and Discussion

6.4.1 PCE and TCE biodegradation

In batch reactors, all PFAA concentrations tested (up to 101 mg/L) did not impede the transformation of PCE and TCE to *cis*-DCE over the entire period PCE and TCE were

detected (<0.0014 mM): 6.0 (±0.0) days in reactors without PFAAs and an average of 5.2 (±0.99) days in reactors with PFAAs (Figure 6-1). Similarly, in the presence of soil (microcosm experiments), there was no difference in the time to dechlorinate PCE and TCE to *cis*-DCE at any of the PFAA concentrations tested. PCE or TCE were no longer detected 9 days after bioaugmentation in all microcosms (Figure 6-2).

Batch reactors with EGMBE and PFAAs required additional time to fully transform PCE and TCE to *cis*-DCE at all concentrations tested. In the sets of bioaugmented reactors, the average time until PCE and TCE were no longer detected was 81% longer (6.3 ±0.9 days) in those containing 28.7 and 65.5 mg/L PFAAs, 100% longer (7.0 ±0.0 days) in those containing 112.6 mg/L PFAAs, and 195% longer (10.3 ±0.9 days) in those containing 138.5 mg/L PFAAs as compared to reactors without PFAAs (3.5 ±0.5 days) (Figure 6-3).

The rapid dechlorination of PCE and TCE to *cis*-DCE is likely facilitated by *Geo* as they have been shown to outcompete *Dhc* when PCE and TCE are present.[257,314] These results suggest that *Geo* are not likely to be inhibited by PFAAs alone but may be negatively impacted by the combination of PFAAs and EGMBE.

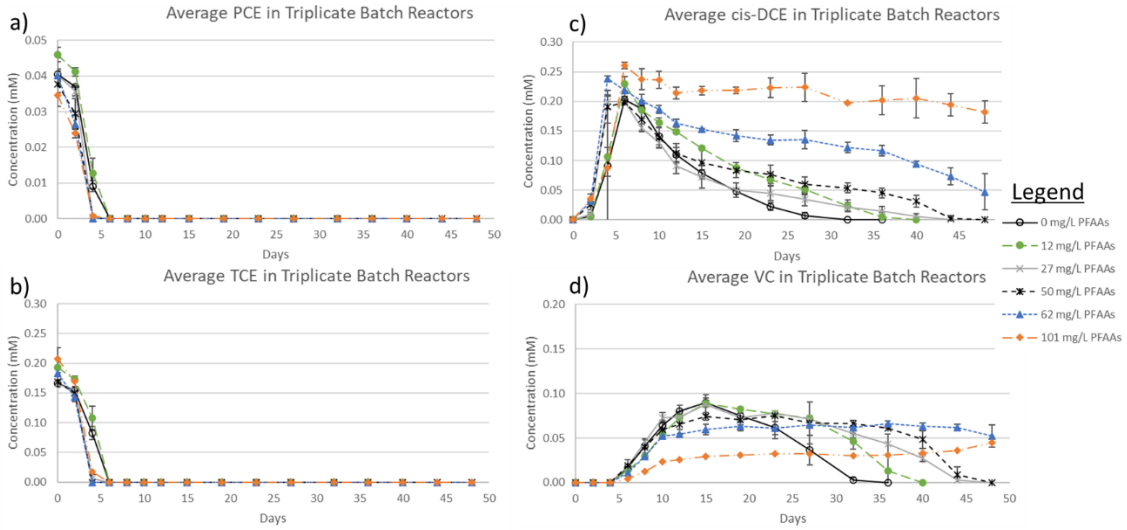

Figure 6-1. Average **a)** PCE **b)** TCE **c)** *cis*-DCE and **d)** VC concentrations in triplicate batch reactors. Vertical error bars represent standard deviation between triplicate batch reactors.

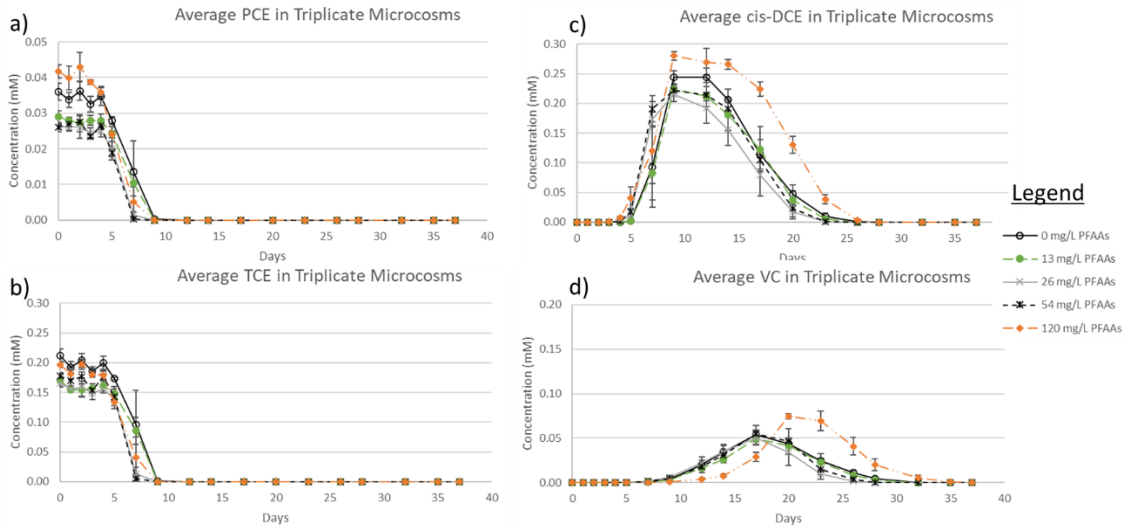

Figure 6-2. Average **a)** PCE **b)** TCE **c)** *cis*-DCE and **d)** VC concentrations in triplicate microcosms. Vertical error bars represent standard deviation between triplicate microcosms.

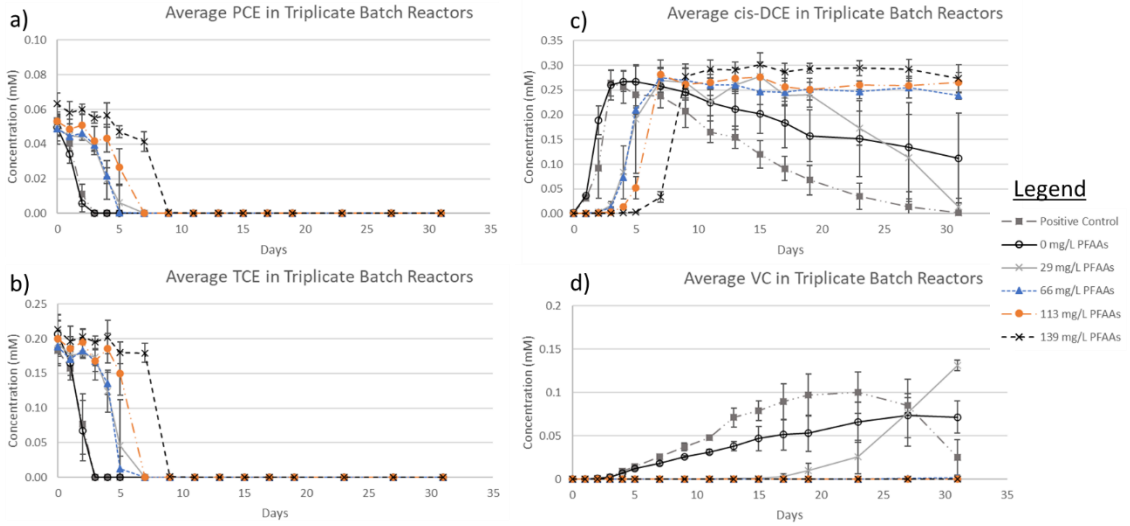

Figure 6-3. Average **a)** PCE **b)** TCE **c)** *cis*-DCE and **d)** VC concentrations in triplicate batch reactors contained EGMBE. Vertical error bars represent standard deviation between triplicate microcosms.

6.4.2 cis-DCE and VC biodegradation

Reductive dechlorination of *cis*-DCE to VC and VC to ethene was impeded by PFAAs concentrations in batch reactor experiments. Batch reactors without PFAAs fully transformed *cis*-DCE to VC within 32.0 (± 0.0) days and transformed VC to ethene within 34.0 (+/- 2.0) days, while reactors with 11.7 mg/L PFAAs required 21% longer (38.6 ±1.9 days) to transform *cis*-DCE to VC, and 18% longer (40.0 ±0.0 days) to transform VC to ethene (Figure 6-1). Similarly, transformation of *cis*-DCE to VC required 38% longer (44.0

±0.0 days) and 46% longer (46.7 ±1.9 days) in reactors with 26.5 mg/L and 49.8 mg/L PFAAs, respectively. Transforming VC to ethene also required 37% longer (46.7 ±1.9 days) in reactors with 26.5 and 49.8 mg/L PFAAs when compared with reactors containing 0 mg/L PFAAs (Figure 6-1). At the end of the experiment, 48 days after bioaugmentation, reactors with 61.7 and 101 mg/L PFAAs did not fully dechlorinate *cis*-DCE to ethene (Figure 6-1).

In contrast, the presence of a solid phase prevented the inhibition of MRD of *cis*-DCE. Transformation of *cis*-DCE to VC and VC to ethene was not impeded by PFAA concentrations of 53.5 mg/L and lower with *cis*-DCE no longer detected after 26.3 (±1.7) days in all bioaugmented microcosms with 53.5, 25.9, 12.8, or 0.0 mg/L PFAAs (Figure 6-2). Only the microcosms prepared with 119.8 mg/L PFAS required additional time (6% longer, 28.0 ±0.0 days) to fully transform *cis*-DCE to VC. Similarly, transformation of VC to ethene required 9% longer (37.0 ±0.0 days) in reactors with 119.8 mg/L PFAAs whend compared to microcosms with 53.5 mg/L PFAA and lower (33.8 ±3.2 days). In the absence of soil, however, PFAA concentrations of 61.7 and 101 mg/L prevented complete transformation of VC to ethene over the course of the experiment. This difference could be caused by protective microenvironments around solid particles. In previous studies, the presence of certain porous media, even at low solid to liquid ratios (10 g soil to 100 mL aqueous phase), prevented complete inhibition of dechlorination at low pH.[463] The authors attributed this phenomenon to more favorable pH conditions at the solid-aqueous interface; similarly, cells attached to soil particles may not be exposed to the same detrimental effects of PFAAs as those in the bulk aqueous phase.

In batch reactors prepared with PFAAs and EGBE, dechlorination of *cis*-DCE to VC was impacted by the presence and concentration of PFAAs. The time until VC was detected (at > 0.001 mM) was 4.5 times longer (13.7 ±0.9 days) in reactors with 28.7 mg/L PFAAs and

10.9 times longer (29.7 ±1.9 days) in reactors with 65.5 mg/L PFAAs when compared to reactors without PFAAs (2.5 ± 0.5 days) (Figure 6-3). The sets of reactors containing EGMBE and 112.6 mg/L and 138.5 mg/L PFAAs did not exhibit dechlorination of *cis*-DCE to VC over the course of the experiment (31 days). The greater inhibition observed in these reactors could be due to a synergistic effect between EGMBE and PFAS.

6.4.3 Total and strain-specific growth of Dehalococcoides

In microcosm experiments, analysis of the *Dhc* population, via qPCR of the *Dhc* 16S rRNA gene, revealed that total *Dhc* 16S rRNA gene increased from an average initial abundance of 1.21×10^{6} ($\pm3.59\times10^{5}$) gene copies/mL to 4.97×10^{7} ($\pm3.36\times10^{7}$) gene copies/mL over the first 28 days of the experiments (while chlorinated ethenes were present) (Figures 6-5 and C-4). Growth occurred regardless of PFAA concentration with increases of 25-, 21-, 22-, 27- and 84- fold in the reactors containing 0, 12.8, 25.9, 53.5, and 119.8 mg/L PFAAs, respectively.

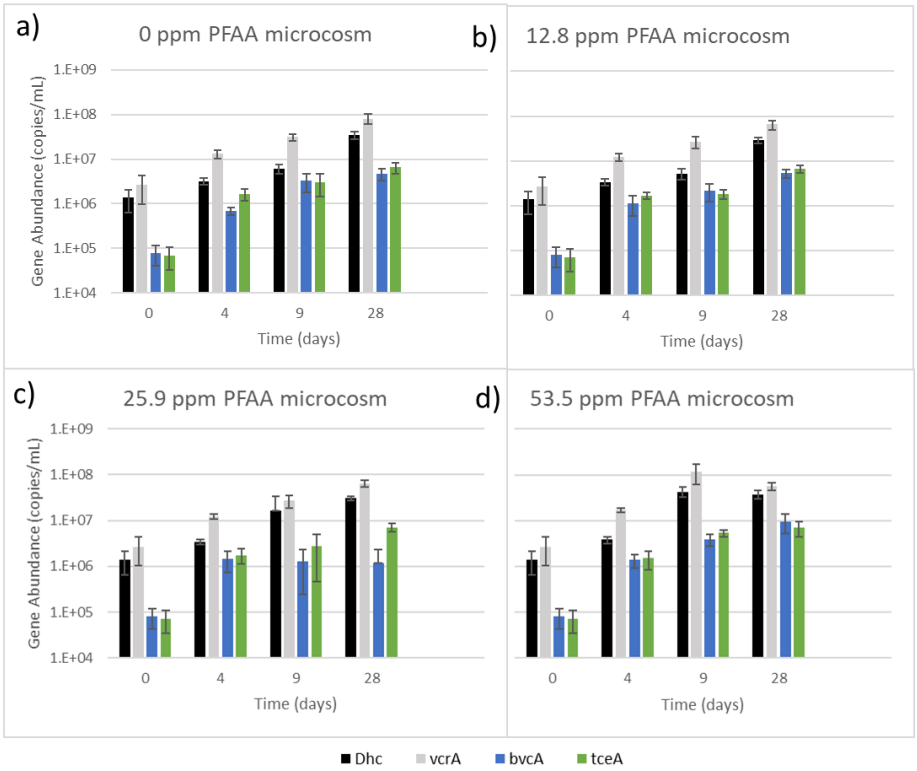

Figure 6-4. *Dhc* and RDase abundance in microcosm experiments with a) 0 ppm, b) 12.8 ppm, c) 25.9 ppm, and d) 53.5 ppm PFAAs

In the presence of EGMBE, total *Dhc* 16S rRNA gene abundance was 1 to 3 orders-of-magnitude lower in reactors containing more than 28.7 mg/L PFAAs than in reactors with 28.7 mg/L or 0 mg/L PFAAs (Figures 6-6 and C-5). Total *Dhc* abundance increased an average of 54.3-fold (±3.1) in the positive control reactors (no EGMBE), 18.7 (±13.2) -fold in reactors containing 0 mg/L PFAAs and EGMBE, and 45.8 (±8.5) -fold in reactors containing 28.7 mg/L PFAAs and EGMBE. In comparison, *Dhc* growth was inhibited in reactors with greater than 28.7 mg/L PFAAs with 2.8 (±1.0)-, 1.7 (±0.3)-, and 0.9 (±0.1) -fold increases in reactors containing EGMBE and 65.5, 112.6, and 138.5 mg/L PFAAs, respectively.

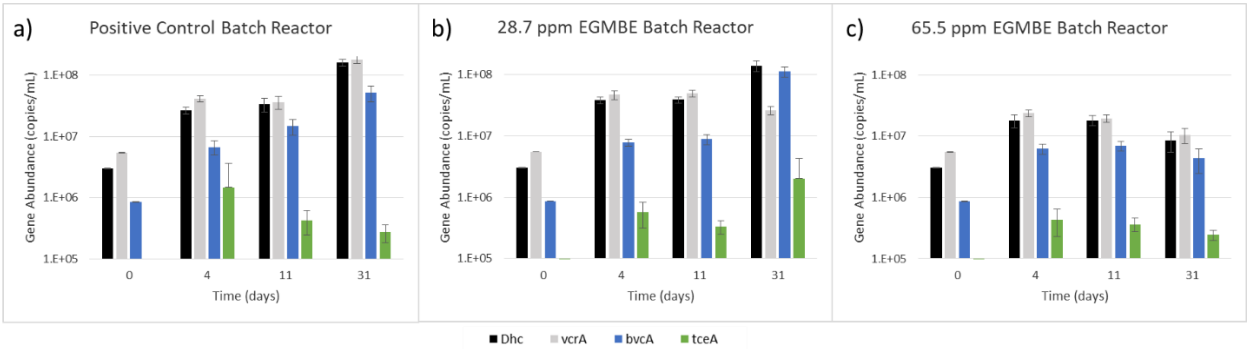

Figure 6-5. *Dhc* and RDase abundance in EGMBE batch reactor experiments with a) 0 ppm and no EGMBE (Positive Control), b) 28.7 ppm, and c) 65.5 ppm PFAAs

This analysis also demonstrated differential growth of *Dhc* strains in the presence of PFAAs. In microcosm experiments with initial concentrations of 25.9 mg/L PFAAs and lower, the increase in *Dhc* 16S rRNA and RDase gene abundance was within 20% of the average increase in all experiments (Table 6-2), although the greatest increase in *vcrA* abundance occurred in the absence of PFAAs. At an initial PFAA concentration of 53.5 mg/L, the abundance of the *bvcA* gene increased an order-of-magnitude (118-fold) compared to lower growth in reactors with lower PFAA concentrations (average of 62.6-±3.18-fold). This difference could be due to a greater tolerance of non-ideal conditions by *Dhc* cells harboring *bvcA* which has been observed in studies of oxygen exposure.[350] The microcosms prepared with the highest initial PFAA concentration (119.8 mg/L) was

bioaugmented from a different bottle of KB-1® inoculum with different initial gene abundances (Figure C-4) so it is not possible to compare the -fold increases with the other microcosms.

Table 6-2. Increase in *Dhc* 16S rRNA and RDase gene abundance in microcosm experiments

Initial PFAS mg/L	-fold increase (day 28)			
	Dhc	*vcrA*	*bvcA*	*tceA*
0	25.1	31.1	60.1	93.0
12.8	21.0	22.8	67.1	93.0
25.9	22.0	24.3	60.7	98.2
53.5	26.7	20.8	118.4	95.2

In microcosms with the highest PFAA concentrations (53.5 and 119.8 mg/L), *Dhc* cells harboring the *bvcA* gene made up a larger percentage of the total RDase genes (13.2% and 20.3%, respectively) than in reactors with 25.9 mg/L PFAS and less (average 6.3% ±0.94%). In microcosm containing 53.5 and 119.8 mg/L PFAAs, cells harboring the *vcrA* gene comprised a smaller proportion of the RDase genes (77% and 74%, respectively) than in reactors with 25.9 mg/L PFAS and less (85% ±1.9%), likely due to the higher efficiency of cells harboring *bvcA* under non-ideal conditions. The relative abundance of cells harboring the *tceA* gene was less variable (average 8.1% ±1.6%) across all PFAA concentrations with the lowest proportion (5.6% ±1.3%) in microcosms with 119.8 mg/L PFAS.

In reactors containing EGMBE, *Dhc* cells harboring the *vcrA* gene (associated with the transformation of TCE and *cis*-DCE to ethene) increased in abundance by 33.2 (±3.6)- and 12.5 (±8.0)-fold over the course of the experiment in the positive control and 0 mg/L PFAAs control reactors, respectively, but only 4.8 (±0.52)-fold in reactors containing 28.7 mg/L PFAAs. Alternatively, cells harboring the *bvcA* gene (associated with the transformation of DCE isomers to ethene), increased to a higher abundance in the reactors

containing 28.7 mg/L than in the reactors containing no PFAAs with increases of 131 (±8.9)-,25.1 (±23.8)-, and 36.7 (±19.2)-fold in the 28.7 mg/L PFAS, 0 mg/L PFAAs, and positive control reactors, respectively (Figures 6 and C-5).

These analyses revealed a shift in the *Dhc* strain responsible for ethene formation from cells harboring *vcrA* in the absence of PFAAs to cells harboring *bvcA* when PFAAs concentrations were high and in the presence of PFAAs and EGMBE. The shift was observed in microcosms with an initial PFAA concentration of 53.5 mg/L and a final PFAA concentration of 38.7 mg/L (Table C-2) but not in microcosms with an initial concentration of 25.9 mg/L and a final concentration of 19.4 mg/L. Similarly, cells harboring the *bvcA* gene were more resilient than cells harboring the *vcrA* gene in the presence of EGMBE at a PFAA concentration of 28.7 mg/L.

6.4.4 Sorption of PFAAs

There was no evidence of PFAA transformation in the batch reactor experiments. Although measured concentrations of total PFAA varied from -13% to +0% over the course of the experiment and concentrations of individual PFAAs varied from -17% to +20% (Table C-1), there was no downward trend with time and fluoride was not detected in IC analyses. Batch reactors containing EGMBE showed greater variability (total PFAAs varied -35% to +6%; individual compounds varied -78% to +131%; Table C-1) but also showed no downward trend over time.

In the microcosms, the concentration of PFAAs decreased over the first 20 days, then remained constant, likely due to sorption of the materials to the organic carbon in the porous media (Table C-2, Figure C-6)).[82,468,469] As the concentrations dropped in both abiotic and bioaugmented microcosms and fluoride was not detected in IC analyses, it is unlikely that PFAAs were transformed or degraded. The total PFAA concentrations dropped to 72% to 75% of the initial concentration while the concentration of individual

compounds remained constant or dropped to as low as 37% of the initial concentration (Table C-2). PFDA and PFOS showed the greatest declines in concentration averaging 39% and 59% of the initial concentration, respectively (Table C-2). The greater decreases in PFOS and PFDA concentrations are expected due to the affinity of longer carbon chain PFAAs to adsorb to organic carbon.[383,385,470]

6.5 Conclusions

Total PFAA concentrations of 11.7 mg/L and higher inhibited the reductive dechlorination of *cis*-DCE to VC and ethene by *Dhc* strains harboring the *vcrA* and *bvcA* genes in batch reactor systems. The presence of a solid phase, however, prevented this inhibition. Microcosm experiments performed with total initial PFAAs concentrations of 53.5 mg/L or lower (38.7 mg/L final) did not exhibit any slowdown of microbial reductive dechlorination. This protection results from a combination of PFAA sorption to the solid phase, decreasing the total aqueous concentration by approximately 30%, and microenvironments around solid particles that may protect microbial cells from the high concentrations in the bulk liquid, as has been observed in low pH conditions.[463] The presence EGMBE, in conjunction with PFAAs, exacerbated the inhibition of MRD. Transformation of all chlorinated ethenes was inhibited in experiments with total PFAA concentrations of 28.7 mg/L and higher.

Although Weathers et al. (2016) did not show inhibition of reductive dechlorination by *Dhc* strain 195 in experiments performed with 22 mg/L PFAAs, the discrepancy is likely caused by the mixture of PFAAs used in each experiment and the presence of EGMBE. In the Weathers et al. (2016) study, the 22 mg/L PFAA experiments contained equal concentrations of each PFAA (i.e. 2 mg/L PFOS), while in these experiments concentrations of each compound were unequal (*i.e.* 20.0%, 5.7 mg/L PFOS). These results indicate the concentration of individual PFAA compounds may inhibit reductive

dechlorination even if the total PFAA concentration is less that the total concentration shown to cause inhibition. Preliminary batch reactor experiments performed with PFOS alone (not shown) revealed a lag in the time to transform all chlorinated ethenes (PCE, TCE, *cis*-DCE, and VC) at PFOS concentrations of 2 mg/L and higher. There was no trend with increasing PFOS concentration, however, and additional investigation is necessary to determine the impact of single PFAAs on microbial reductive dechlorination by *Dhc*.

The presence of PFAAs did not impede total *Dhc* growth in microcosm experiments, but the composition of the population was altered with *bvcA*-harboring *Dhc* strains superseding *vcrA*-harboring strains as the key contributors to ethene production when initial PFAA concentrations were 53.5 mg/L and higher. In the presence of PFAAs and EGMBE, a similar shift in the predominant *Dhc* strain was observed at a PFAA concentration of 28.7 mg/L. Similar resilience of *bvcA*-harboring *Dhc* strains has been measured under elevated temperatures (35°C[29]), suggesting these strains are more resilient to conditions typically considered non-ideal for *Dhc* growth and activity. The total growth of *Dhc* was inhibited by higher concentrations of PFAAs (66.5. 112.6, and 135.8 mg/L) when EGMBE was present.

This study documents complete dechlorination of PCE to ethene by a microbial consortium containing multiple strains of *Dhc* even at initial PFAA concentrations as high as 120 mg/L (86.3 mg/L after sorption) if porous media is present. Although the PFAA concentration was reduced by 72%-75% due to sorption to the solid phase, sorption alone does not account for the reduced inhibition. The equilibrium PFAA concentration of 86.3 mg/L in the microcosms exceeded the batch reactor concentration (61.7 mg/L) at which PCE and TCE were not fully transformed to ethene. These results suggest that MRD is a suitable treatment for chlorinated ethenes in groundwater, even if PFAAs are present, as there will be a solid phase to protect microorganisms from high aqueous concentrations. The shift in

the *Dhc* strains capable of metabolically transforming *cis*-DCE to ethene, from cells harboring the *vcrA* gene to cells harboring the *bvcA* gene, measured at high PFAA concentrations and in the presence of EGMBE, demonstrates the advantage of maintaining a diverse *Dhc* population containing multiple strains.

Acknowledgements

Funding for this research was provided by the Strategic Environmental Research and Development Program (SERDP) under Project ER-2714: Development of Coupled Physiochemical and Biological Systems for In situ Remediation of Mixed Perfluorinated Chemical and Chlorinated Solvent Groundwater Plumes. The contents of this document have not been subject to agency review and do not necessarily represent the views of the sponsoring agency.

Appendix C. Supplementary data

The supplementary material contains additional information on the organic carbon and sorption properties of the porous media used in microcosms and additional details of experimental PFAA concentrations and *Dhc* and RDase abundance.

7.0 Key Findings, publications, and recommendations for future work

The studies completed are intended to enhance the understanding of *Dehalococcoides mccartyi (Dhc)* strains, as measured by the reductive dehalogenase *(*RDase) genes they harbor, and the microbial reductive dechlorination (MRD) of chlorinated ethenes for use in *in situ* bioremediation (ISB). The work focuses on the RDase genes implicated in complete transformation of tetrachloroethene (PCE) and trichloroethene (TCE) to ethene, as a surrogate for strain-specific response, and the factors that impact abundance and expression of these genes. This information may be used by practitioners of ISB to design efficient remedies and avoid some of the pitfalls that prevent complete dechlorination of chlorinated ethenes to benign ethene.

7.1 Key Findings

7.1.1 Bioenhanced back diffusion and population dynamics of Dehalococcoides mccartyi strains in heterogeneous porous media

- Differences in hydraulic conductivity and organic carbon (OC) content-controlled desorption and back diffusion of sequestered chlorinated solvents from OC and low-permeability zones.
- Organohalide respiring bacteria enhanced the mass transfer of TCE out of the low-permeability regions over abiotic dissolution processes alone.
    - MRD enhanced back diffusion by 12%, with local enhancements up to 53% measured where TCE was stored in low-permeability and high-OC lenses, resulting in increased overall mass flux of chlorinated ethenes from the aquifer cell.
    - The greatest bioenhancement of back diffusion occurred in regions of contrasting hydraulic conductivity and OC content.

- The distribution of specific *Dhc* strains was influenced by the availability of electron acceptors within and near soils of differing physical properties.
    - Subsurface heterogeneity represented in the aquifer cell resulted in variations electron acceptor availability, shifting the *Dhc* strains present from cells harboring *tceA* in locations where TCE was available to cells harboring *vcrA* where vinyl chloride was available.
    - Cells harboring *bvcA* were most abundant near low-permeability, high OC materials where *cis*-DCE was available due to the preferential utilization of this electron acceptor.
- *Dhc* cells were capable of penetrating low-permeability porous media including clays, contributing to enhanced back diffusion.

7.1.2 Impact of residence time on extent of trichloroethene degradation

- The average residence time of contaminants and amendments in a bioactive zone determined the extent of TCE biodegradation in the field pilot test and aquifer cell experiment.
    - Increasing the average residence time from 8 days to 16 days in the aquifer cell increased the proportion of ethene in the effluent from 17% of total ethenes on a molar basis to 78% ethene.
    - In the field-pilot test, a 50% increase in average residence time (from 14 days to 21 days) increased the proportion of ethene in the downgradient well from 5% to 46% of total ethenes on a molar basis.
- Localized heterogeneity in the permeability of porous media influenced the extent of TCE dechlorination in both experiments.

- A high permeability layer caused local residence times to vary from the predicted average residence time, allowing contaminants in the treatment zone to reach the downgradient location without being fully transformed to ethene.

7.1.3 Dehalococcoides mccartyi reductive dehalogenase gene expression during pulsed lactate delivery

- The absence of electron donor did not appear to cause down-regulation of *vcrA* gene transcription in the aquifer cell experiment.
    - The abundance of *vcrA* transcripts decreased slowly, with a half-life of 15.3 (±1.68) days, when electron donor was depleted.
- The increase in RDase transcript abundance lagged the increase in RDase gene abundance after an electron donor pulse in the *in situ* pilot test.
    - Increasing electron donor availability first increased the abundance of *vcrA* and *bvcA* DNA, indicating increase growth of cells harboring these genes.
    - RDase gene transcripts increased at a later time as the increased number of cells transcribed the *vcrA* and *bvcA* gene in response to the presence of electron acceptor.

7.1.4 Strain-specific response of Dehalococcoides mccartyi to perfluoroalkyl substances and impact on microbial reductive dechlorination

- Total perfluoroalkyl acid (PFAA) concentrations as low as 11.7 mg/L inhibited the reductive dechlorination of *cis*-DCE to VC and ethene by *Dhc* in batch reactor systems.
- The presence of a solid phase presented inhibition at PFAA concentrations of 53.5 mg/L or lower. This protection results from a combination of PFAA sorption to the solid phase, decreasing the total aqueous concentration by approximately 30%,

and microenvironments around solid particles that protect microbial cells from the high concentrations in the bulk liquid.

- The presence EGMBE in conjunction with PFAAs exacerbates the inhibition of MRD. Transformation of all chlorinated ethenes was inhibited in experiments with total PFAA concentrations of 28.7 mg/L and higher.
- The presence of PFAAs did not impede total *Dhc* growth in microcosm experiments but, in the presence of PFAAs and EGMBE, the total growth of *Dhc* was inhibited by PFAA concentrations of 66.5 mg/L.
- PFAAs shifted the strain of *Dhc* responsible for transforming *cis*-DCE to ethene. In microcosms with initial PFAA concentrations of 53.5 mg/L and in batch reactors containing 28.7 mg/L PFAAs and EGMBE, the composition of the dechlorinating population was altered with *bvcA*-harboring *Dhc* strains superseding *vcrA*-harboring strains as the key contributors to ethene production.

7.2 Implications for Bioremediation

7.2.1 Bioenhanced back diffusion and population dynamics of Dehalococcoides mccartyi strains in heterogeneous porous media

- Future predictions of bioremediation performance should incorporate bioenhanced desorption and diffusion to improve the accuracy of predicting cleanup times. By accounting for this bioenhancement, predicted cleanup times may be reduced and bioremediation can be proposed as a remedy for sites where chlorinated solvent mass is stored in low-permeability materials or those with a high capacity to adsorb contaminants.
- The observed shift in the predominant *Dhc* strain with changes in electron acceptor abundance demonstrates the importance of maintaining a robust dechlorinating community harboring multiple RDase genes and monitoring multiple strains to

obtain more complete information for the assessment of bioremediation progress. If the necessary strains are present, the dechlorinating microbial population (e.g., *Geobacter lovleyi* and *Dhc* strains) adapts to changes in electron acceptor availability caused by the transport of chlorinated ethenes into and out of low-permeability and highly sorptive soils. Such shifts in the microbial population allow efficient transformation of chlorinated ethenes to ethene over the course of a bioremediation application.

7.2.2 Impact of residence time on extent of trichloroethene degradation

- Increasing the average residence time in the treatment zone is a useful tool to increase the extent of chlorinated solvent biodegradation, especially if aquifer heterogeneity is unknown.

7.2.3 Dehalococcoides mccartyi reductive dehalogenase gene expression during pulsed lactate delivery

- This study supports the current practice of pulsed electron donor delivery as RDase RNA is not rapidly depleted when electron donor is limited and will remain up-regulated as cells await future electron donor amendments.
- Because *vcrA* transcripts do not decay rapidly if electron acceptor is present but electron donor is depleted, transcript abundance is not necessarily indicative of active MRD.

7.2.4 Strain-specific response of Dehalococcoides mccartyi to perfluoroalkyl substances and impact on microbial reductive dechlorination

- This study did not measure an impact on MRD of PCE and TCE by a consortium containing multiple *Dhc* strains at PFAA concentrations of 53.5 mg/L or lower when porous media was present. This finding suggests that ISB is an appropriate

remedy for chlorinated ethene plumes even if they are comingled with per- and polyfluorinated alkyl substances (PFAS) below this concentration.

- The preferred growth of *Dhc* strains harboring the *bvcA* gene over cells harboring the *vcrA* gene at high PFAA concentrations reinforces the necessity of maintaining a robust microbial community with multiple *Dhc* strains, especially in conditions that are considered non-ideal.

7.3 Publications and Presentations

The research in this dissertation is the subject of one published manuscript and three manuscripts currently in preparation for publication. Portions of this research has contributed to previously presented material in conference platform and poster presentations.

7.3.1 Publications

1. Hnatko, J.P., L. Yang, K.D. Pennell, L.M. Abriola, N.L. Cápiro. (2020) "Bioenhanced back diffusion and population dynamics of *Dehalococcoides mccartyi* strains in heterogeneous porous media." *Chemosphere*. **2020.** https://doi.org/10.1016/j. chemosphere.2020.126842.
2. Hnatko, J.P., L. Yang, T. Tang, L. Chu, J.L. Elsey, M. Arshadi, K.D. Pennell, L.M. Abriola, N.L. Cápiro. (2020) "Impact of Residence time on extent of trichloroethene biodegradation and comparison of laboratory and field models." *(manuscript in preparation)*
3. Hnatko, J.P. and N.L. Cápiro. (2020) "*Dehalococcoides mccartyi* reductive dehalogenase gene expression during pulsed lactate delivery." *(manuscript in preparation)*

4. Hnatko, J.P., C. Liu, J.L. Elsey, K.D. Pennell, J.D. Fortner, L.M. Abriola, N.L. Cápiro. "Response of *Dehalococcoide mccartyi* strains and dechlorination capability in the presence of pefluoroalkyl substances." *(manuscript in preparation)*

7.3.2 Selected presentations

1. Hnatko, J.P., L. Yang, L.M. Abriola, N.L. Cápiro. "Bioenhanced diffusion and dynamics of *Dehalococcoides mccartyi* strains in heterogeneous porous media." Platform Presentation. 256th American Chemical Society National Meeting; Boston, MA. August 2018.
2. Hnatko, J.P., L. Yang, J.L. Elsey, T. Tang, M. Arshadi, J.A. Christ, K.D. Pennell, N.L. Cápiro, L.M. Abriola. "Comparison of chlorinated solvent dechlorination rates across batch-, laboratory-, and pilot-scales." Poster Presentation. 256th American Chemical Society National Meeting; Boston, MA. August 2018.
3. Hnatko, J.P., L. Yang, J.L. Elsey, T. Tang, M. Arshadi, J.A. Christ, K.D. Pennell, N.L. Cápiro, L.M. Abriola. "Comparison of chlorinated solvent dechlorination rates across batch-, laboratory-, and pilot-scales." Poster Presentation. Association for Environmental Health and Sciences Foundation 34th Annual International Conference on Soils, Sediments, Water, and Energy; Amherst, MA. October 2018.
4. Hnatko, J.P., L. Yang, J.L. Elsey, L.M. Abriola, N.L. Cápiro, L. Chu, J.A. Christ, K.D. Pennell. "Comparison of Microbial Reductive Dechlorination Rates Observed at Laboratory and Field Scales." Poster Presentation. 2017 Strategic Environmental Research and Development Program & Environmental Security Technology Certification Program Symposium; Washington, DC. November 2017.
5. Liu, C., J.P. Hnatko, C. Kim, J. Lee, K. Manz, J. Constanza, N.L. Cápiro, J.D. Fortner, K.D. Pennell. "Development of Coupled Physiochemical and Biological Systems for In situ Remediation of Mixed Perfluorinated Chemical and Chlorinated Solvent

Groundwater Plumes (ER-2714).” Poster Presentation. 2019 Strategic Environmental Research and Development Program & Environmental Security Technology Certification Program Symposium; Washington, DC. December 2019.

7.4 Recommendations for Future Research

This research aims to improve the implementation of ISB by advancing the understanding of *Dhc* strains and MRD. However, additional research is needed to expand upon the findings presented above.

In Chapter 3, MRD was shown to enhance transport of TCE from low-permeability materials by up to 52% in an aquifer cell experiment with four lenses. Additional laboratory studies using more realistic porous media heterogeneities (e.g., interbedded materials, long and narrow lenses, and/or thick layers) and field-scale studies of bioenhancement would provide more evidence and data to incorporate this phenomenon into ISB designs. The study also examined the distribution of *Dhc* strains around low-permeability lenses and strain-specific abundance was found to vary with electron acceptor availability (caused by permeability variations). An additional study in which the electron acceptor was continuously supplied would allow examination of the impact of porous media heterogeneity alone on *Dhc* strains.

Although residence time is a well-understood and commonly used design parameter in ISB, the results of Chapter 4 demonstrate that local residence time controls the extent of biotransformation in heterogeneous systems. In the absence of sufficient site characterization data to identify local variations in permeability, increasing average residence time will increase the extent of TCE biodegradation. In order to use average residence time as a simple design parameter, additional data are needed. A systematic investigation of microbial reductive dechlorination in homogeneous porous media could provide a correlation between hydraulic conductivity, residence time, and chlorinated

ethene degradation. With sufficient data, the appropriate residence time could be selected prior to implementing ISB.

The results presented in Chapter 5 demonstrate that *vcrA* RNA transcripts decay slowly when electron donor is depleted and, thus, are not indicative of active MRD. Additional studies should be completed to examine the impact of electron donor variation on *bvcA* and *tceA* gene expression to provide additional evidence that RDase genes will remain up-regulated when electron donor is provided intermittently. Additional conditions under which RDase genes are transcribed and decay (e.g. pH, oxidation-reduction potential, co-contaminant concentrations) could also assist in the use of dechlorinating microorganisms at complex sites where conditions may vary significantly across the aquifer and over time.

Terminal PFAS (PFAAs) have a greater impact on *Dhc* strains harboring the *vcrA* gene than on strains harboring the *bvcA* and *tceA* genes as presented in Chapter 6. This impact on specific strains may cause the overall inhibition of MRD observed at high PFAA concentrations. Although these conditions are unlikely to exist in *in situ* plume regions, continued research into the impact of PFAAs on MRD may help improve the efficiency of ISB in comingled plumes. As the mixtures of PFAAs in the groundwater can vary substantially from site to site, additional studies examining the impact of individual PFAAs on *Dhc* strains and dechlorination rates may help identify conditions which are not favorable to MRD. As *Dhc* strains harboring the *bvcA* gene have been found to be resilient to multiple non-ideal conditions, additional research into these *Dhc* strains and the conditions that favor them could advance the implementation of bioremediation in conditions that are considered non-ideal.

Appendix A: Supplementary Material for Chapter 3: Bioenhanced back diffusion and population dynamics of *Dehalococcoides mccartyi* strains in heterogeneous porous media

A1.0 Methods

A1.1 Chemicals and Porous Media

Sodium bromide at a concentration of 10 mM (Fisher Scientific; Hampton, NH) and sodium fluorescein at a concentration of 0.075 mM (Sigma Aldrich; St. Louis, MO) were used as non-reactive tracers. Sodium chloride at 10 mM (Fisher Scientific; Hampton, NH) was used as a background electrolyte. TCE (ACS reagent, >99.5%) with a density of 1.46 g/mL and an aqueous solubility of 8.37 mM was obtained from Sigma Aldrich; St. Louis, MO. Aqueous solutions were prepared in 18.2 MΩ deionized water produced by a Milli-Q® Reference Water Purification System (EMD Millipore; Burlington, MA).

ASTM International Standard 20-/30 mesh sand (US Silica Company; Ottawa, IL) was used as the background matrix for the aquifer cell system experiment based on its high hydraulic conductivity (200 m/day[471]) and uniform grain size. Within the background matrix, there were four lenses consisting of Webster soil, a silty clay loam (23% sand, 44% silt, 33% clay)[472] collected from the upper 30 cm of the soil horizon at the Agricultural Experiment Station (Ames, IA), Appling soil, a loamy coarse sand (77% sand, 14% silt, 9% clay) [472] collected from the Ap1 and Ap2 horizons (upper 30 cm of the soil profile) at the University of Georgia Agricultural Experiment Station (Eastville, GA), F-95 fraction of Ottawa Sand Standard sand (Fisher Scientific; Hampton, NH), and loamy sand (69% sand, 22.5% silt, 3.5% clay) collected from the Commerce Street Superfund site (Williston, VT). Webster soil was selected due to its high OC content (1.96%[442]); it has a hydraulic conductivity of 0.86 m/day [443]. Appling soil has a slightly lower OC content (0.66%[442]) and a hydraulic conductivity of 10.2 m/day.[445] F-95 low-permeability sand was selected because it has minimal OC (0.01%[442]) and, therefore, minimal sorption potential, but has a

hydraulic conductivity lower than that of the background matrix (1.9 m/day[447]). The soil from the Commerce Street site is from a location where bioremediation is being considered and has an OC content of 0.09% and a hydraulic conductivity of 1.7-6.9 m/day.[446] The underlying clay layer (45% silt, 55% sand), collected from the Commerce Street Site, contains 0.3% OC.[446] Natural soils (Webster, Appling, and Commerce Street) were ground with a mortar and pestle, then passed through a #30 mesh sieve to remove large particles.

A1.2 Tracer Test

A non-reactive tracer test was performed in the aquifer cell using a 10 mM sodium bromide (Fisher Scientific; Hampton, NH) and 0.075 mM sodium fluorescein (Sigma Aldrich; St. Louis, MO) solution at a flow rate of 2.3 to 2.6 mL/min (200-227 cm/day seepage velocity). After a 750 mL pulse of this solution (approximately 0.66 PVs), the influent was changed to the background electrolyte solution of 10 mM sodium chloride. Effluent samples were collected continuously in 19-minute fractions using a CF-2 fraction collector (Spectrum Laboratories; Rancho Dominguez, CA). Additional 0.6 mL samples were collected from 12 of the sampling ports throughout the tracer experiment approximately once every 90 minutes. Effluent sample bromide concentration was measured using a bromide combination electrode; port sample bromide concentrations were measured by ion exclusion chromatography (IC) as described below. Black light, time-lapse photographs were taken with an EOS Rebel T2 digital camera (Canon; Melville, NY) throughout the tracer experiment to visually verify the flow of fluorescein through the aquifer cell.

A1.3 Analytical methods

Chlorinated ethene and ethene concentrations were measured using an Agilent 7890B GC system with a DB-625 column and an FID (Agilent Technologies; Santa Clara, CA).[336] A 1mL sample was placed in a 20mL headspace vial containing 20 mL of air and sealed with a septum and aluminum crimp cap. The oxygen in the air inhibits continued reductive

dechlorination.[25,277,336] Samples were introduced to the GC by a Telemark HT3 headspace autosampler (Teledyne Technologies; Thousand Oaks, CA) using a constant heating program. Large volume bromide samples (effluent) were measured using a bromide combination electrode (Cole Parmer; Vernon Hills, IL) connected to a Model 50 conductivity meter (Accumet Engineering; Hudson, MA); for small volume (port) samples, bromide concentrations were measured by IC using a Dionex ICS-2100 IC system with IonPac AS-18 Fast column (Thermo Scientific; Waltham, MA). VFA concentrations were measured using a HPLC connected to an Aminex HPX-87H column (Bio-Rad Laboratories; Hercules, CA) as described by He et al. (2003), using an 1200 Agilent HPLC System with diode array detector (DAD; Agilent Technologies; Santa Clara, CA).

Chlorinated ethenes in soil samples were determined using a methanol extraction method modified from Costanza, 2005. Briefly, 5 to 10 mg of soil were placed in 10mL of methanol in a 20mL crimp cap vial and allowed to equilibrate for 24 to 48 hours. After equilibration, vials were centrifuged at room temperature at 800 rpm (129×g) in an Eppendorf 5810R centrifuge (Eppendorf, Happauge, NY) and samples were collected using a needle and syringe. Methanol from soil extractions was sampled and analyzed by GC-ECD using a direct liquid injection into an Agilent 7890B GC with DB-5MS capillary column (0.25 mm i.d., 30 m length, 0.1 μm film thickness; Agilent Technologies; Santa Clara, CA). A 1 μL aliquot of sample was injected by the autosampler into a 300˚C split inlet with a constant stream of helium carrier gas at pressure of 5.3 psi. The inlet was operated with a 3mL/minute septum purge flow and a 40:1 split ratio. The GC oven was held at 30˚C for 8 minutes followed up a rapid (100˚C/min) increase to 60˚C where it was held for 2 minutes after which the oven was heated to 200˚C at a rate of 25˚C/min. Compounds were detected with and micro ECD operated at 300˚C with 30 mL/min of nitrogen gas makeup flow. The

method was calibrated at the start of the experiment using a standard curve of 5 replicates of 5 samples with known concentrations.

A1.4. Solid Phase Sampling

Following collection of the final round of aqueous samples from the side ports, the aquifer cell was partially dewatered by pumping out approximately ½ of the aqueous phase using a peristaltic pump to facilitate aquifer cell unpacking. The solid phase from the aquifer cell was then destructively sampled by placing the aquifer cell on its side, and removing one pane of glass. Soil samples were collected from the porous media corresponding to the 13 ports where aqueous samples were collected with an additional 3 samples collected from each of the soil lenses and 6 samples collected from the clay confining layer (Figure 3-1). Each sample was immediately placed in a sterile 50 mL centrifuge tube and frozen at -80°C for future DNA extraction and microbial quantification. An additional thirty-five samples (5 of background sand, 5 of each lens, and 10 of the clay confining layer) were collected and analyzed for TCE using the methanol extraction procedure described above.

A1.5 Microbial quantification

Aqueous biomass samples (15 mL effluent samples and 1 mL sampling port samples) were prepared by centrifugation as described by Cápiro et al. (2015). After removing the supernatant, pellets were stored at -20°C. Microbial genomic DNA was extracted from the pellets using the QIAamp DNA Mini Kit (Qiagen; Hilden, Germany) and following the manufacturer's protocol. Microbial DNA was also extracted from 0.24 to 0.34 g wet soil samples using the PowerSoil DNA Isolation Kit (Mo-Bio Laboratories; Carlsbad, CA) in accordance with the manufacturer's protocol. All extracted DNA was stored at -20°C until quantitative polymerase chain reaction (qPCR) analysis.

Dhc cell abundance was quantified by qPCR analysis targeting the *Dhc* 16S rRNA gene with additional analysis targeting the *tceA, vcrA, and bvcA* RDase genes. All qPCR

analyses were measured in triplicate using a Step One Plus Real-Time PCR System (Applied Biosystems; Foster City, CA) under standard operating conditions and TaqMan-based chemistry [37]. Primers and probes were obtained from IDT Technologies (Coralville, IA) or ThermoFisher and the TaqMan Universal PCR Master Mix from Applied Biosystems (Foster City, CA). *GeoSZ* 16S rRNA gene copies were measured using SYBR Green detection chemistry according to described protocols [317,474] with the modifications introduced by Amos et al. (2009). For each analysis, a standard curve was generated using 10-fold serial dilutions of a stock solution containing a known concentration of plasmid DNA with a single copy of the target gene [37]. *Dhc* cell abundance was calculated on the basis of a single 16S rRNA gene copy per cell [475,476] and *GeoSZ* abundance based on 2 16S rRNA gene copies per cell [477]. Attached gene copies were calculated by subtracting the product of the aqueous gene copy concentration and the volume of water contained in the soil sample from the total number of cells measured in the solid sample.

A1.6 Modeling aquifer cell and flow field

The governing equation for aqueous transport of non-reactive components in the simulator MT3DMS is given as:

$$\frac{\partial}{\partial t}(\theta C^a) + \boldsymbol{\nabla} \cdot \left(\theta C^a \underline{v}^a\right) - \boldsymbol{\nabla} \cdot (\theta \boldsymbol{D}_h^a \cdot \boldsymbol{\nabla} C^a) = E^{as} \quad (1)$$

where ϕ is the porosity of the aquifer material (dimensionless), C^a is the mass concentration in aqueous phase (ML^{-3}), $\underline{v}^a$ is the aqueous phase linear pore water velocity (LT^{-1}), $\boldsymbol{D}_h^a$ is the aqueous phase hydrodynamic dispersion tensor (L^2T^{-1}), and E^{as} is the mass transfer between sorbed and aqueous phases:

$$E^{as} = -\rho_b \frac{\partial S}{\partial t} \quad (2)$$

where ρ_b is the porous media bulk density (ML^{-3}) and S is the sorbed concentration of the component with respect to the solid mass (MM^{-1}). In this work, consistent with available

batch data, linear equilibrium sorption of TCE to soil materials was assumed, $S = K_d C^a$, where K_d is the distribution coefficient (L^3M^{-1}). This version of MT3DMS was coupled with MODFLOW [478] to account for transient groundwater flow.

To represent the actual experimental conditions of the aquifer cell, the model domain was tailored to account for all of its features, including the lenses, clay layer, and most importantly, the influent delivery system. Prediction accuracy for compound concentrations in the aquifer cell depends primarily on a simulation of the resultant flow field. A schematic diagram of the model domain for the aquifer cell is shown in Figure A-1. The aquifer cell was conventionally modeled as a pseudo two-dimensional domain, as transverse transport along its thickness was considered to be minimal. Flow chambers, constructed as slotted stainless-steel wells to promote uniform flow distribution into the aquifer cell, were simulated by assigning a hydraulic conductivity six orders –of-magnitude higher than that of the background sand to the first and last column of the numerical grid cells. A stainless-steel drop tube in the influent chamber was used to allow the influent solution to flow from a constant head reservoir to create a steady flow rate, and an effluent drop tube was open to the atmosphere at a fixed height. In order to simulate these conditions, the numerical grids at the inlet and outlet points (Figure A-1) of the flow tubes were assigned as constant head cells. A fine spatial discretization was applied to the model domain with a grid spacing of 1 cm (length) × 0.25 cm (height) to capture mass transfer processes (e.g., diffusion) in the vicinity of lens and clay layers. An implicit finite difference scheme with upstream weighting on advection was used to solve the transport equations, providing computational efficiency and robust numerical solutions. An adaptive temporal discretization was applied to minimize numerical dispersion.

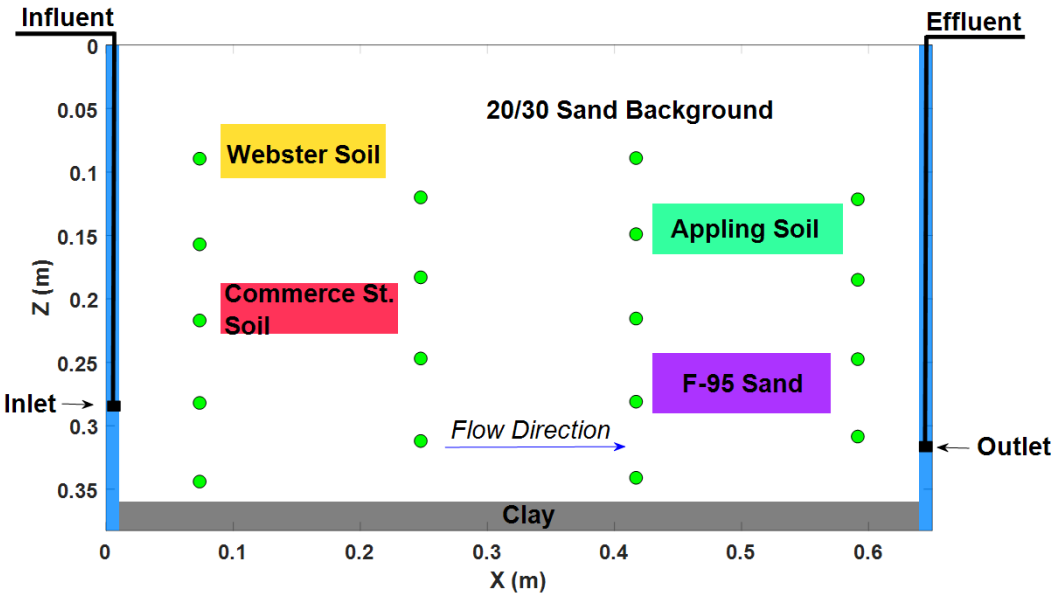

Figure A-1. Aquifer cell construction for numerical simulation. Figure by Lurong Yang.

As the hydraulic head gradient was controlled and known throughout the experiments, hydraulic conductivity and dispersivity coefficients were adjusted by running numerical simulations to match 1) the average effluent flow rate and 2) the breakthrough curves of the initial bromide tracer test. Effluent tracer breakthrough curves (BTC) were used to calibrate the hydraulic conductivity of the background sand while sampling port tracer data was mainly used to fit the hydraulic conductivities of the lenses and the clay. Iterative revision of parameters was used to minimize the root mean square errors between model simulation and experimental observation of the BTC as the complexity of the system and the number of adjustable variables prevented the use of a parameter optimization procedure.

A2.0 Supplemental Information Results:

A2.1 Bromide Tracer Breakthrough

Calibrated parameters used in the tracer test model are listed in Table 2. The hydraulic conductivity values of the emplaced media were reduced by a factor of 1.5 to 2 from initial values in order to match both measured hydraulic gradient and flow rate. An initial

longitudinal dispersivity value of 0.1 cm and a vertical to longitudinal ratio of 0.1 cm were employed, following Lyon-Marion et al. (2017). The longitudinal dispersivity was then slightly adjusted to a value of 0.24 cm after calibration in order to match the rise and tailing of the BTC. Experimental measurements and the associated numerical simulation of the bromide BTC are plotted in Figure A-2. Using the calibrated parameters, the model matched the experimental BTC with goodness of fit of 0.86, 0.60, 0.82, and 0.79, calculated by "goodnessOfFit" (MATLAB, The Mathworks, Natick, MA), for data collected in effluent, and ports 1E, 2C, and 4D, respectively. The model simulation matched the asymmetrical shape of the BTCs, but under-predicted the magnitude of the effluent tailing at late times, possibly due to simulation of the diffusive mass transport within the clay layer at the bottom (Figure A-3). However, a mass balance calculation by using experimental data of influent mass (750.8 gram) and effluent mass (831.9 gram) yielded a mass recovery of 110%, suggesting that the high tailing could be attributed to mass retention from a prior tracer test (not modeled). The model predictions for sampling ports matched the breakthrough times and the plateau maximum concentrations (10mM). In general, the model results displayed good agreement with experimental BTCs in terms of the shape, arrival time, and plateau concentration, demonstrating the capability of the model to simulate the heterogeneous aquifer cell and the suitability of calibrated parameters used in the model.

A2.2 Modeling of Desorption and Diffusion Under Abiotic and Biotic Conditions

In predicting desorption and diffusion under abiotic conditions, the model accounted for the variability of TCE concentration in the influent chamber/well throughout the experiment. Since the influent TCE concentration was not uniform over the experiment, the measured concentration time series was used as the

boundary condition for the presented simulations, resulting in irregular curves for predicted chlorinated ethene concentrations.

Model-experimental comparisons for the abiotic experiment revealed small predictions errors (RMSE<19%), averaging 10%. Thus, while some of the discrepancy reported between abiotic simulations and biotic experimental observations may be attributed to lack of model prediction accuracy, the discrepancy (δ_{MRD} (%)) for the period from PV 2.9 to the end is significantly (p=0.018) greater than the abiotic prediction error at all ports (Figure 3-3).

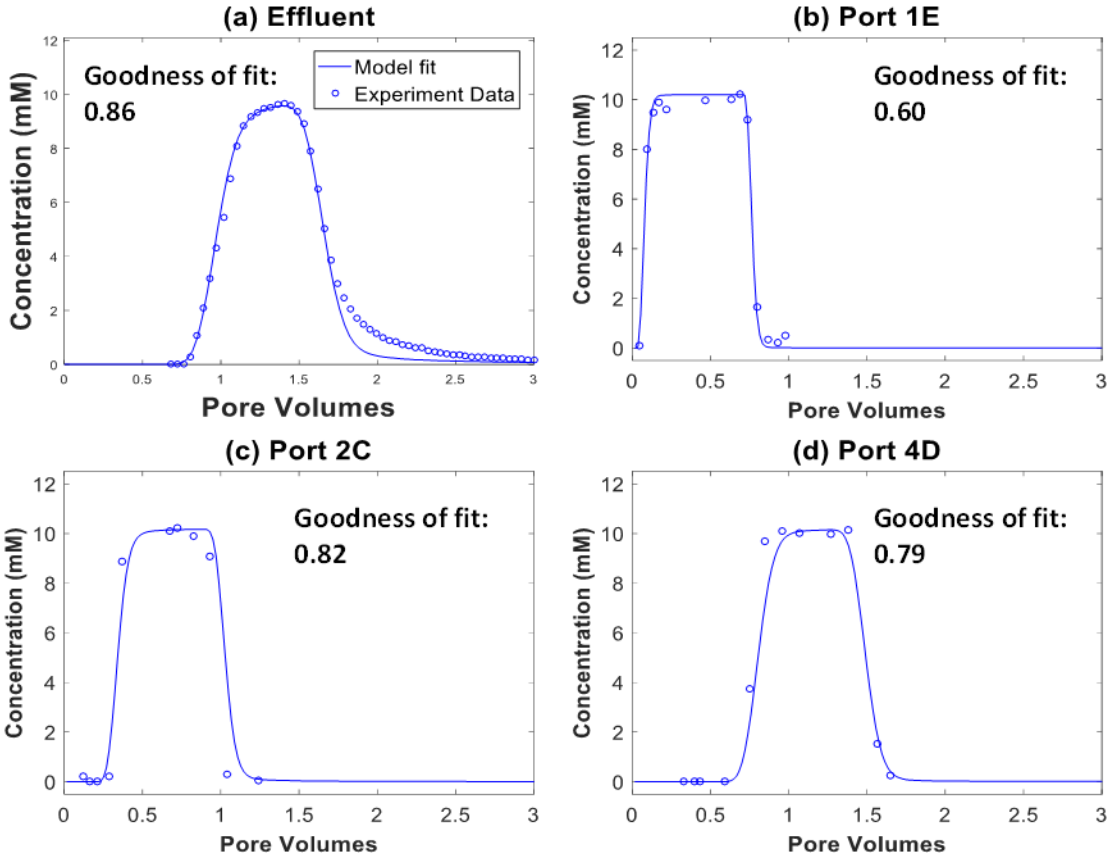

Figure A-2. Comparison of bromide tracer concentration measurements (open circles) and model fit (solid lines) in (a) effluent and (b-d) ports. Figure by Lurong Yang.

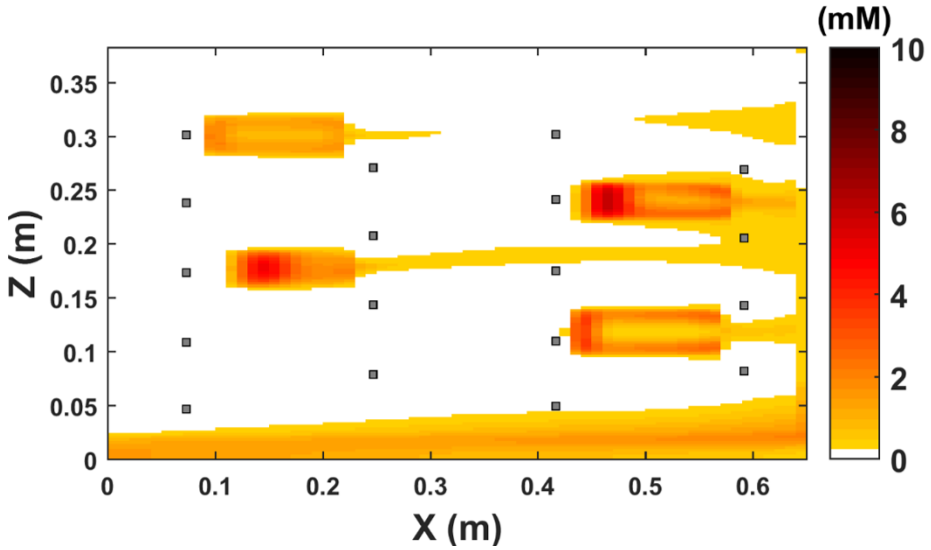

Figure A-3. Simulated aqueous concentration of bromide in aquifer cell at PV 1.96 (hour 15) of tracer experiment. Figure by Lurong Yang.

2.3 Impact of moisture content on microbial quantification

Moisture content in the background material varied substantially due to the sampling and dewatering procedure described above (Table A-1b). Despite this variation, there was no relationship between gene abundance and moisture content in the background porous media (Figure A-4). Moisture content did not vary withing the lenses or clay layer.

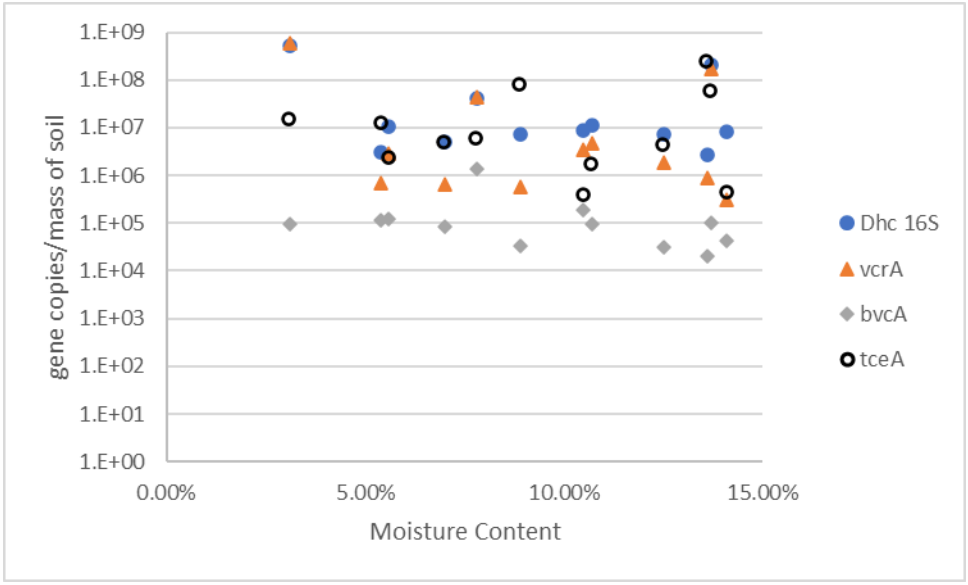

Figure A-4. Solid sample gene abundance (gene copies/mass of soil containing 1mL of pore water) vs. moisture content in background sand samples.

Table A-1. qPCR results for *Dhc* 16S rRNA and RDase genes for (a) aqueous and (b) soil samples.

(a)

Sample Location	Sample PV[a]	Sample Day[a]	*Dhc* 16S rRNA[b]	*vcrA*[b]	*bvcA*[b]	*tceA*[b]	*GeoSZ* 16S rRNA[b]
Inoculum	0	0	2.40E+07	9.83E+07	2.94E+06	5.97E+05	1.57E+06
Port 1B	0.5	1.6	3.84E+04	2.09E+04	2.06E+04	3.13E+04	
Port 1E	0.5	1.6	1.47E+06	4.76E+04	1.64E+04	6.62E+06	7.67E+03
Port 2A	0.6	1.8	3.26E+04	5.53E+05	8.56E+03	5.99E+03	
Port 2B	0.6	1.7	3.46E+04	1.25E+05	7.52E+04		
Port 2C	0.6	1.7	1.01E+05	1.00E+06	7.63E+04		3.34E+04
Port 3A	0.9	2.6	1.31E+05	3.53E+06	3.45E+05		
Port 3C	0.9	2.6	3.51E+04	5.85E+04	1.31E+04	1.72E+04	
Port 3E	0.6	1.8	3.38E+04	1.37E+05	1.96E+04		1.96E+04
Port 4A	0.9	2.8	9.42E+05	1.51E+07	1.78E+06		
Port 4B	0.9	2.8	4.77E+05	4.63E+06	4.79E+05	1.19E+04	
Port 4C	0.9	2.7	6.17E+04	1.89E+06	1.15E+04	2.57E+03	
Port 4D	0.9	2.7	5.36E+04	1.53E+05	1.20E+04	1.38E+04	2.06E+06
Port 1B	2.3	7.5	2.98E+06	3.65E+06	3.48E+06	4.70E+06	
Port 1E	2.3	7.5	4.43E+04	5.59E+04	3.45E+04	1.23E+04	6.20E+05
Port 2A	2.3	7.7		4.37E+06	7.56E+06	2.37E+06	
Port 2B	2.3	7.6		8.22E+05	3.44E+05		
Port 2C	2.3	7.6	1.74E+05	7.31E+05	5.42E+05	5.66E+05	1.32E+06
Port 3A	2.4	7.8	9.97E+04	1.62E+06	5.96E+05		
Port 3C	2.4	7.8	4.24E+05	2.98E+05	2.01E+05	1.07E+05	1.23E+07
Port 3E	2.3	7.7	5.17E+06	3.36E+06	1.42E+05	2.87E+04	
Port 4A	2.5	8.0	6.32E+06	6.07E+06	2.29E+05	1.97E+05	
Port 4B	2.5	8.0	5.94E+06	3.56E+06	2.14E+05	6.24E+04	
Port 4C	2.4	7.9		9.72E+05	5.04E+04		
Port 4D	2.4	7.9	1.28E+06	1.13E+06	1.10E+06	1.79E+06	3.15E+06
Port 1B	5.0	15.6	1.77E+06	2.68E+06	2.15E+06	2.79E+06	
Port 1E	5.0	15.5	9.74E+06	3.94E+06	1.96E+06	2.11E+05	4.90E+06
Port 2A	5.1	15.7		2.46E+07	1.29E+07	3.73E+06	
Port 2B	5.1	15.7		6.62E+12	1.91E+05		
Port 2C	5.0	15.6	4.90E+06	8.62E+06	2.96E+06		6.55E+05
Port 3A	5.4	16.6	6.32E+05	1.38E+07	5.02E+05		
Port 3C	5.4	16.5	5.15E+07	5.15E+07	4.07E+06	2.94E+06	
Port 3E	5.1	15.8	1.26E+07	1.11E+07	2.89E+05		5.24E+06
Port 4A	5.5	16.8	1.04E+08	1.20E+08	1.96E+06		
Port 4B	5.5	16.8	1.29E+08	1.32E+08	3.92E+05	5.37E+04	
Port 4C	5.4	16.7		1.03E+08	1.39E+06		
Port 4D	5.4	16.7	9.09E+07	7.96E+07	2.94E+06	1.40E+06	3.63E+06
Port 1B	9.8	37.3	4.44E+07	7.10E+07	1.17E+07	3.12E+06	5.77E+06
Port 1E	9.8	37.3	5.42E+07	5.67E+07	2.00E+07	1.23E+07	8.45E+06
Port 2A	9.8	37.3	3.84E+07	1.13E+08	2.04E+07	9.96E+05	1.67E+06
Port 2B	9.8	37.3	1.89E+07	0.00E+00	0.00E+00	1.67E+07	
Port 2C	9.8	37.3	2.51E+07	8.36E+07	7.55E+06	8.88E+04	2.28E+06
Port 2D	9.8	37.3	6.37E+07	1.23E+08	1.75E+07	5.18E+07	
Port 3A	9.8	37.3	3.35E+07	5.21E+07	9.44E+06	2.54E+06	3.55E+06

Sample Location	Sample PV[a]	Sample Day[a]	*Dhc* 16S rRNA[b]	*vcrA*[b]	*bvcA*[b]	*tceA*[b]	*GeoSZ* 16S rRNA[b]
Port 3C	9.8	37.3	2.11E+07	1.85E+07	3.38E+06	3.48E+05	9.97E+06
Port 3E	9.8	37.3	3.94E+07	1.27E+08	8.29E+06	9.05E+05	2.06E+06
Port 4A	9.8	37.3	2.55E+07	2.89E+07	6.52E+06	4.72E+05	1.77 E+06
Port 4B	9.8	37.3	2.65E+07	3.95E+07	6.35E+06	1.20E+06	2.04 E+06
Port 4C	9.8	37.3	3.39E+07	4.69E+07	4.61E+06	7.92E+04	
Port 4D	9.8	37.3	6.65E+07	9.54E+07	1.10E+07	1.62E+04	5.37 E+06

[a]since bioaugmentation [b]gene copies/mL

(b)

Sample Location	Sample moisture content	*Dhc* 16S rRNA[b]	*vcrA*[b]	*bvcA*[b]	*tceA*[b]
Port 1B	3.1%	5.29E+08	5.86E+08	9.40E+04	1.41E+05
Port 1E	13.7%	2.04E+08	1.69E+08	1.04E+05	2.92E+05
Port 2A	7.0%	5.06E+06	6.68E+05	8.26E+04	6.42E+04
Port 2B	8.9%	7.29E+06	5.79E+05	3.32E+04	9.92E+05
Port 2C	14.1%	8.46E+06	3.10E+05	4.25E+04	6.14E+04
Port 3A	13.6%	2.70E+06	8.88E+05	2.01E+04	2.44E+06
Port 3C	5.4%	3.12E+06	6.91E+05	1.15E+05	2.89E+04
Port 3E	10.7%	1.12E+07	4.79E+06	9.34E+04	5.19E+04
Port 4A	12.5%	7.40E+06	1.84E+06	3.16E+04	1.66E+04
Port 4B	5.6%	1.08E+07	2.86E+06	1.25E+05	8.13E+03
Port 4C	7.8%	4.11E+07	4.49E+07	1.34E+06	5.35E+04
Port 4D	10.5%	9.06E+06	3.50E+06	1.85E+05	3.23E+04
Webster Lens	14.7%	1.58E+07	8.39E+06	1.06E+05	4.88E+04
Webster Lens	14.7%	3.70E+08	7.52E+07	1.11E+07	3.45E+05
Webster Lens	14.7%	3.16E+08	2.79E+07	1.34E+07	6.62E+04
Appling Lens	32.9%	3.03E+07	5.07E+06	1.42E+05	4.73E+04
Appling Lens	32.9%	1.98E+06	0.00E+00	0.00E+00	2.63E+04
Appling Lens	32.9%	2.92E+06	5.06E+05	1.33E+06	5.61E+04
Comm. St. Lens	18.2%	4.97E+06	8.75E+05	1.02E+06	4.79E+04
Comm. St. Lens	18.2%	1.83E+06	1.65E+05	8.98E+05	6.65E+04
Comm. St. Lens	18.2%	8.35E+06	1.12E+06	1.04E+06	5.35E+04
F95 Sand Lens	19.4%	4.30E+06	1.51E+05	9.75E+05	4.74E+04
F95 Sand Lens	19.4%	9.47E+06	2.42E+06	1.13E+05	5.79E+05
F95 Sand Lens	19.4%	1.13E+07	5.04E+05	1.30E+07	5.19E+04
Clay Layer	28.8%	1.19E+07	7.40E+05	1.34E+07	8.77E+04
Clay Layer	28.8%	9.68E+06	8.20E+06	3.23E+06	9.30E+06
Clay Layer	28.8%	2.03E+07	5.31E+05	1.59E+06	4.94E+04
Clay Layer	28.8%	2.12E+07	1.38E+06	1.19E+06	1.08E+05
Clay Layer	28.8%	2.56E+07	3.43E+06	1.08E+06	7.73E+05
Clay Layer	28.8%	1.95E+08	2.75E+07	5.17E+06	3.59E+04

[a]all samples at end of experiment, 9.8 PVs (37.3 days) after bioaugmentation
[b]gene copies/ mass of porous media containing 1mL of pore water

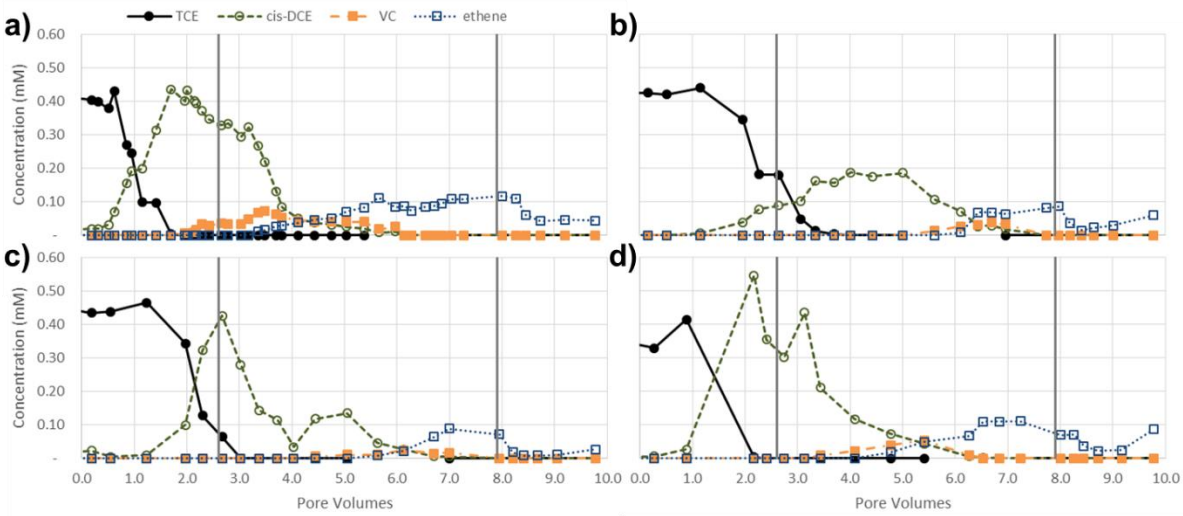

Figure A-5. Chlorinated ethene concentrations during biotic experiment in (a) effluent, (b) port 1E, (c) port 2C, and (d) port 4D. Bioaugmentation occurred at PV 0. Vertical lines represent the reduction of influent TCE concentration from 0.5 mM to 0.04 mM and from 0.04 mM to 0.01 mM, respectively.

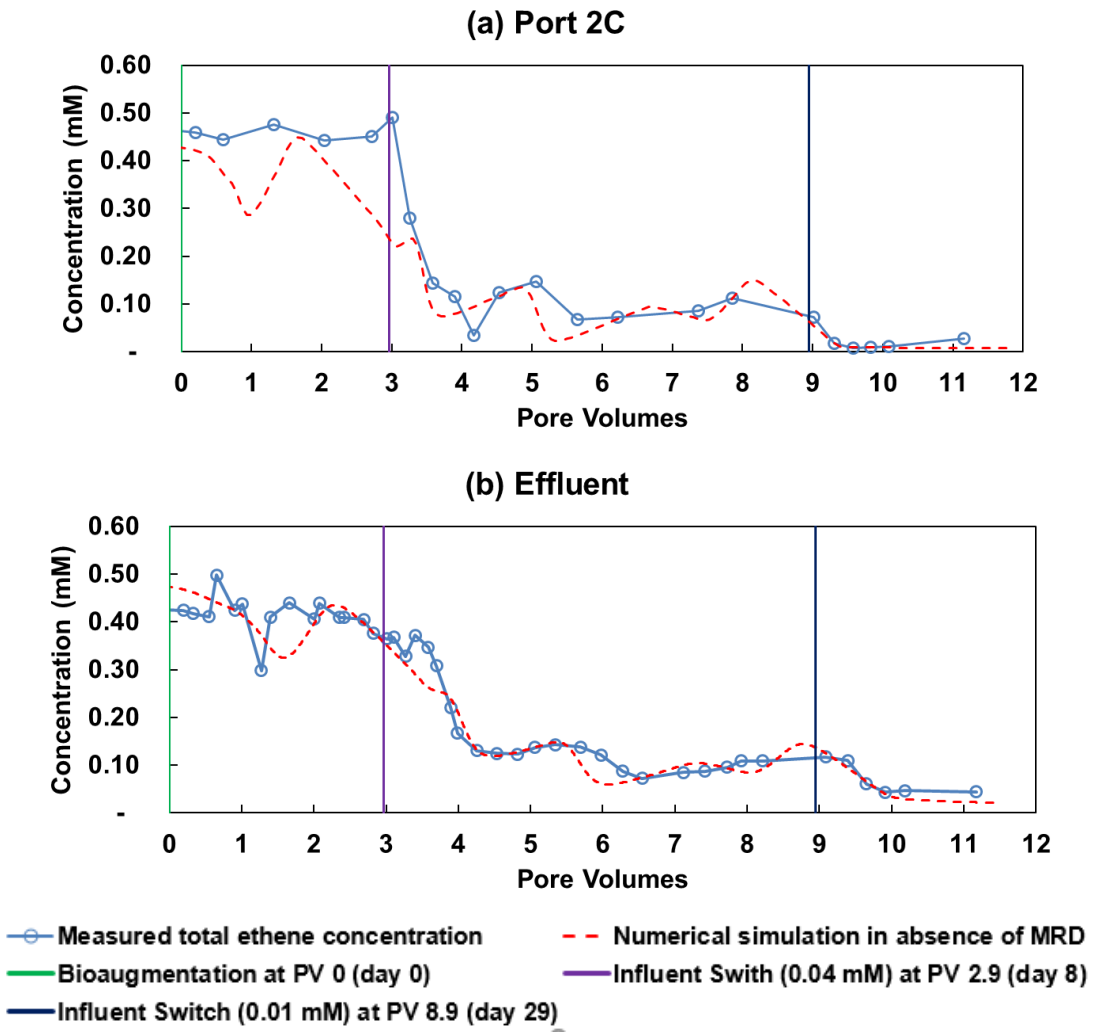

Figure A-6. Selected results for the total molar concentration of chlorinated ethenes and ethene observed during biotic experiment compared with model simulations of abiotic flushing in port 2C and effluent.

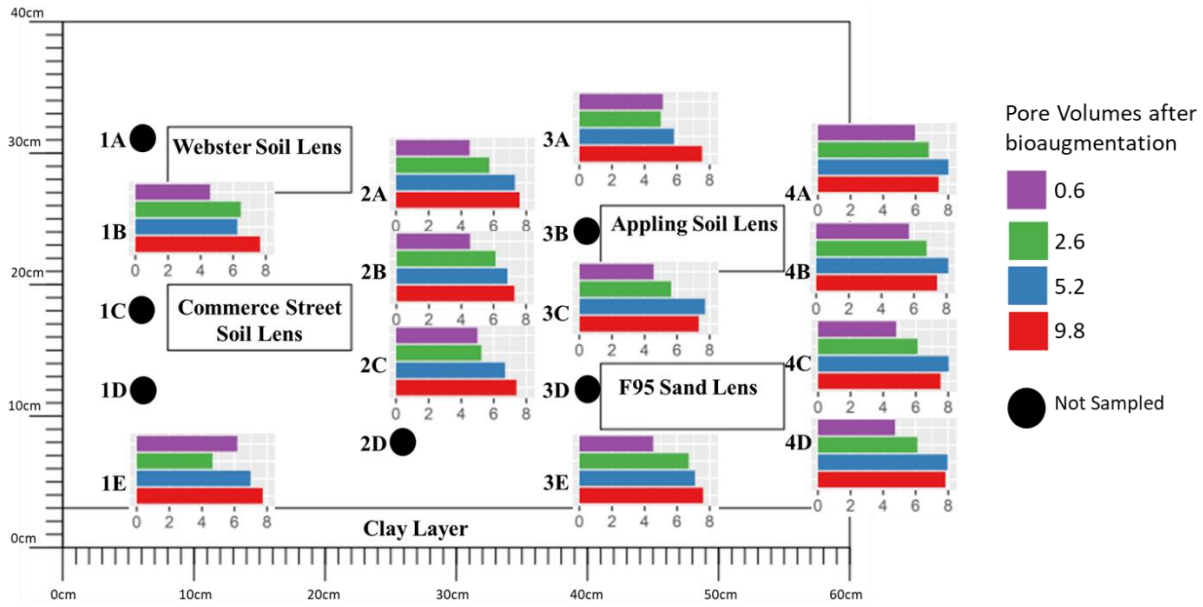

Figure A-7. Log aqueous *Dhc* 16S rRNA gene abundance (gene copies/mL) in sampling ports for samples collected 0.6, 2.6, 5.2, and 9.8 PVs (2-, 8-, 16-, and 37-days) following bioaugmentation.

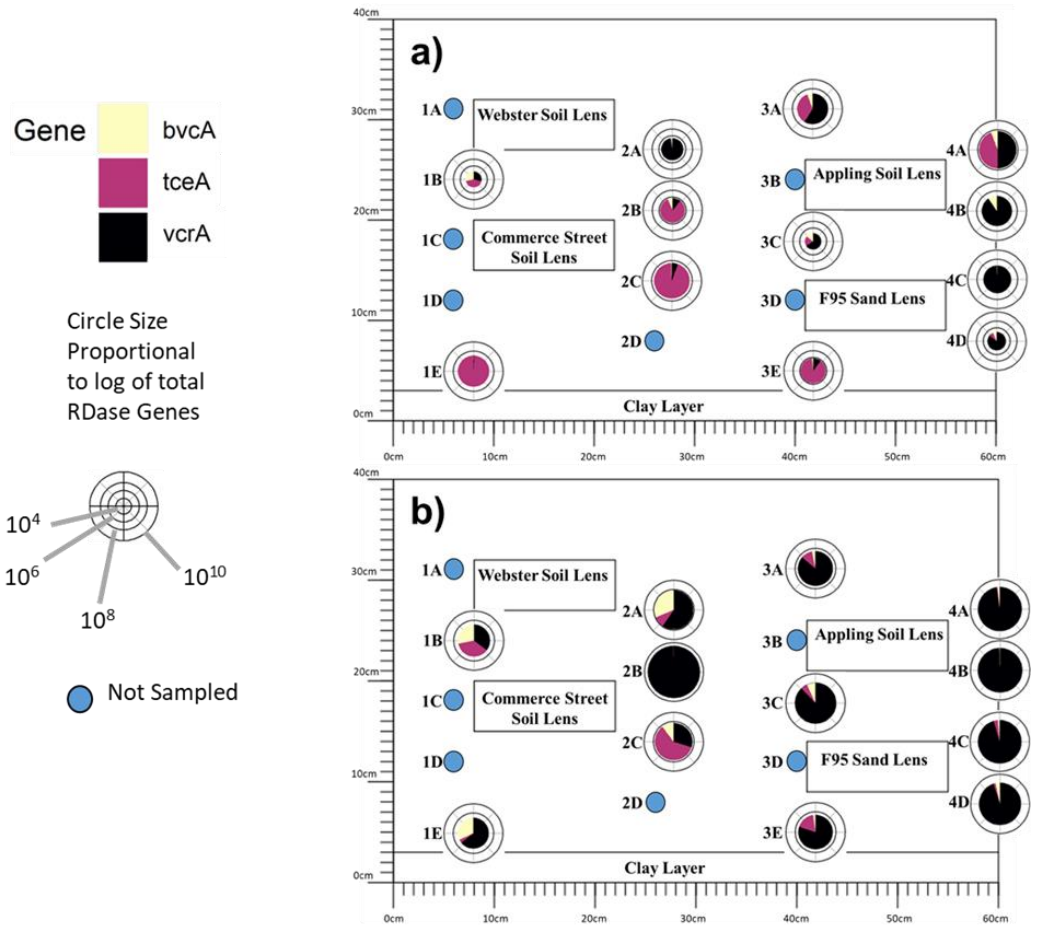

Figure A-8. Aqueous RDase gene abundance and composition (a) 0.6 PVs (2 days) following bioaugmentation and (b) 5.2 PVs (16 days) following bioaugmentation.

Appendix B: Supplementary Material for Chapter 4: Impact of residence time on extent of trichloroethene biodegradation

B1.0 Chemicals, Porous Media, Reduced Growth Media and Inoculum

Sodium bromide at a concentration of 10 mM (Fisher Scientific; Hampton, NH) and erioglaucine A (Fluka Chemical; Seelze, Germany) at a concentration of 50 mg/L were used as non-reactive tracers. Sodium sulfide nonahydrate (Fisher Scientific; Hampton, NH) and L-cysteine (Sigma Aldrich; St. Louis, MO) were used as reductants to maintain anoxic conditions and sodium DL-lactate solution, 60% w/w (Sigma Aldrich; St. Louis, MO) was used as an electron donor. TCE (ACS reagent, >99.5%) with a density of 1.46 g/mL and an aqueous solubility of 1,100 mg/L was obtained from Sigma Aldrich; St. Louis, MO. Aqueous solutions were prepared in deionized water produced by a Milli-Q® Integral Water Purification System (EMD Millipore; Burlington, MA).

Groundwater used in laboratory experiments was collected from numerous wells across the site and was comingled to create a representative groundwater. Groundwater was collected using a modified U.S. Environmental Protection Agency (EPA) low-flow sampling protocol (Section B6.0). Prior to use in laboratory experiments, stored groundwater was sparged with nitrogen gas for at least four hours and amended with 1 mM L-cysteine and 0.2 mM sodium sulfide to remove oxygen and reduce the oxidation-reduction potential (ORP) to less than -150mV, similar to the site conditions.

Porous media from the Commerce Street Site was obtained from soil cores collected during the installation of wells as described in B5.0. Silty clay was collected from the 40 to 42-foot depth of borehole CMT-2 and the remaining soil was collected from the 21 to 35-foot depth of borehole DHT-2. With the exception of the silty clay, porous media used in the aquifer cell was collected from soil cores that were opened in an anaerobic chamber to minimize exposure to oxygen and maintain a viable native community. The silty clay was

collected from the soil core under aerobic conditions, dried, ground with a mortar and pestle, and re-saturated prior to use.

The inoculum used in the aquifer cell and pilot test studies, KB-1® (SiREM; Guelph, ON), is a methanogenic dechlorinating consortium as described above. This inoculum contains several dechlorinating cultures including the PCE to *cis*-DCE dechlorinating species, *Dehalobacter* and *Geo*SZ, as well as three *Dhc* strains (FL2, GT, and BAV1) capable of completing the transformation of PCE to ethene.

B2.0 Chemical Analytical Methods

Groundwater samples for chlorinated ethene and ethene analysis were prepared and analyzed according to previously described methods.[32,257,336] Laboratory samples were placed into headspace analysis vials immediately after collection and analyzed within 24-hours. Chlorinated ethene and ethene concentrations were measured using an Agilent 7890B GC system with a DB-625 column and a flame ionization detector (Agilent Technologies; Santa Clara, CA).[336] Samples were introduced to the GC by a Telemark HT3 headspace autosampler (Teledyne Technologies; Thousand Oaks, CA) using a constant heating program.

Volatile fatty acid concentrations were measured using a high pressure liquid chromatograph (HPLC) connected to an Aminex HPX-87H column (Bio-Rad Laboratories; Hercules, CA) as described by He et al. (2003), using an 1200 Agilent HPLC System with diode array detector (DAD; Agilent Technologies; Santa Clara, CA).

Dissolved organic carbon analysis was performed with a TOC-L analyzer using the non-purgeable organic carbon method (Shimadzu; Kyoto, Japan). Soil sample organic and inorganic carbon content was determined using a total organic carbon (TOC)-L analyzer

(Shimadzu; Kyoto, Japan) using the subtraction method (total carbon minus inorganic carbon equals organic carbon) as described in Marcet et al. (2018).

B3.0 Soil Physical Analyses

Soil cores from the installation of site wells (Section B5.0) were delivered to Tufts University where they were opened, visually inspected and logged with sample aliquots collected at specific locations for analyses. The soil was then segmented and segregated into Ziploc® bags representing 6 inches of borehole depth. For select locations and depth, soil was oven dried and ground with a mortar and pestle, then sample grain size distribution was determined using sieve and hydrometer tests according to Gaeth (2017) and Das et al (1997).

Soil hydraulic conductivity was measured using a static head test in a 15 cm by 2.5 cm inner diameter borosilicate glass chromatography column (ACE Glass Inc, Vineland, NJ). Oven-dried, ground soil was added to the column in approximately 2 cm intervals where it was well mixed using a metal spatula and settled using a gentle vibration tool. The settled material was manually compacted before another 2 cm of material was added to the column and the process was repeated. Once the column was packed completely full of material, it was flushed with carbon dioxide gas for at least 30 minutes, after which Milli-Q® water was driven through the column at a constant flow rate using a Rainin Dynamax RP-1 peristaltic pump (Mettler-Toledo; Columbus, OH). After the column was saturated with at least 5 PV of Milli-Q® at 0.5 mL/min, the pump was removed and column was configured so flow was driven by a static head maintained at a constant height. The head height was measured with a ruler and the flow rate was measured by collecting and weighing the column effluent during a fixed period of time (1 to 10 minutes).

B4.0 Biological Analytical Methods

Aqueous biomass samples from laboratory experiments, including 15 mL aquifer cell effluent samples and 1 mL aquifer cell sampling port samples were prepared by centrifugation as described by Cápiro et al. (2015). After removing the supernatant, pellets were stored at -20°C. Microbial genomic DNA was extracted from the pellets using the QIAamp DNA Mini Kit (Qiagen; Hilden, Germany) and following the manufacturer's protocol. DNA was extracted from field-collected groundwater using the Mo-bio PowerWater Kit (Qiagen; Hilden, Germany) within 48-hours of collection. Alternatively, groundwater was field-filtered using 0.22 μm pore size Sterivex filter cartridges (Millipore; Burlington, MA) which were immediately placed on ice and stored at -80°C prior to DNA extraction using the Mo-bio PowerSoil Kit (Qiagen; Hilden, Germany). Microbial DNA was also extracted from 0.24 to 0.34 g wet soil samples collected from soil cores or laboratory experiments using the PowerSoil DNA Isolation Kit (Mo-Bio Laboratories; Carlsbad, CA). All extractions were performed in accordance with the manufacturers' protocols and extracted DNA was stored at -20°C until qPCR analysis.

Dhc cell abundance was quantified by qPCR analysis targeting the *Dhc* 16S rRNA gene with additional analysis targeting the *tceA, vcrA, and bvcA* RDase genes. All qPCR analyses were measured in triplicate using a Step One Plus Real-Time PCR System (Applied Biosystems; Foster City, CA) under standard operating conditions and TaqMan-based chemistry.[37] *Geobacter lovelyi* Strain SZ (*Geo*SZ) 16S rRNA gene copies were measured using SYBR Green detection chemistry according to described protocols[317,474] with the modifications introduced by Amos et al. (2009). Primers and probes were obtained from IDT Technologies (Coralville, IA) or ThermoFisher and the TaqMan Universal PCR Master Mix from Applied Biosystems (Foster City, CA). For each analysis, a standard

curve was generated using 10-fold serial dilutions of a stock solution containing a known concentration of plasmid DNA with a single copy of the target gene.[37]

B5.0 Well installation and soil core collection

Soil was collected during two well installation events. All borings were completed using a direct-push drill rig to the depth of the clay confining layer, 11.3 to 12.2 m bgs, with soil samples collected in 1.2 m (4 foot) acetate sleeves. Five CMT wells were installed in the proposed treatment area to provide additional data to guide the design and configuration of the pilot test. CMT well locations were selected based on groundwater elevation data, earlier groundwater sampling results, the TCE and *cis*-DCE concentration data from the preliminary soil borings, and the location of subsurface utilities. The wells were installed in two transects perpendicular to the expected groundwater flow direction; two wells in the upgradient transect and an additional three wells in a transect downgradient.

Each CMT well consisted of seven discrete channels screened at discrete intervals to allow groundwater samples to be collected from specified depths beneath the water table.[481] Well screens were installed at 4.7 to 4.9 m bgs, 6.1 to 6.2 m bgs, 7.9 to 8.1 m bgs, 8.8 to 9.0 m bgs, 9.6 to 9.8 m bgs, 10.4 to 10.5 m bgs, and 11.1 to 11.3 m bgs. During CMT well installation, field personnel cut the recovered soil cores into 0.61 m (2 foot) sections, capped each section, and placed them in coolers on ice for storage and transport to Tufts University. While awaiting analysis, the soil cores were stored at 4°C to minimize microbial activity and the volatilization of compounds in the soils.

In September 2016, prior to implementing the pilot test, 3 additional wells were installed in the vicinity of CMT-1 (Figure 4-1 inset). Two wells (DHT-1 and DHT-2) were 5.1 cm (2-inch) diameter PVC-wells, screened between 10.1 and 10.7 m bgs to deliver amendments into and collect samples from the depths of the aquifer with high TCE and

cis-DCE concentrations. The fourth well, CMT-6, was located 5m upgradient of CMT-1, allowing monitoring of constituents entering the pilot test and had a similar construction to the existing CMT wells with 6 screened intervals between 6.2 and 6.4 m bgs, 7.9 to 8.1 m bgs, 8.8 to 9.0 m bgs, 9.6 to 9.8 m bgs, 10.4 to 10.5 m bgs, and 11.1 to 11.3 m bgs. Well DHT-1 was located 3 m upgradient of CMT-1 and was used as an injection well for bioaugmentation and biostimulation. The third well (DHT-2) was 2.0 m upgradient of CMT-1 and served as an extraction well during recirculation and a monitoring well afterward. This configuration allowed CMT-1 to be used as an extraction well during the pilot test.

All wells were developed by rapidly pumping approximately 2.0 L of water from the well after installation and at least 72-hours prior to sampling to remove fine materials from the well screen and any water that was introduced during drilling.

B6.0 Groundwater monitoring and sampling

Site-wide groundwater elevations were measured using a 101 or 102 water level meter (Solinst; Georgetown, ON). Measurements were collected at 35 existing site groundwater wells in August 2014 with additional measurements prior to and during groundwater sampling events. Groundwater samples were collected using U.S. Environmental Protection Agency (EPA) low-flow sampling protocols for most wells and using a modified low-flow protocol for CMT-wells. The modified protocol limited purging to the slowest flow rate, approximately 100 mL per minute, for a maximum of 25 minutes and omitted turbidity measurements. Water was removed from the wells using a Geopump 2 peristaltic pump (Geotech; Denver, CO) and high-density polyethylene tubing. Water quality parameters (temperature, pH, dissolved oxygen, and specific conductivity) were measured using a 556 MPS or Professional Plus 1060 meter (YSI; Yellow Springs, OH) and turbidity

was measured with a microTPW Handheld Turbidity Meter (HF Scientific; Fort Meyers, FL).

Samples for chlorinated ethene and ethene analysis were collected in 40 mL glass volatile organic analysis (VOA) sampling vials with septa caps, completely filled to eliminate headspace; additional sample from select VOA vials was used for volatile fatty acid (VFA) and dissolved organic carbon (DOC). Samples for biological analysis were collected in 1.0 L polyethylene bottles for laboratory filtration or 0.3 to 2.0 L of groundwater was filtered in the field using a 0.2 μm pore size Sterivex filter cartridge (Millipore; Burlington, MA). All samples were collected in triplicate, stored on ice, and transported to Tufts ESL for storage and analysis. VOA vials were stored at 4°C, then sampled and analyzed within 72-hours. Biological samples were stored at -80°C prior to analysis. During operation of the pilot test, groundwater samples from the extraction wells were collected from a sample port in the treatment trailer connected to the extraction tubing without additional purging.

B7.0 Additional Site Background Data

B7.1 Groundwater Elevation

Site wide groundwater elevations varied from 98.4 to 102.6 m above sea level (North American Vertical Datum of 1988) as measured in site monitoring wells in August 2014 (Figure B-1). Groundwater generally flows north to south with a slight west to east gradient in the pilot test area. The unnamed brook does not appear to influence groundwater flow with a groundwater elevation of 101.0 m on the west side of the brook (MW-06) and 101.1 m in a nearby well west of the brook (ASI-05D2). In the pilot test area, groundwater elevation measured in the CMT-wells ranged from 100.9 to 101.1 m in September 2014 with no discernable vertical or horizontal gradients.

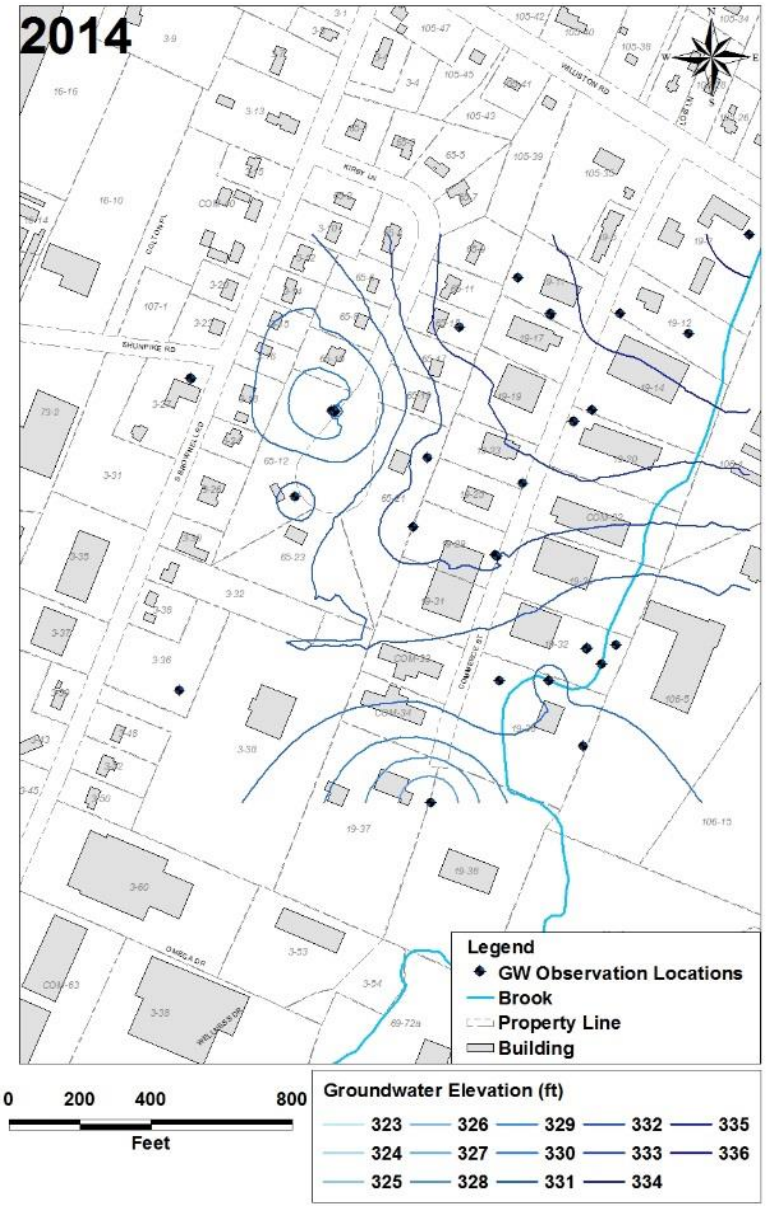

Figure B-1. Interpolated head contours in 2014. The interpolation was based on available head measurements from wells displayed in the maps. Figure by Tian Tang.

B7.2 Soil Permeability and Grain Size

Soil permeability ranged from 4.01×10^{-12} m^2 and 3.88×10^{-12} m^2 in shallow sandy soils and 9.5×10^{-13} m^2 and 2.32×10^{-12} m^2 in deeper, finer grain sediments (Table B-1). In DHT-2, at the screened depth used in the pilot test (10.1 to 10.7 m bgs), the permeability was 1.01×10^{-13} m^2. Grain size analysis indicated that soils in DHT-2 and DHT-4 consist primarily of silty fine sands with some clay (Table B-2). In boring DHT-2, a silty clay layer was encountered at 10.9 m bgs.

Table B-1. Hydraulic conductivities estimated for field and permeability of soil samples collected from monitoring wells.

Depth bgs (m)	Estimated Hydraulic Conductivity (m/d)	Measured Permeability (m^2)	Permeability Measurement Location
0.00-3.05	3.4471		
3.05-3.66	5.6667	8.00E-12 4.70E-12	CMT-5 CMT-1
3.66-4.27	7.5503		
4.27-4.88	4.4221		
4.88-5.49	1.1475	2.00E-12	CMT-1
5.49-6.10	1.2263	2.60E-12	CMT-5
6.10-6.71	1.2239		
6.71-7.32	1.042		
7.32-7.92	2.1358	1.02E-12	DHT-2
7.92-8.53	0.4982		
8.53-8.69	0.6869	9.97E-13	DHT-2
8.69-8.84	0.6869		
8.84-8.99	0.6869		
8.99-9.14	0.6869		
9.14-9.30	0.8076		
9.30-9.45	0.8076		
9.45-9.60	0.8076		
9.60-9.75	0.3917		
9.75-9.91	0.3917	1.00E-13	CMT-4
9.91-10.1	0.403		
10.1-10.2	0.3621		
10.2-10.4	0.3621		
10.4-10.5	0.2836		
10.5-10.7	0.2836		
10.7-10.8	0.2288	1.04E-13	DHT-2
10.8-11.0	0.2285		
11.0-11.1	0.2019		
11.1-11.3	0.2019		
11.3-11.4	0.2313		
11.4-11.6	0.2313		
11.6-11.7	0.2313		
11.7-11.9	0.2313		
11.9-12.0	0.2313		
12.0-12.2	0.2313		
12.2-bottom	0.131		

Table B-2. Grain size of material collected from boring DHT-2^ and DHT-4*

Depth bgs (m)	% larger than 0.42 mm (coarse sand)	% larger than 0.21 mm (medium sand)	% larger than 0.07 mm (fine sand)	% smaller than 0.07 mm, not suspended (very fine sand)	% smaller than 0.07 mm, suspended (silt)	% smaller than 0.07 mm, suspended (clay)
0.00-0.76^	36.9%	16.3%	31.7%	2.5%	12.5%	0.3%
0.76-3.05^	2.3%	10.8%	37.3%	9.6%	34.4%	5.6%
3.05-3.81^	5.8%	30.9%	58.4%	1.1%	3.3%	0.5%
3.81-4.57^	7.0%	33.9%	55.5%		3.7%	
4.57-5.33^	3.7%	0.30%	55.9%	7.9%	5.8%	26.5%
5.33-6.10^	0.20%	0.10%	43.0%	16.6%	38.5%	1.5%
6.10-6.86^	10.5%	1.4%	41.0%	14.9%	29.5%	2.7%
6.86-7.62^	0.00%	0.30%	64.8%	15.6%	16.7%	2.6%
7.62-8.38^	1.5%	0.30%	29.8%	28.7%	37.3%	2.5%
8.38-9.14^	0.10%	0.10%	23.4%	33.4%	42.0%	1.1%
9.60-9.91*	5.5%	0.40%	5.4%	9.1%	71.2%	8.4%
9.91-10.1*	0.30%	0.10%	24.5%	12.6%	54.5%	8.0%
10.1-10.4^	0.10%	0.20%	49.7%	10.5%	32.8%	6.7%
10.4-10.7*	0.0%	0.10%	53.9%	10.1%	28.6%	7.0%
10.7-10.8^	1.5%	1.9%	6.2%	5.3%	76.6%	8.6%
10.8-10.9^	0.40%	0.60%	7.2%	17.5%	70.8%	3.8%
10.9-11.0^	0.00%	0.00%	0.00%	0.00%	66.2%	33.8%

B7.3 Soil Organic Carbon and Sorption Capacity

Organic carbon was not detected in samples collected from the sandy aquifer below 4.0 m bgs but was detected at 0.3% of sample mass in the clay layer. The low amounts of organic carbon limited adsorption of TCE to the soil with sorption equilibrium partitioning coefficients, K_d, of 1.0×10^{-4} to 4.8×10^{-4} L/g (Figure B-2). Site soils are mildly caustic with a soil pH of 7.71 to 9.44.

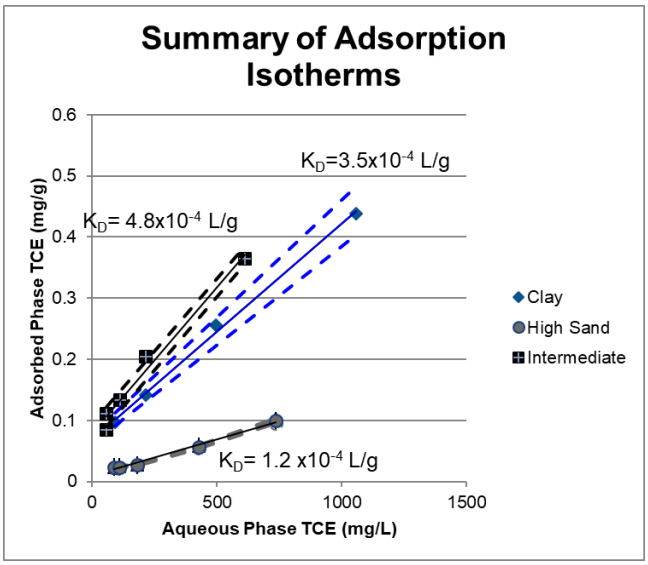

Figure B-2. Adsorption isotherms for soils collected from CMT-1 at depths of 2.6 to 2.9 m bgs (High sand), 2.4 to 3.0 m bgs (Intermediate), and 12.2 to 1.8 m bgs (Clay). Figure by Sam Gaeth.

Adsorption equilibrium experiments were conducted with soils collected from CMT-1 at depths of 2.6 to 2.9 m bgs, 2.4 to 3.0 m bgs, 3.2 to 3.5 m bgs, and 12.2 to 12.8 m bgs as reported in Gaeth (2017). The materials were chosen for their range of particle size and organic carbon content. Depth 2.6 to 2.9 m bgs consisted of primarily sand (90.5% sand, 7.8% silt, and 1.7% clay) with lowest organic carbon content (0.1% by weight) of the three materials tested. The material from this depth also had the lowest sorption equilibrium partitioning coefficient, K_d, (mass of TCE/mass of soil)/(mass of TCE/volume of solution) of the materials with a value of 1.0×10^{-4} L/g. Similar material from a wider range of 2.4 to 3.0 m bgs, consisted of 73.67% sand, 22.5% silt, 3.5 % clay with a slightly higher organic carbon content of 0.2% by weight. The K_d for this depth was higher, 4.8×10^{-4} (L/g), due to the increased organic carbon content. A high clay material, collected from the 12.2 to 1.8 m bgs depth of boring CMT-1, consisted of primarily clay (54.9%) and silt (45.1%), with no sand and 0.3% organic carbon by weight. The adsorption isotherm for this depth was also 3.5×10^{-4}(L/g). The K_d values for each of these isotherms each differ less than a factor of two from their theoretical K_d values, as calculated using the method from Cwiertny and Scherer (2010). The small K_d values and relatively similar amount of adsorption among all

three materials suggests that contaminant sorption throughout the selected pilot test site is limited and confined to a narrow range.

B8.0 Site Groundwater Flow Model Development

In order to determine the appropriate pumping and injection rates, a site groundwater flow model was developed by Dr. Tian Tang (Tufts University). The model was based on site data and implemented using Visual MODFLOW Flex, encompassing a domain that is considerably larger than the DHT study area. The elevations of the ground surface and clay layer were prescribed based on existing topographical and geophysical data. Heterogeneous hydraulic conductivity fields corresponding to different depths below ground surface were generated by Dr. Masoud Arshadi (Tufts University) using a Kriging interpolation method based on permeability measurements in CMT-1 and CMT-5. The measured values vary within one order-of-magnitude.

To account for the formation layering, modeled vertical conductivities were set to be half of those in the horizontal direction. Prescribed heads were set at all lateral boundaries in the modeling process. These values were first obtained based on the interpolated groundwater elevation contour at the boundaries, and then calibrated to better fit the measured and interpolated groundwater levels within the domain. Natural recharge was prescribed based upon the available hydrologic data, while no-recharge boundary conditions were prescribed at the locations of paved roads and buildings. The small brook was treated as a very shallow and narrow river with a riverbed conductivity one order of magnitude lower than the average measured horizontal hydraulic conductivity. In addition, two pumping wells with different screen depths and pumping rates were included at the western and southern parts of the site (Figure B-3), to capture the effect of intermittent sump pump discharge.

The flow model was calibrated to approximate measured groundwater levels. The sump pump discharge rates were used as another fitting parameter to capture the measured drawdown at these locations. In general, the simulation reproduces the interpolated groundwater elevation contours quite well and the normalized root mean squared error of the simulated versus observed head is small (Figure B-3).

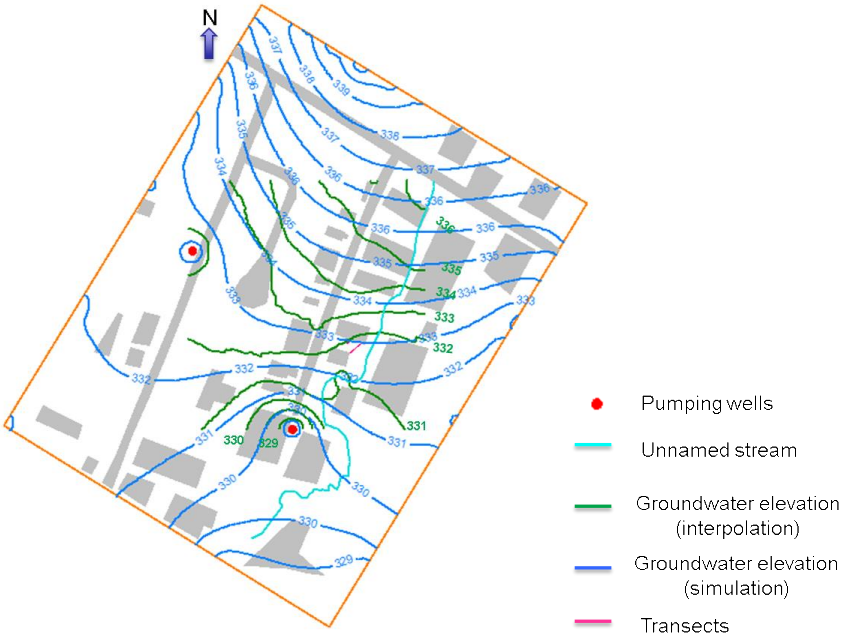

Figure B-3. Comparison of interpolated groundwater elevation contour based on well observations (2011) and the simulated groundwater elevation contour. Figure by Tian Tang.

B9.0 Pilot Test Bromide Tracer

At the inception of the pilot test, bromide injected into DHT-1 was detected in DHT-2 approximately 9 days after beginning the injection, peaking after 11 days (Figure B-4). The pulse was injected over the course of 4 days indicating a residence time of approximately 7 days between DHT-1 and DHT-2. The successful detection of bromide in DHT-2 indicated good hydraulic connectivity between the wells.

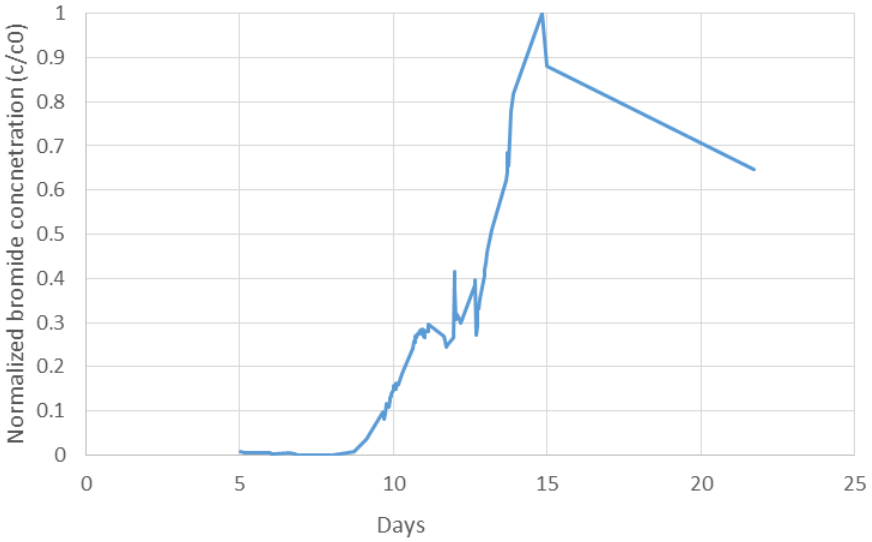

Figure B-4. Bromide breakthrough curve in downgradient well DHT-2

B10.0 Aquifer cell Tracer Test

A tracer test was performed in the aquifer cell using a 385 mL (approximately 1/3 pore volume) pulse of 10 mM sodium bromide and 0.06 mM erioglaucine A solution at a flow rate of approximately 0.15 mL/min. Effluent samples were collected continuously in 75 minute fractions using a CF-2 fraction collector (Spectrum Laboratories; Rancho Dominguez, CA) and bromide concentrations were measured using a bromide combination electrode (Cole Parmer; Vernon Hills, IL). Time-lapse photographs were taken with an EOS Rebel T2 digital camera (Canon; Melville, NY) throughout the tracer experiment to visually verify the flow of erioglaucine A tracer through the aquifer cell.

The photographs (Figure B-5) reveal more rapid flushing of the blue dye through the center of the aquifer cell with delayed transport through the top and bottom layers. This indicates the existence of layers of varying permeability with higher permeability in the center and lower permeabilities above and below. As the aquifer cell was constructed to mimic the stratigraphy of the Commerce Street Site, these layers are likely present in the pilot test location and explain the irregular shape of the pilot test bromide tracer curve (Figure B-4).

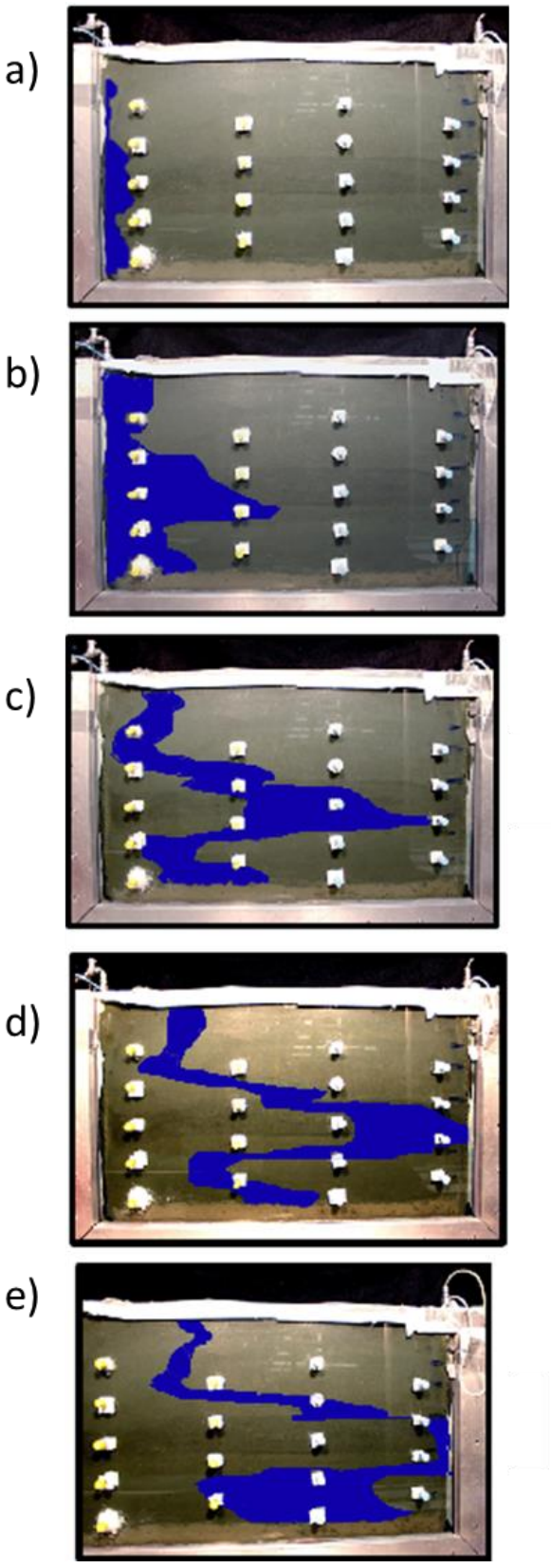

Figure B-5. Photographed tracer position for selected times: (a) hour 5.4, (b) day 1.8, (c) day 3.1, (d) day 4.1, and (e) day 4.9. Color digitally enhanced for clarity.

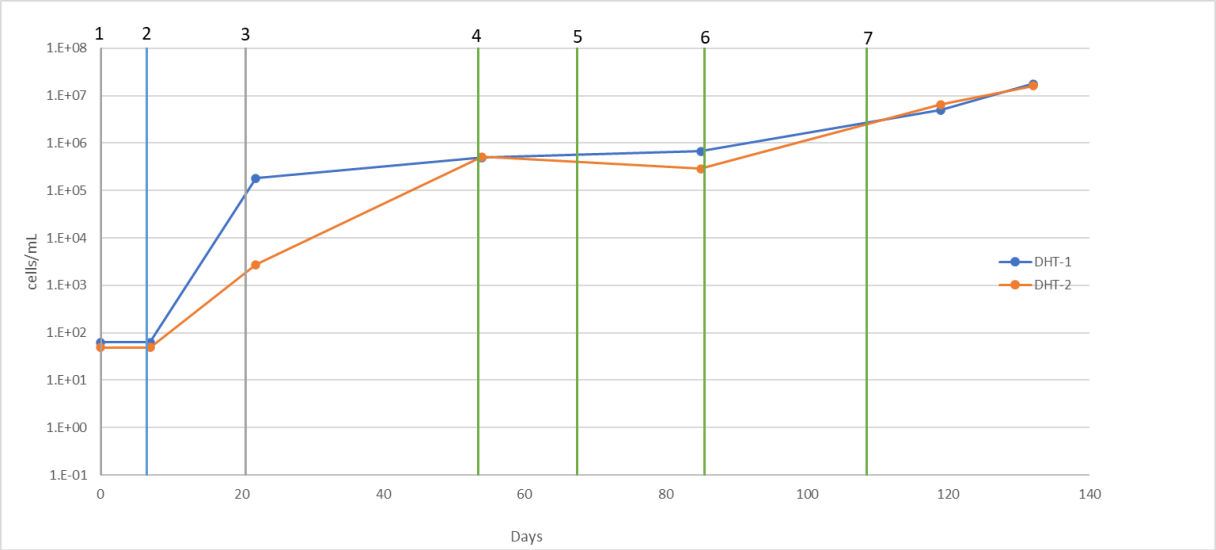

Figure B-6. *Dhc* abundance during pilot test in injection well DHT-1 and downgradient well DHT-2. Vertical lines represent, from left to right: 1. Beginning of recirculation with lactate; 2. Bioaugmentation 3. End of recirculation; 4. Beginning of lactate pulse; 5. End of lactate pulse; 6. Beginning of lactate pulse; and 7. End of lactate pulse.

Appendix C: Supplementary Material for Chapter 6: Strain-specific response of *Dehalococcoides mccartyi* to perfluoroalkyl substances and impact on microbial reductive dechlorination

C1.0 Soil organic carbon and sorption properties

Porous media recovered via shovel in the vicinity of soil boring AA07SB04 at Loring Air Force Base (Aroostook County, ME) in October 2017 was analyzed for total organic carbon and PCE and TCE sorption parameters. Prior to testing the material was air dried, ground with a mortar and pestle, and passed through a No. 40 mesh sieve. Organic carbon was measured using a Shimadzu TOC-L and SSM-5000 (Shimadzu; Kyoto, Japan) via the subtraction method as detailed in Gaeth (2017). Briefly, 50 mg samples were analyzed for total carbon via heating at 900°C. A second 50 mg sample was then analyzed for inorganic carbon by digestion with phosphoric acid at 250°C and organic carbon content was calculated by subtracting the inorganic carbon from the total carbon. Using this methodology, the Loring Air Force base soil was found to have a total organic carbon content of 0.0167 mg carbon/mg soil (1.7% by mass).

To create PCE and TCE isotherms, 5 mg samples of Loring Air Force base soil (dried, ground and sieved as described above) were placed in 20 mL crimp cap vials with teflon-lined rubber caps. After adding soil, each vial was filled with sterile low salts anaerobic medium containing dissolved PCE or TCE and sealed. Vials were filled to minimize headspace (<8% headspace by volume) with an average headspace volume of 2.0% (±2.4%). Negative control vials were set up with anaerobic medium and PCE or TCE but no soil to account for losses of chlorinated ethenes from the vial over the duration of the experiment. Sets of 6 vials (3 with soil and 3 without) were prepared with 10, 25, 50, 100, and 200 mg/L TCE and 5, 10, 25, 50, and 100 mg/L PCE. An additional 26 vials (15 with soil and 11 without) were prepared with 100 mg/L TCE to determine the time to sorption

equilibrium. All vials were placed on a shaker tray and incubated at room temperature (21°C) for up to 21 days.

Vials were destructively sampled after reaching equilibrium. Vials were centrifuged at 400 rpm (65×g) for 30 minutes in an Eppendorf 5810R centrifuge (Eppendorf, Hauppauge, NY) to settle soil particles. After centrifuging, a 1 mL aqueous sample was removed using a needle and syringe and placed in a crimp-cap headspace vial for chlorinated ethene analysis by GC-FID. The vial was then opened and the remaining aqueous volume was removed and replaced with 10 mL of methanol for extraction of sorbed chlorinated ethenes as described by Costanza (2005). Vials containing the soil-methanol mixture were shaken manually, then placed on a shaker tray to equilibrate for 24 to 48 hours at room temperature. The vials were then centrifuged at room temperature and methanol was removed using a needle and syringe, placed in a 1.8 mL glass autosampler vial, and analyzed by GC with ECD. After analysis, the methanol was removed and replaced and the extraction was repeated three times (until chlorinated ethenes were no longer detected in the sample).

Vials containing 100 mg/L TCE were destructively sampled after 3, 7, 10, and 15 days to monitor the extent of TCE sorption over time. The aqueous concentration in these vials dropped to 72% (±3.5%) of the initial concentration after 3 days and remained constant in subsequent samples (71% ± 5.6%). The remaining samples were destructively sampled after 21 days to measure the aqueous and sorbed chlorinated ethene concentrations.

Equilibrium soil and aqueous concentrations were used to create sorption isotherms for PCE and TCE as shown in Figures C-1 and C-2. The linear sorption isotherm best fit both sets of data (average R^2=0.97) resulting in K_d values of 1.30×10^{-3} for TCE and 4.70×10^{-3} for PCE. Freundlich sorption isotherms also fit the data well (average R^2=0.96) with K_d values of 7.13×10^{-4} for TCE and 2.69×10^{-3} for PCE and N values of 0.879 and 0.929 for

TCE and PCE, respectively. The Langmuir form sorption isotherm did not fit the measurements (Figures C-1 and C-2).

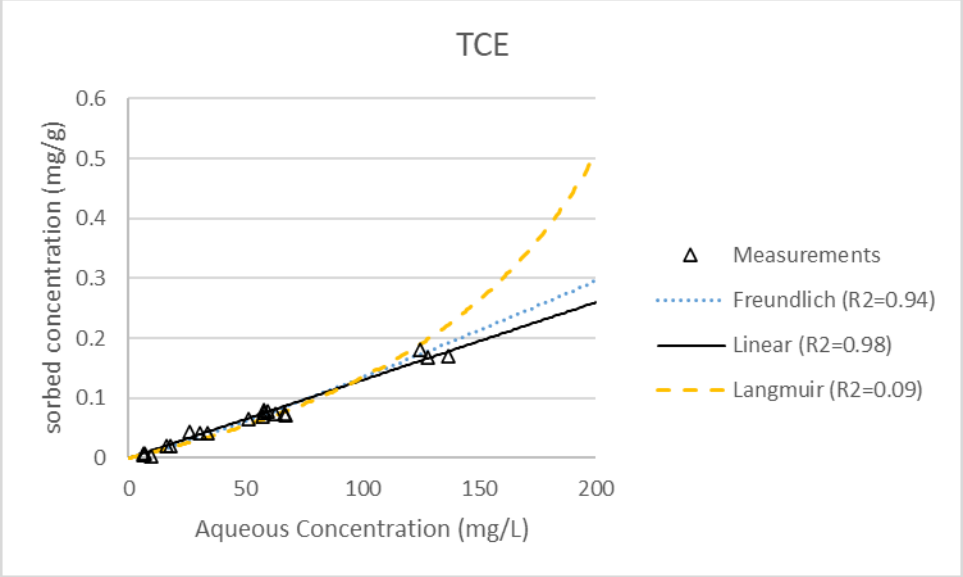

Figure C-1. TCE adsorption isotherms and equilibrium measurements

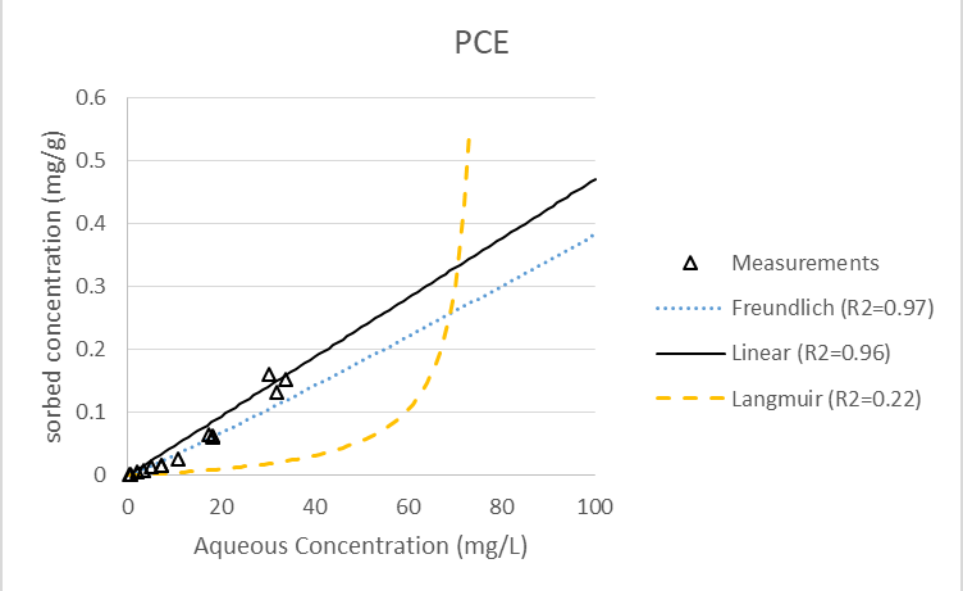

Figure C-2. PCE adsorption isotherms and equilibrium measurements

Table C-1. PFAS concentrations in batch reactors

	PFBA		PFPeA		PFBS		PFHxA		PFHpA		PFHxS		PFOA		PFNA		PFOS		PFDA		TOTAL	
	AVG	STDEV	AVG	STDEV	AVG	STDEV	AVG	STDEV	AVG	STDEV	AVG	STDEV	AVG	STDEV	AVG	STDEV	AVG	STDEV	AVG	STDEV	AVG	STDEV
11.7 ppm Batch Reactor Initial	0.90	0.04	1.88	0.08	0.41	0.26	0.93	0.64	0.81	0.05	2.20	0.10	1.17	0.05	0.45	0.02	2.54	0.10	0.37	0.04	11.67	0.58
Variability (high|Low)	0%	-21%	0%	-5%	0%	-13%	20%	0%	0%	-63%	0%	-82%	0%	-3%	0%	-9%	3%	0%	5%	0%	0%	-2%
Proportion of total PFAS (by mass)	8%		16%		3%		8%		7%		19%		10%		4%		22%		3%			
26.5 ppm Batch Reactor Initial	1.83	0.25	3.99	0.53	1.26	0.88	3.17	0.54	1.65	0.23	4.74	0.61	2.49	0.34	0.95	0.10	5.75	0.85	0.64	0.13	26.46	4.05
Variability (high|Low)	0%	-17%	0%	-10%	0%	-10%	0%	-8%	0%	-5%	0%	-9%	0%	-9%	0%	-13%	0%	-7%	0%	-3%	0%	-13%
Proportion of total PFAS (by mass)	7%		15%		5%		12%		6%		18%		9%		4%		22%		2%			
49.8 ppm Batch Reactor Initial	3.45	0.12	7.49	0.14	3.33	0.05	5.18	1.86	3.06	0.11	8.72	0.04	4.57	0.11	1.78	0.08	11.04	0.73	1.17	0.05	49.80	2.27
Variability (high|Low)	0%	-17%	0%	-2%	0%	-11%	8%	0%	3%	0%	4%	0%	1%	0%	0%	-8%	2%	0%	0%	-1%	0%	0%
Proportion of total PFAS (by mass)	7%		15%		7%		10%		6%		18%		9%		4%		22%		2%			
61.7 ppm Batch Reactor	3.90	0.13	8.94	0.14	4.22	0.10	7.43	0.25	3.65	0.09	10.66	0.36	5.54	0.08	2.15	0.03	13.74	0.42	1.45	0.06	61.68	1.15
Variability (high|Low)	0%	-12%	0%	-328%	0%	-1%	0%	-3%	0%	0%	0%	0%	0%	-1%	0%	-10%	1%	0%	2%	0%	0%	0%
Proportion of total PFAS (by mass)	6%		14%		7%		12%		6%		17%		9%		3%		22%		2%			
101 ppm Batch Reactor	6.44	0.18	14.47	0.16	7.23	0.15	11.79	0.33	5.93	0.19	17.19	0.13	8.98	0.04	3.29	0.10	23.50	1.07	2.26	0.12	101.08	1.03
Variability (high|Low)	0%	-16%	0%	-3%	0%	-3%	1%	0%	0%	0%	0%	-1%	0%	-2%	0%	-7%	3%	0%	3%	0%	0%	-1%
Proportion of total PFAS (by mass)	6%		14%		7%		12%		6%		17%		9%		3%		23%		2%			
29 ppm EGMBE Batch Reactor Initial	1.40	0.11	3.43	1.17	2.18	0.28	4.73	0.65	2.13	0.22	4.19	0.56	2.59	0.04	0.89	0.03	6.37	0.87	0.75	0.10	28.66	0.82
Variability (high|Low)	74%	-53%	33%	0%	0%	-74%	6%	-42%	6%	-38%	8%	-33%	5%	-34%	0%	-62%	33%	-53%	2%	-78%	0%	-35%
Proportion of total PFAS (by mass)	5%		12%		8%		17%		7%		15%		9%		3%		22%		3%			
66 ppm EGMBE Batch Reactor Initial	5.28	0.63	7.90	1.23	3.49	0.16	10.26	0.50	4.70	0.33	10.10	0.60	6.51	0.26	2.43	0.12	13.26	1.03	1.59	0.04	65.54	3.25
Variability (high|Low)	0%	-66%	51%	0%	0%	-37%	131%	-12%	7%	-10%	29%	-18%	4%	-12%	31%	-34%	24%	-30%	8%	-68%	6%	-9%
Proportion of total PFAS (by mass)	8%		12%		5%		16%		7%		15%		10%		4%		20%		2%			
113 ppm EGMBE Batch Reactor Initial	8.06	0.93	18.05	2.82	4.76	0.25	17.45	0.40	8.13	0.31	16.16	1.11	11.33	0.42	4.37	0.19	21.55	1.00	2.72	0.09	112.58	1.39
Variability (high|Low)	24%	-47%	8%	0%	3%	-27%	7%	-18%	2%	-16%	21%	14%	1%	-20%	9%	-34%	14%	-23%	12%	-46%	1%	-9%
Proportion of total PFAS (by mass)	7%		16%		4%		16%		7%		14%		10%		4%		19%		2%			
139 ppm EGMBE Batch Reactor Initial	10.67	2.44	23.71	2.59	5.58	0.35	21.13	0.93	9.68	0.40	19.93	0.87	13.54	0.53	5.29	0.24	25.69	1.41	3.31	0.25	138.52	3.92
Variability (high|Low)	10%	-53%	2%	-6%	5%	-20%	12%	-16%	10%	-12%	27%	-25%	5%	-15%	14%	-30%	21%	-24%	20%	-44%	0%	-7%
Proportion of total PFAS (by mass)	8%		17%		4%		15%		7%		14%		10%		4%		19%		2%			

Table C-2. Initial and final PFAS concentrations in microcosms

	PFBA		PFPeA		PFBS		PFHxA		PFHpA		PFHxS		PFOA		PFNA		PFOS		PFDA		TOTAL	
	AVG	STDEV	AVG	STDEV	AVG	STDEV	AVG	STDEV	AVG	STDEV	AVG	STDEV	AVG	STDEV	AVG	STDEV	AVG	STDEV	AVG	STDEV	AVG	STDEV
13 ppm Micorcosom Initial	1.38	0.15	2.42	0.20	0.56	0.08	2.44	0.19	0.78	0.09	1.80	0.18	1.11	0.09	0.44	0.14	1.70	0.27	0.14	0.03	12.80	1.03
13 ppm Micorcosom Final	1.01	0.09	1.84	0.13	0.46	0.05	1.83	0.14	0.63	0.04	1.36	0.08	0.87	0.06	0.32	0.06	1.14	0.13	0.05	0.02	9.52	0.70
13 ppm % decrease	73%		76%		82%		75%		81%		75%		79%		73%		67%		37%		74%	
Proportion Initial	11%		19%		4%		19%		6%		14%		9%		3%		13%		1%			
Proportion Final	11%		19%		5%		19%		7%		14%		9%		3%		12%		1%			
26 ppm Micrcocosm Initial	2.59	0.43	4.86	0.21	1.12	0.14	4.95	0.32	1.62	0.08	3.51	0.15	2.26	0.10	0.80	0.17	3.95	0.61	0.33	0.04	25.93	1.66
26 ppm Micrcocosm Final	2.14	0.09	3.64	0.05	0.95	0.04	3.63	0.12	1.30	0.04	2.83	0.16	1.75	0.04	0.68	0.06	2.35	0.27	0.13	0.04	19.40	0.44
% decrease	83%		75%		84%		73%		80%		81%		78%		85%		60%		39%		75%	
Proportion Initial	10%		19%		4%		19%		6%		14%		9%		3%		15%		1%			
Proportion Final	11%		19%		5%		19%		7%		15%		9%		3%		12%		1%			
54 ppm Microcosm Initial	5.41	0.26	9.58	0.25	2.45	0.12	10.12	0.18	3.42	0.12	7.66	0.34	4.61	0.06	1.70	0.15	8.00	0.58	0.67	0.03	53.54	0.83
54 ppm Microcosm Final	4.20	0.07	7.32	0.04	1.97	0.05	7.28	0.11	2.55	0.04	5.69	0.38	3.51	0.03	1.36	0.05	4.51	0.29	0.29	0.06	38.69	0.60
% decrease	78%		76%		80%		72%		75%		74%		76%		80%		56%		44%		72%	
Proportion Initial	10%		18%		5%		19%		6%		14%		9%		3%		15%		1%			
Proportion Final	11%		19%		5%		19%		7%		15%		9%		4%		12%		1%			
120 ppm Microcosm Initial	11.89	0.49	20.31	0.41	5.28	0.11	21.43	0.52	7.13	0.17	16.54	0.51	9.91	0.22	3.81	0.25	21.86	0.76	1.75	0.12	119.81	1.62
120 ppm Microcosm Final	9.54	0.18	15.65	0.27	4.29	0.05	15.54	0.34	5.44	0.08	12.93	0.29	7.51	0.14	3.01	0.17	11.70	0.62	0.65	0.09	86.25	0.66
% decrease	80%		77%		81%		73%		76%		78%		76%		79%		54%		37%		72%	
Proportion Initial	10%		17%		4%		18%		6%		14%		8%		3%		18%		1%			
Proportion Final	11%		18%		5%		18%		6%		15%		9%		3%		14%		1%			

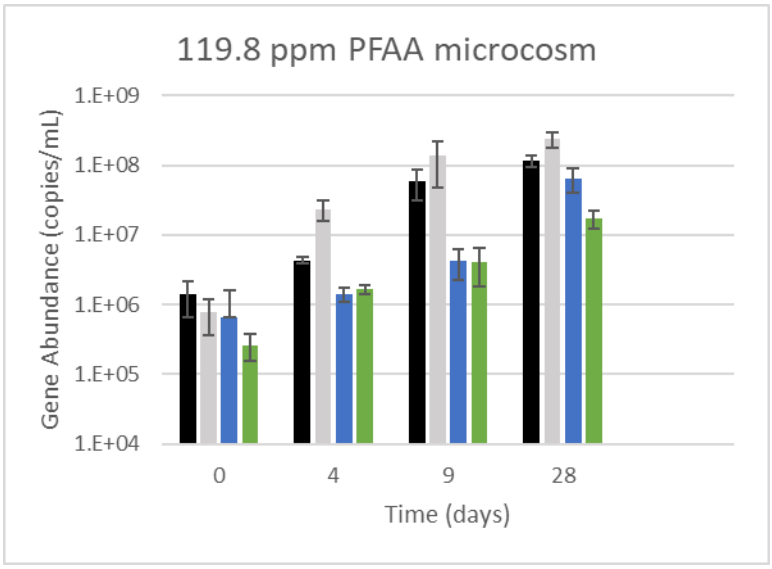

Figure C-4. *Dhc* and RDase abundance in in microcosms with 119.8 ppm PFAAs

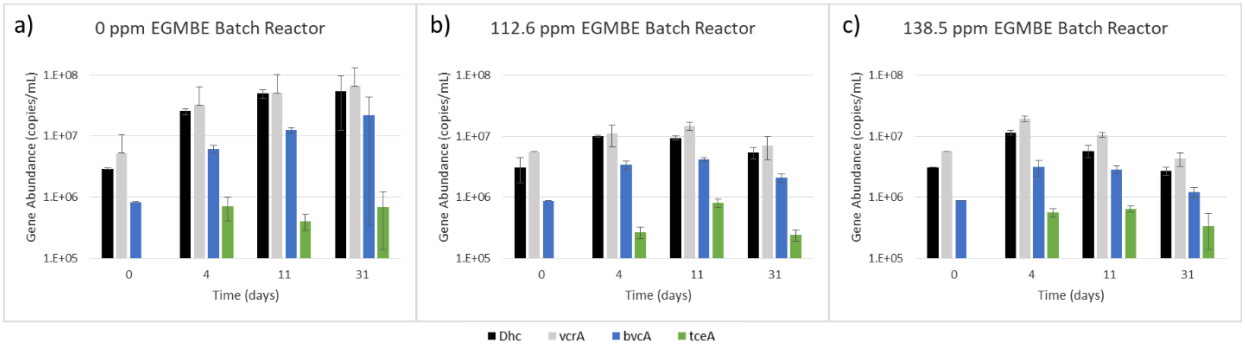

Figure C-5. *Dhc* and RDase abundance in EGMBE batch reactors with a) 0 ppm, b) 112.6 ppm, and c) 138.5 ppm PFAAs

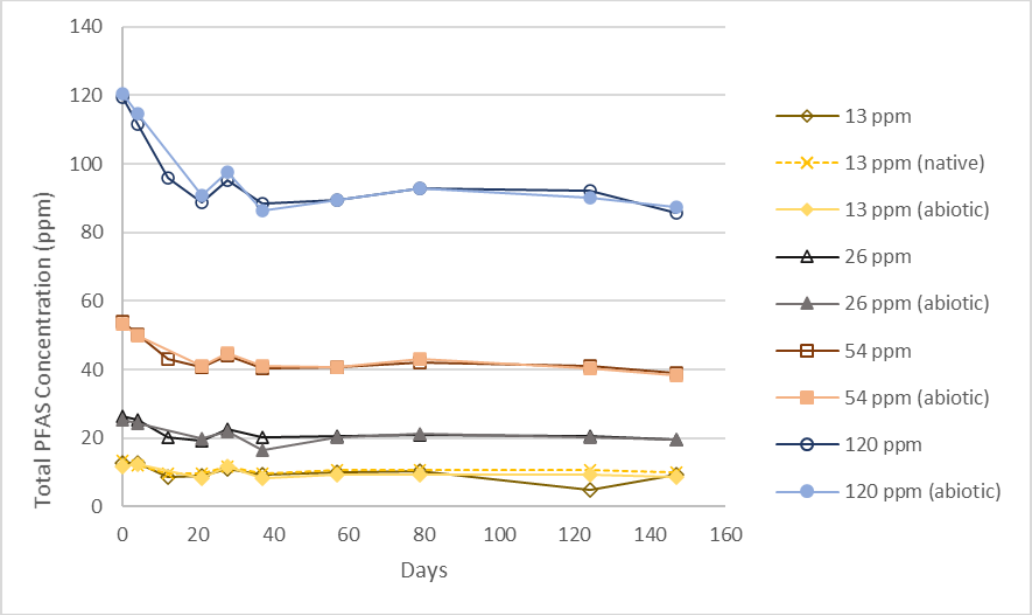

Figure C-6. Total PFAA concentration in microcosms

References

(1) USEPA. *Superfund Remedy Report 15th Edition*; 2017.

(2) McGuire, T. M.; McDade, J. M.; Newell, C. J. Performance of DNAPL Source Depletion Technologies at 59 Chlorinated Solvent-Impacted Sites. *Gr. Water Monit. Remediat.* **2006**, *26* (1), 73–84. https://doi.org/10.1111/j.1745-6592.2006.00054.x.

(3) Steffan, R. J.; Schaefer, C. E. Current and Future Bioremediation Applications; Bioremediation from a Practical and Regulatory Perspective. In *Organohalide Respiring Bacteria*; Adrian, L., Loffler, F. E., Eds.; Springer-Verlag: Berlin, Heidelberg, 2016; pp 517–540.

(4) Fiedler, L.; Pachon, C. Recent Trends in the Selection of Remedies for Groundwater, Soil, and Sediment at Superfund Sites. *Groundw. Monit. Remediat.* **2018**, *38* (1), 13–18. https://doi.org/10.1111/gwmr.12260.

(5) Huang, B.; Lei, C.; Wei, C.; Zeng, G. Chlorinated Volatile Organic Compounds (Cl-VOCs) in Environment - Sources, Potential Human Health Impacts, and Current Remediation Technologies. *Environ. Int.* **2014**, *71*, 118–138. https://doi.org/10.1016/j.envint.2014.06.013.

(6) Moran, M. J.; Zogorski, J. S.; Squillace, P. J. Chlorinated Solvents in Groundwater of the United States. *Environ. Sci. Technol.* **2007**, *41* (1), 74–81. https://doi.org/10.1021/es061553y.

(7) National Research Council. *Alternatives for Managing the Nation's Complex Contaminated Groundwater Sites*; National Academies Press: Washington, D.C., D.C., 2013. https://doi.org/10.17226/14668.

(8) Grostern, A.; Edwards, E. A. Growth of Dehalobacter and Dehalococcoides Spp. during Degradation of Chlorinated Ethanes. *Appl. Environ. Microbiol.* **2006**, *72* (1), 428–436. https://doi.org/10.1128/AEM.72.1.428-436.2006.

(9) Loffler, F. E.; Ritalahti, K. M.; Zinder, S. H. Dehalococcoides and Reductive Dechlorination of Chlorinated Solvents. In *Bioaugmentation for Groundwater Remediation*; Stroo, H. F., Leeson, A., Ward, C. H., Eds.; Springer: New York, NY, 2013; pp 39–88.

(10) Futagami, T.; Goto, M.; Furukawa, K. Biochemical and Genetic Bases of Dehalorespiration. *Chem. Rec.* **2008**, *8* (1), 1–12. https://doi.org/10.1002/tcr.20134.

(11) Doğan-Subaşi, E.; Bastiaens, L.; Leys, N.; Boon, N.; Dejonghe, W. Quantitative and Functional Dynamics of Dehalococcoides Spp. and Its TceA and VcrA Genes under TCE Exposure. *Biodegradation* **2014**, *25* (4), 493–504. https://doi.org/10.1007/s10532-013-9676-8.

(12) Molenda, O.; Tang, S.; Lomheim, L.; Edwards, E. Eight New Genomes of Organohalide-Respiring Dehalococcoides Mccartyi Reveal Evolutionary Trends in Reductive Dehalogenase Enzymes. **2018**. https://doi.org/10.1101/345173.

(13) Duhamel, M.; Mo, K.; Edwards, E. a. Characterization of a Highly Enriched Dehalococcoides -Containing Culture That Grows on Vinyl Chloride And. *Appl.*

Environ. Microbiol. **2004**, *70* (9), 5538–5545. https://doi.org/10.1128/AEM.70.9.5538.

(14) He, J.; Ritalahti, K. M.; Aiello, M. R.; Löffler, F. E. Complete Detoxification of Vinyl Chloride by an Anaerobic Enrichment Culture and Identification of the Reductively Dechlorinating Population as a Dehalococcoides Species. *Appl. Environ. Microbiol.* **2003**, *69* (2), 996–1003. https://doi.org/10.1128/AEM.69.2.996-1003.2003.

(15) Baldwin, B. R.; Taggart, D.; Chai, Y.; Wandor, D.; Biernacki, A.; Sublette, K. L.; Wilson, J. T.; Walecka-Hutchison, C.; Coladonato, C.; Goodwin, B. Bioremediation Management Reduces Mass Discharge at a Chlorinated DNAPL Site. *Groundw. Monit. Remediat.* **2017**, *37* (2), 58–70. https://doi.org/10.1111/gwmr.12211.

(16) Suthersan, S. S.; Schnobrich, M.; Martin, J.; Horst, J. F.; Gates, E. Advances in Remediation Solutions Three Decades of Solvent Bioremediation : The Practice. **2017**, No. 2.

(17) Tillotson, J. M.; Borden, R. C. Rate and Extent of Chlorinated Ethene Removal at 37 ERD Sites. *J. Environ. Eng. (United States)* **2017**, *143* (8), 1–10. https://doi.org/10.1061/(ASCE)EE.1943-7870.0001224.

(18) Kielhorn, J.; Melber, C.; Wahnschaffe, U.; Aitio, a; Mangelsdorf, I. Vinyl Chloride: Still a Cause for Concern. *Environ. Health Perspect.* **2000**, *108* (7), 579–588. https://doi.org/10.2307/3434875.

(19) Major, D. W.; McMaster, M. L.; Cox, E. E.; Edwards, E. a.; Dworatzek, S. M.; Hendrickson, E. R.; Starr, M. G.; Payne, J. A.; Buonamici, L. W. Field Demonstration of Successful Bioaugmentation to Achieve Dechlorination of Tetrachloroethene to Ethene. *Environ. Sci. Technol.* **2002**, *36* (23), 5106–5116. https://doi.org/10.1021/es0255711.

(20) Lendvay, J. M.; Löffler, F. E.; Dollhopf, M.; Aiello, M. R.; Daniels, G.; Fathepure, B. Z.; Gebhard, M.; Heine, R.; Helton, R.; Shi, J.; et al. Bioreactive Barriers: A Comparison of Bioaugmentation and Biostimulation for Chlorinated Solvent Remediation. *Environ. Sci. Technol.* **2003**, *37* (7), 1422–1431. https://doi.org/10.1021/es025985u.

(21) McCarty, P. L. Groundwater Contamination by Chlorinated Solvents: History, Remediation Technologies and Strategies. In *In Situ Remediation of Chlorinated Solvent Plumes*; Stroo, H. F., Ward, C. H., Eds.; Springer: New York, 2010; pp 1–28.

(22) Sale, T.; Parker, B. L.; Newell, C. J.; Devlin, J. F. *Management of Contaminants Stored in Low Permeability Zones*; SERDP Project ER-1740, 2013.

(23) van Genuchten, M. T.; Alves, W. J. *Analytical Solutions of the One-Dimensional Convective-Dispersive Solute Transport Equation*; Technical Bulletins; 157268; United States Department of Agriculture, Economic Research Service, 1982.

(24) Simpkin, T. J.; Norris, R. D. Engineering and Implementation Challenges for Chlorinated Solvent Remediation. In *In Situ Remediation of Chlorinated Solvent Plumes1*; Stroo, H. F., Ward, C. H., Eds.; Springer: New York, 2010; pp 109–143.

(25) Amos, B. K.; Ritalahti, K. M.; Cruz-Garcia, C.; Padilla-Crespo, E.; Löffler, F. E. Oxygen Effect on Dehalococcoides Viability and Biomarker Quantification. *Environ. Sci. Technol.* **2008**, *42* (15), 5718–5726. https://doi.org/10.1021/es703227g.

(26) Yang, Y.; Cápiro, N. L.; Yan, J.; Marcet, T. F.; Pennell, K. D.; Löffler, F. E. Resilience and Recovery of Dehalococcoides Mccartyi Following Low PH Exposure. *FEMS Microbiol. Ecol.* **2017**, *93* (12), 1–9. https://doi.org/10.1093/femsec/fix130.

(27) Behrens, S.; Azizian, M. F.; McMurdie, P. J.; Sabalowsky, A.; Dolan, M. E.; Semprini, L.; Spormann, A. M. Monitoring Abundance and Expression of "Dehalococcoides" Species Chloroethene-Reductive Dehalogenases in a Tetrachloroethene-Dechlorinating Flow Column. *Appl. Environ. Microbiol.* **2008**, *74* (18), 5695–5703. https://doi.org/10.1128/AEM.00926-08.

(28) Liang, X.; Molenda, O.; Tang, S.; Edwards, E. a. Identity and Substrate Specificity of Reductive Dehalogenases Expressed in Dehalococcoides-Containing Enrichment Cultures Maintained on Different Chlorinated Ethenes. *Appl. Environ. Microbiol.* **2015**, *81* (14), 4626–4633. https://doi.org/10.1128/AEM.00536-15.

(29) Marcet, T. F.; Cápiro, N. L.; Yang, Y.; Löffler, F. E.; Pennell, K. D. Impacts of Low-Temperature Thermal Treatment on Microbial Detoxification of Tetrachloroethene under Continuous Flow Conditions. *Water Res.* **2018**, *145*, 21–29. https://doi.org/10.1016/j.watres.2018.07.076.

(30) Mayer-Blackwell, K.; Fincker, M.; Molenda, O.; Callahan, B.; Sewell, H.; Holmes, S.; Edwards, E. A.; Spormann, A. M. 1,2-Dichloroethane Exposure Alters the Population Structure, Metabolism, and Kinetics of a Trichloroethene-Dechlorinating Dehalococcoides Mccartyi Consortium. *Environ. Sci. Technol.* **2016**, *50* (22), 12187–12196. https://doi.org/10.1021/acs.est.6b02957.

(31) Sale, T. C.; Zimbron, J. A.; Dandy, D. S. Effects of Reduced Contaminant Loading on Downgradient Water Quality in an Idealized Two-Layer Granular Porous Media. *J. Contam. Hydrol.* **2008**, *102* (1–2), 72–85. https://doi.org/10.1016/j.jconhyd.2008.08.002.

(32) Amos, B. K.; Suchomel, E. J.; Pennell, K. D.; Löffler, F. E. Microbial Activity and Distribution during Enhanced Contaminant Dissolution from a NAPL Source Zone. *Water Res.* **2008**, *42* (12), 2963–2974. https://doi.org/10.1016/j.watres.2008.03.015.

(33) Glover, K. C.; Munakata-Marr, J.; Illangasekare, T. H. Biologically Enhanced Mass Transfer of Tetrachloroethene from DNAPL in Source Zones: Experimental Evaluation and Influence of Pool Morphology. *Environ. Sci. Technol.* **2007**, *41* (4), 1384–1389. https://doi.org/10.1021/es060922n.

(34) Chen, M.; Abriola, L. M.; Amos, B. K.; Suchomel, E. J.; Pennell, K. D.; Löffler, F. E.; Christ, J. A. Microbially Enhanced Dissolution and Reductive Dechlorination of PCE by a Mixed Culture: Model Validation and Sensitivity Analysis. *J. Contam. Hydrol.* **2013**, *151*, 117–130. https://doi.org/10.1016/j.jconhyd.2013.05.005.

(35) Cápiro, N. L.; Löffler, F. E.; Pennell, K. D. Spatial and Temporal Dynamics of Organohalide-Respiring Bacteria in a Heterogeneous PCE-DNAPL Source Zone. *J. Contam. Hydrol.* **2015**, *182*, 78–90. https://doi.org/10.1016/j.jconhyd.2015.08.007.

(36) Aziz, C. E.; Wymore, R. A.; Steffan, R. J. Bioaugmentation Considerations. In *Bioaugmentation for Groundwater Remediation*; Stroo, H. F., Leeson, A., Ward, C. H., Eds.; Springer: New York, NY, 2013; pp 141–170.

(37) Ritalahti, K. M.; Amos, B. K.; Sung, Y.; Wu, Q.; Koenigsberg, S. S.; Löffler, F. E. Quantitative PCR Targeting 16S RRNA and Reductive Dehalogenase Genes Simultaneously Monitors Multiple Dehalococcoides Strains. *Appl. Environ. Microbiol.* **2006**, *72* (4), 2765–2774. https://doi.org/10.1128/AEM.72.4.2765-2774.2006.

(38) Clark, K.; Taggart, D. M.; Baldwin, B. R.; Ritalahti, K. M.; Murdoch, R. W.; Hatt, J. K.; Lo, F. E. Normalized Quantitative PCR Measurements as Predictors for Ethene Formation at Sites Impacted with Chlorinated Ethenes. **2018**. https://doi.org/10.1021/acs.est.8b04373.

(39) Adrian, L.; Löffler, F. E.; Field, J. a.; Dolfng, J.; McCarty, P. L.; Atashgahi, S.; Lu, Y.; Smidt, H.; Zinder, S. H.; Moe, W. M.; et al. *Organohalide-Respiring Bacteria*; 2016. https://doi.org/10.1007/978-3-662-49875-0.

(40) Chiu, H. Y.; Liu, J. K.; Chien, H. Y.; Surampalli, R. Y.; Kao, C. M. Evaluation of Enhanced Reductive Dechlorination of TCE Using Gene Analysis: A Pilot-Scale Study. *J. Environ. Eng.* **2012**, *139* (March), 120913015545000. https://doi.org/10.1061/(ASCE)EE.1943-7870.0000654.

(41) Hazen, T. C.; Chakraborty, R.; Fleming, J. M.; Gregory, I. R.; Bowman, J. P.; Jimenez, L.; Zhang, D.; Pfiffner, S. M.; Brockman, F. J.; Sayler, G. S. Use of Gene Probes to Assess the Impact and Effectiveness of Aerobic in Situ Bioremediation of TCE. *Arch. Microbiol.* **2009**, *191* (3), 221–232. https://doi.org/10.1007/s00203-008-0445-8.

(42) Lee, P. K. H.; Johnson, D. R.; Holmes, V. F.; He, J.; Alvarez-Cohen, L. Reductive Dehalogenase Gene Expression as a Biomarker for Physiological Activity of Dehalococcoides Spp. *Appl. Environ. Microbiol.* **2006**, *72* (9), 6161–6168. https://doi.org/10.1128/AEM.01070-06.

(43) Weathers, T. S.; Harding-Marjanovic, K.; Higgins, C. P.; Alvarez-Cohen, L.; Sharp, J. O. Perfluoroalkyl Acids Inhibit Reductive Dechlorination of Trichloroethene by Repressing Dehalococcoides. *Environ. Sci. Technol.* **2016**, *50* (1), 240–248. https://doi.org/10.1021/acs.est.5b04854.

(44) Moody, C. A.; Field, J. A. Perfluorinated Surfactants and the Environmental Implications of Their Use in Fire-Fighting Foams. *Environ. Sci. Technol.* **2000**, *34* (18), 3864–3870. https://doi.org/10.1021/es991359u.

(45) McGuire, M. E.; Schaefer, C.; Richards, T.; Backe, W. J.; Field, J. A.; Houtz, E.; Sedlak, D. L.; Guelfo, J. L.; Wunsch, A.; Higgins, C. P. Evidence of Remediation-Induced Alteration of Subsurface Poly- and Perfluoroalkyl Substance Distribution at a Former Firefighter Training Area. *Environ. Sci. Technol.* **2014**, *48* (12), 6644–6652. https://doi.org/10.1021/es5006187.

(46) Harding-Marjanovic, K. C.; Yi, S.; Weathers, T. S.; Sharp, J. O.; Sedlak, D. L.; Alvarez-Cohen, L. Effects of Aqueous Film-Forming Foams (AFFFs) on Trichloroethene (TCE) Dechlorination by a Dehalococcoides Mccartyi-Containing Microbial Community. *Environ. Sci. Technol.* **2016**, *50* (7), 3352–3361. https://doi.org/10.1021/acs.est.5b04773.

(47) Harkness, M. R.; Konzuk, J. S. Cost Analyses for Remedial Options. In *Chlorinated Solvent Source Zone Remediation*; Kueper, B. H., Stroo, H. F., Vogel, C., Ward, C. H., Eds.; Springer: New York, NY, 2014; pp 599–626.

(48) Vidali, M. K. Bioremediation - An Overview. *J. Ind. Pollut. Control* **2001**, *73* (7), 1163–1172.

(49) Stroo, H. F.; West, M. R.; Kueper, B. H.; Borden, R. C.; Major, D. W.; Ward, C. H. In Situ Bioremediation of Chlorinated Ethene Source Zones. In *Chlorinated Solvent Source Zone Remediation*; Kueper, B. H., Stroo, H. F., Vogel, C., Ward, C. H., Eds.; Springer: New York, NY, 2014; pp 395–458.

(50) Stroo, H. F. Bioremediation of Chlorinated Solvent Plumes. In *In Situ Remediation of Chlorinated Solvent Plumes*; Stroo, H. F., Ward, C. H., Eds.; Springer: New York, NY, 2010; pp 309–324.

(51) He, J.; Sung, Y.; Krajmalnik-Brown, R.; Ritalahti, K. M.; Löffler, F. E. Isolation and Characterization of Dehalococcoides Sp. Strain FL2, a Trichloroethene (TCE)- and 1,2-Dichloroethene-Respiring Anaerobe. *Environ. Microbiol.* **2005**, *7* (9), 1442–1450. https://doi.org/10.1111/j.1462-2920.2005.00830.x.

(52) Mertens, J. A. Trichloroethylene. In *Kirk-Othmer Encyclopedia of Chemical Technology*; John Wiley & Sons, Inc.: Hoboken, NJ, USA, 2000. https://doi.org/10.1002/0471238961.2018090313051820.a01.

(53) Hickman, J. C. Tetrachloroethylene. In *Kirk-Othmer Encyclopedia of Chemical Technology*; John Wiley & Sons, Inc.: Hoboken, NJ, USA, 2000; Vol. 5, pp 566–579. https://doi.org/10.1002/0471238961.2005201808090311.a01.

(54) Doherty, R. E. A History of the Production and Use of Carbon Tetrachloride, Tetrachloroethylene, Trichloroethylene and 1,1,1-Trichloroethane in the United States: Part 1 - Historical Background; Carbon Tetrachloride and Tetrachloroethylene. *Environ. Forensics* **2000**, *1* (2), 69–81. https://doi.org/10.1006/enfo.2000.0010.

(55) USEPA. *Problem Formulation of the Risk Evaluation for Perchloroethylene*; 2018.

(56) USEPA. Preliminary Information on Manufacturing , Processing , Distribution , Use , and Disposal: Tetrachloroethylene. **2017**, No. February, 1–15.

(57) USEPA. Preliminary Information on Manufacturing , Processing , Distribution , Use , and Disposal: Trichloroethylene. **2017**, No. February, 1–15.

(58) USEPA. *Toxics Release Inventory*; 2016.

(59) Dow Chemical Company, T. Product Safety Assessment: Perchloroethylene. **2008**, 1–6.

(60) Doucette, W. J.; Chard, J. K.; Fabrizius, H.; Crouch, C.; Petersen, M. R.; Carlsen,

T. E.; Chard, B. K.; Gorder, K. Trichloroethylene Uptake into Fruits and Vegetables: Three-Year Field Monitoring Study. *Environ. Sci. Technol.* **2007**, *41* (7), 2505–2509. https://doi.org/10.1021/es0621804.

(61) Riley, R. G.; Zachara, J. M. Chemical Contaminants on DOE Lands and Selection of Contaminant Mixtures for Subsurface Science Research. **1992**. https://doi.org/10.2172/5202264.

(62) Beamer, P. I.; Luik, C. E.; Abrell, L.; Campos, S.; Martínez, M. E.; Sáez, A. E. Concentration of Trichloroethylene in Breast Milk and Household Water from Nogales, Arizona. *Environ. Sci. Technol.* **2012**, *46* (16), 9055–9061. https://doi.org/10.1021/es301380d.

(63) *Chlorinated Solvent Source Zone Remediation*; Kueper, B. H., Stroo, H. F., Vogel, C. M., Ward, C. H., Eds.; Springer New York: New York, NY, 2014.

(64) 3M. *The Science of Organic Fluorochemistry.*; 1999. https://doi.org/OPPT-2002-0043-0006.

(65) Kissa, E. *Flourinated Surfactants and Repellents*, 2nd ed.; CRC Press: Boca Raton, 2001.

(66) Schultz, M. M.; Barofsky, D. F.; Field, J. A. Fluorinated Alkyl Surfactants. *Environ. Eng. Sci.* **2003**, *20* (5), 487–501. https://doi.org/10.1089/109287503768335959.

(67) Stroo, H. F.; Leeson, A.; Deeb, R. a.; Higgins, C. P.; Mills, M. A.; Patton, C.; Porter, R.; Sedlak, D. L.; Sepulveda, M.; Thompson, T.; et al. *SERDP and ESTCP Workshop on Research and Demonstration Needs for Management of AFFF-Impacted Sites*; 2017.

(68) Buck, R. C.; Franklin, J.; Berger, U.; Conder, J. M.; Cousins, I. T.; Voogt, P. De; Jensen, A. A.; Kannan, K.; Mabury, S. A.; van Leeuwen, S. P. J. Perfluoroalkyl and Polyfluoroalkyl Substances in the Environment: Terminology, Classification, and Origins. *Integr. Environ. Assess. Manag.* **2011**, *7* (4), 513–541. https://doi.org/10.1002/ieam.258.

(69) Rahman, M. F.; Peldszus, S.; Anderson, W. B. Behaviour and Fate of Perfluoroalkyl and Polyfluoroalkyl Substances (PFASs) in Drinking Water Treatment: A Review. *Water Res.* **2014**, *50*, 318–340. https://doi.org/10.1016/j.watres.2013.10.045.

(70) Yamashita, N.; Kannan, K.; Taniyasu, S.; Horii, Y.; Petrick, G.; Gamo, T. A Global Survey of Perfluorinated Acids in Oceans. *Mar. Pollut. Bull.* **2005**, *51* (8–12), 658–668. https://doi.org/10.1016/j.marpolbul.2005.04.026.

(71) Hoehn, E.; Plumlee, M. H.; Reinhard, M. Natural Attenuation Potential of Downwelling Streams for Perfluorochemicals and Other Emerging Contaminants. *Water Sci. Technol.* **2007**, *56* (11), 59–64. https://doi.org/10.2166/wst.2007.804.

(72) Quiñones, O.; Snyder, S. A. Occurrence of Perfluoroalkyl Carboxylates and Sulfonates in Drinking Water Utilities and Related Waters from the United States. *Environ. Sci. Technol.* **2009**, *43* (24), 9089–9095. https://doi.org/10.1021/es9024707.

(73) Ji, B.; Kang, P.; Wei, T.; Zhao, Y. Challenges of Aqueous Per- and

Polyfluoroalkyl Substances (PFASs) and Their Foreseeable Removal Strategies. *Chemosphere* **2020**, *250*. https://doi.org/10.1016/j.chemosphere.2020.126316.

(74) Barzen-Hanson, K. A.; Roberts, S. C.; Choyke, S.; Oetjen, K.; McAlees, A.; Riddell, N.; McCrindle, R.; Ferguson, P. L.; Higgins, C. P.; Field, J. A. Discovery of 40 Classes of Per- and Polyfluoroalkyl Substances in Historical Aqueous Film-Forming Foams (AFFFs) and AFFF-Impacted Groundwater. *Environ. Sci. Technol.* **2017**, *51* (4), 2047–2057. https://doi.org/10.1021/acs.est.6b05843.

(75) Barzen-Hanson, K. A.; Field, J. A. Discovery and Implications of C2and C3perfluoroalkyl Sulfonates in Aqueous Film-Forming Foams and Groundwater. *Environ. Sci. Technol. Lett.* **2015**, *2* (4), 95–99. https://doi.org/10.1021/acs.estlett.5b00049.

(76) Dauchy, X.; Boiteux, V.; Bach, C.; Rosin, C.; Munoz, J. F. Per- and Polyfluoroalkyl Substances in Firefighting Foam Concentrates and Water Samples Collected near Sites Impacted by the Use of These Foams. *Chemosphere* **2017**, *183*, 53–61. https://doi.org/10.1016/j.chemosphere.2017.05.056.

(77) Place, B. J.; Field, J. A. Identification of Novel Fluorochemicals in Aqueous Film-Forming Foams Used by the US Military. *Environ. Sci. Technol.* **2012**, *46* (13), 7120–7127. https://doi.org/10.1021/es301465n.

(78) Houtz, E. F.; Higgins, C. P.; Field, J. A.; Sedlak, D. L. Persistence of Perfluoroalkyl Acid Precursors in AFFF-Impacted Groundwater and Soil. **2013**. https://doi.org/10.1021/es4018877.

(79) Darwin, R. L. *Estimated Quantities of Aqueous Film-Forming Foam (AFFF) in the United States*; Arlington, VA, 2004.

(80) Moody, C. A.; Field, J. A. Determination of Perfluorocarboxylates in Groundwater Impacted by Fire-Fighting Activity Determination of Perfluorocarboxylates in Groundwater Impacted by Fire-Fighting Activity. *Environ. Sci. Technol.* **1999**, *33* (16), 2800–2806. https://doi.org/10.1021/es981355+.

(81) Banzhaf, S.; Filipovic, M.; Lewis, J.; Sparrenbom, C. J.; Barthel, R. A Review of Contamination of Surface-, Ground-, and Drinking Water in Sweden by Perfluoroalkyl and Polyfluoroalkyl Substances (PFASs). *Ambio* **2017**, *46* (3), 335–346. https://doi.org/10.1007/s13280-016-0848-8.

(82) Higgins, C. P.; Luthy, R. G. Sorption of Perfluorinated Surfactants on Sediments. *Environ. Sci. Technol.* **2006**, *40* (23), 7251–7256. https://doi.org/10.1021/es061000n.

(83) Higgins, C. P.; Luthy, R. G. Modeling Sorption of Anionic Surfactants onto Sediment Materials: An a Priori Approach for Perfluoroalkyl Surfactants and Linear Alkylbenzene Sulfonates. *Environ. Sci. Technol.* **2007**, *41* (9), 3254–3261. https://doi.org/10.1021/es062449j.

(84) Johnson, R. L.; Anschutz, A. J.; Smolen, J. M.; Simcik, M. F.; Lee Penn, R. The Adsorption of Perfluorooctane Sulfonate onto Sand, Clay, and Iron Oxide Surfaces. *J. Chem. Eng. Data* **2007**, *52* (4), 1165–1170. https://doi.org/10.1021/je060285g.

(85) Custer, C. M.; Custer, T. W.; Dummer, P. M.; Etterson, M. A.; Thogmartin, W. E.; Wu, Q.; Kannan, K.; Trowbridge, A.; McKann, P. C. Exposure and Effects of Perfluoroalkyl Substances in Tree Swallows Nesting in Minnesota and Wisconsin, USA. *Arch. Environ. Contam. Toxicol.* **2014**, *66* (1), 120–138. https://doi.org/10.1007/s00244-013-9934-0.

(86) *Resource Conservation and Recovery Act*; 1976; pp 1023–1024.

(87) USEPA. *Provisional Health Advisories for Perfluorooctanoic Acid (PFOA) and Perfluorooctane Sulfonate (PFOS)*; 2009.

(88) Danziger, H. Accidental Poisoning by Vinyl Chloride: Report of Two Cases. **1960**, *82* (1958), 828–830.

(89) Mastromatteo, E.; Fisher, A. M.; Christie, H.; Danziger, H. Acute Inhalation Toxicity of Vinyl Chloride to Laboratory Animals. *Am. Ind. Hyg. Assoc. J.* **1960**, *21* (5), 394–398. https://doi.org/10.1080/00028896009344092.

(90) Prodan, L.; Suciu, I.; Pîslaru, V.; Ilea, E.; Pascu, L. Experimental Acute Toxicity of Vinyl Chloride (Monochloroethene). *Ann. N. Y. Acad. Sci.* **1975**, *246*, 154–158.

(91) Bell, A. Death from Trichlorethylene in a Dry-Cleaning Establishment. *N. Z. Med. J.* **1951**, *50* (276), 119–126.

(92) Coopman, V. A. E.; Cordonnier, J. A. C. M.; De Letter, E. A.; Piette, M. H. A. Tissue Distribution of Trichloroethylene in a Case of Accidental Acute Intoxication by Inhalation. *Forensic Sci. Int.* **2003**, *134* (2–3), 115–119. https://doi.org/10.1016/S0379-0738(03)00131-2.

(93) Thorburn, T. G.; Paterson, P.; Doward, W. A.; Mahmoud, M. A Fatal Chemical Burn Associated with the Industrial Use of Trichloroethylene Vapour. *Burns* **2004**, *30* (4), 405–406. https://doi.org/10.1016/j.burns.2003.12.011.

(94) Amadasi, A.; Mastroluca, L.; Marasciuolo, L.; Caligara, M.; Sironi, L.; Gentile, G.; Zoja, R. Death Due to Acute Tetrachloroethylene Intoxication in a Chronic Abuser. *Int. J. Legal Med.* **2015**, *129* (3), 487–493. https://doi.org/10.1007/s00414-015-1143-0.

(95) Dehon, B.; Humbert, L.; Devisme, L.; Stievenart, M.; Mathieu, D.; Houdret, N.; Lhermitte, M. Tetrachloroethylene and Trichloroethylene Fatality: Case Report and Simple Headspace SPME-Capillary Gas Chromatographic Determination in Tissues. *J. Anal. Toxicol.* **2000**, *24* (1), 22–26. https://doi.org/10.1093/jat/24.1.22.

(96) Isenschmid, D. S.; Cassin, B. J.; Hepler, B. R.; Kanluen, S. Tetrachloroethylene Intoxication in an Autoerotic Fatality. *J. Forensic Sci.* **1998**, *43* (1), 231–234.

(97) Langauer-Lewowicka, H.; Kurzbauer, H.; Byczkowska, Z.; Wocka-Marek, T. Vinyl Chloride Disease-Neurological Disturbances. *Int. Arch. Occup. Environ. Health* **1983**, *52* (2), 151–157. https://doi.org/10.1007/BF00405418.

(98) Lilis, R.; Anderson, H.; Nicholson, W. J.; Daum, S.; Fischbein, A. S.; Selikoff, I. J. Prevalence of Disease among Vinyl Chloride and Polyvinyl Chloride Workers. *Ann. N. Y. Acad. Sci.* **1975**, *246*, 22–41.

(99) Suciu, I.; Prodan, L.; Ilea, E.; Paduraru, A.; Pascu, L. Clinical Manifestations in Vinyl Chloride Poisoning . *Ann. New York Acad. Sci.* **1975**, *246*, 53–69.

(100) Veltman, G.; Lange, C. E.; Jühe, S.; Stein, G.; Bachner, U. Clinical Manifestations and Course of Vinyl Chloride Disease. *Ann. N. Y. Acad. Sci.* **1975**, *246*, 6–17.

(101) Rowe, V. K.; McCollister, D. D.; Spencer, H. C.; Adams, E. M.; Irish, D. D. Vapor Toxicity of Tetrachloroethylene for Laboratory Animals and Human Subjects. *AMA. Arch. Ind. Hyg. Occup. Med.* **1952**, *5* (6), 566–579.

(102) Buxton, P. H.; Hayward, M. Polyneuritis Cranialis Associated with Industrial Trichloroethylene Poisoning. *J. Neurol. Neurosurg. Psychiatry* **1967**, *30* (6), 511–518. https://doi.org/10.1136/jnnp.30.6.511.

(103) David, N. J.; Wolman, R.; Milne, F. J.; Van, N. I. Acute Renal Failure Due to Trichloroethylene Poisoning. *Br. J. Ind. Med.* **1989**, *46* (5), 347–349.

(104) Liotier, J.; Barbier, M.; Plantefeve, G.; Duale, C.; Deteix, P.; Souweine, B.; Coudoré, F. A Rare Cause of Abdominal Compartment Syndrome: Acute Trichlorethylene Overdose. *Clin. Toxicol.* **2008**, *46* (9), 905–907. https://doi.org/10.1080/15563650802269893.

(105) Mortiz, F.; de La, C. A.; Bauer, F.; Leroy, J. P.; Goulle, J. P.; Bonmarchand, G. Esmolol in the Treatment of Severe Arrhythmia after Acute Trichloroethylene Poisoning. *Intensive Care Med.* **2000**, *26* (0342–4642 (Print)), 256.

(106) Nomiyama, K.; Nomiyama, H. Dose-Response Relationship for Trichloroethylene in Man. *Int. Arch. Occup. Environ. Health* **1977**, *39* (4), 237–248. https://doi.org/10.1007/BF00409369.

(107) Barret, L.; Garrel, S.; Danel, V.; Debru, J. L. Chronic Trichloroethylene Intoxication: A New Approach by Trigeminal-Evoked Potentials? *Arch. Environ. Health* **1987**, *42* (5), 297–302. https://doi.org/10.1080/00039896.1987.9935824.

(108) Goldman, S. M.; Quinlan, P. J.; Webster Ross, G.; Marras, C.; Meng, C.; Bhudhikanok, G. S.; Comyns, K.; Korell, M.; Chade, A. R.; Kasten, M.; et al. Solvent Exposures and Parkinson's Disease Risk in Twins. *Ann Neurol* **2012**, *71* (6), 776–784. https://doi.org/10.1002/ana.22629.

(109) Grandjean, E.; Munchinger, R.; Turrian, V.; Haas, P. A.; Knoepfel, H.-K.; Rosenmund, H. Investigations into the Effects of Exposure to Trichlorethylene in Mechanical Engineering. *Br. J. Ind. Med.* **1955**, *12* (2), 131–142.

(110) Kilburn, K. H.; Warshaw, R. H. Prevalence of Symptoms of Systemic Lupus Erythematosus (SLE) and of Fluorescent Antinuclear Antibodies Associated with Chronic Exposure to Trichloroethylene and Other Chemicals in Well Water. *Environ. Res.* **1992**, *57* (1), 1–9. https://doi.org/10.1016/S0013-9351(05)80014-3.

(111) Kilburn, K. H.; Warshaw, R. H.; Hanscom, B. Balance Measured by Head (and Trunk) Tracking and a Force Platform in Chemically (PCB and TCE) Exposed and Referent Subjects. *Occup. Environ. Med.* **1994**, *51* (6), 381–385. https://doi.org/10.1136/oem.51.6.381.

(112) Milby, T. H. Chronic Trichloroethylene Intoxication. *J. Occup. Med.* **1968**, *10* (5), 252–254. https://doi.org/10.1080/00039896.1987.9935824.

(113) Mitchell, A. B. S.; Parsons-Smith, B. G. Trichloroethylene Neuropathy. *Br. Med. J.* **1969**, *2* (5655), 516. https://doi.org/10.1136/bmj.2.5655.516.

(114) Smith, G. F. Trichlorethylene: A Review. *Br J Ind Med* **1966**, *23* (4), 249–262.

(115) Trabert, W. Psychiatric Disorders Related to Solvent-Exposure *. *Zentralblatt fur Hyg. und Umweltmedizin* **1998**, *202* (2–4), 121–126. https://doi.org/10.1016/S0934-8859(99)80013-3.

(116) Blair, A.; Hartge, P.; Stewart, P. A.; McAdams, M.; Lubin, J. Mortality and Cancer Incidence of Aircraft Maintenance Workers Exposed to Trichloroethylene and Other Organic Solvents and Chemicals: Extended Follow Up. *Occup. Environ. Med.* **1998**, *55* (3), 161–171. https://doi.org/10.1136/oem.55.3.161.

(117) Radican, L.; Blair, A.; Stewart, P.; Wartenberg, D. Mortality of Aircraft Maintenance Workers Exposed to Trichloroethylene and Other Hydrocarbons and Chemicals: Extended Follow-Up. *J. Occup. Environ. Med.* **2008**, *50* (11), 1306–1319. https://doi.org/10.1097/JOM.0b013e3181845f7f.

(118) Magnavita, N.; Bergamaschi, A.; Garcovich, A.; Giuliano, G. Vasculitic Purpura in Vinyl Chloride Disease: A Case Report. *Angiology* **1986**, *37* (5), 382–388. https://doi.org/10.1177/000331978603700508.

(119) Ostlere, L. S.; Harris, D.; Buckley, C.; Black, C.; Rustin, M. H. Atypical Systemic Sclerosis Following Exposure to Vinyl Chloride Monomer. A Case Report and Review of the Cutaneous Aspects of Vinyl Chloride Disease. *Clin. Exp. Dermatol.* **1992**, *17* (3), 208–210.

(120) Brodkin, C. A.; Daniell, W.; Checkoway, H.; Echeverria, D.; Johnson, J.; Wang, K.; Sohaey, R.; Green, D.; Redlich, C.; Gretch, D. Hepatic Ultrasonic Changes in Workers Exposed to Perchloroethylene. *Occup. Environ. Med.* **1995**, *52* (10), 679–685. https://doi.org/10.1136/oem.52.10.679.

(121) Hanioka, N.; Jinno, H.; Toyo, T.; Nishimura, T.; Ando, M. Induction of Rat Liver Drug-Metabolizing Enzymes by Tetrachloroethylene. **1995**, *280*, 273–280.

(122) Neghab, M.; Qu, S.; Bai, C. L.; Caples, J.; Stacey, N. H. Raised Concentration of Serum Bile Acids Following Occupational Exposure to Halogenated Solvents, 1,1,2-Trichloro-1,2,2-Trifluoroethane and Trichloroethylene. *Int. Arch. Occup. Environ. Health* **1997**, *70* (3), 187–194.

(123) Hayes, J. R.; Condie, L. W.; Borzelleca, J. F. The Subchronic Toxicity of Tetrachloroethylene (Perchloroethylene) Administered in the Drinking Water of Rats. *Toxicol. Sci.* **1986**, *7* (1), 119–125. https://doi.org/10.1093/toxsci/7.1.119.

(124) Meckler, L. C.; Phelps, D. K. Liver Disease Secondary to Tetrachloroethylene Exposure. *JAMA* **1966**, *197* (8), 662. https://doi.org/10.1001/jama.1966.03110080102037.

(125) Mutti, A.; Alinovi, R.; Bergamaschi, E.; Biagini, C.; Cavazzini, S.; Franchini, I.; Lauwerys, R. R.; Bernard, A. M.; Roels, H.; Gelpi, E.; et al. Nephropathies and Exposure to Perchloroethylene in Dry-Cleaners. *Lancet* **1992**, *340* (8813), 189–193. https://doi.org/10.1016/0140-6736(92)90463-D.

(126) Philip, B. K.; Mumtaz, M. M.; Latendresse, J. R.; Mehendale, H. M. Impact of Repeated Exposure on Toxicity of Perchloroethylene in Swiss Webster Mice. *Toxicology* **2007**, *232* (1–2), 1–14. https://doi.org/10.1016/j.tox.2006.12.018.

(127) Berk, P. D.; Martin, J. F.; Waggoner, J. G. Persistence of Vinyl Chloride-Induced

Liver Injury After Cessation of Exposure. *Ann. N. Y. Acad. Sci.* **1975**, *246* (1), 70–77. https://doi.org/10.1111/j.1749-6632.1975.tb51081.x.

(128) Du, C. L.; Wang, J. Der. Increased Morbidity Odds Ratio of Primary Liver Cancer and Cirrhosis of the Liver among Vinyl Chloride Monomer Workers. *Occup. Environ. Med.* **1998**, *55* (8), 528–532. https://doi.org/10.1136/oem.55.8.528.

(129) Maroni, M.; Mocci, F.; Visentin, S.; Preti, G.; Fanetti, A. C. Periportal Fibrosis and Other Liver Ultrasonography Findings in Vinyl Chloride Workers. *Occup. Environ. Med.* **2003**, *60* (1), 60–65. https://doi.org/10.1136/oem.60.1.60.

(130) Malaguarnera, G.; Cataudella, E.; Giordano, M.; Nunnari, G.; Chisari, G.; Malaguarnera, M. Toxic Hepatitis in Occupational Exposure to Solvents. *World J. Gastroenterol.* **2012**, *18* (22), 2756–2766. https://doi.org/10.3748/wjg.v18.i22.2756.

(131) Forand, S. P.; Lewis-Michl, E. L.; Gomez, M. I. Adverse Birth Outcomes and Maternal Exposure to Trichloroethylene and Tetrachloroethylene through Soil Vapor Intrusion in New York State. *Environ. Health Perspect.* **2012**, *120* (4), 616–621. https://doi.org/10.1289/ehp.1103884.

(132) McDonald, G. J.; Wertz, W. E. PCE, TCE, and TCA Vapors in Subslab Soil Gas and Indoor Air: A Case Study in Upstate New York. *Gr. Water Monit. Remediat.* **2007**, *27* (4), 86–92. https://doi.org/10.1111/j.1745-6592.2007.00164.x.

(133) IARC. Vinyl Chloride. *IARC Monogr.* **2012**, *100F*, 1–39.

(134) IARC. Trichloroethylene. *IARC Monogr.* **2014**, *106* (IARC Monographs on the Evaluation of Carcinogenic risks to humans), 219–351.

(135) IARC. Tetrachloroethylene. *IARC Monogr.* **2014**, *106*, 219–351.

(136) Karami, S.; Bassig, B.; Stewart, P. A.; Lee, K. M.; Rothman, N.; Moore, L. E.; Lan, Q. Occupational Trichloroethylene Exposure and Risk of Lymphatic and Haematopoietic Cancers: A Meta-Analysis. *Occup. Environ. Med.* **2013**, *70* (8), 591–599. https://doi.org/10.1136/oemed-2012-101212.

(137) Kelsh, M. A.; Alexander, D. D.; Mink, P. J.; Mandel, J. H. Occupational Trichloroethylene Exposure and Kidney Cancer. *Epidemiology* **2010**, *21* (1), 95–102. https://doi.org/10.1097/EDE.0b013e3181c30e92.

(138) Moore, L. E.; Boffetta, P.; Karami, S.; Brennan, P.; Stewart, P. S.; Hung, R.; Zaridze, D.; Matveev, V.; Janout, V.; Kollarova, H.; et al. Occupational Trichloroethylene Exposure and Renal Carcinoma Risk: Evidence of Genetic Susceptibility by Reductive Metabolism Gene Variants. *Cancer* **2011**, *70* (16), 6527–6536. https://doi.org/10.1158/0008-5472.CAN-09-4167.Occupational.

(139) Scott, C. S.; Jinot, J. Trichloroethylene and Cancer: Systematic and Quantitative Review of Epidemiologic Evidence for Identifying Hazards. *Int. J. Environ. Res. Public Health* **2011**, *8* (11), 4238–4272. https://doi.org/10.3390/ijerph8114238.

(140) Wartenberg, D.; Reyner, D.; Scott, C. S. Trichloroethylene and Cancer: Epidemiologic Evidence. *Environ. Health Perspect.* **2000**, *108* (SUPPL. 2), 161–176. https://doi.org/10.1289/ehp.00108s2161.

(141) Bosetti, C.; La Vecchia, C.; Lipworth, L.; McLaughlin, J. K. Occupational

Exposure to Vinyl Chloride and Cancer Risk: A Review of the Epidemiologic Literature. *Eur. J. Cancer Prev.* **2003**, *12* (5), 427–430. https://doi.org/10.1097/01.cej.0000090184.08740.10.

(142) Byren, D.; Engholm, G.; Englund, A.; Westerholm, P. Mortality and Cancer Morbidity in a Group of Swedish VCM and PCV Production Workers. *Environ. Health Perspect.* **1977**, *Vol. 17* (October), 167–170.

(143) Wu, W.; Steenland, K.; Brown, D.; Wells, V.; Jones, J.; Schulte, P.; Halperin, W. Cohort and Case-Control Analyses of Workers Exposed to Vinyl Chloride: An Update. *J. Occup. Med.* **1989**, *31* (6), 518–523.

(144) Creech, J. L.; Johnson, M. N. Angiosarcoma of Liver in the Manufacture of Polyvinyl Chloride. *J. Occup. Med.* **1974**, *16* (3), 150–151. https://doi.org/4856325.

(145) Laplanche, A.; Clavel-Chapelon, F.; Contassot, J. C.; Lanouziere, C. Exposure to Vinyl Chloride Monomer: Results of a Cohort Study after a Seven Year Follow up. The French VCM Group. *Br. J. Ind. Med.* **1992**, *49* (2), 134–137. https://doi.org/10.1136/oem.49.2.134.

(146) Lee, F. I.; Smith, P. M.; Bennett, B.; Williams, D. M. Occupationally Related Angiosarcoma of the Liver in the United Kingdom 1972-1994. *Gut* **1996**, *39* (2), 312–318.

(147) Monson, R. R.; Peters, J. M.; Johnson, M. N. Proportional Mortality among Vinyl Chloride Workers. *Env. Heal. Perspect* **1975**, *11* (June), 75–77.

(148) Simonato, L.; L'Abbé, K. A.; Andersen, A.; Belli, S.; Comba, P.; Engholm, G.; Ferro, G.; Hagmar, L.; Langård, S.; Lundberg, I. A Collaborative Study of Cancer Incidence and Mortality among Vinyl Chloride Workers. *Scand. J. Work. Environ. Health* **1991**, *17* (3), 159–169.

(149) Thériault, G.; Allard, P. Cancer Mortality of a Group of Canadian Workers Exposed to Vinyl Chloride Monomer. *J. Occup. Med.* **1981**, *23* (10), 671–676.

(150) Waxweiler, R. J.; Stringer, W.; Wagoner, J. K.; Jones, J.; Falk, H.; Carter, C. Exposed To Vinyl Chloride. **1974**, 40–48.

(151) Weber, H.; Reinl, W.; Greiser, E. German Investigations on Morbidity and Mortality of Workers Exposed to Vinyl Chloride. *Environ. Health Perspect.* **1981**, *Vol. 41* (October), 95–99.

(152) Raaschou-Nielsen, O.; Hansen, J.; McLaughlin, J. K.; Kolstad, H.; Christensen, J. M.; Tarone, R. E.; Olsen, J. H. Cancer Risk among Workers at Danish Companies Using Trichloroethylene: A Cohort Study. *Am. J. Epidemiol.* **2003**, *158* (12), 1182–1192. https://doi.org/10.1093/aje/kwg282.

(153) Vartiainen, T.; Pukkala, E.; Rienoja, T.; Strandman, T.; Kaksonen, K. Population Exposure to Tri- and Tetrachloroethene and Cancer Risk: Two Cases of Drinking Water Pollution. *Chemosphere* **1993**, *27* (7), 1171–1181. https://doi.org/10.1016/0045-6535(93)90165-2.

(154) Clark Cooper, W. Epidemiologic Study of Vinyl Chloride Workers: Mortality through December 31, 1972. *Environ. Health Perspect.* **1981**, *Vol. 41* (October), 101–106.

(155) Infante, P. F.; Wagoner, J. K.; Waxweiler, R. J. Carcinogenic, Mutagenic and Teratogenic Risks Associated with Vinyl Chloride. *Mutat. Res.* **1976**, *41* (1 spel. no), 131–141.

(156) Smulevich, V. B.; Fedotova, I. V; Filatova, V. S. Increasing Evidence of the Rise of Cancer in Workers Exposed to Vinylchloride. *Br. J. Ind. Med.* **1988**, *45* (2), 93–97.

(157) Wong, R.-H. .; Chen, P.-C. .; Wang, J.-D. . b; Du, C.-L. .; Cheng, T.-J. . Interaction of Vinyl Chloride Monomer Exposure and Hepatitis B Viral Infection on Liver Cancer. *J. Occup. Environ. Med.* **2003**, *45* (4), 379–383. https://doi.org/10.1097/01.jom.0000063622.37065.fd.

(158) Wong, R.; Chen, P.; Du, C.; Wang, J.; Cheng, T. An Increased Standardised Mortality Ratio for Liver Cancer among Polyvinyl Chloride Workers in Taiwan. *Occup. Environ. Med.* **2002**, *59* (6), 405–409.

(159) Boice, J. D.; Marano, D. E.; Fryzek, J. P.; Sadler, C. J.; Mclaughlin, J. K.; Jr, J. D. B.; Marano, D. E.; Fryzek, J. P.; Sadler, C. J. Mortality among Aircraft Manufacturing Workers Mortality among Aircraft Manufacturing Workers. **1999**, No. February 2007, 581–597.

(160) Calvert, G. M.; Ruder, A. M.; Petersen, M. R. Mortality and End-Stage Renal Disease Incidence among Dry Cleaning Workers. *Occup. Environ. Med.* **2011**, *68* (10), 709–716. https://doi.org/10.1136/oem.2010.060665.

(161) Lynge, E.; Andersen, A.; Rylander, L.; Tinnerberg, H.; Lindbohm, M. L.; Pukkala, E.; Romundstad, P.; Jensen, P.; Clausen, L. B.; Johansen, K. Cancer in Persons Working in Dry Cleaning in the Nordic Countries. *Environ. Health Perspect.* **2006**, *114* (2), 213–219. https://doi.org/10.1289/ehp.8425.

(162) Seldén, A. I.; Ahlborg, G. Cancer Morbidity in Swedish Dry-Cleaners and Laundry Workers: Historically Prospective Cohort Study. *Int. Arch. Occup. Environ. Health* **2011**, *84* (4), 435–443. https://doi.org/10.1007/s00420-010-0582-7.

(163) Bahr, D. E.; Aldrich, T. E.; Seidu, D.; Brion, G. M.; Tollerud, D. J. Occupational Exposure to Trichloroethylene and Cancer Risk for Workers at the Paducah Gaseous Diffusion Plant. *Int. J. Occup. Med. Environ. Health* **2011**, *24* (1), 67–77. https://doi.org/10.2478/s13382-011-0007-1.

(164) Cohn, P.; Klotz, J.; Bove, F.; Berkowitz, M.; Fagliano, J. Drinking Water Contamination and the Incidence of Leukemia and Non-Hodgkin/s Lymphoma. *Environ. Health Perspect.* **1994**, *102* (6–7), 556–561. https://doi.org/sc271_5_1835 [pii].

(165) Fagliano, J.; Berry, M.; Bove, F.; Burke, T. Drinking Water Contamination and the Incidence of Leukemia: An Ecologic Study. *Am. J. Public Health* **1990**, *80* (10), 1209–1212. https://doi.org/10.2105/AJPH.80.10.1209.

(166) Hansen, J.; Sallmén, M.; Seldén, A. I.; Anttila, A.; Pukkala, E.; Andersson, K.; Bryngelsson, I. L.; Raaschou-Nielsen, O.; Olsen, J. H.; McLaughlin, J. K. Risk of Cancer among Workers Exposed to Trichloroethylene: Analysis of Three Nordic Cohort Studies. *J. Natl. Cancer Inst.* **2013**, *105* (12), 869–877. https://doi.org/10.1093/jnci/djt107.

(167) Hansen, J.; Raaschou-Nielsen, O.; Christensen, J. M.; Johansen, I.; McLaughlin, J. K.; Lipworth, L.; Blot, W. J.; Olsen, J. H. Cancer Incidence among Danish Workers Exposed to Trichloroethylene. *J. Occup. Environ. Med.* **2001**, *43* (2), 133–139.

(168) Hardell, L.; Eriksson, M.; Degerman, A. Exposure to Phenoxyacetic Acids, Chlorophenols or Organic Solvents in Relation to Histopathology, Stage and Anatomical Localization of Non-Hodgkin's Lymphoma . *Cancer Res.* **1994**, *54* (9), 2386–2389.

(169) National Archives and Records Administration. *Federal Register: 54 Fed. Reg. 2081*; 1989; Vol. 54, pp 4607–5000.

(170) USEPA. *National Primary Drinking Water Regulations*; 2009; Vol. 1, p 7.

(171) U.S. Dept. of HHS. Draft - Toxicological Profile for Perfluroroalkyls. **2015**, No. August.

(172) Griffith, F. D.; Long, J. E. Animal Toxicity Studies with Ammonium Perfluorooctanoate. *Am. Ind. Hyg. Assoc. J.* **1980**, *41* (8), 576–583. https://doi.org/10.1080/15298668091425301.

(173) Steenland, K.; Woskie, S. Cohort Mortality Study of Workers Exposed to Perfluorooctanoic Acid. *Am. J. Epidemiol.* **2012**, *176* (10), 909–917. https://doi.org/10.1093/aje/kws171.

(174) Leonard, R. C.; Kreckmann, K. H.; Sakr, C. J.; Symons, J. M. Retrospective Cohort Mortality Study of Workers in a Polymer Production Plant Including a Reference Population of Regional Workers. *Ann. Epidemiol.* **2008**, *18* (1), 15–22. https://doi.org/10.1016/j.annepidem.2007.06.011.

(175) Kudo, N. K.; Akajima, S. U.; Itsumoto, A. M.; Awashima, Y. K. Responses of the Liver to Perfluorinated Fatty Acids with Different.Pdf. **2006**, *29* (9), 1952–1957.

(176) Cook, J. C.; Murray, S. M.; Frame, S. R.; Hurtt, M. E. Induction of Leydig Cell Adenomas by Ammonium Perfluorooctanoate: A Possible Endocrine-Related Mechanism. *Toxicol. Appl. Pharmacol.* **1992**, *113* (2), 209–217. https://doi.org/10.1016/0041-008X(92)90116-A.

(177) Dong, G. H.; Tung, K. Y.; Tsai, C. H.; Liu, M. M.; Wang, D.; Liu, W.; Jin, Y. H.; Hsieh, W. S.; Lee, Y. L.; Chen, P. C. Serum Polyfluoroalkyl Concentrations, Asthma Outcomes, and Immunological Markers in a Case-Control Study of Taiwanese Children. *Environ. Health Perspect.* **2013**, *121* (4), 507–513. https://doi.org/10.1289/ehp.1205351.

(178) Humblet, O.; Diaz-Ramirez, L. G.; Balmes, J. R.; Pinney, S. M.; Hiatt, R. A. Perfluoroalkyl Chemicals and Asthma among Children 12-19 Years of Age: Nhanes (1999-2008). *Environ. Health Perspect.* **2014**, *122* (10), 1129–1133. https://doi.org/10.1289/ehp.1306606.

(179) Anderson-Mahoney, P.; Kotlerman, J.; Takhar, H.; Gray, D.; Dahlgren, J. Self-Reported Health Effects among Community Residents Exposed to Perfluorooctanoate. *NEW Solut. A J. Environ. Occup. Heal. Policy* **2008**, *18* (2), 129–143. https://doi.org/10.2190/NS.18.2.d.

(180) Min, J.-Y.; Lee, K.-J.; Park, J.-B.; Min, K.-B. Perfluorooctanoic Acid Exposure Is

Associated with Elevated Homocysteine and Hypertension in US Adults. *Occup. Environ. Med.* **2012**, *69* (9), 658–662. https://doi.org/10.1136/oemed-2011-100288.

(181) Shankar, A.; Xiao, J.; Ducatman, A. Perfluorooctanoic Acid and Cardiovascular Disease in US Adults. *Arch. Intern. Med.* **2012**, *172* (18), 1397–1403. https://doi.org/10.1001/archinternmed.2012.3393.

(182) Eriksen, K. T.; Raaschou-Nielsen, O.; McLaughlin, J. K.; Lipworth, L.; Tjønneland, A.; Overvad, K.; Sørensen, M. Association between Plasma PFOA and PFOS Levels and Total Cholesterol in a Middle-Aged Danish Population. *PLoS One* **2013**, *8* (2), 1–7. https://doi.org/10.1371/journal.pone.0056969.

(183) Nelson, J. W.; Hatch, E. E.; Webster, T. F. Exposure to Polyfluoroalkyl Chemicals and Cholesterol, Body Weight, and Insulin Resistance in the General U.S. Population. *Environ. Health Perspect.* **2010**, *118* (2), 197–202. https://doi.org/10.1289/ehp.0901165.

(184) Fitz-Simon, N.; Fletcher, T.; Luster, M. I.; Steenland, K.; Calafat, A. M.; Kato, K.; Armstrong, B. Reductions in Serum Lipids with a 4-Year Decline in Serum Perfluorooctanoic Acid and Perfluorooctanesulfonic Acid. *Epidemiology* **2013**, *24* (4), 569–576. https://doi.org/10.1097/EDE.0b013e31829443ee.

(185) Eldasher, L. M.; Wen, X.; Little, M. S.; Bircsak, K. M.; Yacovino, L. L.; Aleksunes, L. M. Hepatic and Renal Bcrp Transporter Expression in Mice Treated with Perfluorooctanoic Acid. *Toxicology* **2013**, *306* (4), 108–113. https://doi.org/10.1016/j.tox.2013.02.009.

(186) Qazi, M. R.; Dean Nelson, B.; DePierre, J. W.; Abedi-Valugerdi, M. High-Dose Dietary Exposure of Mice to Perfluorooctanoate or Perfluorooctane Sulfonate Exerts Toxic Effects on Myeloid and B-Lymphoid Cells in the Bone Marrow and These Effects Are Partially Dependent on Reduced Food Consumption. *Food Chem. Toxicol.* **2012**, *50* (9), 2955–2963. https://doi.org/10.1016/j.fct.2012.06.023.

(187) Xie, Y.; Yang, Q.; Nelson, B. D.; DePierre, J. W. The Relationship between Liver Peroxisome Proliferation and Adipose Tissue Atrophy Induced by Peroxisome Proliferator Exposure and Withdrawal in Mice. *Biochem. Pharmacol.* **2003**, *66* (5), 749–756. https://doi.org/10.1016/S0006-2952(03)00386-1.

(188) Biegel, L. B.; Hurtt, M. E.; Frame, S. R.; O'Connor, J. C.; Cook, J. C. Mechanisms of Extrahepatic Tumor Induction by Peroxisome Proliferators in Male CD Rats. *Toxicol. Sci.* **2001**, *60* (1), 44–55. https://doi.org/10.1093/toxsci/60.1.44.

(189) Ahmed, D. Y.; Abd Ellah, M. R. Effect of Exposure to Perfluorooctanoic Acid on Hepatic Antioxidants in Mice. *Comp. Clin. Path.* **2012**, *21* (6), 1643–1645. https://doi.org/10.1007/s00580-011-1341-1.

(190) Elcombe, C. R.; Elcombe, B. M.; Foster, J. R.; Chang, S. C.; Ehresman, D. J.; Noker, P. E.; Butenhoff, J. L. Evaluation of Hepatic and Thyroid Responses in Male Sprague Dawley Rats for up to Eighty-Four Days Following Seven Days of Dietary Exposure to Potassium Perfluorooctanesulfonate. *Toxicology* **2012**, *293* (1–3), 30–40. https://doi.org/10.1016/j.tox.2011.12.015.

(191) Cui, L.; Zhou, Q. F.; Liao, C. Y.; Fu, J. J.; Jiang, G. Bin. Studies on the Toxicological Effects of PFOA and PFOS on Rats Using Histological Observation and Chemical Analysis. *Arch. Environ. Contam. Toxicol.* **2009**, *56* (2), 338–349. https://doi.org/10.1007/s00244-008-9194-6.

(192) Seacat, A. M.; Thomford, P. J.; Hansen, K. J.; Clemen, L. A.; Eldridge, S. R.; Elcombe, C. R.; Butenhoff, J. L. Sub-Chronic Dietary Toxicity of Potassium Perfluorooctanesulfonate in Rats. *Toxicology* **2003**, *183* (1–3), 117–131. https://doi.org/10.1016/S0300-483X(02)00511-5.

(193) Steenland, K.; Zhao, L.; Winquist, A.; Parks, C. Ulcerative Colitis and Perfluorooctanoic Acid (PFOA) in a Highly Exposed Population of Community Residents and Workers in the Mid-Ohio Valley. *Environ. Health Perspect.* **2013**, *121* (8), 900–905. https://doi.org/10.1289/ehp.1206449.

(194) Grandjean, P.; Andersen, E. W.; Budtz-Jørgensen, E.; Nielsen, F.; Mølbak, K.; Weihe, P.; Heilmann, C. Serum Vaccine Antibody Concentrations in Children Exposed to Perfluorinated Compounds. *JAMA* **2012**, *307* (4), 391–397. https://doi.org/10.1001/jama.2011.2034.

(195) Looker, C.; Luster, M. I.; Calafat, A. M.; Johnson, V. J.; Burleson, G. R.; Burleson, F. G.; Fletcher, T. Influenza Vaccine Response in Adults Exposed to Perfluorooctanoate and Perfluorooctanesulfonate. *Toxicol. Sci.* **2014**, *138* (1), 76–88. https://doi.org/10.1093/toxsci/kft269.

(196) Granum, B.; Haug, L. S.; Namork, E.; Stølevik, S. B.; Thomsen, C.; Aaberge, I. S.; Van Loveren, H.; Løvik, M.; Nygaard, U. C. Pre-Natal Exposure to Perfluoroalkyl Substances May Be Associated with Altered Vaccine Antibody Levels and Immune-Related Health Outcomes in Early Childhood. *J. Immunotoxicol.* **2013**, *10* (4), 373–379. https://doi.org/10.3109/1547691X.2012.755580.

(197) Knox, S. S.; Jackson, T.; Javins, B.; Frisbee, S. J.; Shankar, A.; Ducatman, A. M. Implications of Early Menopause in Women Exposed to Perfluorocarbons. *J. Clin. Endocrinol. Metab.* **2011**, *96* (6), 1747–1753. https://doi.org/10.1210/jc.2010-2401.

(198) Louis, G. M. B.; Peterson, C. M.; Chen, Z.; Hediger, M. L.; Croughan, M. S.; Sundaram, R.; Stanford, J. B.; Fujimoto, V. Y.; Varner, M. W.; Giudice, L. C.; et al. Perfluorochemicals and Endometriosis: The ENDO Study. *Epidemiology* **2012**, *23* (6), 799–805. https://doi.org/10.1097/EDE.0b013e31826cc0cf.

(199) Hoffman, K.; Webster, T. F.; Weisskopf, M. G.; Weinberg, J.; Vieira, V. M. Exposure to Polyfluoroalkyl Chemicals and Attention Deficit/Hyperactivity Disorder in U.S. Children 12–15 Years of Age. *Environ. Health Perspect.* **2010**, *118* (12), 1762–1767. https://doi.org/10.1289/ehp.1001898.

(200) Stein, C. R.; Savitz, D. A. Serum Perfluorinated Compound Concentration and Attention Deficit/Hyperactivity Disorder in Children 5-18 Years of Age. *Environ. Health Perspect.* **2011**, *119* (10), 1466–1471. https://doi.org/10.1289/ehp.1003538.

(201) Gump, B. B.; Wu, Q.; Dumas, A. K.; Kannan, K. Perfluorochemical (PFC) Exposure in Children: Associations with Impaired Response Inhibition. *Environ.*

Sci. Technol. **2011**, *45* (19), 8151–8159. https://doi.org/10.1021/es103712g.

(202) Wan, H. T.; Zhao, Y. G.; Wong, M. H.; Lee, K. F.; Yeung, W. S. B.; Giesy, J. P.; Wong, C. K. C. Testicular Signaling Is the Potential Target of Perfluorooctanesulfonate-Mediated Subfertility in Male Mice1. *Biol. Reprod.* **2011**, *84* (5), 1016–1023. https://doi.org/10.1095/biolreprod.110.089219.

(203) Hansen, K. J.; Johnson, H. O.; Eldridge, J. S.; Butenhoff, J. L.; Dick, L. A. Quantitative Characterization of Trace Levels of PFOS and PFOA in the Tennessee River. *Environ. Sci. Technol.* **2002**, *36* (8), 1681–1685. https://doi.org/10.1021/es010780r.

(204) DeWitt, J. C.; Copeland, C. B.; Strynar, M. J.; Luebke, R. W. Perfluorooctanoic Acid-Induced Immunomodulation in Adult C57BL/6J or C57BL/6N Female Mice. *Environ. Health Perspect.* **2008**, *116* (5), 644–650. https://doi.org/10.1289/ehp.10896.

(205) Iwai, H.; Yamashita, K. A Fourteen-Day Repeated Dose Oral Toxicity Study of APFO in Rats. *Drug Chem. Toxicol.* **2006**, *29* (3), 323–332. https://doi.org/10.1080/01480540600653143.

(206) Loveless, S. E.; Hoban, D.; Sykes, G.; Frame, S. R.; Everds, N. E. Evaluation of the Immune System in Rats and Mice Administered Linear Ammonium Perfluorooctanoate. *Toxicol. Sci.* **2008**, *105* (1), 86–96. https://doi.org/10.1093/toxsci/kfn113.

(207) Yang, Q.; Xie, Y.; Eriksson, A. M.; Nelson, B. D.; DePierre, J. W. Further Evidence for the Involvement of Inhibition of Cell Proliferation and Development in Thymic and Splenic Atrophy Induced by the Peroxisome Proliferator Perfluoroctanoic Acid in Mice. *Biochem. Pharmacol.* **2001**, *62* (8), 1133–1140. https://doi.org/10.1016/S0006-2952(01)00752-3.

(208) Butenhoff, J. L.; Chang, S. C.; Olsen, G. W.; Thomford, P. J. Chronic Dietary Toxicity and Carcinogenicity Study with Potassium Perfluorooctanesulfonate in Sprague Dawley Rats. *Toxicology* **2012**, *293* (1–3), 1–15. https://doi.org/10.1016/j.tox.2012.01.003.

(209) Seacat, A. M.; Thomford, P. J.; Hansen, K. J.; Olsen, G. W.; Case, M. T.; Butenhoff, J. L. Subchronic Toxicity Studies on Perfluoroctanesulfonate Potassium Salt in Cynomolgus Monkeys. *Toxicol Sci* **2002**, *68* (November), 249–264. https://doi.org/10.1093/toxsci/68.1.249.

(210) IARC. *IARC Monograph - Perfluorooctanoic Acid*; 2016.

(211) Woskie, S. R.; Gore, R.; Steenland, K. Retrospective Exposure Assessment of Perfluorooctanoic Acid Serum Concentrations at a Fluoropolymer Manufacturing Plant. *Ann. Occup. Hyg.* **2012**, *56* (9), 1025–1037. https://doi.org/10.1093/annhyg/mes023.

(212) Raleigh, K. K.; Alexander, B. H.; Olsen, G. W.; Ramachandran, G.; Morey, S. Z.; Church, T. R.; Logan, P. W.; Scott, L. L. F.; Allen, E. M. Mortality and Cancer Incidence in Ammonium Perfluorooctanoate Production Workers. *Occup. Environ. Med.* **2014**, *71* (7), 500–506. https://doi.org/10.1136/oemed-2014-102109.

(213) Barry, V.; Winquist, A.; Steenland, K. Perfluorooctanoic Acid (PFOA) Exposures and Incident Cancers among Adults Living near a Chemical Plant. *Environ. Health Perspect.* **2013**, *121* (11–12), 1313–1318. https://doi.org/10.1289/ehp.1306615.

(214) Vieira, V. M.; Hoffman, K.; Shin, H. M.; Weinberg, J. M.; Webster, T. F.; Fletcher, T. Perfluorooctanoic Acid Exposure and Cancer Outcomes in a Contaminated Community: A Geographic Analysis. *Environ. Health Perspect.* **2013**, *121* (3), 318–323. https://doi.org/10.1289/ehp.1205829.

(215) Caverly Rae, J. M.; Frame, S. R.; Kennedy, G. L.; Butenhoff, J. L.; Chang, S. C. Pathology Review of Proliferative Lesions of the Exocrine Pancreas in Two Chronic Feeding Studies in Rats with Ammonium Perfluorooctanoate. *Toxicol. Reports* **2014**, *1*, 85–91. https://doi.org/10.1016/j.toxrep.2014.04.005.

(216) USEPA. Emerging Contaminants – Perfluorooctane Sulfonate (PFOS) and Perfluorooctanoic Acid (PFOA). *USEPA Fact Sheet* **2014**, No. March, 6.

(217) USEPA. *Revisions to the Unregulated Contaminant Monitoring Regulation (UCMR 3) for Public Water Systems: Final Rule*; 2012; Vol. 77, pp 1–31.

(218) Pant, P.; Pant, S. A Review: Advances in Microbial Remediation of Trichloroethylene (TCE). *J. Environ. Sci.* **2010**, *22* (1), 116–126. https://doi.org/10.1016/S1001-0742(09)60082-6.

(219) Jacoby, W. A.; Blake, D. M.; Watt, A. S. Remediation of Trichloroethylene or Perchloroethylene Contamination. In *Encyclopediat Series in Environmental Sciences: Environmental Analysis & Remediation*; Myers, R. A., Ed.; Wiley Blackwell, 1998; pp 4847–4873.

(220) Chiao, F. F.; Currie, R. C.; McKone, T. E. Intermedia Transfer Factors for Contaminants Found at Hazardous Waste Sites: Trichloroethylene (TCE). **1994**, No. December, 1-- 44.

(221) Chiao, F. F.; Currie, R. C.; McKone, T. E. Intermedia Transfer Factors for Contaminants Found at Hazardous Waste Sites: Tetrachloroethylene (PCE). **1994**, No. December, 1-- 44.

(222) Russell, H. H.; Matthews, J. E.; Sewell, G. W. TCE Removal from Contaminated Soil and Ground Water. *USEPA Gr. Water Issue* **1992**, 1–10. https://doi.org/10.1056/NEJMoa030660.

(223) Mackay, D. M.; Roberts, P. V.; Cherry, J. A. Transport of Organic Contaminants in Groundwater. *Environ. Sci. Technol.* **1985**, *19* (5), 384–392. https://doi.org/10.1021/es00135a001.

(224) Marrin, D. L.; Kerfoot, H. B. Soil-Gas Surveying Techniques. *Environ. Sci. Technol.* **1988**, *22* (7), 740–745. https://doi.org/10.1021/es00172a001.

(225) Bourg, A. C. M.; Mouvet, C.; Lerner, D. N. A Review of the Attenuation of Trichloroethylene in Soils and Aquifers. *Q. J. Eng. Geol.* **1992**, *25* (WHO 1984), 359–370. https://doi.org/0481-2085/92.

(226) Agarwal, D.; Singh, M. Densities and Viscosities of Binary Liquid Mixtures of Trichloroethylene and Tetrachloroethylene with Some Polar and Nonpolar Solvents. *J. Chem. Eng. Data* **2004**, *49* (5), 1218–1224.

https://doi.org/10.1021/je034203p.

(227) Aggarwal, V.; Li, H.; Boyd, S. A.; Teppen, B. J. Enhanced Sorption of Trichloroethene by Smectite Clay Exchanged with Cs +. *Environ. Sci. Technol.* **2006**, *40* (3), 894–899. https://doi.org/10.1021/es0500411.

(228) Li, J.; Werth, C. J. Evaluating Competitive Sorption Mechanisms of Volatile Organic Compounds in Soils and Sediments Using Polymers and Zeolites. *Environ. Sci. Technol.* **2001**, *35* (3), 568–574. https://doi.org/10.1021/es001366e.

(229) Lin, T. F.; Little, J. C.; Nazaroff, W. W.; Nazaroff, W. W.; Little, J. C. Transport and Sorption of Volatile Organic Compounds and Water Vapor within Dry Soil Grains. *Environ. Sci. Technol.* **1994**, *28* (2), 322–330. https://doi.org/10.1021/es00051a020.

(230) Smith, J. A.; Chiou, C. T.; Kammer, J. A.; Kile, D. E. Effect of Soil Moisture on the Sorption of Trichloroethene Vapor to Vadose-Zone Soil at Picatinny Arsenal, New Jersey. *Environ. Sci. Technol.* **1990**, *24* (5), 676–683. https://doi.org/10.1021/es00075a010.

(231) Lee, C.; Cheng, S.; Chang, C.; Lee, F.; Liao, C. Simplified Approach for Rapid Estimation of Trichloroethylene Adsorption onto Soils. *Control* **2007**, *11* (July), 172–176. https://doi.org/10.1061/(ASCE)1090-025X(2007)11:3(172).

(232) Poulsen, T. G.; Yamaguchi, T.; Moldrup, P.; de Jonge, L. W.; Rolston, D. E. Predicting Volatile Organic Vapor Sorption from Soil Specific Surface Area and Texture. *J. Environ. Qual.* **2000**, *29* (5), 1642–1649. https://doi.org/10.2134/jeq2000.00472425002900050035x.

(233) Mihelcic, J. R.; Lueking, D. R.; Mitzell, R. J.; Stapleton, J. M. Bioavailability of Sorbed- and Separate-Phase Chemicals. *Biodegradation* **1993**, *4* (3), 141–153. https://doi.org/10.1007/BF00695116.

(234) Sims, J. L.; Suflita, J. M.; Russell, H. H. In-Situ Bioremediation of Contaminated Groundwater. *Gr. Water Issue* **1992**, 1–25. https://doi.org/10.1056/NEJMoa030660.

(235) Bankston, J. L.; Sola, D. L.; Komor, A. T.; Dwyer, D. F. Degradation of Trichloroethylene in Wetland Microcosms Containing Broad-Leaved Cattail and Eastern Cottonwood. *Water Res.* **2002**, *36* (6), 1539–1546. https://doi.org/10.1016/S0043-1354(01)00368-2.

(236) Lee, M. D.; Wilson, J. T.; Ward, C. H. In Situ Restoration Techniques for Aquifers Contaminated with Hazardous Wastes. *J. Hazard. Mater.* **1987**, *14* (1), 71–82. https://doi.org/10.1016/0304-3894(87)87006-1.

(237) Keely, J. F. Performance Evaluations of Pump-and-Treat Remediations. *Gr. Water Issue* **1989**, 1–12. https://doi.org/10.1056/NEJMoa030660.

(238) Johnson, R. L.; Johnson, P. C.; McWhorter, D. B.; Hinchee, R. E.; Goodman, I. An Overview of In Situ Air Sparging. *Groundw. Monit. Remediat.* **1993**, *13* (4), 127–135. https://doi.org/10.1111/j.1745-6592.1993.tb00456.x.

(239) Stroo, H. F.; Ward, C. H. *In Situ Remediation of Chlorinated Solvent Plumes*; 2010. https://doi.org/10.1007/978-1-4419-1401-9.

(240) Kavanaugh, M. C. The DNAPL Remediation Challenge: Is There a Case for Source Depletion? *USEPA Publ.* **2004**, *EPA/600/R-*, 1–129.

(241) Stroo, H. F.; Leeson, A.; Marqusee, J. A.; Johnson, P. C.; Ward, C. H.; Kavanaugh, M. C.; Sale, T. C.; Newell, C. J.; Pennell, K. D.; Lebrón, C. A.; et al. Chlorinated Ethene Source Remediation: Lessons Learned. *Environ. Sci. Technol.* **2012**, *46* (12), 6438–6447. https://doi.org/10.1021/es204714w.

(242) USEPA. *Introduction to in Situ Bioremediation of Groundwater*; 2013.

(243) Stroo, H. F.; Leeson, A.; Ward, C. H. *Bioaugmentation for Groundwater Remediation: An Overview*; Springer: New York, NY, 2013. https://doi.org/10.1007/978-1-4614-4115-1_1.

(244) Ellis, D. E.; Lutz, E. J.; Odom, J. M.; Buchanan, R. J.; Bartlett, C. L.; Lee, M. D.; Harkness, M. R.; Deweerd, K. A. Bioaugmentation for Accelerated in Situ Anaerobic Bioremediation. *Environ. Sci. Technol.* **2000**, *34* (11), 2254–2260. https://doi.org/10.1021/es990638e.

(245) Pandey, J.; Chauhan, A.; Jain, R. K. Integrative Approaches for Assessing the Ecological Sustainability of in Situ Bioremediation. *FEMS Microbiol. Rev.* **2009**, *33* (2), 324–375. https://doi.org/10.1111/j.1574-6976.2008.00133.x.

(246) Yang, Q.; Xie, Y.; Alexson, S. E. H.; Dean Nelson, B.; DePierre, J. W. Involvement of the Peroxisome Proliferator-Activated Receptor Alpha in the Immunomodulation Caused by Peroxisome Proliferators in Mice. *Biochem. Pharmacol.* **2002**, *63* (10), 1893–1900. https://doi.org/10.1016/S0006-2952(02)00923-1.

(247) Huling, S. G.; Ross, R. R.; Meeker Prestbo, K. In Situ Chemical Oxidation: Permanganate Oxidant Volume Design Considerations. *Groundw. Monit. Remediat.* **2017**, *37* (2), 78–86. https://doi.org/10.1111/gwmr.12195.

(248) Geosyntec Consultants. *Assessing the Feasibility of DNAPL Source Zone Remediation : Review of Saties*; 2004.

(249) Siegrist, R.; Petri, B.; Krembs, F. *In Situ Chemical Oxidation for Remediation of Contaminated Groundwater : Summary Proceedings of an ISCO Technology*; 2008.

(250) Mundle, K.; Reynolds, D. A.; West, M. R.; Kueper, B. H. Concentration Rebound Following in Situ Chemical Oxidation in Fractured Clay. *Ground Water* **2007**, *45* (6), 692–702. https://doi.org/10.1111/j.1745-6584.2007.00359.x.

(251) Adamson, D. T.; Newell, C. J. Support of Source Zone Bioremediation through Endogenous Biomass Decay and Electron Donor Recycling. *Bioremediat. J.* **2009**, *13* (1), 29–40. https://doi.org/10.1080/10889860802690539.

(252) McGuire, T. M.; Adamson, D. T.; Burcham, M. S.; Bedient, P. B.; Newell, C. J. Evaluation of Long-Term Performance and Sustained Treatment at Enhanced Anaerobic Bioremediation Sites. *Groundw. Monit. Remediat.* **2016**, *36* (2), 32–44. https://doi.org/10.1111/gwmr.12151.

(253) Suthersan, S.; Nelson, D.; Schnobrich, M.; Kalve, E.; Mccaughey, M. Role of Biomass Recycling in the Successful Completion of Enhanced Reductive Dechlorination (ERD) Systems. *Groundw. Monit. Remediat.* **2013**, *33* (1), 31–36.

https://doi.org/10.1111/gwmr.12001.

(254) Adamson, D. T.; McDade, J. M.; Hughes, J. B. Inoculation of a DNAPL Source Zone to Initiate Reductive Dechlorination of PCE. *Environ. Sci. Technol.* **2003**, *37* (11), 2525–2533. https://doi.org/10.1021/es020236y.

(255) Philips, J.; Hamels, F.; Smolders, E.; Springael, D. Distribution of a Dechlorinating Community in Relation to the Distance from a Trichloroethene Dense Nonaqueous Phase Liquid in a Model Aquifer. *FEMS Microbiol. Ecol.* **2012**, *81* (3), 636–647. https://doi.org/10.1111/j.1574-6941.2012.01395.x.

(256) Christ, J. A.; Ramsburg, C. A.; Abriola, L. M.; Pennell, K. D.; Löffler, F. E. Coupling Aggressive Mass Removal with Microbial Reductive Dechlorination for Remediation of DNAPL Source Zones: A Review and Assessment. *Environ. Health Perspect.* **2005**, *113* (4), 465–477. https://doi.org/10.1289/ehp.6932.

(257) Amos, B. K.; Suchomel, E. J.; Pennell, K. D.; Löffler, F. E. Spatial and Temporal Distributions of Geobacter Lovleyi and Dehalococcoides Spp. during Bioenhanced PCE-NAPL Dissolution. *Environ. Sci. Technol.* **2009**, *43* (6), 1977–1985. https://doi.org/10.1021/es8027692.

(258) Freedman, D. L.; Gossett, J. M. Biological Reductive Dechlorination of Tetrachloroethylene and Trichloroethylene to Ethylene under Methanogenic Conditions. *Appl. Environ. Microbiol.* **1989**, *55* (9), 2144–2151.

(259) Griffin, B. M.; Tiedje, J. M.; Löffler, F. E. Anaerobic Microbial Reductive Dechlorination of Tetrachloroethene to Predominately Trans-1,2-Dichloroethene. *Environ. Sci. Technol.* **2004**, *38* (16), 4300–4303. https://doi.org/10.1021/es035439g.

(260) Mohn, W. W.; Tiedje, J. M. Microbial Reductive Dehalogenation. *Microbiol. Rev.* **1992**, *56* (3), 482–507. https://doi.org/DOI 10.1111/j.1574-6941.2000.tb00693.x.

(261) Alvarez-Cohen, L.; McCarty, P. L. A Cometabolic Biotransformation Model for Halogenated Aliphatic Compounds Exhibiting Product Toxicity. *Environ. Sci. Technol.* **1991**, *25* (8), 1381–1387. https://doi.org/10.1021/es00020a003.

(262) Hanson, R. S.; Tsien, H. C.; Tsuji, K.; Brusseau, G. A.; Wackett, L. P. Biodegradation of Low-Molecular-Weight Halogenated Hydrocarbons by Methanotrophic Bacteria. *FEMS Microbiol. Lett.* **1990**, *87* (3–4), 273–278. https://doi.org/10.1016/0378-1097(90)90466-4.

(263) Phelps, T. J.; Niedzielski, J. J.; Schram, R. M.; Herbes, S. E.; White, D. C. Biodegradation of Trichloroethylene in Continuous-Recycle Expanded-Bed Bioreactors. *Appl. Environ. Microbiol.* **1990**, *56* (6), 1702–1709.

(264) Enzien, M. V.; Picardal, F.; Hazen, T. C.; Arnold, R. G.; Fliermans, C. B. Reductive Dechlorination of Trichloroethylene and Tetrachloroethylene under Aerobic Conditions in a Sediment Column. *Appl. Environ. Microbiol.* **1994**, *60* (6), 2200–2204.

(265) Hopkins, G. D.; McCarty, P. L. Field Evaluation of in Situ Aerobic Cometabolism of Trichloroethylene and Three Dichloroethylene Isomers Using Phenol and Toluene as the Primary Substrates. *Environ. Sci. Technol.* **1995**, *29* (6), 1628–1637. https://doi.org/10.1021/es00006a029.

(266) Hartmans, S.; De Bont, J. A. Aerobic Vinyl Chloride Metabolism in Mycobacterium Aurum L1. *Appl. Environ. Microbiol.* **1992**, *58* (4), 1220–1226.

(267) Bradley, P. M.; Chapelle, F. H. Effect of Contaminant Concentration on Aerobic Microbial Mineralization of DCE and VC in Stream-Bed Sediments. *Environ. Sci. Technol.* **1998**, *32* (5), 553–557. https://doi.org/10.1021/es970498d.

(268) Bradley, P. M.; Chapelle, F. H. Kinetics of DCE and VC Mineralization under Methanogenic and Fe(III)- Reducing Conditions. *Environ. Sci. Technol.* **1997**, *31* (9), 2692–2696. https://doi.org/10.1021/es970110e.

(269) Moore, A. T.; Vira, A.; Fogel, S. Biodegradation of Trans-1,2-Dichloroethylene by Methane-Utilizing Bacteria in an Aquifer Simulator. *Environ. Sci. Technol.* **1989**, *23* (4), 403–406. https://doi.org/10.1021/es00181a003.

(270) Mattes, T. E.; Alexander, A. K.; Coleman, N. V. Aerobic Biodegradation of the Chloroethenes: Pathways, Enzymes, Ecology, and Evolution. **2010**, *1*. https://doi.org/10.1111/j.1574-6976.2010.00210.x.

(271) Jin, Y. O. H.; Mattes, T. E. Adaptation of Aerobic , Mycobacterium Strains to Vinyl Chloride as a Growth Substrate. **2008**, *42* (13), 4784–4789.

(272) Nocardioides, A.; Coleman, N. V; Wilson, N. L.; Barry, K.; Brettin, T. S.; Bruce, D. C.; Copeland, A.; Dalin, E.; Detter, J. C.; Glavina, T.; et al. Genome Sequence of the Ethene- and Vinyl Chloride-Oxidizing. **2011**, *193* (13), 3399–3400. https://doi.org/10.1128/JB.05109-11.

(273) Coleman, N. V; Mattes, T. E.; Gossett, J. M. Phylogenetic and Kinetic Diversity of Aerobic Vinyl Chloride-Assimilating Bacteria from Contaminated Sites. **2002**, *68* (12), 6162–6171. https://doi.org/10.1128/AEM.68.12.6162.

(274) Coleman, N. V; Mattes, T. E.; Gossett, J. M. Biodegradation of Cis - Dichloroethene as the Sole Carbon Source by a -Proteobacterium. **2002**, *68* (6), 2726–2730. https://doi.org/10.1128/AEM.68.6.2726.

(275) De Bruin, W. P.; Kotterman, M. J. J.; Posthumus, M. A.; Schraa, G.; Zehnder, A. J. B. Complete Biological Reductive Transformation of Tetrachloroethene to Ethane. *Appl. Environ. Microbiol.* **1992**, *58* (6), 1996–2000.

(276) Maymó-Gatell, X.; Anguish, T.; Zinder, S. H. Reductive Dechlorination of Chlorinated Ethenes and 1, 2-Dichloroethane by “Dehalococcoides Ethenogenes” 195. *Appl. Environ. Microbiol.* **1999**, *65* (7), 3108–3113.

(277) Adrian, L.; Hansen, S. K.; Fung, J. M.; Görisch, H.; Zinder, S. H. Growth of Dehalococcoides Strains with Chlorophenols as Electron Acceptors. *Environ. Sci. Technol.* **2007**, *41* (7), 2318–2323. https://doi.org/10.1021/es062076m.

(278) Holliger, C.; Schraa, G.; Stams, A. J. M.; Zehnder, A. J. B. A Highly Purified Enrichment Culture Couples the Reductive Dechlorination of Tetrachloroethene to Growth. *Appl. Environ. Microbiol.* **1993**, *59* (9), 2991–2997.

(279) Mccarty, P. L. Biotic and Abiotic Transformations of Chlorinated Solvents in Ground Water. *Proc. Symp. Nat. Attenuation Chlorinated Org. Gr. Water* **1997**.

(280) Byl, T. D.; Williams, S. D. Biodegradation of Chlorinated Ethenes at a Karst Site in Middle Tennessee. *Water-Resources Investig. Rep. 99-4285* **2000**.

(281) Noell, A. L. Estimation of Sequential Degradation Rate Coefficients for Chlorinated Ethenes. *Pract. Period. hazardous, toxic, Radioact. waste Manag.* **2009**, *13* (1), 35–44. https://doi.org/10.1061/(ASCE)1090-025X(2009)13:1(35).

(282) Franke, S.; Lihl, C.; Renpenning, J.; Elsner, M.; Nijenhuis, I. Triple-Element Compound-Specific Stable Isotope Analysis of 1,2-Dichloroethane for Characterization of the Underlying Dehalogenation Reaction in Two Dehalococcoides Mccartyi Strains. *FEMS Microbiol. Ecol.* **2017**, *93* (12), 1–9. https://doi.org/10.1093/femsec/fix137.

(283) Neumann, A.; Scholz-Muramatsu, H.; Diekert, G. Tetrachloroethene Metabolism of Dehalospirillum Multivorans. *Arch. Microbiol.* **1994**, *162* (4), 295–301. https://doi.org/10.1007/BF00301854.

(284) Neumann, A.; Siebert, A.; Trescher, T.; Reinhardt, S.; Wohlfarth, G.; Diekert, G. Tetrachloroethene Reductive Dehalogenase of Dehalospirillum Multivorans: Substrate Specificity of the Native Enzyme and Its Corrinoid Cofactor. *Arch. Microbiol.* **2002**, *177* (5), 420–426. https://doi.org/10.1007/s00203-002-0409-3.

(285) Sharma, P. K.; McCarty, P. L. Isolation and Characterization of a Facultatively Aerobic Bacterium That Reductively Dehalogenates Tetrachloroethene to Cis-1,2-Dichloroethene. *Appl. Environ. Microbiol.* **1996**, *62* (3), 761–765.

(286) Gerritse, J.; Renard, V.; Gomes, T. M. P.; Lawson, P. A.; Collins, M. D.; Gottschal, J. C. Desulfitobacterium Sp. Strain PCE1, an Anaerobic Bacterium That Can Grow by Reductive Dechlorination of Tetrachloroethene or Ortho - Chlorinated Phenols. *Arch. Microbiol.* **1996**, *165* (2), 132–140. https://doi.org/10.1007/s002030050308.

(287) Holliger, C.; Wohlfarth, G.; Y, G. D. Reductive Dechlorination in the Energy Metabolism of Anaerobic Bacteria. *FEMS Microbiol. Rev.* **1999**, *22* (June), 383–398. https://doi.org/10.1016/S0168-6445(98)00030-8.

(288) Luijten, M. L. G. C.; de Weert, J.; Smidt, H.; Boschker, H. T. S.; de Vos, W. M.; Schraa, G.; Stams, A. J. M. Description of Sulfurospirillum Halorespirans Sp. Nov., an Anaerobic, Tetrachloroethene-Respiring Bacterium, and Transfer of Dehalospirillum Multivorans to the Genus Sulfurospirillum a Sulfurospirillum Multivorans Comb. Nov. *Int. J. Syst. Evol. Microbiol.* **2003**, *53* (3), 787–793. https://doi.org/10.1099/ijs.0.02417-0.

(289) Sung, Y.; Fletcher, K. E.; Ritalahti, K. M.; Apkarian, R. P.; Ramos-Hernandez, N.; Sanford, R. a; Mesbah, N. M.; Loffler, F. E. Geobacter Lovleyi Sp. Nov. Strain SZ, a Novel Metal-Reducing and Tetrachloroethene-Dechlorinating Bacterium. *Appl. Environ. Microbiol.* **2006**, *72* (4), 2775–2782. https://doi.org/10.1128/AEM.72.4.2775-2782.2006.

(290) Patil, S. S.; Adetutu, E. M.; Ball, A. S. Microbiology of Chloroethene Degradation in Groundwater. *Microbiol. Aust.* **2014**, 211–214.

(291) Maymo-Gatell, X. Isolation of a Bacterium That Reductively Dechlorinates Tetrachloroethene to Ethene. *Science (80-.).* **1997**, *276* (5318), 1568–1571. https://doi.org/10.1126/science.276.5318.1568.

(292) Loffler, F. E.; Yan, J.; Ritalahti, K. M.; Adrian, L.; Edwards, E. A.; Konstantinidis, K. T.; Muller, J. A.; Fullerton, H.; Zinder, S. H.; Spormann, A. M.

Dehalococcoides Mccartyi Gen. Nov., Sp. Nov., Obligately Organohalide-Respiring Anaerobic Bacteria Relevant to Halogen Cycling and Bioremediation, Belong to a Novel Bacterial Class, Dehalococcoidia Classis Nov., Order Dehalococcoidales Ord. Nov. and Famil. *Int. J. Syst. Evol. Microbiol.* **2013**, *63* (Pt 2), 625–635. https://doi.org/10.1099/ijs.0.034926-0.

(293) Sung, Y.; Ritalahti, K. M.; Apkarian, R. P.; Löffler, F. E.; Lo, F. E. Quantitative PCR Confirms Purity of Strain GT , a Novel Dehalococcoides Isolate Quantitative PCR Confirms Purity of Strain GT , a Novel Trichloroethene-to-Ethene-Respiring Dehalococcoides Isolate. *Society* **2006**, *72* (3), 1980. https://doi.org/10.1128/AEM.72.3.1980.

(294) Cupples, A. M.; Spormann, A. M.; McCarty, P. L. Growth of a Dehalococcoides-like Microorganism on Vinyl Chloride and Cis-Dichloroethene as Electron Acceptors as Determined by Competitive PCR. *Appl. Environ. Microbiol.* **2003**, *69* (2), 953–959. https://doi.org/10.1128/AEM.69.2.953.

(295) Yan, J.; Yang, Y.; Li, X.; Löffler, F. E. Complete Genome Sequence of Dehalococcoides Mccartyi Strain FL2, a Trichloroethene-Respiring Anaerobe Isolated from Pristine Freshwater Sediment. *Microbiol. Resour. Announc.* **2019**, *8* (33), 10–11. https://doi.org/10.1128/MRA.00558-19.

(296) Cheng, D.; He, J. Isolation and Characterization of "Dehalococcoides" Sp. Strain MB, Which Dechlorinates Tetrachloroethene to Trans-1,2-Dichloroethene. *Appl. Environ. Microbiol.* **2009**, *75* (18), 5910–5918. https://doi.org/10.1128/AEM.00767-09.

(297) Krajmalnik-Brown, R.; Holscher, T.; Thomson, I. N.; Saunders, F. M.; Ritalahti, K. M.; Loffler, F. E. Genetic Identification of a Putative Vinyl Chloride Reductase in Strain BAV1. *Appl. Environ. Microbiol.* **2004**, *70* (10), 6347–6351. https://doi.org/10.1128/AEM.70.10.6347.

(298) Hölscher, T.; Krajmalnik-brown, R.; Ritalahti, K. M.; von Wintzingerode, F.; Görisch, H.; Löffler, F. E.; Adrian, L. Multiple Nonidentical Genes Are Common in Dehalococcoides. *Appl. Environ. Microbiol.* **2004**, *70* (9), 5290–5297. https://doi.org/10.1128/AEM.70.9.5290.

(299) Magnuson, J. K.; Romine, M. F.; Burris, D. R.; Kingsley, M. T. Trichloroethene Reductive Dehalogenase from Dehalococcoides Ethenogenes: Sequence of TceA and Substrate Range Characterization. *Appl. Environ. Microbiol.* **2000**, *66* (12), 5141–5147. https://doi.org/10.1128/AEM.66.12.5141-5147.2000.

(300) Müller, J. a.; Rosner, B. M.; Von Abendroth, G.; Meshulam-Simon, G.; McCarty, P. L.; Spormann, A. M. Molecular Identification of the Catabolic Vinyl Chloride Reductase from Dehalococcoides Sp. Strain VS and Its Environmental Distribution. *Appl. Environ. Microbiol.* **2004**, *70* (8), 4880–4888. https://doi.org/10.1128/AEM.70.8.4880-4888.2004.

(301) Zhao, S.; Ding, C.; He, J. Genomic Characterization of Dehalococcoides Mccartyi Strain 11a5 Reveals a Circular Extrachromosomal Genetic Element and a New Tetrachloroethene Reductive Dehalogenase Gene. *FEMS Microbiol. Ecol.* **2017**, *93* (4), 1–11. https://doi.org/10.1093/femsec/fiw235.

(302) Zhao, S.; He, J. Reductive Dechlorination of High Concentrations of

Chloroethenes by a Dehalococcoides Mccartyi Strain 11G. *FEMS Microbiol. Ecol.* **2019**, *95* (1), 1–9. https://doi.org/10.1093/femsec/fiy209.

(303) Molenda, O.; Tang, S.; Edwards, E. A. Complete Genome Sequence of *Dehalococcoides Mccartyi* Strain WBC-2, Capable of Anaerobic Reductive Dechlorination of Vinyl Chloride. *Genome Announc.* **2016**, *4* (6), e01375-16. https://doi.org/10.1128/genomeA.01375-16.

(304) Hao, F.; Guo, W.; Wang, A.; Leng, Y.; Li, H. Intensification of Sonochemical Degradation of Ammonium Perfluorooctanoate by Persulfate Oxidant. *Ultrason. Sonochem.* **2014**, *21* (2), 554–558. https://doi.org/10.1016/j.ultsonch.2013.09.016.

(305) Pöritz, M.; Schiffmann, C. L.; Hause, G.; Heinemann, U.; Seifert, J.; Jehmlich, N.; von Bergen, M.; Nijenhuis, I.; Lechner, U. Dehalococcoides Mccartyi Strain DCMB5 Respires a Broad Spectrum of Chlorinated Aromatic Compounds. *Appl. Environ. Microbiol.* **2015**, *81* (2), 587–596. https://doi.org/10.1128/AEM.02597-14.

(306) Wang, S.; Chng, K. R.; Chen, C.; Bedard, D. L.; He, J. Genomic Characterization of Dehalococcoides Mccartyi Strain JNA That Reductively Dechlorinates Tetrachloroethene and Polychlorinated Biphenyls. *Environ. Sci. Technol.* **2015**, *49* (24), 14319–14325. https://doi.org/10.1021/acs.est.5b01979.

(307) Higgins, S. A.; Padilla-Crespo, E.; Löffler, F. E. Draft Genome Sequences of the 1,2-Dichloropropane-Respiring Dehalococcoides Mccartyi Strains RC and KS. *Microbiol. Resour. Announc.* **2018**, *7* (10), 1–2. https://doi.org/10.1128/MRA.01081-18.

(308) Molenda, O.; Tang, S.; Lomheim, L.; Gautam, V. K.; Lemak, S.; Yakunin, A. F.; Maxwell, K. L.; Edwards, E. A. Extrachromosomal Circular Elements Targeted by CRISPR-Cas in Dehalococcoides Mccartyi Are Linked to Mobilization of Reductive Dehalogenase Genes. *ISME J.* **2019**, *13* (1), 24–38. https://doi.org/10.1038/s41396-018-0254-2.

(309) Scheutz, C.; Durant, N. D.; Dennis, P.; Hansen, M. H.; J??rgensen, T.; Jakobsen, R.; Cox, E. E.; Bjerg, P. L. Concurrent Ethene Generation and Growth of Dehalococcoides Containing Vinyl Chloride Reductive Dehalogenase Genes during an Enhanced Reductive Dechlorination Field Demonstration. *Environ. Sci. Technol.* **2008**, *42* (24), 9302–9309. https://doi.org/10.1021/es800764t.

(310) Kanitkar, Y. H.; Stedtfeld, R. D.; Hatzinger, P. B.; Hashsham, S. A.; Cupples, A. M. Development and Application of a Rapid, User-Friendly, and Inexpensive Method to Detect Dehalococcoides Sp. Reductive Dehalogenase Genes from Groundwater. *Appl. Microbiol. Biotechnol.* **2017**, *101* (11), 4827–4835. https://doi.org/10.1007/s00253-017-8203-y.

(311) Yang, Y.; Mccarty, P. L. Biologically Enhanced Dissolution of Tetrachloroethene DNAPL. *Environ. Sci. Technol.* **2000**, *34* (14), 2979–2984. https://doi.org/10.1021/es991410u.

(312) He, J.; Holmes, V. F.; Lee, P. K. H.; Alvarez-Cohen, L. Influence of Vitamin B12 and Cocultures on the Growth of Dehalococcoides Isolates in Defined Medium. *Appl. Environ. Microbiol.* **2007**, *73* (9), 2847–2853. https://doi.org/10.1128/AEM.02574-06.

(313) Yan, J.; Şimşir, B.; Farmer, A. T.; Bi, M.; Yang, Y.; Campagna, S. R.; Löffler, F. E. The Corrinoid Cofactor of Reductive Dehalogenases Affects Dechlorination Rates and Extents in Organohalide-Respiring Dehalococcoides Mccartyi. *ISME J.* **2016**, *10* (5), 1092–1101. https://doi.org/10.1038/ismej.2015.197.

(314) Duhamel, M.; Wehr, S. D.; Yu, L.; Rizvi, H.; Seepersad, D.; Dworatzek, S.; Cox, E. E.; Edwards, E. a. Comparison of Anaerobic Dechlorinating Enrichment Cultures Maintained on Tetrachloroethene, Trichloroethene, Cis-Dichloroethene and Vinyl Chloride. *Water Res.* **2002**, *36* (17), 4193–4202. https://doi.org/10.1016/S0043-1354(02)00151-3.

(315) Stupperich, E.; Eisinger, H. J.; Kräutler, B. Diversity of Corrinoids in Acetogenic Bacteria. P-Cresolylcobamide from Sporomusa Ovata, 5-Methoxy-6-Methylbenzimidazolylcobamide from Clostridium Formicoaceticum and Vitamin B12 from Acetobacterium Woodii. *Eur. J. Biochem.* **1988**, *172* (2), 459–464. https://doi.org/10.1111/j.1432-1033.1988.tb13910.x.

(316) Yan, J.; Ritalahti, K. M.; Wagner, D. D.; Löffler, F. E. Unexpected Specificity of Interspecies Cobamide Transfer from Geobacter Spp. to Organohalide-Respiring Dehalococcoides Mccartyi Strains. *Appl. Environ. Microbiol.* **2012**, *78* (18), 6630–6636. https://doi.org/10.1128/AEM.01535-12.

(317) Duhamel, M.; Edwards, E. A. Microbial Composition of Chlorinated Ethene-Degrading Cultures Dominated by Dehalococcoides. *FEMS Microbiol. Ecol.* **2006**, *58* (3), 538–549. https://doi.org/10.1111/j.1574-6941.2006.00191.x.

(318) Men, Y.; Feil, H.; Verberkmoes, N. C.; Shah, M. B.; Johnson, D. R.; Lee, P. K. H.; West, K. A.; Zinder, S. H.; Andersen, G. L.; Alvarez-Cohen, L. Sustainable Syntrophic Growth of Dehalococcoides Ethenogenes Strain 195 with Desulfovibrio Vulgaris Hildenborough and Methanobacterium Congolense: Global Transcriptomic and Proteomic Analyses. *ISME J.* **2012**, *6* (2), 410–421. https://doi.org/10.1038/ismej.2011.111.

(319) Ding, C.; Alvarez-Cohen, L.; He, J. Growth of Dehalococcoides Mccartyi Species in an Autotrophic Consortium Producing Limited Acetate. *Biodegradation* **2018**, *29* (5), 487–498. https://doi.org/10.1007/s10532-018-9846-9.

(320) Freeborn, R. A.; West, K. A.; Bhupathiraju, V. K.; Chauhan, S.; Rahm, B. G.; Richardson, R. E.; Alvarez-Cohen, L. Phylogenetic Analysis of TCE-Dechlorinating Consortia Enriched on a Variety of Electron Donors. *Environ. Sci. Technol.* **2005**, *39* (21), 8358–8368. https://doi.org/10.1021/es048003p.

(321) Richardson, R. E.; Bhupathiraju, V. K.; Song, D. L.; Goulet, T. A.; Alvarez-Cohen, L. Phylogenetic Characterization of Microbial Communities That Reductively Dechlorinate TCE Based upon a Combination of Molecular Techniques. *Environ. Sci. Technol.* **2002**, *36* (12), 2652–2662. https://doi.org/10.1021/es0157797.

(322) Ritalahti, K. M.; Loffler, F. E. Populations Implicated in Anaerobic Reductive Dechlorination of 1 , 2-Dichloropropane in Highly Enriched Bacterial Communities †. *Appl. Environ. Microbiol.* **2004**, *70* (7), 4088–4095. https://doi.org/10.1128/AEM.70.7.4088.

(323) Guimaraes, D. H.; Weber, A.; Klaiber, I.; Vogler, B.; Renz, P. Guanylcobamide

and Hypoxanthylcobamide-Corrinoids Formed by Desulfovibrio Vulgaris. *Arch. Microbiol.* **1994**, *162* (4), 272–276. https://doi.org/10.1007/BF00301850.

(324) Men, Y.; Lee, P. K. H.; Harding, K. C.; Alvarez-Cohen, L. Characterization of Four TCE-Dechlorinating Microbial Enrichments Grown with Different Cobalamin Stress and Methanogenic Conditions. *Appl. Microbiol. Biotechnol.* **2013**, *97* (14), 6439–6450. https://doi.org/10.1007/s00253-013-4896-8.

(325) Semprini, L.; Hopkins, G. D.; Roberts, P. V; McCarty, P. L. Pilot Scale Field Studies of Insitu Bioremediation of Chlorinated Solvents. *J. Hazard. Mater.* **1992**, *32* (2–3), 145–162.

(326) Harkness, M. R.; Bracco, A. A.; Brennan, M. J.; Deweerd, K. A.; Spivack, J. L. Use of Bioaugmentation to Stimulate Complete Reductive Dechlorination of Trichloroethene in Dover Soil Columns. *Environ. Sci. Technol.* **1999**, *33* (7), 1100–1109. https://doi.org/10.1021/es9807690.

(327) Pfiffner, S. M.; Palumbo, A. V.; Sayles, G. D.; Gannon, D. Microbial Population and Degradation Activity Changes Monitored During a Chlorinated Solvent Biovent Demonstration. *Ground Water Monit. Remediat.* **2010**, *24* (3), 102–110. https://doi.org/10.1111/j.1745-6592.2004.tb01297.x.

(328) Lowe, M.; Madsen, E. L.; Schindler, K.; Smith, C.; Emrich, S.; Robb, F.; Halden, R. U. Geochemistry and Microbial Diversity of a Trichloroethene-Contaminated Superfund Site Undergoing Intrinsic in Situ Reductive Dechlorination. *FEMS Microbiol. Ecol.* **2002**, *40* (2), 123–134. https://doi.org/10.1016/S0168-6496(02)00229-5.

(329) Beeman, R. E.; Bleckmann, C. A. Sequential Anaerobic-Aerobic Treatment of an Aquifer Contaminated by Halogenated Organics: Field Results. *J. Contam. Hydrol.* **2002**, *57* (3–4), 147–159. https://doi.org/10.1111/j.1745-6592.2004.tb01297.x.

(330) Schaefer, C. E.; Lavorgna, G. M.; White, E. B.; Annable, M. D. Bioaugmentation in a Well-Characterized Fractured Rock DNAPL Source Area. *Groundw. Monit. Remediat.* **2017**, *37* (2), 35–42. https://doi.org/10.1111/gwmr.12208.

(331) Scheutz, C.; Broholm, M. M.; Durant, N. D.; Weeth, E. B.; Jorgensen, T. H.; Dennis, P.; Jacobsen, C. S.; Cox, E. E.; Chambon, J. C.; Bjerg, P. L. Field Evaluation of Biological Enhanced Reductive Dechlorination of Chloroethenes in Clayey Till. *Environ. Sci. Technol.* **2010**, *44* (13), 5134–5141. https://doi.org/10.1021/es1003044.

(332) Damgaard, I.; Bjerg, P. L.; Jacobsen, C. S.; Tsitonaki, A.; Kerrn-Jespersen, H.; Broholm, M. M. Performance of Full-Scale Enhanced Reductive Dechlorination in Clay Till. *Ground Water Monit. Remediat.* **2013**, *33* (1), 48–61. https://doi.org/10.1111/j1745-6592.2012.01405.x.

(333) Imfeld, G.; Nijenhuis, I.; Nikolausz, M.; Zeiger, S.; Paschke, H.; Drangmeister, J.; Grossmann, J.; Richnow, H. H.; Weber, S. Assessment of in Situ Degradation of Chlorinated Ethenes and Bacterial Community Structure in a Complex Contaminated Groundwater System. *Water Res.* **2008**, *42* (4–5), 871–882. https://doi.org/10.1016/j.watres.2007.08.035.

(334) Borden, R. C.; Beckwith, W. J.; Lieberman, M. T.; Akladiss, N.; Hill, S. R.

Enhanced Anaerobic Bioremediation of a TCE Source at the Tarheel Army Missile Plant Using EOS. *Remediation* **2007**, *17* (3), 5–19. https://doi.org/10.1002/rem.20130.

(335) Hood, E. D.; Major, D. W.; Quinn, J. W.; Yoon, W. S.; Gavaskar, A.; Edwards, E. A. Demonstration of Enhanced Bioremediation in a TCE Source Area at Launch Complex 34, Cape Canaveral Air Force Station. *Gr. Water Monit. Remediat.* **2008**, *28* (2), 98–107. https://doi.org/10.1111/j.1745-6592.2008.00197.x.

(336) Amos, B. K.; Christ, J. A.; Abriola, L. M.; Pennell, K. D.; Löffler, F. E. Experimental Evaluation and Mathematical Modeling of Microbially Enhanced Tetrachloroethene (PCE) Dissolution. *Environ. Sci. Technol.* **2007**, *41* (3), 963–970. https://doi.org/10.1021/es061438n.

(337) Sleep, B. E.; Seepersad, D. J.; Mo, K.; Heidorn, C. M.; Hrapovic, L.; Morrill, P. L.; McMaster, M. L.; Hood, E. D.; Lebron, C.; Lollar, B. S.; et al. Biological Enhancement of Tetrachloroethene Dissolution and Associated Microbial Community Changes. *Environ. Sci. Technol.* **2006**, *40* (11), 3623–3633. https://doi.org/10.1021/es051493g.

(338) Carr, C. S.; Garg, S.; Hughes, J. B. Effect of Dechlorinating Bacteria on the Longevity and Composition of PCE-Containing Nonaqueous Phase Liquids under Equilibrium Dissolution Conditions. *Environ. Sci. Technol.* **2000**, *34* (6), 1088–1094. https://doi.org/10.1021/es990989t.

(339) Lima, G. da P.; Sleep, B. E. The Spatial Distribution of Eubacteria and Archaea in Sand-Clay Columns Degrading Carbon Tetrachloride and Methanol. *J. Contam. Hydrol.* **2007**, *94* (1–2), 34–48. https://doi.org/10.1016/j.jconhyd.2007.05.001.

(340) Chambon, J. C.; Broholm, M. M.; Binning, P. J.; Bjerg, P. L. Modeling Multi-Component Transport and Enhanced Anaerobic Dechlorination Processes in a Single Fracture-Clay Matrix System. *J. Contam. Hydrol.* **2010**, *112* (1–4), 77–90. https://doi.org/10.1016/j.jconhyd.2009.10.008.

(341) Aulenta, F.; Di Tomassi, C.; Cupo, C.; Papini, M. P.; Majone, M. Influence of Hydrogen on the Reductive Dechloination of Tetrachloroethene (PCE) to Ethene in a Methanogenic Biofilm Reactor: Role of Mass Transport Phenomena. *J. Chem. Technol. Biotechnol.* **2006**, *81*, 1520–1529. https://doi.org/10.1002/jctb.1562.

(342) Chung, J.; Rittmann, B. E. Simultaneous Bio-Reduction of Trichloroethene, Trichloroethane, and Chloroform Using a Hydrogen-Based Membrane Biofilm Reactor. *Water Sci. Technol.* **2008**, *58* (3), 495–501. https://doi.org/10.2166/wst.2008.432.

(343) Karataş, S.; Hasar, H.; Taşkan, E.; Özkaya, B.; Şahinkaya, E. Bio-Reduction of Tetrachloroethen Using a H2-Based Membrane Biofilm Reactor and Community Fingerprinting. *Water Res.* **2014**, *58*, 21–28. https://doi.org/10.1016/j.watres.2014.03.053.

(344) Mirza, B. S.; Sorensen, D. L.; Dupont, R. R.; McLean, J. E. Dehalococcoides Abundance and Alternate Electron Acceptor Effects on Large, Flow-through Trichloroethene Dechlorinating Columns. *Appl. Microbiol. Biotechnol.* **2016**, *100* (5), 2367–2379. https://doi.org/10.1007/s00253-015-7112-1.

(345) Perez De Mora, A.; Lacourt, A.; McMaster, M. L.; Liang, X.; Dworatzek, S. M.; Edwards, E. A. Chlorinated Electron Acceptor Abundance Drives Selection of Dehalococcoides Mccartyi (D. Mccartyi) Strains in Dechlorinating Enrichment Cultures and Groundwater Environments. *Front. Microbiol.* **2018**, *9* (May), 812. https://doi.org/10.3389/FMICB.2018.00812.

(346) Perez-de-Mora, A.; Lacourt, A.; McMaster, M. L.; Liang, X.; Dworatzek, S. M.; Edwards, E. A. Chlorinated Electron Acceptor Availability Selects for Specific Dehalococooides Populations in Dechlorinating Inrichment Cultures and in Groundwater. **2017**. https://doi.org/10.1101/175182.

(347) Johnson, D. R.; Lee, P. K. H.; Holmes, V. F.; Fortin, A. C.; Alvarez-cohen, L. Transcriptional Expression of The. *Microbiology* **2005**, *71* (11), 7145–7151. https://doi.org/10.1128/AEM.71.11.7145.

(348) Mirza, B. S.; Sorensen, D. L.; McGlinn, D. J.; Dupont, R. R.; McLean, J. E. Dehalococcoides and General Bacterial Ecology of Differentially Trichloroethene Dechlorinating Flow-through Columns. *Appl. Microbiol. Biotechnol.* **2017**, *101* (11), 4799–4813. https://doi.org/10.1007/s00253-017-8180-1.

(349) Mayer-Blackwell, K.; Azizian, M. F.; Green, J. K.; Spormann, A. M.; Semprini, L. Survival of Vinyl Chloride Respiring Dehalococcoides Mccartyi under Long-Term Electron Donor Limitation. *Environ. Sci. Technol.* **2017**, *51* (3), 1635–1642. https://doi.org/10.1021/acs.est.6b05050.

(350) Heavner, G.; Mansfeldt, C.; Debs, G.; Hellerstedt, S.; Rowe, A.; Richardson, R. Biomarkers' Responses to Reductive Dechlorination Rates and Oxygen Stress in Bioaugmentation Culture KB-1TM. *Microorganisms* **2018**, *6* (1), 13. https://doi.org/10.3390/microorganisms6010013.

(351) Fletcher, K. E.; Costanza, J.; Cruz-Garcia, C.; Ramaswamy, N. S.; Pennell, K. D.; Löffler, F. E. Effects of Elevated Temperature on Dehalococcoides Dechlorination Performance and DNA and RNA Biomarker Abundance. *Environ. Sci. Technol.* **2011**, *45* (2), 712–718. https://doi.org/10.1021/es1023477.

(352) Kaya, D.; Kjellerup, B. V.; Chourey, K.; Hettich, R. L.; Taggart, D. M.; Löffler, F. E. Impact of Fixed Nitrogen Availability on Dehalococcoides Mccartyi Reductive Dechlorination Activity. *Environ. Sci. Technol.* **2019**, *53* (24), 14548–14558. https://doi.org/10.1021/acs.est.9b04463.

(353) Robinson, C.; Barry, D. A.; McCarty, P. L.; Gerhard, J. I.; Kouznetsova, I. PH Control for Enhanced Reductive Bioremediation of Chlorinated Solvent Source Zones. *Sci. Total Environ.* **2009**, *407* (16), 4560–4573. https://doi.org/10.1016/j.scitotenv.2009.03.029.

(354) Puentes Jácome, L. A.; Wang, P.-H.; Molenda, O.; Li, Y. X. (Jine-J.; Islam, M. A.; Edwards, E. A. Sustained Dechlorination of Vinyl Chloride to Ethene in Dehalococcoides -Enriched Cultures Grown without Addition of Exogenous Vitamins and at Low PH. *Environ. Sci. Technol.* **2019**, *53* (19), 11364–11374. https://doi.org/10.1021/acs.est.9b02339.

(355) Wei, K. Substrates and Substrate Interactions in Anaerobic Dechlorinating Cultures, University of Toronto, 2012.

(356) Im, J.; Mack, E. E.; Seger, E. S.; Löffler, F. E. Biotic and Abiotic Dehalogenation

of 1,1,2-Trichloro-1,2,2-Trifluoroethane (CFC-113): Implications for Bacterial Detoxification of Chlorinated Ethenes. *Environ. Sci. Technol.* **2019**, *53* (20), 11941–11948. https://doi.org/10.1021/acs.est.9b04399.

(357) Chan, W. W. M.; Grostern, A.; Löffler, F. E.; Edwards, E. A. Quantifying the Effects of 1,1,1-Trichloroethane and 1,1-Dichloroethane on Chlorinated Ethene Reductive Dehalogenases. *Environ. Sci. Technol.* **2011**, *45* (22), 9693–9702. https://doi.org/10.1021/es201260n.

(358) Wen, L. L.; Chen, J. X.; Fang, J. Y.; Li, A.; Zhao, H. P. Effects of 1,1,1-Trichloroethane and Triclocarban on Reductive Dechlorination of Trichloroethene in a TCE-Reducing Culture. *Front. Microbiol.* **2017**, *8* (AUG), 1–10. https://doi.org/10.3389/fmicb.2017.01439.

(359) Cápiro, N. L.; Wang, Y.; Hatt, J. K.; Lebron, C.; Pennell, K. D.; Löffler, F. E. Distribution of Organohalide-Respiring Bacteria between Solid and Aqueous Phases. *Environ. Sci. Technol.* **2014**, *48* (18), 10878–10887. https://doi.org/10.1021/es501320h.

(360) Singh, R.; Paul, D.; Jain, R. K. Biofilms: Implications in Bioremediation. *Trends Microbiol.* **2006**, *14* (9), 389–397. https://doi.org/10.1016/j.tim.2006.07.001.

(361) Van Der Zaan, B.; Hannes, F.; Hoekstra, N.; Rijnaarts, H.; De Vos, W. M.; Smidt, H.; Gerritse, J. Correlation of Dehalococcoides 16S RRNA and Chloroethene-Reductive Dehalogenase Genes with Geochemical Conditions in Chloroethene-Contaminated Groundwater. *Appl. Environ. Microbiol.* **2010**, *76* (3), 843–850. https://doi.org/10.1128/AEM.01482-09.

(362) Yoshikawa, M.; Takeuchi, M.; Zhang, M. Distribution of Dehalococcoides 16S RRNA and Dehalogenase Genes in Contaminated Sites. *Environ. Nat. Resour. Res.* **2017**, *7* (2), 37. https://doi.org/10.5539/enrr.v7n2p37.

(363) Luo, J.; Kitanidis, P. K. Fluid Residence Times within a Recirculation Zone Created by an Extraction-Injection Well Pair. *J. Hydrol.* **2004**, *295* (1–4), 149–162. https://doi.org/10.1016/j.jhydrol.2004.03.006.

(364) Elder, C. R.; Daly, M.; Zeeb, P. J.; Poulos, S. J.; Drobinski, J.; Wanty, D. Design and Construction of a Ground Water Recirculation System in Hydraulically Dynamic Fractured Bedrock. *Proc. Third Int. Conf. Remediat. Chlorinated Recalcitrant Compd.* **2002**, No. May, 2457–2466.

(365) Benner, M. L.; Mohtar, R. H.; Lee, L. S. Factors Affecting Air Sparging Remediation Systems Using Field Data and Numerical Simulations. *J. Hazard. Mater.* **2002**, *95* (3), 305–329. https://doi.org/10.1016/S0304-3894(02)00144-9.

(366) Erto, A.; Bortone, I.; Di Nardo, A.; Di Natale, M.; Musmarra, D. Permeable Adsorptive Barrier (PAB) for the Remediation Ofgroundwater Simultaneously Contaminated by Some Chlorinated Organic Compounds. *J. Environ. Manage.* **2014**, *140*, 111–119. https://doi.org/10.1016/j.jenvman.2014.03.012.

(367) Bortone, I.; Di Nardo, A.; Di Natale, M.; Erto, A.; Musmarra, D.; Santonastaso, G. F. Remediation of an Aquifer Polluted with Dissolved Tetrachloroethylene by an Array of Wells Filled with Activated Carbon. *J. Hazard. Mater.* **2013**, *260*, 914–920. https://doi.org/10.1016/j.jhazmat.2013.06.050.

(368) Duba, A. G.; Jackson, K. J.; Jovanovich, M. C.; Knapp, R. B.; Taylor, R. T. TCE Remediation Using in Situ, Resting-State Bioaugmentation. *Environ. Sci. Technol.* **1996**, *30* (6), 1982–1989. https://doi.org/10.1021/es950730k.

(369) Williams, C. L.; Spiers, C. A. Degradation of Trichloroethene (TCE) in a Fractured Bedrock Aquifer Using Sodium Permanganate. *Proc. Third Int. Conf. Remediat. Chlorinated Recalcitrant Compd.* **2002**, No. May, 1431–1438.

(370) Haest, P. J.; Philips, J.; Springael, D.; Smolders, E. The Reactive Transport of Trichloroethene Is Influenced by Residence Time and Microbial Numbers. *J. Contam. Hydrol.* **2011**, *119* (1–4), 89–98. https://doi.org/10.1016/j.jconhyd.2010.09.011.

(371) Schaefer, C. E.; Towne, R. M.; Vainberg, S.; McCray, J. E.; Steffan, R. J. Bioaugmentation for Treatment of Dense Non-Aqueous Phase Liquid in Fractured Sandstone Blocks. *Environ. Sci. Technol.* **2010**, *44* (13), 4958–4964. https://doi.org/10.1021/es1002428.

(372) Roh, Y.; Lee, S. Y.; Elless, M. P.; Moon, H. S. Electro-Enhanced Remediation of Trichloroethene-Contaminated Groundwater Using Zero-Valent Iron. *J. Environ. Sci. Heal. - Part A Toxic/Hazardous Subst. Environ. Eng.* **2000**, *35* (7), 1061–1076. https://doi.org/10.1080/10934520009377020.

(373) Lee, P. K. H.; Macbeth, T. W.; Sorenson, K. S.; Deeb, R. a.; Alvarez-Cohen, L. Quantifying Genes and Transcripts to Assess the in Situ Physiology of "Dehalococcoides" Spp. in a Trichloroethene-Contaminated Groundwater Site. *Appl. Environ. Microbiol.* **2008**, *74* (9), 2728–2739. https://doi.org/10.1128/AEM.02199-07.

(374) Beach, S. A.; Newsted, J. L.; Coady, K.; Giesy, J. P. Ecotoxicological Evaluation of Perfluorooctanesulfonate (PFOS). *Rev. Environ. Contam. Toxicol.* **2006**, *186*, 133–174.

(375) Guelfo, J. L.; Higgins, C. P. Subsurface Transport Potential of Perfluoroalkyl Acids at Aqueous Film-Forming Foam (AFFF)-Impacted Sites. *Environ. Sci. Technol.* **2013**, *47* (9), 4164–4171. https://doi.org/10.1021/es3048043.

(376) Minnesota Department of Health. MDH Evaluation of Point-of-Use Water Treatment Devices for Perfluorochemical Removal. **2008**, 1–6.

(377) Vecitis, C.; Park, H.; Cheng, J. Treatment Technologies for Aqueous Perfluorooctanesulfonate (PFOS) and Perfluorooctanoate (PFOA). *Front. Environ. Sci. Eng.* **2009**, *3* (2), 129–151. https://doi.org/10.1007/s11783-009-0022-7.

(378) Tsai, Y. T.; Yu-Chen Lin, A.; Weng, Y. H.; Li, K. C. Treatment of Perfluorinated Chemicals by Electro-Microfiltration. *Environ. Sci. Technol.* **2010**, *44* (20), 7914–7920. https://doi.org/10.1021/es101964y.

(379) Steinle-Darling, E.; Reinhard, M. Nanofiltration for Trace Organic Contaminant Removal: Structure, Solution, and Membrane Fouling Effects on the Rejection of Perfluorochemicals. *Environ. Sci. Technol.* **2008**, *42* (14), 5292–5297. https://doi.org/10.1021/es703207s.

(380) Appleman, T. D.; Higgins, C. P.; Quiñones, O.; Vanderford, B. J.; Kolstad, C.;

Zeigler-Holady, J. C.; Dickenson, E. R. V. Treatment of Poly- and Perfluoroalkyl Substances in U.S. Full-Scale Water Treatment Systems. *Water Res.* **2014**, *51*, 246–255. https://doi.org/10.1016/j.watres.2013.10.067.

(381) Eschauzier, C.; Beerendonk, E.; Scholte-Veenendaal, P.; De Voogt, P. Impact of Treatment Processes on the Removal of Perfluoroalkyl Acids from the Drinking Water Production Chain. *Environ. Sci. Technol.* **2012**, *46* (3), 1708–1715. https://doi.org/10.1021/es201662b.

(382) Takagi, S.; Adachi, F.; Miyano, K.; Koizumi, Y.; Tanaka, H.; Watanabe, I.; Tanabe, S.; Kannan, K. Fate of Perfluorooctanesulfonate and Perfluorooctanoate in Drinking Water Treatment Processes. *Water Res.* **2011**, *45* (13), 3925–3932. https://doi.org/10.1016/j.watres.2011.04.052.

(383) Hansen, M. C.; Børresen, M. H.; Schlabach, M.; Cornelissen, G. Sorption of Perfluorinated Compounds from Contaminated Water to Activated Carbon. *J. Soils Sediments* **2010**, *10* (2), 179–185. https://doi.org/10.1007/s11368-009-0172-z.

(384) Yu, Q.; Zhang, R.; Deng, S.; Huang, J.; Yu, G. Sorption of Perfluorooctane Sulfonate and Perfluorooctanoate on Activated Carbons and Resin: Kinetic and Isotherm Study. *Water Res.* **2009**, *43* (4), 1150–1158. https://doi.org/10.1016/j.watres.2008.12.001.

(385) Ochoa-Herrera, V.; Sierra-Alvarez, R. Removal of Perfluorinated Surfactants by Sorption onto Granular Activated Carbon, Zeolite and Sludge. *Chemosphere* **2008**, *72* (10), 1588–1593. https://doi.org/10.1016/j.chemosphere.2008.04.029.

(386) Zaggia, A.; Conte, L.; Falletti, L.; Fant, M.; Chiorboli, A. Use of Strong Anion Exchange Resins for the Removal of Perfluoroalkylated Substances from Contaminated Drinking Water in Batch and Continuous Pilot Plants. *Water Res.* **2016**, *91*, 137–146. https://doi.org/10.1016/j.watres.2015.12.039.

(387) Deng, S.; Yu, Q.; Huang, J.; Yu, G. Removal of Perfluorooctane Sulfonate from Wastewater by Anion Exchange Resins: Effects of Resin Properties and Solution Chemistry. *Water Res.* **2010**, *44* (18), 5188–5195. https://doi.org/10.1016/j.watres.2010.06.038.

(388) Lee, M. C.; Choi, W. Development of Thermochemical Destruction Method of Perfluorocarbons (PFCs). *J. Ind. Eng. Chem.* **2004**, *10* (1), 107–114.

(389) Yang, S.; Cheng, J.; Sun, J.; Hu, Y.; Liang, X. Defluorination of Aqueous Perfluorooctanesulfonate by Activated Persulfate Oxidation. *PLoS One* **2013**, *8* (10), 6–15. https://doi.org/10.1371/journal.pone.0074877.

(390) Mitchell, S. M.; Ahmad, M.; Teel, A. L.; Watts, R. J. Degradation of Perfluorooctanoic Acid by Reactive Species Generated through Catalyzed H2O2 Propagation Reactions. *Environ. Sci. Technol. Lett.* **2013**, *1* (1), 117–121. https://doi.org/10.1021/ez4000862.

(391) Jin, L.; Zhang, P. Photochemical Decomposition of Perfluorooctane Sulfonate (PFOS) in an Anoxic Alkaline Solution by 185nm Vacuum Ultraviolet. *Chem. Eng. J.* **2015**, *280*, 241–247. https://doi.org/10.1016/j.cej.2015.06.022.

(392) Rodriguez-Freire, L.; Balachandran, R.; Sierra-Alvarez, R.; Keswani, M. Effect of

Sound Frequency and Initial Concentration on the Sonochemical Degradation of Perfluorooctane Sulfonate (PFOS). *J. Hazard. Mater.* **2015**, *300*, 662–669. https://doi.org/10.1016/j.jhazmat.2015.07.077.

(393) Vecitis, C. D.; Park, H.; Cheng, J.; Mader, B. T.; Hoffmann, M. R. Enhancement of Perfluorooctanoate and Perfluorooctanesulfonate Activity at Acoustic Cavitation Bubble Interfaces. *J. Phys. Chem. C* **2008**, *112* (43), 16850–16857. https://doi.org/10.1021/jp804050p.

(394) Gole, V. L.; Fishgold, A.; Sierra-Alvarez, R.; Deymier, P.; Keswani, M. Treatment of Perfluorooctane Sulfonic Acid (PFOS) Using a Large-Scale Sonochemical Reactor. *Sep. Purif. Technol.* **2018**, *194* (July 2017), 104–110. https://doi.org/10.1016/j.seppur.2017.11.009.

(395) Moriwaki, H.; Takagi, Y.; Tanaka, M.; Tsuruho, K.; Okitsu, K.; Maeda, Y. Sonochemical Decomposition of Perfluorooctane Sulfonate and Perfluorooctanoic Acid. *Environ. Sci. Technol.* **2005**, *39* (9), 3388–3392. https://doi.org/10.1021/es040342v.

(396) Hori, H.; Hayakawa, E.; Einaga, H.; Kutsuna, S.; Koike, K.; Ibusuki, T.; Kiatagawa, H.; Arakawa, R. Decomposition of Environmentally Persistent Perfluorooctanoic Acid in Water by Photochemical Approaches. *Environ. Sci. Technol.* **2004**, *38* (22), 6118–6124. https://doi.org/10.1021/es049719n.

(397) Cheng, J.; Vecitis, C. D.; Park, H.; Mader, B. T.; Hoffmann, M. R. Sonochemical Degradation of Perfluorooctane Sulfonate (PFOS) and Perfluorooctanoate (PFOA) in Groundwater: Kinetic Effects of Matrix Inorganics. *Environ. Sci. Technol.* **2010**, *44* (1), 445–450. https://doi.org/10.1021/es902651g.

(398) Thompson, J.; Eaglesham, G.; Reungoat, J.; Poussade, Y.; Bartkow, M.; Lawrence, M.; Mueller, J. F. Removal of PFOS, PFOA and Other Perfluoroalkyl Acids at Water Reclamation Plants in South East Queensland Australia. *Chemosphere* **2011**, *82* (1), 9–17. https://doi.org/10.1016/j.chemosphere.2010.10.040.

(399) Hori, H.; Yamamoto, A.; Hayakawa, E.; Taniyasu, S.; Yamashita, N.; Kutsuna, S.; Kiatagawa, H.; Arakawa, R. Efficient Decomposition of Environmentally Persistent Perfluorocarboxylic Acids by Use of Persulfate as a Photochemical Oxidant. *Environ. Sci. Technol.* **2005**, *39* (7), 2383–2388. https://doi.org/10.1021/es0484754.

(400) Hori, H.; Nagaoka, Y.; Murayama, M.; Kutsuna, S. Efficient Decomposition of Perfluorocarboxylic Acids and Alternative Fluorochemical Surfactants in Hot Water. *Environ. Sci. Technol.* **2008**, *42* (19), 7438–7443. https://doi.org/10.1021/es800832p.

(401) Hori, H.; Yamamoto, A.; Koike, K.; Kutsuna, S.; Osaka, I.; Arakawa, R. Persulfate-Induced Photochemical Decomposition of a Fluorotelomer Unsaturated Carboxylic Acid in Water. *Water Res.* **2007**, *41* (13), 2962–2968. https://doi.org/10.1016/j.watres.2007.02.033.

(402) Park, S.; Lee, L. S.; Medina, V. F.; Zull, A.; Waisner, S. Heat-Activated Persulfate Oxidation of PFOA, 6:2 Fluorotelomer Sulfonate, and PFOS under Conditions Suitable for in-Situ Groundwater Remediation. *Chemosphere* **2016**,

145, 376–383. https://doi.org/10.1016/j.chemosphere.2015.11.097.

(403) Tabe, S.; Yang, P.; Zhao, X.; Hao, C.; Seth, R.; Schweitzer, L.; Jamal, T. Occurrence and Removal of PPCPs and EDCs in the Detroit River Watershed. *Water Pract. Technol.* **2010**, *5* (1), wpt2010015-wpt2010015. https://doi.org/10.2166/wpt.2010.015.

(404) Liu, C. S.; Shih, K.; Wang, F. Oxidative Decomposition of Perfluorooctanesulfonate in Water by Permanganate. *Sep. Purif. Technol.* **2012**, *87*, 95–100. https://doi.org/10.1016/j.seppur.2011.11.027.

(405) Liu, C. S.; Higgins, C. P.; Wang, F.; Shih, K. Effect of Temperature on Oxidative Transformation of Perfluorooctanoic Acid (PFOA) by Persulfate Activation in Water. *Sep. Purif. Technol.* **2012**, *91*, 46–51. https://doi.org/10.1016/j.seppur.2011.09.047.

(406) Eberle, D.; Ball, R.; Boving, T. B. Impact of ISCO Treatment on PFAA Co-Contaminants at a Former Fire Training Area. *Environ. Sci. Technol.* **2017**, *51* (9), 5127–5136. https://doi.org/10.1021/acs.est.6b06591.

(407) Lange, C. C. *Aerobic Biodegradation of N-EtFOSE Alcohol by the Microbial Activity Present in Municipal Wastewater Treatment Sludge. Biodegradation Study Report; 3M Project ID: LIMS E00-2252*; St. Paul, MN, 2000.

(408) Prevedouros, K.; Cousins, I. T.; Buck, R. C.; Korzeniowski, S. H. Sources, Fate and Transport of Perfluorocarboxylates. *Environ. Sci. Technol.* **2006**, *40* (1), 32–44. https://doi.org/10.1021/es0512475.

(409) Dinglasan, M. J. A.; Ye, Y.; Edwards, E. A.; Mabury, S. A. Fluorotelomer Alcohol Biodegradation Yields Poly- and Perfluorinated Acids. *Environ. Sci. Technol.* **2004**, *38* (10), 2857–2864. https://doi.org/10.1021/es0350177.

(410) Wallington, T. J.; Hurley, M. D.; Xia, J.; Wuebbles, D. J.; Sillman, S.; Ito, A.; Penner, J. E.; Ellis, D. A.; Martin, J.; Mabury, S. A.; et al. Formation of C7F15COOH (PFOA) and Other Perfluorocarboxylic Acids during the Atmospheric Oxidation of 8:2 Fluorotelomer Alcohol. *Environ. Sci. Technol.* **2006**, *40* (3), 924–930. https://doi.org/10.1021/es051858x.

(411) Lee, H.; D'eon, J.; Mabury, S. A. Biodegradation of Polyfluoroalkyl Phosphates as a Source of Perfluorinated Acids to the Environment. *Environ. Sci. Technol.* **2010**, *44* (9), 3305–3310. https://doi.org/10.1021/es9028183.

(412) Liu, J.; Wang, N.; Buck, R. C.; Wolstenholme, B. W.; Folsom, P. W.; Sulecki, L. M.; Bellin, C. A. Aerobic Biodegradation of [14C] 6:2 Fluorotelomer Alcohol in a Flow-through Soil Incubation System. *Chemosphere* **2010**, *80* (7), 716–723. https://doi.org/10.1016/j.chemosphere.2010.05.027.

(413) D'Agostino, L. A.; Mabury, S. A. Aerobic Biodegradation of 2 Fluorotelomer Sulfonamide–based Aqueous Film–forming Foam Components Produces Perfluoroalkyl Carboxylates. *Environ. Toxicol. Chem.* **2017**, *36* (8), 2012–2021. https://doi.org/10.1002/etc.3750.

(414) Wang, N.; Szostek, B.; Buck, R. C.; Folsom, P. W.; Sulecki, L. M.; Capka, V.; Berti, W. R.; Gannon, J. T. Fluorotelomer Alcohol Biodegradation - Direct Evidence That Perfluorinated Carbon Chains Breakdown. *Environ. Sci. Technol.*

2005, *39* (19), 7516–7528. https://doi.org/10.1021/es0506760.

(415) Wang, N.; Szostek, B.; Buck, R. C.; Folsom, P. W.; Sulecki, L. M.; Gannon, J. T. 8-2 Fluorotelomer Alcohol Aerobic Soil Biodegradation: Pathways, Metabolites, and Metabolite Yields. *Chemosphere* **2009**, *75* (8), 1089–1096. https://doi.org/10.1016/j.chemosphere.2009.01.033.

(416) Liu, J.; Wang, N.; Szostek, B.; Buck, R. C.; Panciroli, P. K.; Folsom, P. W.; Sulecki, L. M.; Bellin, C. A. 6-2 Fluorotelomer Alcohol Aerobic Biodegradation in Soil and Mixed Bacterial Culture. *Chemosphere* **2010**, *78* (4), 437–444. https://doi.org/10.1016/j.chemosphere.2009.10.044.

(417) Ochoa-Herrera, V.; Field, J. A.; Luna-Velasco, A.; Sierra-Alvarez, R. Microbial Toxicity and Biodegradability of Perfluorooctane Sulfonate (PFOS) and Shorter Chain Perfluoroalkyl and Polyfluoroalkyl Substances (PFASs). *Environ. Sci. Process. Impacts* **2016**, *18* (9), 1236–1246. https://doi.org/10.1039/c6em00366d.

(418) Benskin, J. P.; Ikonomou, M. G.; Gobas, F. A. P. C.; Begley, T. H.; Woudneh, M. B.; Cosgrove, J. R. Biodegradation of N-Ethyl Perfluorooctane Sulfonamido Ethanol (EtFOSE) and EtFOSE-Based Phosphate Diester (SAmPAP Diester) in Marine Sediments. *Environ. Sci. Technol.* **2013**, *47* (3), 1381–1389. https://doi.org/10.1021/es304336r.

(419) Dasu, K.; Liu, J.; Lee, L. S. Aerobic Soil Biodegradation of 8:2 Fluorotelomer Stearate Monoester. *Environ. Sci. Technol.* **2012**, *46* (7), 3831–3836. https://doi.org/10.1021/es203978g.

(420) Harding-Marjanovic, K. C.; Houtz, E. F.; Yi, S.; Field, J. A.; Sedlak, D. L.; Alvarez-Cohen, L. Aerobic Biotransformation of Fluorotelomer Thioether Amido Sulfonate (Lodyne) in AFFF-Amended Microcosms. *Environ. Sci. Technol.* **2015**, *49* (13), 7666–7674. https://doi.org/10.1021/acs.est.5b01219.

(421) Tseng, N.; Wang, N.; Szostek, B.; Mahendra, S. Biotransformation of 6:2 Fluorotelomer Alcohol (6:2 FTOH) by a Wood-Rotting Fungus. *Environ. Sci. Technol.* **2014**, *48* (7), 4012–4020. https://doi.org/10.1021/es4057483.

(422) Key, B. D.; Howell, R. D.; Criddle, C. S. Defluorination of Organofluorine Sulfur Compounds by Pseudomonas Sp. Strain D2. *Environ. Sci. Technol.* **1998**, *32* (15), 2283–2287. https://doi.org/10.1021/es9800129.

(423) Huang, S.; Jaffé, P. R. Defluorination of Perfluorooctanoic Acid (PFOA) and Perfluorooctane Sulfonate (PFOS) by Acidimicrobium Sp. Strain A6. *Environ. Sci. Technol.* **2019**. https://doi.org/10.1021/acs.est.9b04047.

(424) Yu, Y.; Zhang, K.; Li, Z.; Ren, C.; Liu, J.; Men, Y. Microbial Cleavage of C-F Bonds in per- and Polyfluoroalkyl Substances via Dehalorespiration. *ChemRxiv* **2019**. https://doi.org/10.26434/chemrxiv.8245679.v4.

(425) Cai, Y.; Chen, H.; Yuan, R.; Wang, F.; Chen, Z.; Zhou, B. Toxicity of Perfluorinated Compounds to Soil Microbial Activity: Effect of Carbon Chain Length, Functional Group and Soil Properties. *Sci. Total Environ.* **2019**, *690*, 1162–1169. https://doi.org/10.1016/j.scitotenv.2019.06.440.

(426) Qiao, W.; Xie, Z.; Zhang, Y.; Liu, X.; Xie, S.; Huang, J.; Yu, L. Perfluoroalkyl Substances (PFASs) Influence the Structure and Function of Soil Bacterial

Community: Greenhouse Experiment. *Sci. Total Environ.* **2018**, *642*, 1118–1126. https://doi.org/10.1016/j.scitotenv.2018.06.113.

(427) Fitzgerald, N. J. M.; Temme, H. R.; Simcik, M. F.; Novak, P. J. Aqueous Film Forming Foam and Associated Perfluoroalkyl Substances Inhibit Methane Production and Co-Contaminant Degradation in an Anaerobic Microbial Community. *Environ. Sci. Process. Impacts* **2019**, *21* (11), 1915–1925. https://doi.org/10.1039/c9em00241c.

(428) Weathers, T. S.; Higgins, C. P.; Sharp, J. O. Enhanced Biofilm Production by a Toluene-Degrading Rhodococcus Observed after Exposure to Perfluoroalkyl Acids. *Environ. Sci. Technol.* **2015**, *49* (9), 5458–5466. https://doi.org/10.1021/es5060034.

(429) Chapman, S. W.; Parker, B. L.; Sale, T. C.; Doner, L. A. Testing High Resolution Numerical Models for Analysis of Contaminant Storage and Release from Low Permeability Zones. *J. Contam. Hydrol.* **2012**, *136–137*, 106–116. https://doi.org/10.1016/j.jconhyd.2012.04.006.

(430) Rodriguez, D. Significance of Diffused Zone Mass Storage and Rebound in Determing the Longevity of Solute Plumes Emanating from Heterogeneous DNAPL Source Zones, 2006. https://doi.org/10.1073/pnas.0703993104.

(431) Chapman, S. W.; Parker, B. L. Plume Persistence Due to Aquitard Back Diffusion Following Dense Nonaqueous Phase Liquid Source Removal or Isolation. *Water Resour. Res.* **2005**, *41* (12), 1–16. https://doi.org/10.1029/2005WR004224.

(432) Parker, B. L.; Chapman, S. W.; Guilbeault, M. A. Plume Persistence Caused by Back Diffusion from Thin Clay Layers in a Sand Aquifer Following TCE Source-Zone Hydraulic Isolation. *J. Contam. Hydrol.* **2008**, *102* (1–2), 86–104. https://doi.org/10.1016/j.jconhyd.2008.07.003.

(433) Suchomel, E. J.; Ramsburg, C. A.; Pennell, K. D. Evaluation of Trichloroethene Recovery Processes in Heterogeneous Aquifer Cells Flushed with Biodegradable Surfactants. *J. Contam. Hydrol.* **2007**, *94* (3–4), 195–214. https://doi.org/10.1016/j.jconhyd.2007.05.011.

(434) Löffler, F. E.; Sanford, R. A.; Ritalahti, K. M. Enrichment, Cultivation, and Detection of Reductively Dechlorinating Bacteria. *Methods Enzymol.* **2005**, *397* (1996), 77–111. https://doi.org/10.1016/S0076-6879(05)97005-5.

(435) Yang, L.; Wang, X.; Mendoza-Sanchez, I.; Abriola, L. M. Modeling the Influence of Coupled Mass Transfer Processes on Mass Flux Downgradient of Heterogeneous DNAPL Source Zones. *J. Contam. Hydrol.* **2018**, *211*, 1–14. https://doi.org/10.1016/j.jconhyd.2018.02.003.

(436) Verschueren, K. *Handbook of Environmental Data on Organic Chemicals*; Wiley, 2001.

(437) Li, Y.-H.; Gregory, S. Diffusion of Ions in Sea Water and in Deep-Sea Sediments. *Geochim. Cosmochim. Acta* **1974**, *38* (5), 703–714. https://doi.org/10.1016/0016-7037(74)90145-8.

(438) Ball, W. P.; Liu, C.; Xia, G.; Young, D. F. A Diffusion-Based Interpretation of Tetrachloroethene and Trichloroethene Concentration Profiles in a Groundwater

Aquitard. *Water Resour. Res.* **1997**, *33* (12), 2741–2757. https://doi.org/10.1029/97WR02135.

(439) Johnson, R. L.; Cherry, J. A.; Pankow, J. F. Diffusive Contaminant Transport in Natural Clay: A Field Example and Implications for Clay-Lined Waste Disposal Sites. *Environ. Sci. Technol.* **1989**, *23* (3), 340–349. https://doi.org/10.1021/es00180a012.

(440) Yang, L.; Wang, X.; Mendoza-Sanchez, I.; Abriola, L. M. Modeling the Influence of Coupled Mass Transfer Processes on Mass Flux Downgradient of Heterogeneous DNAPL Source Zones. *J. Contam. Hydrol.* **2018**, *211*, 1–14. https://doi.org/10.1016/j.jconhyd.2018.02.003.

(441) Taylor, T. P.; Pennell, K. D.; Abriola, L. M.; Dane, J. H. Surfactant Enhanced Recovery of Tetrachloroethylene from a Porous Medium Containing Low Permeability Lenses. *J. Contam. Hydrol.* **2001**, *48* (3–4), 325–350. https://doi.org/10.1016/S0169-7722(00)00185-6.

(442) Marcet, T. F.; Cápiro, N. L.; Morris, L. A.; Hassan, S. M.; Yang, Y.; Löffler, F. E.; Pennell, K. D. Release of Electron Donors during Thermal Treatment of Soils. *Environ. Sci. Technol.* **2018**, *52* (6), 3642–3651. https://doi.org/10.1021/acs.est.7b06014.

(443) Marcet, T. F. Secondary Impacts of In Situ Chlorinated Solvent Remediation Due to Metal Sulfide Preceipitation and Thermal Treatment, Tufts University, 2014.

(444) Pankow, J. F.; Feenstra, S.; Cherry, J. A.; Ryan, M. C. Dense Chlorinated Solvents and Other DNAPLs in Groundwater : Background and History of the Problem. In *Dense Chlorinated Solvents and Other DNAPLs in Groundwater*; Pankow, J. F., Cherry, J. A., Eds.; Waterloo Press: Guelph, Ontario, Canada, 1996; pp 1–52.

(445) Pennell, K. D.; Boyd, S. a; Abriola, L. M. Surface Area of Soil Organic Matter Reexamined. *Soil Sci. Soc. Am. J.* **1995**, *59* (January), 1012–1018. https://doi.org/10.2136/sssaj1995.03615995005900040008x.

(446) Gaeth, S. P. Examining Reactive Minerals, Sulfide, and Bioremediation Interactions for Improved Chlorinated Solvent Detoxification, Tufts University, 2017.

(447) Chen, L.; Miller, G. A.; Kibbey, T. C. G. Rapid Pseudo-Static Measurement of Hysteretic Capillary Pressure-Saturation Relationships in Unconsolidated Porous Media. *Geotech. Test. J.* **2007**, *30* (6), 474–483. https://doi.org/10.1520/GTJ100850.

(448) Joo, J. C.; Shackelford, C. D.; Reardon, K. F. Association of Humic Acid with Metal (Hydr)Oxide-Coated Sands at Solid-Water Interfaces. *J. Colloid Interface Sci.* **2008**, *317* (2), 424–433. https://doi.org/10.1016/j.jcis.2007.09.061.

(449) Duhamel, M.; Edwards, E. A. Growth and Yields of Dechlorinators, Acetogens, and Methanogens during Reductive Dechlorination of Chlorinated Ethenes and Dihaloelimination of 1,2-Dichloroethane. *Environ. Sci. Technol.* **2007**, *41* (7), 2303–2310. https://doi.org/10.1021/es062010r.

(450) Damgaard, I.; Bjerg, P. L.; Bælum, J.; Scheutz, C.; Hunkeler, D.; Jacobsen, C. S.;

Tuxen, N.; Broholm, M. M. Identification of Chlorinated Solvents Degradation Zones in Clay till by High Resolution Chemical, Microbial and Compound Specific Isotope Analysis. *J. Contam. Hydrol.* **2013**, *146*, 37–50. https://doi.org/10.1016/j.jconhyd.2012.11.010.

(451) Walker, S. L.; Redman, J. a.; Elimelech, M. Influence of Growth Phase on Bacterial Deposition: Interaction Mechanisms in Packed-Bed Column and Radial Stagnation Point Flow Systems. *Environ. Sci. Technol.* **2005**, *39* (17), 6405–6411. https://doi.org/10.1021/es050077t.

(452) Abriola, L. M.; Capiro, N. L.; Christ, J. A.; Chu, L.; Miller, E. L.; Pennell, K. D. *Development of an Integrated Field Test / Modeling Protocol for Efficient In Situ Bioremediation Design and Performance Uncertainty Assessment*; 2019.

(453) Lu, X.; Wilson, J. T.; Kampbell, D. H. Relationship between Dehalococcoides DNA in Ground Water and Rates of Reductive Dechlorination at Field Scale. *Water Res.* **2006**, *40* (16), 3131–3140. https://doi.org/10.1016/j.watres.2006.05.030.

(454) Ritalahti, K. M.; Hatt, J. K.; Petrovskis, E.; Loffler, F. E. Groundwater Sampling for Nucleic Acid Biomarker Analysis. *Handb. Hydrocarb. Lipid Microbiol.* **2010**, *5* (1), 3407–3418. https://doi.org/10.1007/978-3-540-77587-4.

(455) West, K. A.; Lee, P. K. H.; Johnson, D. R.; Zinder, S. H.; Alvarez-Cohen, L. Global Gene Expression of Dehalococcoides within a Robust Dynamic TCE-Dechlorinating Community under Conditions of Periodic Substrate Supply. *Biotechnol. Bioeng.* **2013**, *110* (5), 1333–1341. https://doi.org/10.1002/bit.24819.

(456) Low, A.; Shen, Z.; Cheng, D.; Rogers, M. J.; Lee, P. K. H.; He, J. A Comparative Genomics and Reductive Dehalogenase Gene Transcription Study of Two Chloroethene-Respiring Bacteria, Dehalococcoides Mccartyi Strains MB and 11a. *Sci. Rep.* **2015**, *5* (June), 1–12. https://doi.org/10.1038/srep15204.

(457) Waller, A. S.; Krajmalnik-Brown, R.; Löffler, F. E.; Edwards, E. A. Multiple Reductive-Dehalogenase-Homologous Genes Are Simultaneously Transcribed during Dechlorination by Dehalococcoides-Containing Cultures. *Appl. Environ. Microbiol.* **2005**, *71* (12), 8257–8264. https://doi.org/10.1128/AEM.71.12.8257-8264.2005.

(458) Fung, J. M.; Morris, R. M.; Adrian, L.; Zinder, S. H. Expression of Reductive Dehalogenase Genes in Dehalococcoides Ethenogenes Strain 195 Growing on Tetrachloroethene, Trichloroethene, or 2,3-Dichlorophenol. *Appl. Environ. Microbiol.* **2007**, *73* (14), 4439–4445. https://doi.org/10.1128/AEM.00215-07.

(459) Liang, Y.; Liu, X.; Singletary, M. A.; Wang, K.; Mattes, T. E. Relationships between the Abundance and Expression of Functional Genes from Vinyl Chloride (VC)-Degrading Bacteria and Geochemical Parameters at VC-Contaminated Sites. *Environ. Sci. Technol.* **2017**, *51* (21), 12164–12174. https://doi.org/10.1021/acs.est.7b03521.

(460) Overholser, B. R.; Sowinski, K. M. Biostatistics Primer: Part 2. *Nutr. Clin. Pract.* **2008**, *23* (1), 76–84. https://doi.org/10.1177/011542650802300176.

(461) Maymó-Gatell, X.; Nijenhuis, I.; Zinder, S. H. Reductive Dechlorination of Cis-1,2-Dichloroethene and Vinyl Chloride by "Dehalococcoides Ethenogenes."

Environ. Sci. Technol. **2001**, *35* (3), 516–521. https://doi.org/10.1021/es001285i.

(462) OECD. Toward a New Comprehensive Global Database of Per- and Polyfluoroalkyl Substances (PFASs): Summary Report on Updating the OECD 2007 List of per- and Polyfluoroalkyl Substances (PFASs). *Ser. Risk Manag.* **2018**, *No. 39*. (39), 1–24.

(463) Yang, Y.; Cápiro, N. L.; Marcet, T. F.; Yan, J.; Pennell, K. D.; Löffler, F. E. Organohalide Respiration with Chlorinated Ethenes under Low PH Conditions. *Environ. Sci. Technol.* **2017**, *51* (15), 8579–8588. https://doi.org/10.1021/acs.est.7b01510.

(464) Center, A. F. C. E. *Crash Fire Station Soil and Groundwater Sample Results Former Loring Air Force Base, Limeston, ME*; Lackland, TX, 2017.

(465) OECD. *Hazard Assessment of Perfluorooctane Sulfonate (PFOS) and Its Salts*; 2002.

(466) Wolin, E. A.; Wolin, M. J.; Wolfe, R. S. Formation of Methane by Bacterial Extracts. *J. Biol. Chem.* **1963**, *238* (6), 2882–2886. https://doi.org/10.1016/S0016-0032(13)90081-8.

(467) Backe, W. J.; Day, T. C.; Field, J. A. Zwitterionic, Cationic, and Anionic Fluorinated Chemicals in Aqueous Film Forming Foam Formulations and Groundwater from U.S. Military Bases by Nonaqueous Large-Volume Injection HPLC-MS/MS. *Environ. Sci. Technol.* **2013**, *47* (10), 5226–5234. https://doi.org/10.1021/es3034999.

(468) Field, J. A.; Sedlak, D. L.; Alvarez-Cohen, L. *Characterization of the Fate and Biotransformation of Fluorochemicals in AFFF-Contaminated Groundwater at Fire / Crash Testing Military Sites (ER-2128)*; 2017.

(469) Bräunig, J.; Baduel, C.; Heffernan, A.; Rotander, A.; Donaldson, E.; Mueller, J. F. Fate and Redistribution of Perfluoroalkyl Acids through AFFF-Impacted Groundwater. *Sci. Total Environ.* **2017**, *596–597*, 360–368. https://doi.org/10.1016/j.scitotenv.2017.04.095.

(470) Xiao, X.; Ulrich, B. A.; Chen, B.; Higgins, C. P. Sorption of Poly- and Perfluoroalkyl Substances (PFASs) Relevant to Aqueous Film-Forming Foam (AFFF)-Impacted Groundwater by Biochars and Activated Carbon. *Environ. Sci. Technol.* **2017**, *51* (11), 6342–6351. https://doi.org/10.1021/acs.est.7b00970.

(471) Shang, H. Geotechnical Laboratory Characterization of Sand- Zeolite Mixtures, University of Louisville, 2015.

(472) Wang, Y.; Li, Y.; Kim, H.; Walker, S. L.; Abriola, L. M.; Pennell, K. D. Transport and Retention of Fullerene Nanoparticles in Natural Soils. *J. Environ. Qual.* **2010**, *39* (6), 1925–1933. https://doi.org/10.2134/jeq2009.0411.

(473) Costanza, J. Degradation of Tetrachloroethylene and Trichloroethylene under Thermal Remediation Conditions, Georgia Institute of Technology, 2005.

(474) Amos, B. K.; Sung, Y.; Fletcher, K. E.; Gentry, T. J.; Wu, W. M.; Criddle, C. S.; Zhou, J.; Löffler, F. E. Detection and Quantification of Geobacter Lovleyi Strain SZ: Implications for Bioremediation at Tetrachloroethene- and Uranium-Impacted Sites. *Appl. Environ. Microbiol.* **2007**, *73* (21), 6898–6904.

https://doi.org/10.1128/AEM.01218-07.

(475) Kube, M.; Beck, A.; Zinder, S. H.; Kuhl, H.; Reinhardt, R.; Adrian, L. Genome Sequence of the Chlorinated Compound-Respiring Bacterium Dehalococcoides Species Strain CBDB1. *Nat. Biotechnol.* **2005**, *23* (10), 1269–1273. https://doi.org/10.1038/nbt1131.

(476) Seshadri, R.; Adrian, L.; Fouts, D. E.; Eisen, J. A.; Phillippy, A. M.; Methe, B. A.; Ward, N. L.; Nelson, W. C.; Deboy, R. T.; Khouri, H. M.; et al. Genome Sequence of the PCE-Dechlorinating Bacterium Dehalococcoides Ethenogenes. *Science (80-.).* **2005**, *307* (5706), 105–108. https://doi.org/10.1126/science.1102226.

(477) Wagner, D. D.; Hug, L. A.; Hatt, J. K.; Spitzmiller, M. R.; Padilla-Crespo, E.; Ritalahti, K. M.; Edwards, E. A.; Konstantinidis, K. T.; Löffler, F. E. Genomic Determinants of Organohalide-Respiration in Geobacter Lovleyi, an Unusual Member of the Geobacteraceae. *BMC Genomics* **2012**, *13* (1). https://doi.org/10.1186/1471-2164-13-200.

(478) McDonald, M. .; Harbaugh, A. W. A Modular Three-Dimensional Finite Difference Ground-Water Flow Model. *Tech. Water-Resources Investig. B. 6* **1988**, 588. https://doi.org/10.1016/0022-1694(70)90079-X.

(479) Lyon-Marion, B. A.; Becker, M. D.; Kmetz, A. A.; Foster, E.; Johnston, K. P.; Abriola, L. M.; Pennell, K. D. Simulation of Magnetite Nanoparticle Mobility in a Heterogeneous Flow Cell. *Environ. Sci. Nano* **2017**, *4* (7), 1512–1524. https://doi.org/10.1039/c7en00152e.

(480) Das, B. M. 5 Hydrometer Analysis. In *Soil Mechanics Laboratory Manual. 5th ed.*; Austin, 1997; pp 23–34.

(481) Einarson, M. D.; Cherry, J. A. A New Multilevel Ground Water Monitoring System Using Multichannel Tubing. *Groundw. Monit. Remediat.* **2002**, *22* (4), 52–65. https://doi.org/10.1111/j.1745-6592.2002.tb00771.x.

(482) Cwiertny, D. M.; Scherer, M. M. Abiotic Processes Affecting the Remediation of Chlorinated Solvents; 2010; pp 69–108. https://doi.org/10.1007/978-1-4419-1401-9_4.